Physics – Uspekhi **45** (3) 235 – 291 (2002)

REVIEWS OF TOPICAL PROBLEMS PACS numbers: **41.60. – m**, 52.35.Hr, 95.30.Gv

Transition radiation in media with random inhomogeneities

K Yu Platonov, G D Fleĭshman

DOI: 10.1070/PU2002v045n03ABEH000952

Contents

Abstract. This review analyzes radiation produced by randomly inhomogeneous media excited by fast particles — i.e., polarization bremsstrahlung for thermodynamically equilibrium inhomogeneities or transition radiation for nonthermal ones — taking into account all the effects important for natural sources. Magnetic field effects on both the motion of fast particles and the dispersion of background plasma are considered, and the multiple scattering of fast particles in the medium is examined. Various resonant effects occurring under the conditions of Cherenkov (or cyclotron) emission for a particular eigenmode are discussed. The transition radiation intensity and absorption (amplification) coefficients are calculated for ensembles of fast particles with realistic distributions over momentum and angles. The value of the developed theory of transition radiation is illustrated by applying it to astrophysical objects. Transition radiation is shown to contribute significantly to the radio emission of the Sun, planets (including Earth), and interplanetary and interstellar media. Possible further applications of transition radiation (particularly stimulated) are discussed.

K Yu Platonov St.-Petersburg State Technical University,
ul. Politekhnicheskaya 29, 195251 St.-Petersburg, Russian Federation
Tel. (7-812) 552 65 01
E-mail: platonov@quark.stu.neva.ru
G D Fleĭshman A F Ioffe Physical-Technical Institute,
Russian Academy of Sciences,
ul. Politekhnicheskaya 26, 194021 St.-Petersburg, Russian Federation
Tel. (7-812) 247 93 68. Fax (7-812) 247 10 17
E-mail: gregory@sun.ioffe.rssi.ru

Received 9 February 2001, revised 15 September 2001
Uspekhi Fizicheskikh Nauk **172** (3) 241 – 300 (2002)
Translated by G D Fleĭshman; edited by M V Magnitskaya

1. Introduction

Contrary to the old statement "a particle moving with the constant velocity does not radiate", it seems trivial now that any moving particle produces radiation. The point is that the particle would not radiate only when moving in empty space without external fields. Actually, charged particles propagate in a medium and in the presence of the fields. Moreover, several microscopic mechanisms of electromagnetic emission can typically operate simultaneously. This makes both analysis of experiments and interpretation of natural emissions (e.g., in astrophysics) more complicated.

This paper concentrates on transition radiation generation by fast particles propagating in media with random inhomogeneities, which happens frequently in natural conditions.

Note that various authors define 'transition radiation' differently. Some of them consider transition radiation as emission arising on the sharp boundary of two media only (transition radiation in the narrow sense of the term). They treat other similar emissions (e.g., on a system of boundaries

or in a periodic medium) as independent mechanisms. Others refer to any radiation produced by a particle moving with constant velocity in/near media as transition radiation except for Vavilov – Cherenkov radiation (see papers [1] and references there for the discussion of emission by rectilinearly moving particles).

Thus, it would be useful to start with a formal definition of what transition radiation is. However, an exact (and brief) definition of all the phenomena we regard as transition radiation appears not easy to give. Sections 1.1 and 1.2 explain in detail what processes are classified as transition radiation. For the moment we define transition radiation as follows.

When a source is moving in (*close to*) *a medium, then transition radiation is the part of the radiation that remains non-zero for constant velocity of source motion, while vanishing for a uniform* (*at any spatial and temporal scales*) *medium*.

This definition seems to be the most general, because it includes such phenomena as transition radiation at a single boundary [2], diffraction [3], resonant [4], polarization [5] etc. radiations. Together with the term 'transition radiation' we use further some other particular terms (e.g., polarization bremsstrahlung) when appropriate.

1.1 Classification of emission mechanisms by fast particles in media

An idea of elementary (microscopic) emission mechanisms is exceedingly productive in building a physical classification of the mechanisms (i.e., the simplest radiative processes).

To avoid misunderstanding we should emphasize that the idea of an elementary emission mechanism is a physical idealization that describes actual radiative processes just approximately (while the accuracy can be rather high). When a fast particle is moving in a medium, the radiation is produced due to the interaction between both components (the particle and the medium) of the dynamic system. The total radiation of the system cannot be strictly divided into the two components — emission by the particle and emission by the medium — in any particular case (this separation can be done differently at least).

Nevertheless, the concept of the two emission channels of the system, namely, the *intrinsic emission* by the fast particle and the *emission by the medium* excited by the particle, is very productive and has a wide applicability.

Feynman diagrams represent these two channels in a simple way. *Intrinsic emission* (Fig. 1a) arises when the fast particle exchanges a virtual photon with the medium (and/or external field) with momentum $\mathbf{q}$ and emits a quantum with momentum $\mathbf{k}$. It is important to note, that the produced quantum is assumed to obey the material dispersion relation $\omega = \omega(\mathbf{k})$ (a 'wrapped' quantum).

The intrinsic radiation can be of various kinds depending on the external field's nature. A particle rotating in a magnetic field generates *magneto-bremsstrahlung*. The emission is referred to as *cyclotron* emission for non-relativistic particles and as *synchrotron* for ultra-relativistic particles. The term '*gyro-synchrotron*' is frequently used for the emission by mildly relativistic particles.

A particle moving in a Coulomb field produces *bremsstrahlung*. The same name is used for the emission resulting from particle deceleration in a medium, i.e., when the particle is moving in an electric field created by a huge number of Coulomb centers.

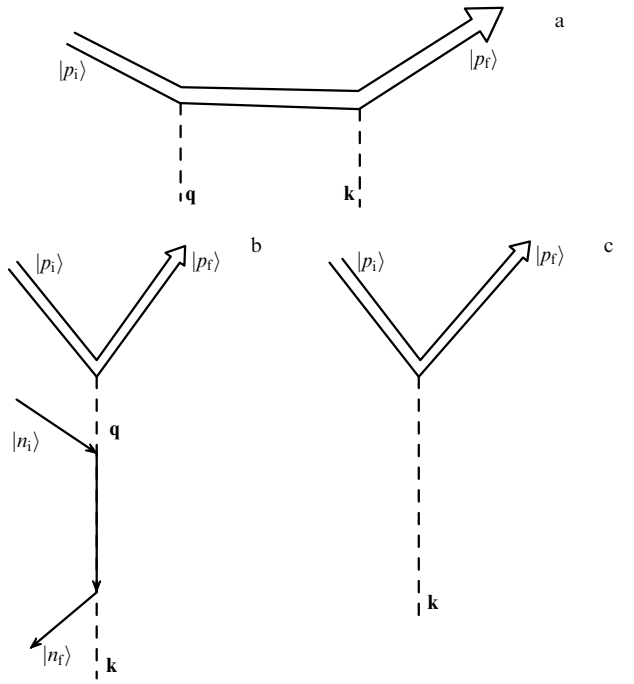

Figure 1. Feynman diagrams for various radiative processes in a medium: (a) bremsstrahlung, (b) polarization bremsstrahlung, (c) Vavilov – Cherenkov radiation.

Figure 1b displays the *emission by the medium* when the exchange between the particle and the medium by the virtual photon with momentum $\mathbf{q}$ results in the production of radiation by background electrons. Thus, the account of the degrees of freedom for the medium is a must to calculate the respective emission. Obviously, the medium may generate without any external particle, while this paper considers only the emission types that are stimulated by fast particle action. We use the name 'transition radiation' in a general sense for all radiative processes of this kind.

This general type of emission is divided in the literature into a few particular types. For example, a particle emits '*diffraction*' *radiation* if it moves near a screen or through a hole, '*resonant*' *radiation* when it propagates in a medium with periodic (in space) dielectric permeability etc. The cases have in common the same physical cause providing the emission, that is inhomogeneities of the medium.

There is one more type of emission, *Vavilov – Cherenkov radiation* (*VCR*). It seems to be outside the proposed classification dividing all emissions into either intrinsic or emission produced by the medium, because no exchange between the particle and the medium occurs by a virtual photon with the momentum $\mathbf{q}$ (Fig. 1c). The formal electrodynamics allows calculation of the intensity of emission by a particle moving rectilinearly without any acceleration. This intensity is proportional to $\delta[\omega(\mathbf{k}) - \mathbf{kv}]$ in both vacuum and medium. Obviously, the equality $\omega(\mathbf{k}) = \mathbf{kv}$ must be fulfilled for the emission to be non-zero. This is only possible for particles moving with a velocity exceeding the phase speed of the generated waves, so VCR is a kind of threshold effect.

The phase speed of the electromagnetic waves in vacuum is the speed of light. Thus, VCR might arise in vacuum for (hypothetical) superluminal particles only. VCR would obviously reveal itself as intrinsic emission by the superluminal particle because no medium is present in this case. Moreover, the photon energy is taken from the particle

energy (this is valid even for a particle of infinitely large mass, when the respective energy decrease does not affect the motion itself).

Let us place the particle in a medium with refractive index larger than unity. The emission still occurs, while its intensity changes due to the different wave dispersion relation $\omega(\mathbf{k})$. It is important that the threshold of the effect also changes because the phase speed in the medium is less than the speed of light. Thus, the condition $\omega(\mathbf{k}) = \mathbf{kv}$ may now be fulfilled for normal (subluminal) particles as well.

This approach allows us to classify VCR as intrinsic emission by the particle, rather than emission by the medium (this is emphasized by Frank in the book [6, p. 56], as well as in papers [7, 8]). The role of the medium is just modification (renormalization) of the vacuum particle field in such a way that subluminal particles produce non-zero intensity in the medium instead of zero intensity in the vacuum. The modification is obviously provided by the response polarization current of the medium, thus, the presence of the medium is substantial to generate VCR by subluminal particles.

This case is very similar to the generation of other kinds of intrinsic radiation, e.g., synchrotron radiation (which we regard as intrinsic radiation in both vacuum and medium). Synchrotron radiation in a medium is known to be suppressed strongly compared to vacuum at low frequencies. This suppression is defined completely by the difference in the wave dispersion, which is provided finally by the polarization current in the medium.

Thus, synchrotron radiation might be treated as a coherent sum of emissions by currents produced by the particle itself and by the medium's response. The calculations based on this approach (i.e., when the two radiation fields are found separately, then their coherent sum is calculated etc.) are much more extensive, so it is much more convenient to include into the study the respective wave dispersion relation in the medium from the very beginning. Accordingly, synchrotron radiation is always regarded in the literature as a kind of intrinsic emission by a particle rotating in a magnetic field. It is important to bear in mind that the physical reason for the emission modification in media is the medium response.

Similarly, VCR is the intrinsic emission by a particle moving rectilinearly with constant velocity. The medium response is the physical reason for the difference in the radiation intensity in vacuum and medium. The difference appears to be most prominent for subliminal particles, which do not radiate in vacuum while generating non-zero VCR in media.

We should note as well that both synchrotron emission and VCR are not associated with momentum transfer between the particle and the medium, the microscopic state of the medium does not change, so the medium plays a 'passive' role. Contrarily, to produce transition radiation the medium receives momentum from the fast particle, which is the basic difference between transition radiation and VCR.

1.2 Coherence effects in electromagnetic emission by fast particles in a medium

Let us discuss the mechanisms of coherent emission in a medium in more detail because the coherence effects are very important to generate transition radiation. Generally, many particles are necessary to provide the coherence.

Radiation is known to be incoherent if its intensity is proportional to the number of particles, while for coherent radiation this dependence is nonlinear. Note that for radiation of fast particles in a medium there are various groups of particles: fast particles, background particles, electrons in an atom (or in a Debye sphere), particles in a coherent volume, etc. Hence, the same radiation may be coherent with respect to one group of particles and incoherent with respect to another one.

For simplicity, let us start with the ideal case of one fast particle moving in a medium. Both intrinsic emission by the particle and emission by the medium may be coherent *with respect to background particles* under certain conditions.

A relativistic electron moving in a monocrystal produces the well-known *coherent bremsstrahlung* (*CB*). The coherence is associated here with the order in atom positions [4, 9, 10]. There is a so-called long-range order in the ideal infinite monocrystal, i.e., atom sites are strictly correlated for any long distance.

Order in particle positions at macroscopic distances may also arise in plasma and amorphous condensed matter [11, 12]. Such order may occur in cases of random inhomogeneities in a medium (plasma turbulence), propagation of acoustic waves or for man-made structures (a pile of plates from different materials). However, the correlation is of statistical nature here, the particles are ordered locally (within the respective correlation length), differently than in a monocrystal.

Macroscopic inhomogeneities in a medium may have a substantial effect on the generation of bremsstrahlung by relativistic particles and lead to extra coherent bremsstrahlung besides the Bethe–Heitler incoherent component. While the emitted wavelength is much less than the scales of the inhomogeneities, the coherence is provided by the smallness of the longitudinal momentum transferred to the medium by the relativistic particle. As a result, the radiation at a frequency ω is produced over a length of order

$$l_c \approx \frac{2c\gamma^2/\omega}{1+\omega_p^2\gamma^2/\omega^2}\,, \tag{1}$$

which can reach a macroscopic value. Here γ is the Lorentz factor of the particle, ω_p is the plasma frequency. The presence of density inhomogeneities of the same or less size, in which the positions of electrons and nuclei are correlated, results in the extra contribution to bremsstrahlung by relativistic particles, CB.

Emission by the medium may be both coherent and incoherent as well. The emission is incoherent if all background electrons radiate independently from each other. For the medium in thermodynamic equilibrium this occurs at rather high frequencies $\omega > c/R$ (where R is the atom radius or Debye screening radius), because the formation zone here is of about the wavelength c/ω, while the correlation length in the medium is R. At lower frequencies, $\omega < c/R$, all electrons in the atom (or within the Debye sphere in a plasma) radiate coherently, hence, the radiation intensity is proportional to the square of the number of atomic electrons. In a partly ionized plasma there are two typical scales, where the positions (and motion) of electrons are correlated: the atom radius R_a and the Debye radius R_D). Hence, all the atomic electrons radiate coherently at $c/R_D < \omega < c/R_a$, while for $\omega < c/R_D$ the coherent emission is produced by the electrons in the Debye sphere, where number of them may be much larger.

Emission by a thermodynamically equilibrium medium (or by individual atoms) excited by a fast particle has received

various names in the literature: dynamic bremsstrahlung, transition bremsstrahlung, polarization bremsstrahlung [5]. Historically, the first name came into being when considering atomic media (or individual atoms); the second appeared when the same processes were considered in plasma. The third name is a kind of 'unifying' term, which emphasizes the fundamental importance of the medium's dynamic polarizability in all radiative processes of this type.

Actually, we regard the term 'bremsstrahlung' in the names as senseless because particle deceleration is unnecessary for this emission mechanism. It would be more appropriate to refer to this radiation as just 'polarization radiation' (or transition radiation on thermodynamically equilibrium inhomogeneities). Nevertheless, this paper keeps up the accepted traditional terminology.

Then, one more coherent effect takes place if there are macroscopic inhomogeneities of a size l in the medium (in other words, the positions of background particles are correlated at macroscopic scales), if $|\mathbf{q}-\mathbf{k}| \sim 2\pi l^{-1}$. Here, all background electrons located in a coherent volume (which is much larger than the Debye volume) produce the coherent radiation. This type of radiation we call transition radiation in a medium with inhomogeneities (or, for brevity, just transition radiation).

To proceed from the models of elementary emission mechanisms to the real conditions of electromagnetic wave generation, we note that an ensemble of fast particles is usually present rather than a single one. Obviously, this modifies both the intrinsic radiation generated by fast particles and the radiation produced by a medium due to integration over the fast particle spectrum. Besides, new (collective) effects appear.

If particles are arranged within bunches with a size of about radiated wave length, the resulting radiation is proportional to the square (instead of the first power) of the number of fast particles in the bunch. The case, when the bunching is produced by the radiation itself and gives rise to radiation amplification (the maser effect) is of special interest. According to the underlying microscopic seed emission mechanism, *cyclotron maser*, *transition maser*, *plasma* emission, etc. can be produced.

Let us briefly consider the methods for theoretical treatment of the transition radiation. Since background electrons generate the transition radiation, it can be calculated if the electric current produced by the electrons is known. The current depends on both the fast particle field and the background particle spatial distribution, and can be found, for example, from the kinetic equation. Sections 2 and 3 apply this approach to detailed study of the transition radiation in media with random non-thermal inhomogeneities.

The same process can be treated as scattering of the quasi-stationary field of the fast particle by the inhomogeneities. This approach reveals the tight similarity between light scattering in a medium and the transition radiation. The analogy with light scattering and the respective formalism appear to be most convenient for the study of emission in thermodynamically equilibrium media (polarization bremsstrahlung, Section 4).

Finally, the formulae of transition radiation in a medium with macroscopic inhomogeneities can be derived from the formulae of polarization bremsstrahlung per atom or background ion by direct summing of radiation fields, their squaring, and subsequent averaging [11]. The coherent nature of the transition radiation is most pronounced in such an approach, since the non-diagonal terms ($i \neq j$) of the formed double sum contribute the bulk to the radiation intensity and the result can be expressed by a pair (two-point) correlator of the particle positions. The respective contribution vanishes in the absence of the macroscopic inhomogeneities.

At least one more way is discussed in the literature to calculate transition radiation, the mean-field reaction method [13–15]. This method is based on the tensor of an effective dielectric permeability [16–18] and is only valid for small-scale inhomogeneities [19] with a size l much less than the formation zone of radiation l_c [see Eqn (1)]. This paper does not use this approach because a broad spectrum of inhomogeneities (with the scales l both less and larger than l_c) is assumed to exist in the medium.

The papers [20, 21] use the tensor of an effective dielectric permeability to calculate the transition radiation by particles moving in a plasma with strong inhomogeneities modeled by parallel narrow infinitely long cylinders ($a \ll l_c$, where a is the radius of the cylinder). Other aspects of the transition radiation in a medium with random inhomogeneities are discussed in papers [22–25] (for transition radiation of acoustic waves see, for example, Refs [26, 27]) and monographs [4, 5, 10, 28] (also see references there).

The paper is arranged as follows. Section 2 considers the emission by relativistic particles. The respective theory is valid for any matter because the plasma dielectric permeability is universal at high frequencies. Section 3 studies the transition radiation of particles with arbitrary energy, particularly, close to plasma eigen frequencies. Section 4 describes the transition radiation generated in thermodynamically equilibrium media and Section 5 applies the theory to various astrophysical conditions.

2. Transition radiation by relativistic particles in magnetized plasma with random inhomogeneities

2.1 Theory of transition radiation by a particle moving along a curve

Let us consider transition radiation generated by a particle moving curvilinearly [19]. TR originates over a length called the coherence length or formation zone, which is described by Eqn (1) in the case of a rectilinearly moving particle. The bulk of energy at frequency ω is emitted within a narrow cone along the velocity vector with the angle

$$\theta_c \approx \left(\gamma^{-2} + \frac{\omega_p^2}{\omega^2}\right)^{1/2}. \qquad (2)$$

The radiation at frequency ω arises due to the interaction of the relativistic particle field with the inhomogeneities of scales $k^{-1} \sim l_c(\omega)$ if density inhomogeneities with a broad spectrum exist in the plasma. The velocity direction is assumed to change by the angle θ_c over a length $l' \ll l_c(\omega)$ for the chosen particle trajectory. Then the TR spectrum is formed over the small length l' due to the high directivity of radiation. Hence, the interaction between the relativistic particle field and the inhomogeneities of scales $k^{-1} \sim l_c(\omega) \gg l'$ (forming TR at the frequency ω) becomes weaker, which results in TR suppression.

Let us deduce general equations for transition radiation by a relativistic particle moving along an arbitrary path. The

energy emitted by the relativistic particle current $\mathbf{j}^{Q}_{\omega,\mathbf{k}}$ might be expressed as [10]

$$\mathcal{E}_{\mathbf{n},\omega} = (2\pi)^4 \int \mathbf{j}^{Q*}_{\omega,\mathbf{k}} \cdot \mathbf{E}_{\omega,\mathbf{k}} k^2 \, \mathrm{d}k \,, \tag{3}$$

where $\mathbf{E}_{\omega,\mathbf{k}}$ is the field produced by the current $\mathbf{j}^{Q}_{\omega,\mathbf{k}}$ in the medium, if the exact Green function for photon propagation in the medium is known. Equation (3) contains all types of emission provided by both curvature of trajectory and response of medium. The Green function can be found approximately (within the geometrical optics approximation) for some inhomogeneous media, e.g., for periodic media [4]. Respectively, Eqn (3) can be applied to calculate resonant radiation. However, the Green function is unknown for media with random inhomogeneities. We calculate TR approximately based on the perturbation theory.

Let us expand the electric field in a series over the magnitude of inhomogeneities

$$\mathbf{E}_{\omega,\mathbf{k}} = \mathbf{E}^{(0)}_{\omega,\mathbf{k}} + \mathbf{E}^{(1)}_{\omega,\mathbf{k}} + \mathbf{E}^{(2)}_{\omega,\mathbf{k}} \ldots \tag{4}$$

that corresponds to the expansion of electric current in the medium:

$$\mathbf{j}_{\omega,\mathbf{k}} = \mathbf{j}^{(0)}_{\omega,\mathbf{k}} + \mathbf{j}^{(1)}_{\omega,\mathbf{k}} + \mathbf{j}^{(2)}_{\omega,\mathbf{k}} \ldots \tag{5}$$

Then the total emitted energy (3) takes the form

$$\begin{aligned}\mathcal{E}_{\mathbf{n},\omega} = (2\pi)^4 \,\mathrm{Re} \int \big(& \mathbf{j}^{Q*}_{\omega,\mathbf{k}} \cdot \mathbf{E}^{(0)}_{\omega,\mathbf{k}} + \langle \mathbf{j}^{*(1)}_{\omega,\mathbf{k}} \cdot \mathbf{E}^{(1)}_{\omega,\mathbf{k}} \rangle \\ & + \mathbf{j}^{Q*}_{\omega,\mathbf{k}} \cdot \langle \mathbf{E}^{(2)}_{\omega,\mathbf{k}} \rangle + \langle \mathbf{j}^{*(2)}_{\omega,\mathbf{k}} \rangle \cdot \mathbf{E}^{(0)}_{\omega,\mathbf{k}} \big) k^2 \, \mathrm{d}k \,. \end{aligned} \tag{6}$$

The first term in Eqn (6) is the intrinsic radiation, while TR is connected with other terms quadratic over the density inhomogeneities $\delta N_{\omega,\mathbf{k}}$. The broken brackets denote averaging over the inhomogeneity spectrum, all terms linear over $\delta N_{\omega,\mathbf{k}}$ disappear due to the averaging. The vectors $\mathbf{j}^{Q*}_{\omega,\mathbf{k}}$ and $\mathbf{E}^{(0)}_{\omega,\mathbf{k}}$ are out of the averaging brackets in Eqn (6) because they do not depend on $\delta N_{\omega,\mathbf{k}}$.

The Maxwell equations provide us with the relation between the transverse electric field and its source (the respective electric current):

$$(c^2k^2 - \omega^2) E^{i}_{\omega,\mathbf{k}} = 4\pi \mathrm{i}\omega \left(\delta_{ij} - \frac{k_i k_j}{k^2} \right) j^{j}_{\omega,\mathbf{k}} \,. \tag{7}$$

It is important that we use here the microscopic (vacuum) Maxwell equations, hence the current $j^{j}_{\omega,\mathbf{k}}$ is the total current in the medium consisting from both the current of the fast particle and current of background particles (in particular, the usual medium response providing the dielectric permeability). Substitution of Eqns (4), (5) into Eqn (7) yields

$$\begin{aligned}(c^2k^2 - \omega^2) & \big(E^{i(0)}_{\omega,\mathbf{k}} + E^{i(1)}_{\omega,\mathbf{k}} + E^{i(2)}_{\omega,\mathbf{k}} + \ldots \big) \\ & = 4\pi \mathrm{i}\omega \left(\delta_{ij} - \frac{k_i k_j}{k^2} \right) \big(j^{j(0)}_{\omega,\mathbf{k}} + j^{j(1)}_{\omega,\mathbf{k}} + j^{j(2)}_{\omega,\mathbf{k}} + \ldots \big) \,. \end{aligned} \tag{8}$$

Within the perturbation theory, the field $E^{i(0)}_{\omega,\mathbf{k}}$ is defined by the current $j^{j(0)}_{\omega,\mathbf{k}}$, the field $E^{i(1)}_{\omega,\mathbf{k}}$ is defined by the current $j^{j(1)}_{\omega,\mathbf{k}}$, which is expressed through the field $E^{i(0)}_{\omega,\mathbf{k}}$ by means of kinetic equation, etc. Thus, we have found the complete scheme for calculating the fields and currents in any order of perturbation.

It is important to note that the denominator of the right-hand side of Eqn (8) contains repeatedly the difference $c^2k^2 - \omega^2$ (or $c^2k^2 - \omega^2\varepsilon$ if taking into account the linear response of unperturbed plasma). The difference vanishes for eigen waves of the medium, e.g., for the usual transverse electromagnetic waves, which results in divergence of expressions for $E^{i(1)}_{\omega,\mathbf{k}}$, $E^{i(2)}_{\omega,\mathbf{k}}$, etc. Thus, the perturbation theory is only valid for the quasi-stationary component of the electric field, when $c^2k^2 - \omega^2\varepsilon$ does not vanish. The electric field of a rectilinearly moving particle is quasi-stationary entirely (if the Vavilov–Cherenkov condition is not satisfied; see Section 4.3) and the perturbation theory can be properly applied to the entire field [28]. The situation is more complicated for motion with acceleration. The particle's field consists here of two components: the field of radiation and the intrinsic quasi-stationary field; the perturbation theory is only valid for the second.

To find the current arising when a relativistic particle is moving in a plasma with random inhomogeneities we apply the kinetic equation [28]:

$$f_{\omega,\mathbf{k}}(\mathbf{p}) = \frac{e}{\mathrm{i}\omega} \int \mathbf{E}_{\omega-\omega',\mathbf{k}-\mathbf{k}'} \frac{\partial}{\partial \mathbf{p}} f_{\omega',\mathbf{k}'}(\mathbf{p}) \, \mathrm{d}\omega' \, \mathrm{d}\mathbf{k}' \,, \tag{9}$$

where e is the charge of an electron. Solution of the equation using the perturbation theory taking into account the electric field expansion (4) provides corrections to the undisturbed distribution function:

$$f^{(0)}_{\omega,\mathbf{k}}(\mathbf{p}) = f(\mathbf{p}) \delta(\omega) \delta(\mathbf{k}) \,, \tag{10}$$

$$f^{(1)}_{\omega,\mathbf{k}}(\mathbf{p}) = \frac{e\mathbf{E}^{(0)}_{\omega,\mathbf{k}}}{\mathrm{i}\omega} \frac{\partial f(\mathbf{p})}{\partial \mathbf{p}} + \delta f_{\omega,\mathbf{k}}(\mathbf{p}) \;\; \text{etc.}, \tag{11}$$

where $f(\mathbf{p})$ is normalized by the background particle number density N, and the correction $\delta f_{\omega,\mathbf{k}}$ describes the density inhomogeneities:

$$\int f(\mathbf{p}) \frac{\mathrm{d}\mathbf{p}}{(2\pi)^3} = N_0 \,, \qquad \int \delta f_{\omega,\mathbf{k}}(\mathbf{p}) \frac{\mathrm{d}\mathbf{p}}{(2\pi)^3} = \delta N_{\omega,\mathbf{k}} \,. \tag{12}$$

The expressions $f^{(i)}_{\omega,\mathbf{k}}$ allow calculation of the respective plasma currents using the well-known formula:

$$\mathbf{j}_{\omega,\mathbf{k}} = e \int \mathbf{v} f_{\omega,\mathbf{k}}(\mathbf{p}) \frac{\mathrm{d}\mathbf{p}}{(2\pi)^3} \,. \tag{13}$$

The integration yields

$$\mathbf{j}^{(0)}_{\omega,\mathbf{k}} = \mathbf{j}^{Q}_{\omega,\mathbf{k}} + \frac{\mathrm{i}e^2 N}{m\omega} \mathbf{E}^{(0)}_{\omega,\mathbf{k}} \big[\Theta(\omega - \mathbf{k}\mathbf{v}) + \Theta(\mathbf{k}\mathbf{v} - \omega) \big] \,, \tag{14}$$

$$\begin{aligned}\mathbf{j}^{(1)}_{\omega,\mathbf{k}} = {} & \frac{\mathrm{i}e^2 N}{m\omega} \mathbf{E}^{(1)}_{\omega,\mathbf{k}} + \frac{\mathrm{i}e^2}{m\omega} \int \mathbf{E}^{(0)}_{\omega-\omega_1,\mathbf{k}-\mathbf{k}_1} \delta N_{\omega_1,\mathbf{k}_1} \\ & \times \Theta\big[\omega - \omega_1 - (\mathbf{k} - \mathbf{k}_1)\mathbf{v}\big] \, \mathrm{d}\omega_1 \, \mathrm{d}\mathbf{k}_1 \\ & + \frac{\mathrm{i}e^2}{m\omega} \int \mathbf{E}^{(0)}_{\omega-\omega_1,\mathbf{k}-\mathbf{k}_1} \delta N_{\omega_1,\mathbf{k}_1} \Theta\big[(\mathbf{k} - \mathbf{k}_1)\mathbf{v} - (\omega - \omega_1)\big] \, \mathrm{d}\omega_1 \, \mathrm{d}\mathbf{k}_1 , \end{aligned} \tag{15}$$

$$\mathbf{j}^{(2)}_{\omega,\mathbf{k}} = \frac{\mathrm{i}e^2 N}{m\omega} \mathbf{E}^{(2)}_{\omega,\mathbf{k}} + \frac{\mathrm{i}e^2}{m\omega} \int \mathbf{E}^{(1)}_{\omega-\omega_2,\mathbf{k}-\mathbf{k}_2} \delta N_{\omega_2,\mathbf{k}_2} \, \mathrm{d}\omega_2 \, \mathrm{d}\mathbf{k}_2 \,. \tag{16}$$

In expression (14) the electric field is artificially split into two components: $\mathbf{E}^{(0)}_{\omega,\mathbf{k}} \Theta(\omega - \mathbf{k}\mathbf{v})$ and $\mathbf{E}^{(0)}_{\omega,\mathbf{k}} \Theta(\mathbf{k}\mathbf{v} - \omega)$, where $\Theta(x)$ is the unit step function, and m is the mass of the

electron. Since $\Theta(x)+\Theta(-x)\equiv 1$, the splitting does not affect Eqn (14) itself, but this allows us to consider separately the radiation field $\Theta(\omega-\mathbf{kv})$ and the quasi-stationary field $\Theta(\mathbf{kv}-\omega)$ in Eqn (8).

Paper [19] studies all four terms in Eqn (6) in detail. The two last terms are found to vanish in a randomly inhomogeneous medium, while the first term is the intrinsic radiation by relativistic particle modified by the density inhomogeneities. The transition radiation is described entirely by the second term (i.e., the intrinsic radiation and the transition radiation can be treated separately within the perturbation theory). Thus, the finding of the first (linear) corrections to the field and current in the medium is sufficient to calculate the transition radiation. Equation (8) reads within this approximation:

$$(c^2k^2-\omega^2)(E^{i(0)}_{\omega,\mathbf{k}}+E^{i(1)}_{\omega,\mathbf{k}})=4\pi\mathrm{i}\omega\left(\delta_{ij}-\frac{k_ik_j}{k^2}\right)\times\left\{j^{Qj}_{\omega,\mathbf{k}}+\frac{\mathrm{i}e^2N}{m\omega}(E^{(0)j}_{\omega,\mathbf{k}}+E^{(1)j}_{\omega,\mathbf{k}})+\frac{\mathrm{i}e^2}{m\omega}\int E^{(0)j}_{\omega-\omega_1,\mathbf{k}-\mathbf{k}_1}\delta N_{\omega_1,\mathbf{k}_1}\times\Theta\big[(\mathbf{k}-\mathbf{k}_1)\mathbf{v}-(\omega-\omega_1)\big]\,\mathrm{d}\omega_1\,\mathrm{d}\mathbf{k}_1\right\}. \quad (17)$$

The linear in electric field terms $(\mathrm{i}e^2N/m\omega)E^j_{\omega,\mathbf{k}}$ correspond to the polarization response of undisturbed plasma. They provide the actual wave dispersion relation in the medium. Indeed, the transfer of the terms into the left-hand side of Eqn (17) replaces $(c^2k^2-\omega^2)$ by $(c^2k^2-\omega^2\varepsilon)$, where

$$\varepsilon=1-\frac{\omega_{\mathrm{pe}}^2}{\omega^2}\,. \quad (18)$$

This expression for plasma dielectric permeability is correct in magnetized plasma if

$$\frac{\omega}{\omega_{B\mathrm{e}}}\gg 1 \quad (19)$$

that is assumed to be fulfilled when considering the effect of the trajectory curvature ($\omega_{B\mathrm{e}}$ is the electron gyrofrequency); the effects of plasma gyrotropy are analyzed separately.

The relations between fields and currents in the respective orders of the perturbation theory can now be written as

$$E^{(0)i}_{\omega,\mathbf{k}}=G^{\mathrm{t}}_{ij}(\omega,\mathbf{k})j^{Qj}_{\omega,\mathbf{k}}\,, \quad (20)$$

$$E^{(1)i}_{\omega,\mathbf{k}}=G^{\mathrm{t}}_{ij}(\omega,\mathbf{k})j^{(1)j}_{\omega,\mathbf{k}}\,, \quad (21)$$

$$j^{(1)j}_{\omega,\mathbf{k}}=\frac{\mathrm{i}e^2}{m\omega}\int E^{(0)j}_{\omega-\omega_1,\mathbf{k}-\mathbf{k}_1}\delta N_{\omega_1,\mathbf{k}_1}\times\Theta\big[(\mathbf{k}-\mathbf{k}_1)\mathbf{v}-(\omega-\omega_1)\big]\,\mathrm{d}\omega_1\,\mathrm{d}\mathbf{k}_1\,, \quad (22)$$

where

$$G^{\mathrm{t}}_{ij}(\omega,\mathbf{k})=\frac{4\pi\mathrm{i}\omega}{c^2k^2-\omega^2\varepsilon}\left(\delta_{ij}-\frac{k_ik_j}{k^2}\right) \quad (23)$$

is the transverse Green function in the medium.

Integration of the second term in Eqn (6) over $\mathrm{d}k$ yields the energy of transition radiation

$$\mathcal{E}^{\mathrm{tr}}_{\mathbf{n},\omega}=(2\pi)^6\,\frac{\omega^2}{c^3}\left\langle|\mathbf{n}\times\mathbf{j}^{(1)}_{\omega,\mathbf{k}}|^2\right\rangle, \quad (24)$$

where $\mathbf{n}$ is the unit vector in the direction of emission, and the current $\mathbf{j}^{(1)}_{\omega,\mathbf{k}}$ is defined by Eqn (22). The electric field $E^{(0)i}_{\omega,\mathbf{k}}$ is defined by the relativistic particle current $\mathbf{j}^{Q}_{\omega,\mathbf{k}}$ that is expressed from its velocity $\mathbf{v}(t)$ and trajectory $\mathbf{r}(t)$:

$$\mathbf{j}^{Q}_{\omega,\mathbf{k}}=Q\int\mathbf{v}(t)\exp\big[-\mathrm{i}\mathbf{kr}(t)+\mathrm{i}\omega t\big]\,\frac{\mathrm{d}t}{(2\pi)^4}\,, \quad (25)$$

where Q is the charge of the relativistic particle.

Further transformations, namely, substitution of Eqns (25) and (23) into Eqn (20), then of Eqn (20) into Eqn (22) and of Eqn (22) into Eqn (24), and the averaging of the obtained expression over random phases of the inhomogeneities by means of

$$\langle\delta N_{\omega_1,\mathbf{k}_1}\delta N^*_{\omega_2,\mathbf{k}_2}\rangle=|\delta N|^2_{\omega_1,\mathbf{k}_1}\delta(\omega_1-\omega_2)\delta(\mathbf{k}_1-\mathbf{k}_2)\,, \quad (26)$$

where $|\delta N|^2_{\omega_1,\mathbf{k}_1}$ is the spectrum of inhomogeneities, yield

$$\mathcal{E}^{\mathrm{tr}}_{\mathbf{n},\omega}=\frac{4Q^2e^4}{m^2c^3\omega^2}\int_V\mathrm{d}\mathbf{k}_1\int_{-\infty}^{\infty}\mathrm{d}t\,\mathrm{Re}\int_{-\infty}^{\infty}\mathrm{d}\tau\times\big[\mathbf{n}\times\mathbf{v}(t)\big]\big[\mathbf{n}\times\mathbf{v}(t+\tau)\big]\times\frac{|\delta N|^2_{\mathbf{k}_1}\exp\big\{\mathrm{i}\omega\tau-\mathrm{i}(\mathbf{k}-\mathbf{k}_1)\big[\mathbf{r}(t+\tau)-\mathbf{r}(t)\big]\big\}}{\big[1-(\mathbf{k}-\mathbf{k}_1)^2c^2/\omega^2\varepsilon(\omega)\big]^2}\,. \quad (27)$$

Here we assume the inhomogeneities to be quasi-static, $|\delta N|^2_{\omega,\mathbf{k}}=|\delta N|^2_{\mathbf{k}}\delta(\omega)$, and the symbol V indicates that the integration over $\mathrm{d}\mathbf{k}_1$ should be performed over the region $\omega-(\mathbf{k}-\mathbf{k}_1)\mathbf{v}\leqslant 0$ that corresponds to the quasi-stationary particle field.

2.2 Suppression of transition radiation by a magnetic field

Let us assume the curvature of the particle path to be caused by a uniform magnetic field $\mathbf{B}$ [19, 29]. Then $l'=l_{\mathrm{s}}=Mc^2/QB_\perp=c/\omega_{B_\perp}$, where $\omega_{B_\perp}=QB_\perp/Mc$ is the gyrofrequency of the particle; the largest value of $l_{\mathrm{c}}(\omega)$ (1) is achieved at $\omega=\omega_{\mathrm{p}}\gamma$: $l_{\mathrm{c}}^{\max}=c\gamma/\omega_{\mathrm{p}}$. Hence, the condition $l'\ll l_{\mathrm{c}}$ receives the form:

$$\gamma\gg\gamma^*=\frac{\omega_{\mathrm{p}}}{\omega_{B_\perp}}\,. \quad (28)$$

Thus, the rotation of the particle in a magnetic field is important when Eqn (28) is fulfilled and gives rise to TR suppression in this region of parameters.

Let us calculate the transition radiation produced by a relativistic particle rotating in a magnetic field in plasma with random density inhomogeneities. First of all, we substitute the standard expressions of the particle path $\mathbf{r}(t)$ and velocity $\mathbf{v}(t)$ into Eqn (27) [30]. The formation zone is much less than the Larmor radius of an ultra-relativistic particle, so the arguments of trigonometric functions in $\mathbf{r}(t)$ and $\mathbf{v}(t)$ are small, $\omega_{B_\perp}\tau/\gamma\ll 1$. This allows the expansion off the sine and cosine in a series over the powers of the small value $\omega_{B_\perp}\tau/\gamma$. This expansion should keep the next terms after the linear ones to take properly into account the difference between the actual particle path and a rectilinear trajectory:

$$\mathbf{v}(t)=\mathbf{n}v\left(1-\frac{\theta^2}{2}\right)+\boldsymbol{\theta}v\,,\quad \mathbf{v}(t+\tau)=\mathbf{v}(t)+v[\mathbf{n}\times\boldsymbol{\Omega}]\tau\,, \quad (29)$$

$$\mathbf{r}(t+\tau)-\mathbf{r}(t)=\mathbf{v}(t)\tau-v[\mathbf{n}\times\boldsymbol{\Omega}]\frac{\tau^2}{2}+v[\boldsymbol{\Omega}\times\boldsymbol{\theta}]\frac{\tau^2}{2}-v\big[\boldsymbol{\Omega}\times[\mathbf{n}\times\boldsymbol{\Omega}]\big]\frac{\tau^3}{6}\,, \quad (30)$$

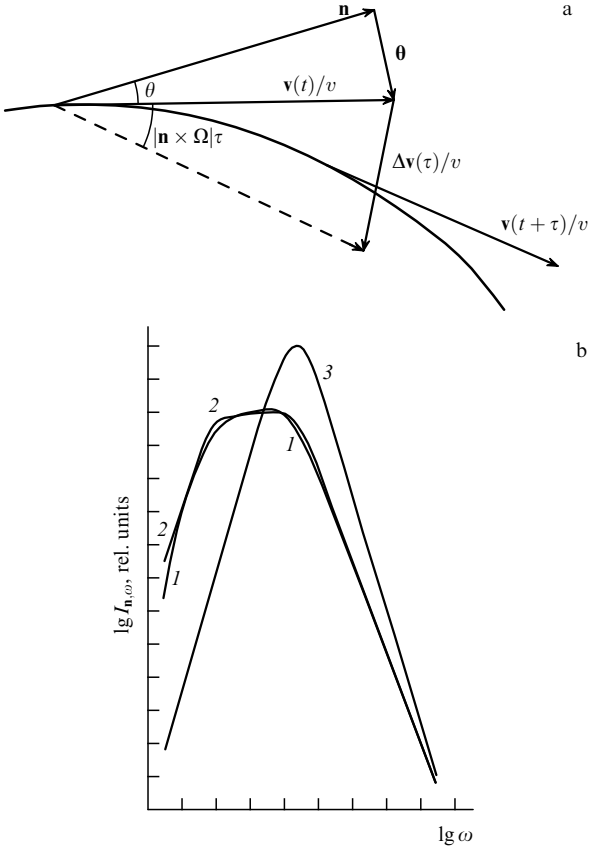

Figure 2. (a) Definition of the vectors $\mathbf{\theta}$, $\mathbf{n}$, $\mathbf{v}/v$, $\Delta\mathbf{v}/v$ and the angles θ and $|\mathbf{n}\times\mathbf{\Omega}|\tau$. (b) Spectral-angular distribution of transition radiation in a fixed direction ($\theta\sim\gamma^{-1}$) with the presence of a magnetic field: (*1*) numerical calculations by Eqn (36), (*2*) asymptotic forms (43), (45), (*3*) the dependence without the magnetic field.

where $\mathbf{\Omega}=Q\mathbf{B}/Mc\gamma$, the length of two-dimensional vector $\mathbf{\theta}$ is equal to the angle between $\mathbf{n}$ and $\mathbf{v}(t)$, see Fig. 2a. This approach is widely used for calculating synchrotron radiation [31].

Let us proceed further to the radiation energy per unit time (the radiation intensity) instead of the total emitted energy. Substitution of Eqns (29), (30) into Eqn (27) omitting the outer integration over the time $\mathrm{d}t$ yields

$$I_\omega^{\mathrm{tr}}=\frac{2\pi Q^2e^4}{m^2c^3}\int \mathrm{d}\mathbf{\theta}'\int\frac{\mathrm{d}\mu\,\mathrm{d}k_1\,|\delta N|^2_{\mathbf{k}_1}}{\mu^2}\,\mathrm{Re}\int_{-\infty}^{\infty}\mathrm{d}\tau \times\left([\mathbf{n}\times\mathbf{\theta}']^2+\mathbf{\theta}'[\mathbf{n}\times\mathbf{\Omega}]\tau\right)\exp\left\{\mathrm{i}\left[\omega-(\mathbf{k}-\mathbf{k}_1)\mathbf{v}\right]\tau -\mathrm{i}\omega\mathbf{\theta}'[\mathbf{n}\times\mathbf{\Omega}]\,\frac{\tau^2}{2}+\mathrm{i}\omega[\mathbf{n}\times\mathbf{\Omega}]^2\frac{\tau^3}{6}\right\}, \tag{31}$$

where $\mu=\cos\vartheta=\mathbf{k}\mathbf{k}_1/kk_1$.

This formula (31) represents the radiation I_ω^{tr} into the full solid angle, which is time-independent. Contrarily, the emission into any particular direction reveals itself as short repetitive pulses like for synchrotron radiation [31]. Integration of Eqn (31) is easy to perform by substitution of the variable $\mathbf{\theta}'=\mathbf{\theta}+[\mathbf{n}\times\mathbf{\Omega}]\tau$. The substitution does not affect the limits of integration over $\mathrm{d}\mathbf{\theta}$, because rapid convergence of the integral allows integration over the angle within infinite limits:

$$I_\omega^{\mathrm{tr}}=\frac{2\pi Q^2e^4}{m^2c^3}\int \mathrm{d}\mathbf{\theta}\int\frac{\mathrm{d}\mu\,\mathrm{d}k_1\,|\delta N|^2_{\mathbf{k}_1}}{\mu^2}\,\mathrm{Re}\int_{-\infty}^{\infty}\mathrm{d}\tau \times\left(\theta^2+2\mathbf{\theta}[\mathbf{n}\times\mathbf{\Omega}]\tau+\frac{3}{4}\,[\mathbf{n}\times\mathbf{\Omega}]^2\tau^2\right) \times\exp\left[\frac{\mathrm{i}\omega\tau}{2}\left(\gamma^{-2}+\frac{\omega_{\mathrm{p}}^2}{\omega^2}+\theta^2+\frac{2\mathbf{k}_1\mathbf{v}}{\omega}\right)+\mathrm{i}\omega\,\frac{\omega_{B_\perp}^2\tau^3}{24\gamma^2}\right]. \tag{32}$$

The inner integral can be expressed with the Airy function $\mathrm{Ai}(\xi)$. The substitution $x=(\omega\omega_{B_\perp}^2/\gamma^2)^{1/3}\tau/2$ together with the account of $\mathrm{Ai}''(\xi)=\xi\,\mathrm{Ai}(\xi)$ and that $\mathrm{Ai}'(\xi)$ gives no real contribution [the function $\mathrm{Ai}(\xi)$ is normalized to unity] yields

$$I_\omega^{\mathrm{tr}}=\frac{8\pi^2Q^2e^4}{\omega m^2c^3}\left(\frac{\omega\gamma}{\omega_{B_\perp}}\right)^{2/3}\int\mathrm{d}\mathbf{\theta}\int\frac{\mathrm{d}\mu\,\mathrm{d}k_1\,|\delta N|^2_{\mathbf{k}_1}}{\mu^2} \times\left[\theta^2-3\left(\frac{\omega_{B_\perp}}{\omega\gamma}\right)^{2/3}\xi\right]\mathrm{Ai}(\xi)\,, \tag{33}$$

where

$$\xi=\left(\gamma^{-2}+\frac{\omega_{\mathrm{p}}^2}{\omega^2}+\theta^2+\frac{2\mathbf{k}_1\mathbf{n}c}{\omega}\right)\left(\frac{\omega\gamma}{\omega_{B_\perp}}\right)^{2/3}. \tag{34}$$

The integration in Eqn (33) is taken over the parameter region $\xi\leqslant 0$ that corresponds to the scattering of the quasi-stationary field of the particle.

The further calculation of transition radiation requires for the spectrum of inhomogeneities $|\delta N|^2_{\mathbf{k}_1}$ to be specified. The spectrum is assumed to be a power-law:

$$|\delta N|^2_{\mathbf{k}_1}=\frac{\nu-1}{4\pi}\,\frac{k_0^{\nu-1}\langle\Delta N^2\rangle}{k_1^{\nu+2}}\,, \tag{35}$$

where $L_0=2\pi/k_0$ is the main scale and $\langle\Delta N^2\rangle$ is the mean square of the inhomogeneities. Substituting Eqn (35) into Eqn (33) and taking into account the actual limits of integration arising from $\xi\leqslant 0$, we find:

$$I_\omega^{\mathrm{tr}}=\frac{2\pi(\nu-1)Q^2e^4k_0^{\nu-1}\langle\Delta N^2\rangle}{\omega m^2c^3}\left(\frac{\omega\gamma}{\omega_{B_\perp}}\right)^{2/3}\int\mathrm{d}\mathbf{\theta}\int_{k_{\min}}^{\infty}\frac{\mathrm{d}k_1}{k_1^{\nu+2}} \times\int_{-1}^{-k_{\min}/k_1}\frac{\mathrm{d}\mu}{\mu^2}\left[\theta^2-3\left(\frac{\omega_{B_\perp}}{\omega\gamma}\right)^{2/3}\xi\right]\mathrm{Ai}(\xi)\,, \tag{36}$$

where

$$k_{\min}(\theta)=\frac{\omega}{2c}\left(\gamma^{-2}+\theta^2+\frac{\omega_{\mathrm{p}}^2}{\omega^2}\right). \tag{37}$$

Expression (36) allows the correct limiting transition to the case of zero magnetic field. Indeed, if $\omega_{B_\perp}\to 0$ then

$$\lim_{b\to 0}\frac{\mathrm{Ai}(a/b)}{b}=\delta(a)=\delta\left[\omega-(\mathbf{k}-\mathbf{k}_1)\mathbf{v}\right], \tag{38}$$

and the integrals in Eqn (36) over $\mathrm{d}\mu$ and $\mathrm{d}k_1$ are taken easily. Thus, the intensity of transition radiation per unit frequency per unit solid angle (the spectral-angular distribution) produced by the rectilinearly moving particle is given by

(with omitting the outer integration over $\mathrm{d}\boldsymbol{\theta}$)

$$I^1_{\mathbf{n},\omega} = \frac{8\pi(\nu-1)Q^2e^4\langle\Delta N^2\rangle}{\nu cm^2\omega^3}\left(\frac{2k_0c}{\omega}\right)^{\nu-1} \times \frac{\theta^2}{(\gamma^{-2}+\theta^2+\omega_\mathrm{p}^2/\omega^2)^{\nu+2}} \tag{39}$$

in agreement with Ref. [28]. Let us discuss equation (36) in more detail. It is important to note that expression (36) omitting the outer integration over $\mathrm{d}\boldsymbol{\theta}$ cannot be interpreted as the radiation intensity into a given direction $\mathbf{n}$ for a curvilinearly moving particle. This originates from the angle θ depending on the instant direction of particle velocity, while the emission occurs over a finite (even if small) part of the particle path, so the direction of the particle velocity is changing during the emission process. This essential difference is caused by degradation of the system symmetry: the system has no axial symmetry with respect to the direction of particle velocity anymore when the particle is moving curvilinearly. Nevertheless, omitting the integral over $\mathrm{d}\boldsymbol{\theta}$ in Eqn (36) is convenient to compare the output expressions with Eqn (39).

Spectral-angular distribution of TR. The integration (36) of combinations of the Airy function with polynomials within finite limits is not easy to perform. Nevertheless, good asymptotic approximations can be found for some restricted frequency ranges.

Let us start with the condition

$$\gamma^{-2}+\frac{\omega_\mathrm{p}^2}{\omega^2} \geqslant \left(\frac{\omega_{B_\perp}}{\omega\gamma}\right)^{2/3} \tag{40}$$

that is valid in the frequency ranges

$$\omega \ll \omega_* = \omega_\mathrm{p}\left(\frac{\omega_\mathrm{p}\gamma}{\omega_{B_\perp}}\right)^{1/2}, \tag{41}$$

$$\omega \geqslant \omega_{B_\perp}\gamma^2. \tag{42}$$

The role of the path curvature is minor here, so the Airy function can be replaced by a δ function (38). However, the second term in the brackets in Eqn (36) requires account of the non-zero bandwidth of the Airy function because it dominates for $\theta \to 0$. The restricted bandwidth of $(\omega\gamma/\omega_{B_\perp})^{2/3}\mathrm{Ai}(\xi)$ allows ξ to vary effectively within the limits $-1 < \xi \leqslant 0$. Hence, we can accept, e.g., $\xi = -1/3$ for a rough estimate and then find

$$I^2_{\mathbf{n},\omega} = \frac{8\pi(\nu-1)Q^2e^4\langle\Delta N^2\rangle}{\nu cm^2\omega^3}\left(\frac{2k_0c}{\omega}\right)^{\nu-1} \times \frac{\theta^2+(\omega_{B_\perp}/\omega\gamma)^{2/3}}{(\gamma^{-2}+\theta^2+\omega_\mathrm{p}^2/\omega^2)^{\nu+2}}. \tag{43}$$

This expression differs from Eqn (39) in the only additional term $(\omega_{B_\perp}/\omega\gamma)^{2/3}$ in the numerator, which has little effect on the intensity of emission into the full solid angle under conditions (41), (42).

For the other case, $\gamma^{-2}+\omega_\mathrm{p}^2/\omega^2 \ll (\omega_{B_\perp}/\omega\gamma)^{2/3}$, or

$$\omega_* \ll \omega \ll \omega_{B_\perp}\gamma^2, \tag{44}$$

the path curvature is essential, the argument of the Airy function occurs to be small effectively: $|\xi| \ll 1$ (due to rapid convergence of the integral over $\mathrm{d}k_1$). This allows us to expand $\mathrm{Ai}(\xi)$ into a series and keep only the first term of the expansion $\mathrm{Ai}(\xi) \approx \mathrm{Ai}(0) = 1/[3^{2/3}\Gamma(2/3)]$. Then, the integration over $\mathrm{d}\mu$ and $\mathrm{d}k_1$ is easy to perform:

$$I^3_{\mathbf{n},\omega} = \frac{24\pi(\nu-1)}{\nu^2(\nu+1)}\frac{Q^2e^4\langle\Delta N^2\rangle\,\mathrm{Ai}(0)}{cm^2\omega^3} \times \frac{(2k_0c/\omega)^{\nu-1}(\omega\gamma/\omega_{B_\perp})^{2/3}}{(\gamma^{-2}+\theta^2+\omega_\mathrm{p}^2/\omega^2)^{\nu+2}} \times \left[1+\frac{\nu\theta^2}{3(\gamma^{-2}+\theta^2+\omega_\mathrm{p}^2/\omega^2)^{\nu+2}}\right]. \tag{45}$$

It is important to note that the possibility of replacement of the Airy function $\mathrm{Ai}(\xi)$ by $\mathrm{Ai}(0)$ implies an essential change in the nature of the transition radiation. In particular, the interaction between the particle and the inhomogeneities loses its resonant character that was ensured by the δ function $\delta[\omega-(\mathbf{k}-\mathbf{k}_1)\mathbf{v}]$ for a rectilinearly moving particle.

According to Eqn (45), the intensity of transition radiation decreases when the magnetic field increases: $I^3_{\mathbf{n},\omega} \propto \omega_{B_\perp}^{-2/3}$ in contrast to what occurs for synchrotron radiation. Thus, suppression of transition radiation by the magnetic field takes place. Figure 2b displays both the asymptotic forms (43), (45) and the respective curve obtained from Eqn (36) numerically. The dependence (39) for zero magnetic field is plotted as well.

Spectral distribution of TR. Integrating Eqns (43), (45) over the angles, we find the spectral distributions of transition radiation in the respective frequency ranges:

$$I^2_\omega = \frac{8\pi^2(\nu-1)}{\nu^2(\nu+1)}\frac{Q^2e^4\langle\Delta N^2\rangle}{cm^2\omega^3}\left(\frac{2k_0c}{\omega}\right)^{\nu-1}\left(\gamma^{-2}+\frac{\omega_\mathrm{p}^2}{\omega^2}\right)^{-\nu} \times \left[1+\frac{\nu(\omega_{B_\perp}/\omega\gamma)^{2/3}}{\gamma^{-2}+\omega_\mathrm{p}^2/\omega^2}\right], \tag{46}$$

$$I^3_\omega = \frac{16\pi^2(2\nu+1)\,\mathrm{Ai}(0)}{\nu^2(\nu+1)^2}\frac{Q^2e^4\langle\Delta N^2\rangle}{cm^2\omega^3}\left(\frac{\omega\gamma}{\omega_{B_\perp}}\right)^{2/3} \times \left[\frac{\omega}{2k_0c}\left(\gamma^{-2}+\frac{\omega_\mathrm{p}^2}{\omega^2}\right)\right]^{1-\nu}. \tag{47}$$

According to Eqns (46), (47), the whole radiation spectrum can conventionally be subdivided into four power-law parts: $I^\mathrm{tr}_\omega \propto \omega^{\nu-2}$ at $\omega \ll \omega_*$, $I^\mathrm{tr}_\omega \propto \omega^{\nu-(10/3)}$ at $\omega_* \ll \omega \ll \omega_\mathrm{p}\gamma$, $I^\mathrm{tr}_\omega \propto \omega^{-\nu-(4/3)}$ at $\omega_\mathrm{p}\gamma \ll \omega \ll \omega_{B_\perp}\gamma^2$, and $I^\mathrm{tr}_\omega \propto \omega^{-\nu-2}$ at $\omega \geqslant \omega_{B_\perp}\gamma^2$ (Fig. 3a). Thus, the intensity of transition radiation decreases rapidly at $\omega > \omega_*$, the bulk of radiation is generated at $\omega \leqslant \omega_*$ (41). The suppression effect occurs if $\omega_* < \omega_\mathrm{p}\gamma$ that coincides with condition (28) found from qualitative consideration.

As a result, the curvature of the particle trajectory gives rise to considerable modification of the transition radiation produced by particles with sufficiently high energy. Firstly, the emission is suppressed at frequencies $\omega \leqslant \omega_\mathrm{p}\gamma$, where a rectilinearly moving particle would have emitted most of the energy. Secondly, the characteristic angle of the TR emission cone increases (but it remains smaller than unity). Indeed, substitution of ω_* into Eqn (2) yields

$$\theta_\mathrm{c} \approx \left(\frac{\omega_{B_\perp}}{\omega_\mathrm{p}\gamma}\right)^{1/2} > \gamma^{-1}. \tag{48}$$

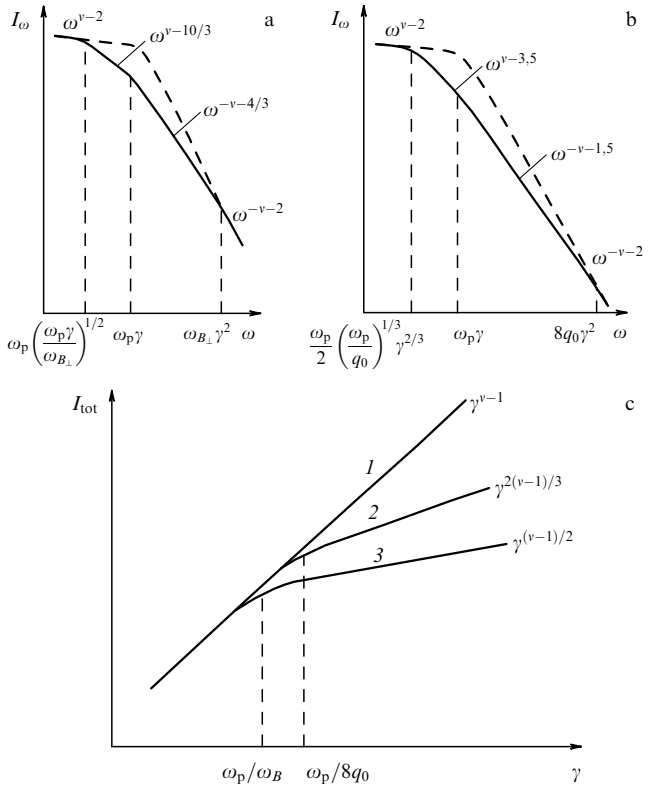

Figure 3. (a) Spectrum of transition radiation in the presence of a magnetic field, (b) spectrum of transition radiation in the presence of multiple scattering, (c) the dependence of total energy emitted by transition mechanism on the energy of relativistic particle for various types of motion: (*1*) rectilinear trajectory, (*2*) multiple scattering (random walk), (*3*) helix.

A particle rotating along a helix in plasma with random inhomogeneities generates synchrotron radiation besides transition radiation. It is important to bear in mind that the former is exponentially small at frequencies $\omega < \omega_p\gamma$, while the latter appears in this very region of frequencies. The suppression of TR by magnetic field occurs at frequencies $\omega_* < \omega < \omega_p\gamma$. Synchrotron emission by protons and other nuclei is exceedingly small because of their large mass, hence, transition radiation can dominate over synchrotron even at $\omega > \omega_p\gamma$ for the nuclei. Thus, the effect of TR suppression by magnetic field takes place at those frequencies where TR is the dominant mechanism of emission for both electrons and heavier particles.

Total energy of TR. Let us calculate now the intensity of transition radiation integrated over frequency:

$$I_{tot}^{tr} = \int_{\omega_p}^{\infty} I_\omega^{tr}\, d\omega\,. \tag{49}$$

Without a magnetic field [more precisely, if condition (28) is not satisfied], the main contribution to the integral (49) comes from the frequency region $\omega < \omega_p\gamma$, since at $\omega > \omega_p\gamma$ the intensity I_ω^{tr} falls rapidly:

$$I_{tot}^{tr} \approx \int_{\omega_p}^{\omega_p\gamma} I_\omega^2\, d\omega = \frac{8\pi^2(\nu-1)}{\nu^2(\nu+1)}\,\frac{Q^2e^4\langle\Delta N^2\rangle}{cm^2\omega_p^2} \times \left(\frac{2k_0c}{\omega_p}\,\gamma\right)^{\nu-1} \propto \gamma^{\nu-1}\,. \tag{50}$$

For a magnetic field obeying Eqn (28), the transition radiation drops already at $\omega \sim \omega_* < \omega_p\gamma$, so

$$I_{tot}^{tr} \approx \int_{\omega_p}^{\omega_*} I_\omega^2\, d\omega = \frac{8\pi^2(\nu-1)}{\nu^2(\nu+1)}\,\frac{Q^2e^4\langle\Delta N^2\rangle}{cm^2\omega_p^2}\left(\frac{2k_0c}{\omega_p}\right)^{\nu-1} \times \left(\frac{\omega_p\gamma}{\omega_{B_\perp}}\right)^{(\nu-1)/2} \propto \gamma^{(\nu-1)/2}\,. \tag{51}$$

For a particular case of a set of sharp boundaries we have $\nu = 2$ (this situation can be ensured by a pile of plates, an ensemble of shock waves etc.), so instead of the linear law $I_{tot}^{tr} \propto \gamma$ we obtain the square-root law $I_{tot}^{tr} \propto \gamma^{1/2}$. This prominent change is provided by the suppression of transition radiation by the magnetic field under condition (28) at those frequencies at which the bulk of emission would be produced if $B = 0$.

Astrophysical estimates. Radiation of astrophysical radio sources is typically generated by electrons distributed with a power-law over the energy. For this case, synchrotron emission is suppressed strongly at $\omega < \omega_p^2/\omega_B$. Contrarily, the effect of TR suppression occurs at frequencies $\omega > \omega_p^2/\omega_B$, while it is generated effectively at the lower frequencies. This allows using standard formulae of TR generated by rectilinearly moving particles for interpretation of low-frequency radio spectra in the range $\omega < \omega_p^2/\omega_B$.

For a more physical feeling, we give a few illustrative estimates of $\gamma_{e,p}^*$ (28) (for both electrons and protons) for various circumstances. For laboratory plasma with $n_e \sim 10^{14}$ cm^{-3} ($\omega_p \sim 5\times10^{11}$ s^{-1}) and $B \sim 10^4$ G ($\omega_{Be} \sim 2\times10^{11}$ s^{-1}, $\omega_{Bp} \sim 10^8$ s^{-1}) we have $\gamma_e^* \sim 2.5$, $\gamma_p^* \sim 5\times10^3$. For solar active regions (loops) with $n_e \sim 2.5\times10^9$ cm^{-3} ($\omega_p \sim 2.5\times10^9$ s^{-1}) and $B \sim 10^2$ G ($\omega_{Be} \sim 2\times10^9$ s^{-1}, $\omega_{Bp} \sim 10^6$ s^{-1}) we find $\gamma_e^* \sim 1$, $\gamma_p^* \sim 2\times10^3$. For interplanetary medium ($n_e \sim 4$ cm^{-3}, $B \sim 5\times10^{-5}$ G) they are respectively $\gamma_e^* \sim 10^2$, $\gamma_p^* \sim 2\times10^5$; and for radio galaxies ($n_e \sim 10^{-2}$ cm^{-3}, $B \sim 10^{-5}$ G) they are $\gamma_e^* \sim 30$, $\gamma_p^* \sim 5\times10^4$. Thus, the typical case is that transition radiation generated by most of the relativistic electrons is suppressed strongly, while the magnetic field effect is unimportant for heavy particles up to rather high energy. Hence, transition radiation by weakly relativistic and non-relativistic particles at relatively low frequencies (of order of the plasma frequency) can be important as well, see Section 3.

Suppression of TR by a strong magnetic field. The essence of the suppression effect is modified a bit if the curvature of the particle trajectory is associated with its motion along a field line of a very strong magnetic field $B \sim 10^{12}$ G (say, in the magnetosphere of a neutron star). Here, the radius of curvature of the field line should replace the Larmor radius, $R_L \to R_{cur}$. Thus, substituting the frequency $\omega_{cur} = c\gamma/R_{cur}$ (instead of gyrofrequency $\omega_{B_\perp}$) into Eqn (28) we obtain

$$\gamma^* = \left(\frac{\omega_p R_{cur}}{c}\right)^{1/2}. \tag{52}$$

As an example, for $\omega_p \sim 10^{12}$ s^{-1}, $R_{cur} \sim 10^7$ cm, we have $\gamma^* \sim 10^4$.

2.3 Influence of multiple scattering on transition radiation

The results obtained in the previous section are correct for transition radiation produced by a relativistic particle propagating along any regular trajectory until it can be approximated by a circle within the formation zone. How-

ever, besides the regular external field, the scattering of a particle in a medium by either Coulomb centers or stochastic electromagnetic fields [32] can cause curvature of the particle path. Here, the very particle path appears to be a random function, hence, the calculation of the TR spectrum requires averaging (27) over the respective ensemble of realizations [19]:

$$\mathcal{E}^{\rm tr}_{\mathbf{n},\omega} = \frac{8Q^2e^4}{m^2c^3\omega^2}\int \frac{|\delta N|^2_{\mathbf{k}_1}\,\mathrm{d}\mathbf{k}_1}{\left[1-(\mathbf{k}-\mathbf{k}_1)^2c^2/\omega^2\varepsilon(\omega)\right]^2} \times \int_{-\infty}^{\infty}\mathrm{d}t\,\mathrm{Re}\int_0^{\infty}\mathrm{d}\tau\exp(\mathrm{i}\omega\tau) \times \left\langle [\mathbf{n}\times\mathbf{v}(t)][\mathbf{n}\times\mathbf{v}(t+\tau)]\exp\left\{-\mathrm{i}(\mathbf{k}-\mathbf{k}_1)\left[\mathbf{r}(t+\tau)-\mathbf{r}(t)\right]\right\}\right\rangle. \quad (53)$$

Averaging over a random particle path. The averaging marked in Eqn (53) by the broken brackets can be performed with the use of distribution functions (the random density inhomogeneities and the random particle trajectory are assumed to be statistically independent of each other):

$$\langle\ldots\rangle = \int \mathrm{d}\mathbf{r}\,\mathrm{d}\mathbf{r}'\,\mathrm{d}\mathbf{v}\,\mathrm{d}\mathbf{v}'[\mathbf{n}\times\mathbf{v}][\mathbf{n}\times\mathbf{v}']\exp\left[-\mathrm{i}(\mathbf{k}-\mathbf{k}_1)(\mathbf{r}'-\mathbf{r})\right] \times F(\mathbf{r},\mathbf{v},t)\,W(\mathbf{r},\mathbf{v},\mathbf{r}',\mathbf{v}',\tau) = \int \mathrm{d}\mathbf{v}\,\mathrm{d}\mathbf{v}'\,[\mathbf{n}\times\mathbf{v}][\mathbf{n}\times\mathbf{v}']\,W_{\mathbf{k}-\mathbf{k}_1}(\mathbf{v},\mathbf{v}',\tau)\,, \quad (54)$$

where $F(\mathbf{r},\mathbf{v},t)$ is the distribution function of the particle at the time t, which (being normalized by unity) is converted to unity after integrating over $\mathrm{d}\mathbf{r}\,\mathrm{d}\mathbf{v}$, $W(\mathbf{r},\mathbf{v},\mathbf{r}',\mathbf{v}',\tau)$ is the conditional probability of the transition of the fast particle (for the time interval τ) from an initial point $(\mathbf{r},\mathbf{v})$ of the phase space into a final point $(\mathbf{r}',\mathbf{v}')$, and $W_{\mathbf{k}-\mathbf{k}_1}$ is its spatial Fourier-transform.

The function W (that obeys the kinetic equation) has been calculated in the frame of radiation theory for both Coulomb collisions [33] and scattering by a random field [32]. It can be expressed as

$$W_{\mathbf{k}-\mathbf{k}_1}(\mathbf{v}_0,\mathbf{v},\tau) = v^{-2}\delta(v-v_0) \times \exp\left\{-\mathrm{i}\left[\frac{\omega v}{c}\left(1-\frac{\omega_{\rm p}^2}{2\omega^2}\right)+\mathbf{k}_1\mathbf{n}v\right]\tau\right\}u(\boldsymbol{\theta}_0,\boldsymbol{\theta},\tau)\,, \quad (55)$$

where the vectors $\boldsymbol{\theta}_0$, $\boldsymbol{\theta}$ are defined like Eqns (29), (30) by

$$\mathbf{v}_0 = \mathbf{n}v\left(1-\frac{\theta_0^2}{2}\right)+\boldsymbol{\theta}_0 v\,, \qquad \mathbf{v} = \mathbf{n}v\left(1-\frac{\theta^2}{2}\right)+\boldsymbol{\theta}v\,, \quad (56)$$

and the function $u(\boldsymbol{\theta}_0,\boldsymbol{\theta},\tau)$ obeys the equation

$$\frac{\partial u}{\partial\tau}-\frac{\mathrm{i}\omega}{2}\,\theta^2 u = q\Delta_\theta u\,. \quad (57)$$

Here, $q = q_0\gamma^{-2}$ is the rate of collisions between the relativistic particle and either Coulomb centers or small-scale fields. For the former case [33]

$$q_0 = 2\pi N v\left(\frac{Ze^2}{Mc^2}\right)^2\ln\frac{183}{Z^{1/3}}\,, \quad (58)$$

where N and Ze are the number density and the charge of the background nuclei, while for the latter case [34]:

$$q_0 = \frac{L_0}{3c}\,\frac{Q^2\langle B_{\rm st}^2\rangle}{M^2c^2} = \frac{\omega_{\rm st}^2}{3\omega_0}\,, \qquad \omega_{\rm st}<\omega_0\,, \quad (59)$$

where L_0 and $\langle B_{\rm st}^2\rangle$ are the correlation length and the magnitude of magnetic irregularities, $\omega_{\rm st} = Q\langle B_{\rm st}^2\rangle^{1/2}/Mc$, $\omega_0 = c/L$; the magnetic field is regarded as a small-scale field if $\omega_{\rm st}<\omega_0$. For purely electric irregularities equation (57) remains unchanged, while the definition of q_0 requires the replacement $\langle B_{\rm st}^2\rangle \to \langle E_{\rm st}^2\rangle$.

The solution of Eqn (57) with the obvious initial condition $u(\boldsymbol{\theta}_0,\boldsymbol{\theta},0) = \delta(\boldsymbol{\theta}_0-\boldsymbol{\theta})$ is

$$u(\boldsymbol{\theta}_0,\boldsymbol{\theta},\tau) = \frac{x}{\pi\sinh z\tau}\exp\left[-x(\theta^2+\theta_0^2)\coth(z\tau) + 2x(\boldsymbol{\theta}_0\cdot\boldsymbol{\theta})\sinh^{-1}(z\tau)\right], \quad (60)$$

where

$$x = (1-\mathrm{i})\left(\frac{\omega}{16q}\right)^{1/2}, \qquad z = (1-\mathrm{i})(\omega q)^{1/2}\,. \quad (61)$$

Spectral-angular distribution of TR. Substituting Eqns (55), (60) into Eqns (54), (53) and proceeding to the intensity of emission (the energy emitted per unit time) like in the previous section, we find

$$I^{\rm tr}_{\mathbf{n},\omega} = \frac{8Q^2e^4}{m^2c\omega^2}\int\frac{|\delta N|^2_{\mathbf{k}_1}\,\mathrm{d}\mathbf{k}_1}{\left[1-(\mathbf{k}-\mathbf{k}_1)^2c^2/\omega^2\varepsilon(\omega)\right]^2}\,\mathrm{Re}\int_0^{\infty}\mathrm{d}\tau \times\int\mathrm{d}\boldsymbol{\theta}\,(\boldsymbol{\theta}_0\cdot\boldsymbol{\theta})\,\frac{x}{\pi\sinh z\tau}\exp\left[\frac{\mathrm{i}\omega\tau}{2}\left(\gamma^{-2}+\frac{\omega_{\rm p}^2}{\omega^2}+\frac{2\mathbf{k}_1\mathbf{n}c}{\omega}\right) - x(\theta^2+\theta_0^2)\,\coth(z\tau)+2x(\boldsymbol{\theta}_0\cdot\boldsymbol{\theta})\sinh^{-1}(z\tau)\right]. \quad (62)$$

It is important that the analysis of emission into a fixed direction can be performed correctly in the presence of multiple scattering, because the system remains axially symmetric (on average) with respect to the initial velocity of the particle. Indeed, any direction of the velocity change has equal probability, so the angle of emission θ_0 can be counted from the vector of initial velocity $\mathbf{v}_0$. The symmetry surely arises for an ensemble (beam) of particles, while each individual particle moves along a unique highly asymmetric (random) trajectory.

The integrand in Eqn (62) is a Gaussian function of the angle, hence, the integration over $\mathrm{d}\theta_x$ and $\mathrm{d}\theta_y$ is easy to perform over the region $[-\infty,+\infty]$. The limits of integration can actually be set as infinities due to rapid convergence of the integrals over $\mathrm{d}\boldsymbol{\theta}$, which is provided by sharp directivity of the emission along the velocity of the particle:

$$I^{\rm tr}_{\mathbf{n},\omega} = \frac{8Q^2e^4}{m^2c\omega^2}\,\theta_0^2\int\frac{|\delta N|^2_{\mathbf{k}_1}\,\mathrm{d}\mathbf{k}_1}{\left[1-(\mathbf{k}-\mathbf{k}_1)^2c^2/\omega^2\varepsilon(\omega)\right]^2} \times\mathrm{Re}\int_0^{\infty}\frac{\mathrm{d}\tau}{\pi\cosh^2 z\tau} \times\exp\left[\frac{\mathrm{i}\omega\tau}{2}\left(\gamma^{-2}+\frac{\omega_{\rm p}^2}{\omega^2}+\frac{2\mathbf{k}_1\mathbf{n}c}{\omega}\right)-x\theta_0^2\tanh z\tau\right]. \quad (63)$$

Like in the previous section, we analyze further different limiting cases of expression (63). If

$$|z| \ll \frac{\omega}{2}\left(\gamma^{-2}+\frac{\omega_p^2}{\omega^2}\right), \tag{64}$$

then the arguments of the hyperbolic functions are small: $|z\tau| \ll 1$, $\tanh z\tau \approx z\tau$, $\cosh z\tau \approx 1$ and Eqn (63) reduces to the familiar expression (39) as for a rectilinearly moving particle. Inequality (64) is valid for low- and high-frequency regions:

$$\omega \ll \omega_{**} = \frac{\omega_p}{2}\left(\frac{\omega_p}{q_0}\right)^{1/3}\gamma^{2/3}, \tag{65}$$

$$\omega \gg 8q_0\gamma^2. \tag{66}$$

For the intermediate frequency range, when

$$|z| \gg \frac{\omega}{2}\left(\gamma^{-2}+\frac{\omega_p^2}{\omega^2}\right), \tag{67}$$

or equally

$$\omega_{**} \ll \omega \ll 8q_0\gamma^2, \tag{68}$$

the multiple scattering is important. Here, the hyperbolic functions can be simplified as well: $\tanh z\tau \approx 1$, $\cosh^2 z\tau \approx \exp(2z\tau)/4$. Then, the integration over the time yields

$$I^{tr}_{\mathbf{n},\omega} = \frac{8Q^2e^4}{m^2c\omega(\omega q)^{1/2}}\,\theta_0^2\int\frac{|\delta N|^2_{\mathbf{k}_1}\,d\mathbf{k}_1}{\left[1-(\mathbf{k}-\mathbf{k}_1)^2c^2/\omega^2\varepsilon(\omega)\right]^2}. \tag{69}$$

The integration of Eqn (69) over $d\mathbf{k}_1$ with the spectrum of inhomogeneities (35) yields

$$I^{tr}_{\mathbf{n},\omega} = \frac{4(\nu-1)}{\nu(\nu+1)}\,\frac{Q^2e^4\langle\Delta N^2\rangle}{cm^2\omega^2(\omega q)^{1/2}}\left(\frac{2k_0c}{\omega}\right)^{\nu-1} \times\frac{\theta_0^2}{\left[\theta_0^2+\gamma^{-2}+\omega_p^2/\omega^2\right]^{\nu+1}}. \tag{70}$$

Here, contrary to the case of the particle rotation in magnetic field, the intensity of radiation along the particle velocity $\theta_0^2 = 0$ remains zero. The difference is provided by the difference in the symmetry in these two cases.

Spectral distribution of TR. Integration of Eqn (70) over the angles gives rise to the spectrum of transition radiation at the frequencies (68):

$$I^{tr}_{\omega} = \frac{2}{\nu^2(\nu+1)}\,\frac{Q^2e^4\langle\Delta N^2\rangle}{cm^2\omega^2(\omega q)^{1/2}}\left\{\left(\frac{\omega}{2k_0c}\right)\left[\gamma^{-2}+\frac{\omega_p^2}{\omega^2}\right]\right\}^{1-\nu}. \tag{71}$$

Hence, the radiation spectrum consists of two power-law parts in the region (68), $I^{tr}_{\omega} \propto \omega^{\nu-3.5}$ at $\omega_{**} \ll \omega \ll \omega_p\gamma$ and $I^{tr}_{\omega} \propto \omega^{-\nu-1.5}$ at $\omega_p\gamma \ll \omega \ll 8q_0\gamma^2$. Thus, at $\omega \geqslant \omega_{**}$ the transition radiation is suppressed considerably (see Fig. 3b) and it decreases as the rate of collisions increases $I^{tr}_{\omega} \propto q^{-1/2}$.

The effect of suppression of transition radiation by multiple scattering (71) is essential if the frequency range (68) actually exists, i.e., $\omega_{**} \ll 8q_0\gamma^2$, which [taking into account Eqn (65)] happens for particles with sufficiently high energy:

$$\gamma \gg \gamma^{**} = \frac{\omega_p}{8q_0}. \tag{72}$$

This inequality is similar (to some extent) to condition (28) of suppression of transition radiation by a magnetic field.

Total energy of TR. Let us calculate the dependence of the total energy emitted by the transition mechanism under condition (72). Integrating Eqn (46) over frequency up to the frequency ω_{**}, like Eqn (51), we find

$$I^{tr}_{tot} \approx \int_{\omega_p}^{\omega_{**}} I^2_{\omega}\,d\omega = \frac{16\pi^2}{2^\nu\nu^2(\nu+1)}\,\frac{Q^2e^4\langle\Delta N^2\rangle}{cm^2\omega_p^2} \times\left(\frac{2k_0c}{\omega_p}\right)^{\nu-1}\left(\frac{\omega_p\gamma^2}{q_0}\right)^{(\nu-1)/3} \propto \gamma^{2(\nu-1)/3}. \tag{73}$$

This case seems to be an intermediate in some sense between rectilinear motion of the particle (50) and its rotation in a magnetic field (51). Figure 3c displays the dependence of the total energy generated by TR on the energy of the particle.

Estimate of TR suppression by multiple scattering. Suppression of transition radiation by multiple scattering on Coulomb centers can be observed in standard condensed media, for example, in carbon for $\gamma_e > 10^4$, in iron for $\gamma_e > 800$ etc., which is the same as for a single boundary case [35]. For interplanetary plasma [36] $\langle B^2_{st}\rangle \approx 3.6\times10^{-10}$ G^2, $L_0 \sim 3\times10^{11}$ cm providing $\omega_{st} = 0.25$ s^{-1}, $\omega_0 = 0.1$ s^{-1}, so we have

$$\gamma_e^{**} \approx \frac{\omega_p\omega_0}{2\omega_{st}^2} \sim 10^5. \tag{74}$$

Let us assume, that there are weak inhomogeneities of the magnetic field (say, Alfven waves) in the magnetosphere of a neutron star with magnitude $B_{st} = \langle B^2_{st}\rangle^{1/2} \approx 5$ G ($\sim 10^{-11}B_0$) and $L_0 \sim 100$ cm, then $\omega_{st} = 10^8$ s^{-1}, $\omega_0 = 3\times10^8$ s^{-1}. With the use of Eqn (74), we find

$$\gamma_e^{**} \sim 10^2. \tag{75}$$

Since the plasma in the vicinity of a neutron star is relativistic and $\gamma \geqslant 10^2$ for most of the particles, the suppression of transition radiation occurs there for most of the electrons and positrons available. We conclude that the application of the theory of transition radiation to natural objects with a strong magnetic field should be done with great caution and paying particular attention to each effect resulting in curvature of the trajectories of emitted particles.

2.4 Transition radiation in a gyrotropic plasma

A method for analyzing the radiation by particles in anisotropic media was proposed by Ginzburg back in 1940 [37]. Ginzburg used this method to analyze Vavilov–Cherenkov radiation [38]. Kolomensky generalized this method to the case of gyrotropic media [39]. He also studied the formation of the Vavilov–Cherenkov radiation emitted by a particle moving along the magnetic field in a magnetized plasma [40]. Barsukov [41] studied the radiation emitted by oscillators moving along the axis of symmetry of a gyrotropic crystal. The results of those early studies, as well as methods for calculating the radiation in anisotropic media, are reviewed in Ref. [42]. Here we mention only those papers which concentrate on the role of the optical anisotropy in generation of radiation in media. The crystal structure, i.e.,

order in the positions of the particles in the medium, if present, gives rise to many interesting effects [9, 43–45], which are beyond the scope of this paper.

Some problems of transition radiation generation in anisotropic media have also been studied. The transition radiation at an interface between an ordinary isotropic medium and an optically active isotropic medium is studied in Ref. [46]. The radiation by particles as they pass through ferroelectric or crystalline plates is studied in Ref. [47].

General treatment. Let us consider the transition radiation generated by a single relativistic particle propagating at an arbitrary angle θ with respect to the magnetic field through a gyrotropic magnetized plasma with a broad spectrum of random density inhomogeneities (35) [48].

As has been shown above (see Refs [28, 19] as well), the calculation of transition radiation in a plasma with weak inhomogeneities

$$\frac{\Delta N}{N} \ll 1 \tag{76}$$

requires one to obtain the current $\mathbf{j}^{(1)}_{\omega,\mathbf{k}}$ in the medium, which is bilinear over the field of the relativistic particle $\mathbf{E}^{Q}_{\omega,\mathbf{k}}$ and over the amplitude of the inhomogeneities $\delta N_{\mathbf{k}}$. The expression for $\mathbf{j}^{(1)}_{\omega,\mathbf{k}}$ can be found by solving the kinetic equation using the perturbation theory (see Section 2.1), like when deriving the dielectric tensor of a magnetized plasma [49]:

$$j^{(1),\alpha}_{\omega,\mathbf{k}} = \frac{\mathrm{i}e^2}{m\omega}\,\chi_{\alpha\beta}\int \mathrm{d}\mathbf{k}'\, E^{Q,\beta}_{\omega,\mathbf{k}-\mathbf{k}'}\delta N_{\mathbf{k}'}\,, \tag{77}$$

where the inhomogeneities are assumed to be quasi-static. The tensor $\chi_{\alpha\beta}$ is given in the cold-plasma approximation by

$$\chi_{\alpha\beta} = \begin{pmatrix} \dfrac{1}{1-u} & \dfrac{-\mathrm{i}\sqrt{u}}{1-u} & 0 \\ \dfrac{\mathrm{i}\sqrt{u}}{1-u} & \dfrac{1}{1-u} & 0 \\ 0 & 0 & 1 \end{pmatrix}. \tag{78}$$

The diagonal components of the tensor $\chi_{\alpha\beta}$ describe the currents which are transverse and longitudinal with respect to the magnetic field ($\mathbf{B} = B\mathbf{e}_z$), while the off-diagonal components describe the Hall current of the plasma electrons. The dimensionless quantity u is determined by the ratio of the electron gyrofrequency to the radiation frequency:

$$u = \frac{\omega^2_{B\mathrm{e}}}{\omega^2}\,. \tag{79}$$

The electric field of the relativistic particle in Eqn (77) is expressed from the current of the particle with the use of the Green function $G_{\beta\sigma}(\omega,\mathbf{k})$, like Eqn (20). The Green function of gyrotropic plasma, however, differs from that in isotropic medium. It can be found by expanding the field in the anisotropic medium into normal modes (the Hamiltonian method [37, 39, 50]). In particular, the Green function can be written as [cf. Eqn (23) for an isotropic plasma]

$$G_{\alpha\beta}(\omega,\mathbf{k}) = 4\pi\mathrm{i}\omega\left(\frac{a^{\alpha}_{\mathrm{o}\mathbf{k}}a^{*\beta}_{\mathrm{o}\mathbf{k}}}{\omega^2_{\mathrm{o}\mathbf{k}}-\omega^2} + \frac{a^{\alpha}_{\mathrm{e}\mathbf{k}}a^{*\beta}_{\mathrm{e}\mathbf{k}}}{\omega^2_{\mathrm{e}\mathbf{k}}-\omega^2}\right) \tag{80}$$

for a cold magnetized plasma, where $\mathbf{a}_{\mathrm{o,e}}$ are the vectors of polarization of the ordinary and extraordinary waves, and $\omega_{\mathrm{o,e}}$ are the corresponding eigenfrequencies. These quantities were derived by Eidman [51] when analyzing the magneto-bremsstrahlung in gyrotropic plasma. While they are reproduced in many treatises (see, e.g., Ref. [52]), we write them down here for convenience in the reading of the paper:

$$\omega^2_{j,\mathbf{k}} = \frac{k^2c^2}{n^2_j}\,, \qquad j = \mathrm{o},\mathrm{e}\,, \tag{81}$$

$$n^2_{\mathrm{o,e}} = 1 - \frac{2v(1-v)}{2(1-v) - u\sin^2\theta \pm \left[u^2\sin^4\theta + 4u(1-v)^2\cos^2\theta\right]^{1/2}}\,, \tag{82}$$

where θ is the angle between the vectors $\mathbf{k}$ and $\mathbf{B}$, and

$$v = \frac{\omega^2_{\mathrm{p}}}{\omega^2}\,, \tag{83}$$

$$\mathbf{a}_{j,\mathbf{k}} = \frac{n_{j,\mathbf{k}}}{(1+\alpha^2_j+\beta^2_j)^{1/2}}(1, \mathrm{i}\alpha_j, \mathrm{i}\beta_j)\,, \qquad j = \mathrm{o},\mathrm{e}\,. \tag{84}$$

Here the brackets contain (x,y,z) components of the vector of polarization. The coordinate system is chosen in such a way that the magnetic field $\mathbf{B}$ is along the z axis, and the vector $\mathbf{k}$ belongs to the (y,z) plane. Further

$$\alpha_j = K_j\cos\theta - \gamma_j\sin\theta\,, \qquad \beta_j = K_j\sin\theta + \gamma_j\cos\theta\,, \tag{85}$$

$$K_{\mathrm{o,e}} = \frac{2\sqrt{u}(1-v)\cos\theta}{u\sin^2\theta \mp (u^2\sin^4\theta + 4u(1-v)^2\cos^2\theta)^{1/2}}\,, \tag{86}$$

$$K_{\mathrm{o}}K_{\mathrm{e}} \equiv -1\,,$$

$$\gamma_{\mathrm{o,e}} = -\frac{v\sqrt{u}\,\sin\theta + uvK_{\mathrm{o,e}}\cos\theta\sin\theta}{1-u-v(1-u\cos^2\theta)}\,. \tag{87}$$

These expressions are correct for the electric fields in a plasma except for the vicinity of the fundamental cyclotron resonance ($u = 1$) and possibly its lowest harmonics, where the thermal motion of the plasma particles (the spatial dispersion) should be taken into account.

The energy radiated by a particle into one of the normal modes during the entire time over which the particle moves through the plasma can be written, like Eqn (24), as [10]

$$\mathcal{E}_{j,\mathbf{n},\omega} = (2\pi)^6\,\frac{\omega^2}{c^3}\left\langle\left|\mathbf{a}^*_{j,\mathbf{k}}\cdot\mathbf{j}^{(1)}_{j,\omega,\mathbf{k}}\right|^2\right\rangle. \tag{88}$$

To be more specific, we consider the energy radiated into the ordinary wave; the expressions for the extraordinary wave are then found by the exchange of the indices $\mathrm{o} \Leftrightarrow \mathrm{e}$. In the calculations we assume the relativistic particles to move rectilinearly. Surely, this approximation is not necessarily valid. For example, under the condition $\omega_{B\mathrm{e}}/\omega_{\mathrm{p}} > 1$, the curvature of the trajectory has a very strong effect on the transition radiation by relativistic electrons of any energy. Nevertheless, it is still worthwhile to examine the rectilinear motion of the particles in this case, since we intend to study the proper effect of the plasma gyrotropy on the radiation only. Furthermore, for protons and heavier nuclei, this approximation may be completely valid even in fairly strong magnetic fields. With these general comments, we end our discussion of the role of trajectory curvature for the time being; more quantitative evaluations and the applicability criteria are given at the end of this section.

The Fourier component of the proper current produced by a rectilinearly moving particle is

$$\mathbf{j}^{Q}_{\omega,\mathbf{k}-\mathbf{k}'} = \frac{Q\mathbf{v}}{(2\pi)^3}\,\delta\big[\omega-(\mathbf{k}-\mathbf{k}')\mathbf{v}\big]\,, \tag{89}$$

where Q is the charge of the relativistic particle. Substitution of all that is required into Eqn (88) yields

$$\begin{aligned}
\mathcal{E}_{\mathrm{o},\mathbf{n},\omega} = {}& \frac{8\pi e^4Q^2\omega^2}{c^3}\,T\Bigg\{|a^{*\alpha}_{\mathrm{o},\mathbf{k}}\chi_{\alpha\beta}\,a^{\beta}_{\mathrm{o},\mathbf{k}}|^2|\mathbf{a}^{*}_{\mathrm{o},\mathbf{k}}\cdot\mathbf{v}|^2\\
&\times\int d\mathbf{k}'\,|\delta N|^2_{\mathbf{k}'}\,\frac{\delta\big[\omega-(\mathbf{k}-\mathbf{k}')\mathbf{v}\big]}{\big[(\mathbf{k}-\mathbf{k}')^2c^2/n_{\mathrm{o}}^2-\omega^2\big]^2}\\
&+|a^{*\alpha}_{\mathrm{o},\mathbf{k}}\chi_{\alpha\beta}a^{\alpha}_{\mathrm{e},\mathbf{k}}|^2|\mathbf{a}^{*}_{\mathrm{e},\mathbf{k}}\cdot\mathbf{v}|^2\int d\mathbf{k}'\,|\delta N|^2_{\mathbf{k}'}\,\frac{\delta\big[\omega-(\mathbf{k}-\mathbf{k}')\mathbf{v}\big]}{\big[(\mathbf{k}-\mathbf{k}')^2c^2/n_{\mathrm{e}}^2-\omega^2\big]^2}\\
&+2\,\mathrm{Re}\,(a^{*\alpha}_{\mathrm{o},\mathbf{k}}\chi_{\alpha\beta}a^{\beta}_{\mathrm{o},\mathbf{k}})(a^{\gamma}_{\mathrm{o},\mathbf{k}}\chi^{*}_{\gamma\delta}a^{*\delta}_{\mathrm{e},\mathbf{k}})\big|(\mathbf{a}^{*}_{\mathrm{o},\mathbf{k}}\cdot\mathbf{v})(\mathbf{a}_{\mathrm{e},\mathbf{k}}\cdot\mathbf{v})\big|\\
&\times\int d\mathbf{k}'\,|\delta N|^2_{\mathbf{k}'}\,\frac{\delta\big[\omega-(\mathbf{k}-\mathbf{k}')\mathbf{v}\big]}{\big[(\mathbf{k}-\mathbf{k}')^2c^2/n_{\mathrm{o}}^2-\omega^2\big]\big[(\mathbf{k}-\mathbf{k}')^2c^2/n_{\mathrm{e}}^2-\omega^2\big]}\Bigg\}\,,
\end{aligned} \tag{90}$$

where T is the total duration of emission. Dividing Eqn (90) by this time yields the radiation intensity (the energy emitted per unit time). In general, the intensity of the radiation of the ordinary wave depends on the refractive indices of both normal modes. The formal reason for this is the difference between the tensor $\chi_{\alpha\beta}$ (78) and $\delta_{\alpha\beta}$. The Green function (80) represents the electric field of the particle as the sum of quasi-stationary ('virtual') ordinary and extraordinary waves. The scattering of the virtual ordinary wave (and of the extra-ordinary wave) by inhomogeneities of the medium leads to the emission of both ordinary and extraordinary waves. Respectively, we refer to the two contributions to the radiation of each normal mode as the 'radiation through the virtual ordinary wave' (or through the 'virtual extraordinary wave').

Since the radiation by relativistic particles reveals high directivity, we use the smallness of the angle ϑ between $\mathbf{k}$ and $\mathbf{v}$ (56), which yields:

$$\begin{aligned}
|\mathbf{a}^{*}_{\mathrm{o},\mathbf{k}}\cdot\mathbf{v}|^2 &\approx c^2\,\frac{K_{\mathrm{o}}^2\vartheta^2\sin^2\phi+\vartheta^2\cos^2\phi}{1+K_{\mathrm{o}}^2}\\
&= c^2\vartheta^2\,\frac{\sin^2\phi+K_{\mathrm{e}}^2\cos^2\phi}{1+K_{\mathrm{e}}^2}\,,\\
|\mathbf{a}^{*}_{\mathrm{e},\mathbf{k}}\cdot\mathbf{v}|^2 &\approx c^2\vartheta^2\,\frac{\cos^2\phi+K_{\mathrm{e}}^2\sin^2\phi}{1+K_{\mathrm{e}}^2}\,,\\
2(\mathbf{a}^{*}_{\mathrm{o},\mathbf{k}}\cdot\mathbf{v})(\mathbf{a}_{\mathrm{e},\mathbf{k}}\cdot\mathbf{v}) &\approx -2K_{\mathrm{e}}c^2\vartheta^2\,\frac{\cos 2\phi}{1+K_{\mathrm{e}}^2}\,.
\end{aligned} \tag{91}$$

Here the condition $K_{\mathrm{o}}K_{\mathrm{e}}\equiv -1$ is taken into account. We have also discarded some terms proportional to γ_j which describe the longitudinal component of the electric field, since the relations $|\gamma_j|\ll 1, |K_j|$ are fulfilled under the conditions of interest. Here ϕ is the azimuth angle of the vector $\boldsymbol{\vartheta}$; we have $\cos\phi = 0$ when $\boldsymbol{\vartheta}$ belongs to the $(\mathbf{B},\mathbf{v})$ plane, and we have $\sin\phi = 0$ when $\boldsymbol{\vartheta}$ is perpendicular to this plane.

Substituting Eqn (91) into Eqn (90), and using $\mathbf{k}\mathbf{k}'/kk'\approx\mathbf{v}\mathbf{k}'/vk'$, we can integrate Eqn (90) over the angles of the vector $\mathbf{k}'$ taking into account the δ function. We obtain further the radiation intensity by dividing Eqn (90) by T:

$$\begin{aligned}
I_{\mathrm{o},\mathbf{n},\omega} = {}& \frac{16\pi^2e^4Q^2}{m^2\omega^2c^2}\int_{k'_{\min}}^{\infty}k'\,dk'\,|\delta N|^2_{\mathbf{k}'}\,\frac{\vartheta^2}{(1+K_{\mathrm{e}}^2)^3}\\
&\times\Bigg(\frac{\big[(\cos^2\theta-2K_{\mathrm{e}}\sqrt{u}\,\cos\theta+K_{\mathrm{e}}^2)/(1-u)+\sin^2\theta\big]^2}{\vartheta^2+\gamma^{-2}+2(1-n_{\mathrm{o}})}\\
&\times\frac{\sin^2\phi+K_{\mathrm{e}}^2\cos^2\phi}{\vartheta^2+\gamma^{-2}+2(1-n_{\mathrm{o}})}\\
&+\frac{\big\{\big[(1-K_{\mathrm{e}}^2)\sqrt{u}\,\cos\theta-uK_{\mathrm{e}}\sin^2\theta\big]/(1-u)\big\}^2}{\vartheta^2+\gamma^{-2}+2(1-n_{\mathrm{e}})}\\
&\times\frac{\cos^2\phi+K_{\mathrm{e}}^2\sin^2\phi}{\vartheta^2+\gamma^{-2}+2(1-n_{\mathrm{e}})}\\
&-2K_{\mathrm{e}}\,\frac{\big[(1-K_{\mathrm{e}}^2)\sqrt{u}\,\cos\theta-uK_{\mathrm{e}}\sin^2\theta\big]/(1-u)}{\vartheta^2+\gamma^{-2}+2(1-n_{\mathrm{e}})}\\
&\times\frac{(1-2K_{\mathrm{e}}\sqrt{u}\,\cos\theta+K_{\mathrm{e}}^2-u\sin^2\theta)/(1-u)}{\vartheta^2+\gamma^{-2}+2(1-n_{\mathrm{o}})}\cos 2\phi\Bigg)\,,
\end{aligned} \tag{92}$$

where

$$k'^{j}_{\min} = \frac{\omega}{2c}\big[\vartheta^2+\gamma^{-2}+2(1-n_j)\big]\,. \tag{93}$$

In deriving Eqn (92) we ignored the difference between the directions of $\mathbf{k}$ and $\mathbf{v}$ everywhere except for expressions like $|\mathbf{a}^{*}_{j,\mathbf{k}}\cdot\mathbf{v}|^2\sim[\mathbf{n}\times\mathbf{v}]^2$. In particular, the angle θ in Eqn (92) is assumed to be equal to the angle between the velocity of the particle and the external magnetic field. Integration of Eqn (92) over the inhomogeneity spectrum (35) yields:

$$\begin{aligned}
I_{\mathrm{o},\mathbf{n},\omega} = {}& \frac{8\pi(\nu-1)}{\nu}\,\frac{e^4Q^2\langle\Delta N^2\rangle}{cm^2\omega^3}\\
&\times\frac{(2k_0c/\omega)^{\nu-1}}{\big[\vartheta^2+\gamma^{-2}+2(1-n_{\mathrm{o}})\big]^{\nu}}\,\frac{\vartheta^2}{(1+K_{\mathrm{e}}^2)^3}\\
&\times\Bigg(\frac{\big[(\cos^2\theta-2K_{\mathrm{e}}\sqrt{u}\,\cos\theta+K_{\mathrm{e}}^2)/(1-u)+\sin^2\theta\big]^2}{\vartheta^2+\gamma^{-2}+2(1-n_{\mathrm{o}})}\\
&\times\frac{\sin^2\phi+K_{\mathrm{e}}^2\cos^2\phi}{\vartheta^2+\gamma^{-2}+2(1-n_{\mathrm{o}})}\\
&+\frac{\big\{\big[(1-K_{\mathrm{e}}^2)\sqrt{u}\,\cos\theta-uK_{\mathrm{e}}\sin^2\theta\big]/(1-u)\big\}^2}{\vartheta^2+\gamma^{-2}+2(1-n_{\mathrm{e}})}\\
&\times\frac{\cos^2\phi+K_{\mathrm{e}}^2\sin^2\phi}{\vartheta^2+\gamma^{-2}+2(1-n_{\mathrm{e}})}-2K_{\mathrm{e}}\cos 2\phi\\
&\times\frac{\big[(1-K_{\mathrm{e}}^2)\sqrt{u}\,\cos\theta-uK_{\mathrm{e}}\sin^2\theta\big]/(1-u)}{\vartheta^2+\gamma^{-2}+2(1-n_{\mathrm{e}})}\\
&\times\frac{(\cos^2\theta-2K_{\mathrm{e}}\sqrt{u}\,\cos\theta+K_{\mathrm{e}}^2)/(1-u)+\sin^2\theta}{\vartheta^2+\gamma^{-2}+2(1-n_{\mathrm{o}})}\Bigg)\,.
\end{aligned} \tag{94}$$

The radiation of the extraordinary wave per unit frequency per unit angle (the spectral-angular distribution of the

radiation) is calculated similarly. The result is

$$I_{\mathrm{e},\mathbf{n},\omega} = \frac{8\pi(\nu-1)}{\nu}\,\frac{e^4Q^2\langle\Delta N^2\rangle}{cm^2\omega^3} \times \frac{(2k_0c/\omega)^{\nu-1}}{\left[\vartheta^2+\gamma^{-2}+2(1-n_\mathrm{e})\right]^{\nu}}\,\frac{\vartheta^2}{(1+K_\mathrm{e}^2)^3} \times \left(\frac{\left[(1+2K_\mathrm{e}\sqrt{u}\cos\theta+K_\mathrm{e}^2\cos^2\theta)/(1-u)+K_\mathrm{e}^2\sin^2\theta\right]^2}{\vartheta^2+\gamma^{-2}+2(1-n_\mathrm{e})} \times \frac{\cos^2\phi+K_\mathrm{e}^2\sin^2\phi}{\vartheta^2+\gamma^{-2}+2(1-n_\mathrm{e})} + \frac{\left\{\left[(1-K_\mathrm{e}^2)\sqrt{u}\cos\theta-uK_\mathrm{e}\sin^2\theta\right]/(1-u)\right\}^2}{\vartheta^2+\gamma^{-2}+2(1-n_\mathrm{o})} \times \frac{\sin^2\phi+K_\mathrm{e}^2\cos^2\phi}{\vartheta^2+\gamma^{-2}+2(1-n_\mathrm{o})} - 2K_\mathrm{e}\cos 2\phi \times \frac{\left[(1-K_\mathrm{e}^2)\sqrt{u}\cos\theta-uK_\mathrm{e}\sin^2\theta\right]/(1-u)}{\vartheta^2+\gamma^{-2}+2(1-n_\mathrm{e})} \times \frac{(1+2K_\mathrm{e}\sqrt{u}\cos\theta+K_\mathrm{e}^2\cos^2\theta)/(1-u)+K_\mathrm{e}^2\sin^2\theta}{\vartheta^2+\gamma^{-2}+2(1-n_\mathrm{o})}\right). \quad (95)$$

Expressions (94) and (95) solve the problem of the transition radiation generated by a relativistic particle moving through a magnetized plasma with random density variations. Let us now analyze various limiting cases in more detail.

The case of weak gyrotropy. Let us consider high frequencies (19) at which the plasma gyrotropy has only a weak effect on the intensity of transition radiation. However, the weak magnetic field is the only reason for polarization of the radiation if the fluctuations of the medium are distributed isotropically. The polarization of the radiation is important for the expected applications of the transition mechanism to astrophysical sources. Observing and analyzing the polarization of radiation appears frequently to be crucial in identifying the mechanisms of astrophysical electromagnetic radiation [53].

To find the degree of polarization of the transition radiation under condition (19), we proceed in the following way. We calculate the intensities of the radiation of the two normal modes (94), (95) by expanding them into power series over u. Since the expressions for both the refractive indices (82) and the polarization vectors (86) contain the quantity u in combinations with $\sin\theta$ and $\cos\theta$, the respective expansions are different depending on the relation between $\cos^2\theta$ and u.

Quasi-longitudinal motion. If

$$\cos^2\theta \gg u\,, \quad (96)$$

the polarization of the normal modes in the plasma is almost circular [53], and the intensities of the ordinary and extraordinary waves are

$$I_{\mathrm{o},\omega} = \frac{I_\omega^{\mathrm{tr}}}{2}\left\{1-2\sqrt{u}\cos\theta\left[1-\frac{\nu}{2(1+\omega^2/\omega_\mathrm{p}^2\gamma^2)}\right]\right\}, \quad (97)$$

$$I_{\mathrm{e},\omega} = \frac{I_\omega^{\mathrm{tr}}}{2}\left\{1+2\sqrt{u}\cos\theta\left[1-\frac{\nu}{2(1+\omega^2/\omega_\mathrm{p}^2\gamma^2)}\right]\right\}, \quad (98)$$

where I_ω^{tr} is the intensity of the transition radiation in an isotropic plasma (46). Obviously, the extraordinary wave is radiated a bit more efficiently than the ordinary wave. The difference between the radiation intensities (97) and (98) (on the one hand) and those in the case of an isotropic plasma (on the other) arises primarily from the existence of the Hall current of the background electrons (the terms $\pm 2\sqrt{u}\cos\theta$). Since the direction of the electron rotation is the same as the direction of the electric field rotation in the extraordinary wave, the respective Hall current increases the radiation of these waves and reduces the radiation of ordinary waves. The other terms arise from a small difference between the refractive indices for the normal modes and they are smaller than the Hall contributions if $\nu < 2$. The degree of polarization of the radiation is

$$P = \frac{I_{\mathrm{o},\omega}-I_{\mathrm{e},\omega}}{I_{\mathrm{o},\omega}+I_{\mathrm{e},\omega}} = -2\,\frac{\omega_{Be}}{\omega}\cos\theta\left[1-\frac{\nu}{2(1+\omega^2/\omega_\mathrm{p}^2\gamma^2)}\right]. \quad (99)$$

According to the definition of the degree of polarization (99), a positive (negative) value of P corresponds to the predominant emission of ordinary (extraordinary) waves.

A point of importance for astrophysical applications is that the degree of polarization (99) at a given frequency is determined almost exclusively by the strength of the magnetic field (more precisely, its longitudinal component). In principle, we thus have a method to measure the magnetic field in radiation sources, e.g., in solar flares.

Quasi-transverse motion. Now we consider quasi-transverse motion of the particle with respect to the magnetic field:

$$\cos^2\theta \ll u\,. \quad (100)$$

Using expansions as in the preceding case, we find

$$I_{\mathrm{o},\omega} = \frac{I_\omega^{\mathrm{tr}}}{2}\left(1+4\cot^2\theta+\frac{\nu\cos^2\theta}{1+\omega^2/\omega_\mathrm{p}^2\gamma^2}\right), \quad (101)$$

$$I_{\mathrm{e},\omega} = \frac{I_\omega^{\mathrm{tr}}}{2}\left(1+2u-4\cot^2\theta-\frac{\nu u\sin^2\theta}{1+\omega^2/\omega_\mathrm{p}^2\gamma^2}\right). \quad (102)$$

Here, the ordinary wave is almost linearly polarized along the magnetic field, while the extraordinary wave is elliptically polarized, in the plane perpendicular to the magnetic field. For $\theta=\pi/2$ the quantity $I_{\mathrm{o},\omega}$ is exactly half the radiation intensity in an isotropic plasma, since the electric field of the ordinary wave is directed strictly along the external magnetic field, so the field has no effect on the radiation and propagation of the ordinary waves. The degree of polarization is

$$P = -u+4\cot^2\theta+\frac{\nu(\cos^2\theta+u\sin^2\theta)}{2(1+\omega^2/\omega_\mathrm{p}^2\gamma^2)}\,. \quad (103)$$

In the case of strictly transverse motion ($\cos\theta=0$), this expression reduces to

$$P = -\left(\frac{\omega_{Be}}{\omega}\right)^2\left[1-\frac{\nu}{2(1+\omega^2/\omega_\mathrm{p}^2\gamma^2)}\right]. \quad (104)$$

In contrast to Eqn (96), the polarization is now inverse quadratic over the magnetic field and for the typical values $1<\nu<2$ we have $P<0$. In other words, the extraordinary waves predominate, as before. The reason for the quadratic (rather than linear) dependence of the degree of polarization on the magnetic field is that the polarization is now dominated by the respective transverse current, rather than by the Hall current of the plasma electrons.

Strong gyrotropy, motion along the magnetic field. Let us consider the condition opposite to Eqn (19) that corresponds to strong gyrotropy. For $\sin\theta = 0$ we have

$$n_{\mathrm{o,e}}^2 = 1 \mp \frac{v}{\sqrt{u} \pm 1}\,, \qquad K_{\mathrm{o,e}} = \mp 1\,, \qquad \gamma_{\mathrm{o,e}} = 0\,, \tag{105}$$

i.e., the normal modes are circularly polarized. The refractive indices under the condition $\sqrt{u} \gg 1$ are

$$n_{\mathrm{o,e}}^2 = 1 \mp \frac{\omega_{\mathrm{p}}^2}{\omega_{Be}\omega}\,. \tag{106}$$

When we substitute Eqns (105), (106) into Eqns (94), (95), the contributions to the emission of the ordinary wave through a virtual extraordinary wave and vice versa vanish exactly. The spectral-angular distribution of the radiation of the normal modes is

$$I_{\mathbf{n},\omega}^{(\mathrm{o,e})} = \frac{4\pi(\nu-1)}{\nu}\,\frac{e^4Q^2\langle\Delta N^2\rangle}{cm^2\omega^3}\left(\frac{\omega}{\omega_{Be}}\right)^2 \times \frac{\vartheta^2(2k_0c/\omega)^{\nu-1}\Theta(\vartheta^2+\gamma^{-2}\pm\omega_{\mathrm{p}}^2/\omega_{Be}\omega)}{(\vartheta^2+\gamma^{-2}\pm\omega_{\mathrm{p}}^2/\omega_{Be}\omega)^{\nu+2}}\,. \tag{107}$$

Here the Θ function is the unit step function. It has been introduced into the numerator because for

$$\gamma^{-2} - \frac{\omega_{\mathrm{p}}^2}{\omega_{Be}\omega} < 0 \tag{108}$$

the Cherenkov condition for the radiation of (slow) extraordinary waves (the so called Z mode) is satisfied. For

$$\vartheta^2 + \gamma^{-2} - \frac{\omega_{\mathrm{p}}^2}{\omega_{Be}\omega} = 0 \tag{109}$$

expression (107) for the extraordinary wave diverges. There is a simple physical basis for this divergence. The matter is, under condition (108), the electric field of a particle moving through a gyrotropic medium has two components: a quasi-stationary intrinsic field and a radiation field (Cherenkov radiation). The scattering of the quasi-stationary field (in other words, the scattering of the virtual photons emitted by the particle) occurs over a finite distance, equal to the formation zone of the transition radiation [19]. There is also a scattering of propagating Cherenkov photons by irregularities of the medium. In an infinite, transparent medium, however, the distance over which the photons interact with irregularities is infinite. This is the reason for these divergences.

Under actual conditions, the intensity of the scattered Cherenkov radiation is affected by the spatial size of the system and by the mean free path of the photons. The respective contribution to the total radiation intensity can be easily found for a specific problem (see Section 4.3). Here, we restrict the discussion to the proper transition radiation, which we regard as the result of a conversion of the quasi-stationary (virtual) field of the particle into electromagnetic radiation on irregularities of the medium [19]. We just mention to finalize the matter at the moment, that when a particle moves through a plate with the Vavilov–Cherenkov condition satisfied in it [28], the respective contribution is simply the result of repeated refraction and reflection of the Cherenkov radiation at the boundaries.

An important difference between Eqn (107) and the radiation intensity in an isotropic medium is the small factor $(\omega/\omega_{Be})^2$. This factor appears because the radiation is dominated in this case by the Hall component of the plasma current, which is described by the off-diagonal terms of the tensor $\chi_{\alpha\beta}$ (78). The reason is that the transverse field of the relativistic particle does not contain any component along the magnetic field in this geometry. Accordingly, in strong fields, as $(\omega/\omega_{Be})^2 \to 0$, the transition radiation associated with the longitudinal electric field of the relativistic particle may become important (this is the radiation through a virtual longitudinal wave). This field is

$$\mathbf{E}_{\omega,\mathbf{k}}^{Q,l} = -\frac{4\pi\mathrm{i}Qc\delta(\omega-\mathbf{kv})}{(2\pi)^3\omega\varepsilon_l(\omega)}\,\frac{\mathbf{B}}{B}\,. \tag{110}$$

Calculating the plasma current excited by the field (110) along the magnetic field, we find the radiation intensity, as has been done in deriving Eqns (94), (95):

$$I_{\mathbf{n},\omega,l}^{(\mathrm{o,e})} = \frac{4\pi(\nu-1)}{\nu}\,\frac{e^4Q^2\langle\Delta N^2\rangle}{cm^2\omega^3\varepsilon_l^2}\,\frac{\vartheta^2(2k_0c/\omega)^{\nu-1}}{(\vartheta^2+\gamma^{-2}\pm\omega_{\mathrm{p}}^2/\omega_{Be}\omega)^{\nu}}\,. \tag{111}$$

The comparison of expressions (107) and (111) shows that for

$$\gamma < \left(\frac{\omega_{Be}}{\omega_{\mathrm{p}}}\right)^{1/2} \tag{112}$$

the radiation (111) through the longitudinal field dominates at frequencies

$$\omega_{\mathrm{p}} < \omega < \omega_{Be}\gamma^{-2}\,, \tag{113}$$

while the radiation (107) through the transverse field dominates at higher frequencies. Note that no Cherenkov radiation appears at any frequency under condition (112). However, the intensity (111) diverges, when $\omega \to \omega_{\mathrm{p}}$, since the condition for Cherenkov emission of longitudinal waves (Langmuir plasma waves) begins to hold (Section 3 discusses the respective regularization method in detail).

Integrating Eqns (107), (111) over angle, we find the respective emission spectra. It occurs that the integration over $\mathrm{d}\vartheta^2$ in Eqn (111) cannot be carried out between infinite limits, since the result turns out to be infinite. Hence, the radiation through a virtual longitudinal wave does not display strong directivity along the velocity of the particle anymore. However, expression (111) is valid only in a small interval of angles with respect to the magnetic field, since in deriving this expression we used the specific expressions (105), (106) for the refractive indices and the polarization vectors of the normal modes. To get a feeling of the magnitudes involved, we estimate the radiation intensity (111) within an angle $\vartheta_* = \gamma^{-1}$ under condition (112):

$$I_{\omega,l}^{(\mathrm{o,e})} \sim \frac{4\pi^2(\nu-1)}{\nu}\,\frac{e^4Q^2\langle\Delta N^2\rangle}{cm^2\omega^3}\,\frac{(2k_0c/\omega)^{\nu-1}}{(\gamma^{-2}\pm\omega_{\mathrm{p}}^2/\omega_{Be}\omega)^{\nu-2}}\,. \tag{114}$$

The integration of Eqn (107) can be carried out between infinite limits, because of the rapid convergence:

$$I_{\omega}^{(\mathrm{o,e})} = \frac{4\pi^2(\nu-1)}{\nu^2(\nu+1)}\,\frac{e^4Q^2\langle\Delta N^2\rangle}{cm^2\omega^3}\left(\frac{\omega}{\omega_{Be}}\right)^2\frac{(2k_0c/\omega)^{\nu-1}}{(\gamma^{-2}\pm\omega_{\mathrm{p}}^2/\omega_{Be}\omega)^{\nu}}\,. \tag{115}$$

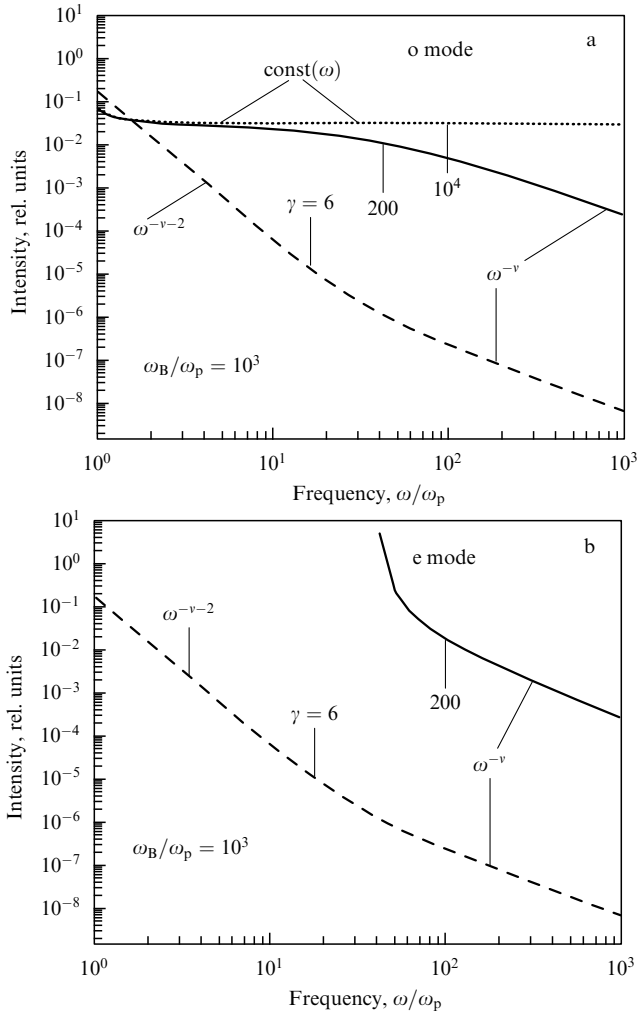

Figure 4. Transition radiation spectra of ordinary (a) and extraordinary (b) waves when a relativistic particle is moving along the magnetic field in highly gyrotropic plasma. The presented values of the particle Lorentz factor (6, 200, 10^4) correspond to the regions $\gamma < (\omega_{Be}/\omega_p)^{1/2} = 31.6$, $(\omega_{Be}/\omega_p)^{1/2} < \gamma < \omega_{Be}/\omega_p = 10^3$, $\gamma > \omega_{Be}/\omega_p$. The spectra of extraordinary waves are plotted only if the Vavilov – Cherenkov condition is not fulfilled.

Thus, $I_\omega^{(o,e)} \sim \omega^{-\nu-2}$ at frequencies $\omega_p \ll \omega \ll \omega_{Be}\gamma^{-2}$ and $I_\omega^{(o,e)} \sim \omega^{-\nu}$ at frequencies $\omega_{Be}\gamma^{-2} \ll \omega \ll \omega_{Be}$ under condition (112) (the dashed curves in Fig. 4, $\omega_{Be}/\omega_p\gamma^2 \approx 28$ is accepted).

For higher-energy particles

$$\left(\frac{\omega_{Be}}{\omega_p}\right)^{1/2} < \gamma < \frac{\omega_{Be}}{\omega_p} \tag{116}$$

the radiation through the longitudinal wave is unimportant. There is a frequency interval in which the condition for Cherenkov radiation is fulfilled. We consider only that region of parameters in which this condition does not hold. For the ordinary wave, this region covers the full frequency range, while for the extraordinary wave it covers the only frequencies

$$\omega > \frac{\omega_p^2}{\omega_{Be}}\,\gamma^2\,. \tag{117}$$

Expression (115) remains valid for these cases [the solid line in Fig. 4b; the line is plotted for the parameters providing the dimensionless separating frequency $(\omega_p/\omega_{Be})\gamma^2 = 40$]. Ordinary wave radiation displays a spectrum composed of two power-law regions: $I_\omega^{(o)} \sim \omega^{-\nu}$ under condition (117) and $I_\omega^{(o)} \sim \text{const}(\omega)$ in the opposite case (the solid line in Fig. 4a).

If $\gamma > \omega_{Be}/\omega_p$, the intensity of the ordinary-wave radiation is constant over the entire frequency interval $\omega_p \ll \omega \ll \omega_{Be}$ (the dotted line in Fig. 4a), while the extraordinary waves are generated by the Cherenkov mechanism here. The intensity of Vavilov – Cherenkov emission (of extraordinary waves) considerably exceeds the intensity of transition radiation (of ordinary waves) at the same frequencies under condition (76), their ratio is

$$\frac{I^{\text{tr(o)}}}{I^{\text{VC(e)}}} \sim \left(\frac{\omega_{Be}}{\omega_p}\right)^{\nu-1} \frac{\langle \Delta N^2\rangle}{N^2}\,. \tag{118}$$

It is worthwhile to consider transition radiation of extraordinary waves only outside the Cherenkov angle, i.e., at $\vartheta > \vartheta_* = \omega_p^2/\omega_{Be}\omega$. As ϑ approaches ϑ_*, the intensity of the transition radiation diverges. Kapitza [54] reported a similar divergence to occur as the respective parameters of the system approach the Cherenkov threshold, back in 1960. The matter is that a virtual photon becomes progressively more 'similar' to a real photon as the Cherenkov threshold is approaching. At the threshold, the mean free path of the photon becomes infinite, and the virtual photon itself becomes the real Cherenkov photon. Under real conditions, this divergence may be restricted by accounting for the following factors: the finite size of the main scale of the inhomogeneities, L_0; the curvature of the particle trajectory; the finite size of the medium and the energy losses in the medium. An example of such a calculation is given at Section 4.3, which could be generalized to this case as well.

Strong gyrotropy, motion across the magnetic field. We consider the motion of a particle across the magnetic field, $\cos\theta = 0$. The curvature of the trajectory of a relativistic particle [19, 29] may in general have an important effect on the spectrum of the transition radiation in this case. However, there is a certain range in which the approximation of rectilinear motion is applicable for protons and heavier nuclei; this range is determined later on.

The refractive indices for normal modes in the case $\cos\theta = 0$ are

$$n_o^2 = 1 - \frac{\omega_p^2}{\omega^2}\,, \qquad n_e^2 = 1 + \frac{\omega_p^2}{\omega_{Be}^2}\,. \tag{119}$$

The spectral-angular distribution of the ordinary waves is

$$I_{\mathbf{n},\omega}^{(o)} = \frac{8\pi(\nu-1)}{\nu}\,\frac{e^4Q^2\langle\Delta N^2\rangle}{cm^2\omega^3}\,\frac{(2k_0c/\omega)^{\nu-1}\vartheta^2\sin^2\phi}{(\vartheta^2+\gamma^{-2}+\omega_p^2/\omega^2)^{\nu+2}}\,. \tag{120}$$

The factor $\sin^2\phi$ provides the directivity pattern to be elongated along the magnetic field. The spectral distribution of the radiation in this case is

$$I_\omega^{(o)} = \frac{4\pi^2(\nu-1)}{\nu^2(\nu+1)}\,\frac{e^4Q^2\langle\Delta N^2\rangle}{cm^2\omega^3}\,\frac{(2k_0c/\omega)^{\nu-1}}{(\gamma^{-2}+\omega_p^2/\omega^2)^{\nu}} \tag{121}$$

that is half of the total intensity of the transition radiation in an isotropic medium. The magnetic field has absolutely no effect on expressions (120), (121), since the direction of the electric field in the wave is the same as the direction of the external magnetic field.

The angular distribution found from Eqn (95) for the extraordinary wave radiation is

$$I^{(e)}_{\mathbf{n},\omega} = \frac{8\pi(\nu-1)}{\nu}\,\frac{e^4Q^2\langle\Delta N^2\rangle}{cm^2\omega^3}\left(\frac{\omega}{\omega_{Be}}\right)^4 \times \frac{(2k_0c/\omega)^{\nu-1}\vartheta^2\cos^2\phi}{(\vartheta^2+\gamma^{-2}-\omega_p^2/\omega_{Be}^2)^{\nu+2}}\,. \tag{122}$$

The respective directivity pattern is elongated perpendicular to the magnetic field. It is clear from the above discussion, that we consider the radiation only by the particles whose energy is not too high,

$$\gamma < \frac{\omega_{Be}}{\omega_p}\,, \tag{123}$$

and the Vavilov–Cherenkov condition is not satisfied. Condition (123) allows us to neglect the term $(\omega_p/\omega_{Be})^2$ in comparison with γ^{-2} in the denominator in Eqn (122). For the radiation spectrum we find

$$I^{(e)}_{\omega} = \frac{4\pi^2(\nu-1)}{\nu^2(\nu+1)}\,\frac{e^4Q^2\langle\Delta N^2\rangle}{cm^2\omega_{Be}^4}\,\omega\gamma^{2\nu}\left(\frac{2k_0c}{\omega}\right)^{\nu-1}. \tag{124}$$

According to this expression, the radiation by particles of any energies within the range (123) increases (in the frequency interval $\omega_p \ll \omega \ll \omega_{Be}$) according to the law:

$$I^{(e)}_{\omega} \sim \omega^{2-\nu} \tag{125}$$

if $\nu < 2$. The ordinary-wave radiation behaves differently: the spectrum (121) decreases slowly, $I^{(o)}_{\omega} \sim \omega^{\nu-2}$, at frequencies $\omega_p \ll \omega \ll \omega_p\gamma$ and then falls off sharply, $I^{(o)}_{\omega} \sim \omega^{-\nu-2}$, at higher frequencies. Comparing Eqns (121) and (124), we conclude the ordinary wave radiation to dominate except for a narrow frequency region near ω_{Be}.

Motion at an arbitrary angle. We turn now to the properties of the transition radiation of the normal modes when the particle is moving at an arbitrary angle with respect to the magnetic field. We start with the angular distribution of the transition radiation, based on the general expressions (94), (95).

Figure 5a displays a typical directivity pattern for the ordinary wave as the relativistic particle is moving at any (but not too small) angle with respect to the external magnetic field. The distribution is obviously elongated along the projection of the magnetic field onto the plane of the figure. The directivity pattern has such a simple shape because the ordinary-wave radiation due to the scattering of the virtual extraordinary wave is always small in comparison with the main contribution, coming from the scattering of the virtual ordinary wave.

For extraordinary waves, however, the radiation through a virtual ordinary wave may be very important. For example, Fig. 5b–d displays the directivity patterns for the intensity of extraordinary waves generated by a particle with $\gamma = 5$ at a frequency $\omega = 5\omega_p$ for various magnetic fields $\omega_{Be}/\omega_p = 300$, 500, 700. For the first case, the emission is provided by the scattering of the virtual extraordinary wave (the pattern is elongated in the direction transverse with respect to the magnetic field). In the second case the two components are comparable, and in the third the component arising from the virtual ordinary wave dominates. This results in the ordinary-wave radiation, integrated over angles, depending only on its own refractive index, while the

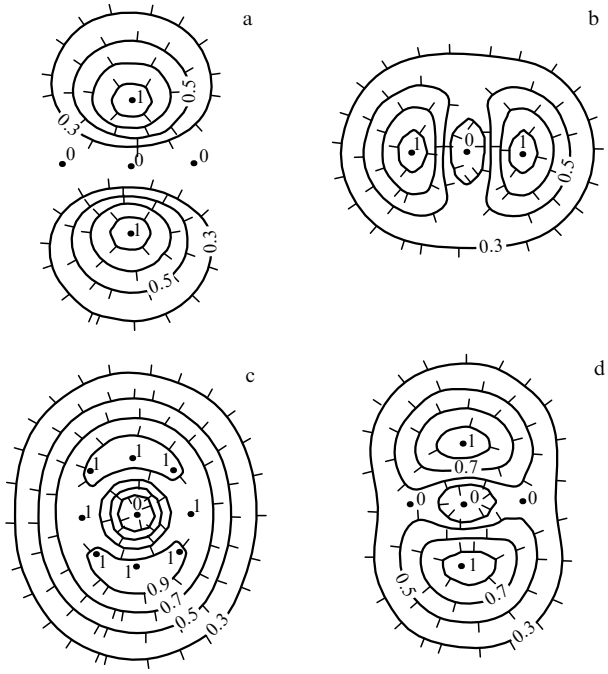

Figure 5. Directivity patterns of transition radiation of normal modes for $\gamma = 5$, $\omega/\omega_p = 5$, $\theta = \pi/4$: (a) o wave, (b) e wave, $\omega_{Be}/\omega_p = 300$, (c) e wave, $\omega_{Be}/\omega_p = 500$, (d) e wave, $\omega_{Be}/\omega_p = 700$.

intensity of the extraordinary waves generally depends on the refractive indices of both normal modes. In this regard the transition radiation is quite different from radiation of other types (e.g., Cherenkov radiation [38, 40] and magneto-bremsstrahlung [51]), for which the intensity of each normal mode is determined exclusively by the refractive index corresponding to the very same mode. This property of the transition radiation has the same physical origin as the mutual conversion of normal modes in a gyrotropic plasma [52].

Let us consider the spectral distribution of the radiation intensity. When expressions (94), (95) are integrated over angles, the terms containing $\cos 2\phi$ vanish (these terms describe the interference between two components of the radiation). Ignoring the small component of the intensity of the ordinary-wave radiation associated with n_e, we find

$$I^{(o)}_{\omega} = \frac{4\pi^2(\nu-1)}{\nu^2(\nu+1)}\,\frac{e^4Q^2\langle\Delta N^2\rangle}{cm^2\omega^3}\left(\frac{2k_0c}{\omega}\right)^{\nu-1} \times \frac{\left[(\cos^2\theta - 2K_e\sqrt{u}\cos\theta + K_e^2)/(1-u) + \sin^2\theta\right]^2}{\left[\gamma^{-2}+2(1-n_o)\right]^{\nu}(1+K_e^2)^2} \tag{126}$$

for the ordinary wave and

$$I^{(e)}_{\omega} = \frac{4\pi^2(\nu-1)}{\nu^2(\nu+1)}\,\frac{e^4Q^2\langle\Delta N^2\rangle}{cm^2\omega^3}\,\frac{(2k_0c/\omega)^{\nu-1}}{\left[\gamma^{-2}+2(1-n_e)\right]^{\nu}(1+K_e^2)^2} \times \left\{\left(\frac{1+2K_e\sqrt{u}\cos\theta+K_e^2\cos^2\theta}{1-u}+K_e^2\sin^2\theta\right)^2 + \left[\frac{(1-K_e^2)\sqrt{u}\cos\theta - uK_e\sin^2\theta}{1-u}\right]^2 \times F\left[2,\nu,\nu+2;1-\frac{\gamma^{-2}+2(1-n_o)}{\gamma^{-2}+2(1-n_e)}\right]\right\} \tag{127}$$

for the extraordinary wave. Here $F(2, v, v+2; 1-z)$ is the hypergeometric function.

Let us first find the asymptotic behavior of Eqns (126), (127) at $u \gg 1$. More precisely, we assume

$$\frac{4\cos^2\theta}{u\sin^4\theta} \ll 1\,. \tag{128}$$

For the refractive indices and the polarization vectors we then find

$$\begin{aligned} &2(1-n_\mathrm{o}) = \frac{\omega_\mathrm{p}^2}{\omega^2}\sin^2\theta\,, \qquad 2(1-n_\mathrm{e}) = -\frac{\omega_\mathrm{p}^2}{\omega_{Be}^2\sin^2\theta}\,,\\ &K_\mathrm{o} \approx -\sqrt{u}\,\frac{\sin^2\theta}{\cos\theta}\,, \qquad K_\mathrm{e} \approx \frac{\cos\theta}{\sqrt{u}\,\sin^2\theta}\,. \end{aligned} \tag{129}$$

Since the condition for Cherenkov radiation of extraordinary waves is fulfilled for particles with $\gamma > \omega_{Be}\sin\theta/\omega_\mathrm{p}$, we consider only particles with lower energies. In this case the argument z of the hypergeometric function in Eqn (127) is restricted as $|z| \geqslant 1$. We can thus approximate the function F by the analytic expression [55]:

$$F(2, v, v+2; 1-z) \approx \left[1 + \frac{z^v - 1}{\Gamma(2+v)\Gamma(2-v)}\right]^{-1}. \tag{130}$$

Substituting Eqn (129) into Eqn (126), and retaining only the largest terms under condition (128), we find

$$I_\omega^{(\mathrm{o})} = \frac{4\pi^2(v-1)}{v^2(v+1)}\,\frac{e^4Q^2\langle\Delta N^2\rangle}{cm^2\omega^3}\,\frac{(2k_0c/\omega)^{v-1}\sin^4\theta}{(\gamma^{-2} + \omega_\mathrm{p}^2\sin^2\theta/\omega^2)^v}\,. \tag{131}$$

This expression differs from that for an isotropic plasma (or for strictly transverse motion of the particle) in the factor $\sin^2\theta$ in the dispersion law for the ordinary waves, and the factor $\sin^4\theta$ in the numerator in Eqn (131). The latter factor describes the projection of the electric field of the ordinary wave onto the external magnetic field.

Figure 6a displays a set of ordinary-wave radiation spectra plotted using Eqn (126) for various angles θ. Obviously, the magnetic field provides no qualitative change in the radiation of the ordinary waves.

Respectively, the transition radiation of extraordinary waves is

$$\begin{aligned} I_\omega^{(\mathrm{e})} = {}& \frac{4\pi^2(v-1)}{v^2(v+1)}\,\frac{e^4Q^2\langle\Delta N^2\rangle}{cm^2\omega^3}\,\gamma^{2v}\left(\frac{2k_0c}{\omega}\right)^{v-1}\\ &\times\left[\frac{1}{u^2\sin^4\theta} + \frac{v^2\cos^2\theta}{u}\,F\left(2, v, v+2; -\frac{\omega_\mathrm{p}^2\gamma^2\sin^2\theta}{\omega^2}\right)\right]. \end{aligned} \tag{132}$$

Taking expression (130) into account, we can easily analyze this expression in various frequency regions. At $\omega \ll \omega_\mathrm{p}\gamma\sin\theta$, we have

$$\begin{aligned} I_\omega^{(\mathrm{e})} = {}& \frac{4\pi^2(v-1)}{v^2(v+1)}\,\frac{e^4Q^2\langle\Delta N^2\rangle}{cm^2\omega^3}\left(\frac{2k_0c}{\omega}\right)^{v-1}\\ &\times\left[\frac{\omega^4\gamma^{2v}}{\omega_{Be}^4\sin^4\theta} + \frac{\Gamma(2+v)\Gamma(2-v)\omega_\mathrm{p}^{4-2v}\omega^{2(v-1)}\cos^2\theta}{\omega_{Be}^2\sin^{2v}\theta}\right]. \end{aligned} \tag{133}$$

The second term, which is associated with the radiation through the virtual ordinary wave, may become dominant at low frequencies, close to ω_p (the mutual transformation of the normal modes in a plasma occurs at the very same frequencies). In the opposite limit,

$$\omega_\mathrm{p}\gamma\sin\theta \ll \omega \ll \omega_{Be}\,, \tag{134}$$

the spectrum is

$$\begin{aligned} I_\omega^{(\mathrm{e})} = {}& \frac{4\pi^2(v-1)}{v^2(v+1)}\,\frac{e^4Q^2\langle\Delta N^2\rangle}{cm^2\omega^3}\,\gamma^{2v}\left(\frac{2k_0c}{\omega}\right)^{v-1}\frac{\omega^4}{\omega_{Be}^4\sin^4\theta}\\ &\times\left(1 + \frac{\omega_\mathrm{p}^4\omega_{Be}^2}{\omega^6}\cos^2\theta\sin^4\theta\right). \end{aligned} \tag{135}$$

The second term may dominate for particles with low energy, at low frequencies [but satisfying Eqn (134)]. Figure 6b displays a set of extraordinary-wave spectra for $\omega_{Be}/\omega_\mathrm{p} = 300$, $\theta = \pi/4$, and various γ. With increasing radiation frequency and/or with increasing energy of the particle, the component of the radiation through the virtual ordinary wave becomes less important. This conclusion agrees with the fact that the mutual conversion of normal modes in a gyrotropic medium occurs most efficiently for the parameter region $\omega_\mathrm{p}/\omega \approx 1$.

Figure 6c displays a set of extraordinary-wave radiation spectra for the same parameters as in Fig. 6a. For $\omega < \omega_{Be}$, the transition radiation differs drastically from that in the case of an isotropic plasma. Indeed, the radiation intensity decreases with decreasing frequency, $I_\omega^{(\mathrm{e})} \sim \omega^{2-v}$, instead of increasing, as it does for an ordinary wave, $I_\omega^{(\mathrm{o})} \sim \omega^{v-2}$.

Figure 6d displays the polarization of the radiation for the same parameter values. The ordinary wave is predominantly radiated in the frequency range $\omega_\mathrm{p} < \omega < \omega_{Be}$, while it is predominantly the extraordinary wave at $\omega > \omega_{Be}$. The frequency dependence of the polarization is quadratic for $\theta = \pi/2$, while it is linear for other angles.

Although the radiation of ordinary waves is usually more efficient at $\omega < \omega_{Be}$, this may not always be the case. For example, Fig. 6e displays the radiation spectra for ordinary and extraordinary waves as the parameter values approach the Cherenkov threshold. In this case, the radiation of extraordinary waves may be several orders of magnitude more intense than the radiation of ordinary waves at certain frequencies. These curves are plotted with the use of Eqns (126), (127), which ignore all the effects that could restrict the enhancement of the radiation.

Discussion of the gyrotropy effect. Transition radiation in magnetized plasma reveals some new features. In particular, divergent expressions appear under certain conditions, e.g., when the condition for Cherenkov radiation is fulfilled for either the extraordinary wave or plasma wave. This happens because the probability of the scattering of the Cherenkov photon over an infinite distance (in a boundless transparent medium) is unity. This divergence can be regularized when specific bound media are analyzed.

Then, an anomalous enhancement of the radiation (of extraordinary waves) may occur as the Cherenkov threshold approaches (but when the Cherenkov condition has not yet become satisfied). A similar enhancement was discovered long ago [54]; it is provided by the increase of the formation zone of radiation as the Cherenkov threshold approaches (virtual photons become almost real ones). Nevertheless, the

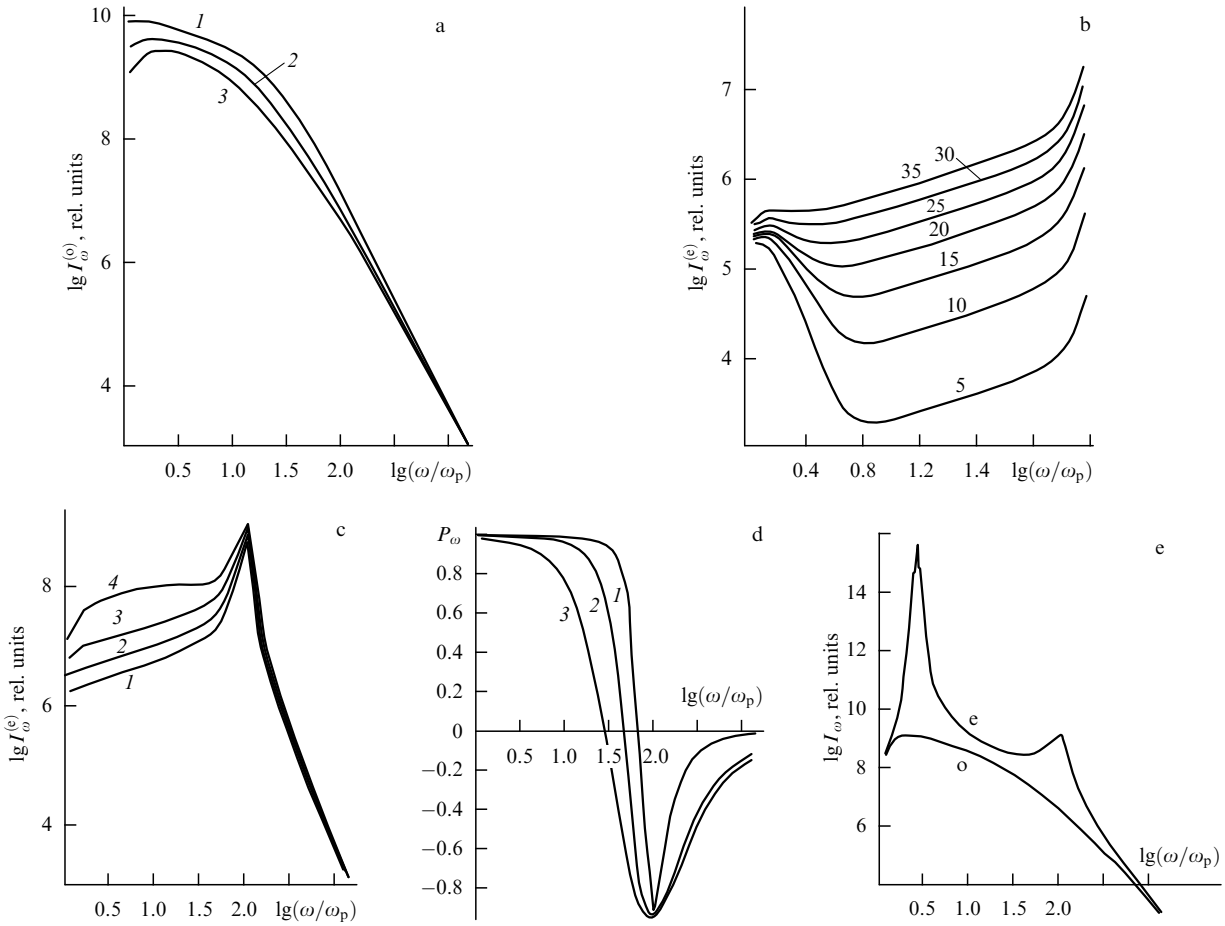

Figure 6. (a) Set of transition radiation spectra of ordinary waves for various pitch angles of the relativistic particle for the parameter values: $\gamma = 25$, $\omega_{Be}/\omega_p = 100$. (*1*) $\theta = \pi/2$, (*2*) $\theta = \pi/4$, (*3*) $\theta = \pi/6$. (b) Set of transition radiation spectra of extraordinary waves for various values of the energy of the relativistic particle for the parameter values: $\omega_{Be}/\omega_p = 300$, $\theta = \pi/4$. The radiation intensity increases with Lorentz-factors (labels at the curves). (c) Set of transition radiation spectra of extraordinary waves for various pitch angles of the relativistic particle for the parameter values: $\gamma = 25$, $\omega_{Be}/\omega_p = 100$. (*1*) $\theta = \pi/2$, (*2*) $\theta = \pi/3$, (*3*) $\theta = \pi/4$, (*4*) $\theta = \pi/6$. (d) Polarization of the transition radiation versus the frequency for various pitch angles of the particle for the parameter values: $\gamma = 25$, $\omega_{Be}/\omega_p = 100$. (*1*) $\theta = \pi/2$, (*2*) $\theta = \pi/4$, (*3*) $\theta = \pi/6$. $P > 0$ corresponds to ordinary waves, $P < 0$ corresponds to extraordinary waves. (e) Transition radiation spectra of ordinary and extraordinary waves as the threshold for Cherenkov generation of extraordinary waves approaches. Here the parameters are $\gamma = 25$, $\omega_{Be}/\omega_p = 100$, $\theta = \pi/15$.

increase in the radiation may be limited by many factors under actual conditions: the finite size of the basic length scale of the plasma density inhomogeneities, the curvature of the particle trajectory, the deceleration of the particle in the plasma, etc.

Furthermore, the expressions for the extraordinary waves diverge as $\omega_{Be}/\omega \to 1$, i.e., at the cyclotron resonance. The cold-plasma approximation, which we have used here, is well known [49] to be incorrect in this region. A correct description would require consideration of the thermal motion of the plasma particles (spatial dispersion). We have not included the spatial dispersion, since the approach presented here becomes incorrect before the spatial dispersion effects become important. The matter is that, as the cyclotron resonance is approaching, the condition

$$|1 - n_e^2| \ll 1 \tag{136}$$

becomes violated at a certain frequency. Hence, the phase velocity of the normal mode starts to differ strongly from the velocity of light in vacuum, c. Consequently, the distinctive features characterizing the radiation by relativistic particles fade away; in particular, there is no longer the sharp directivity of the radiation along the direction of the particle velocity. For this reason, the peaks in the region $\omega \approx \omega_{Be}$ in Fig. 6c, e do not have a quantitative sense; they merely indicate the presence of certain peculiarities there. Actually, the entire analysis of the transition radiation in this region should be done differently (we should also note that extraordinary waves cannot propagate at all in a magnetized plasma in the narrow frequency region

$$\omega_{Be}\left(1 + \frac{\omega_p^2 \sin^2\theta}{2\omega_{Be}^2}\right) < \omega < \omega_{Be}\left(1 + \frac{\omega_p^2}{\omega_{Be}^2}\right).$$

However, such an analysis would not seem to be particularly interesting for applications, since more intense cyclotron radiation is generated at $\omega \approx \omega_{Be}$.

The applicability region. Let us consider when the approximation of the rectilinear motion of the relativistic particle is valid. According to Section 2.2, transition radiation by electrons moving along a helix is strongly suppressed under the condition

$$\gamma > \frac{\omega_p}{\omega_{Be} \sin\theta}. \tag{137}$$

The transition radiation by electrons is thus described by the equations obtained here in weakly gyrotropic plasma and for quasi-longitudinal motion. The situation is more favorable for the radiation by protons and other heavy particles. According to the preceding sections, the curvature of the particle trajectory strongly influences the transition radiation (namely, it suppresses this radiation) if the particle turns through an angle larger than the characteristic angle of the emission cone at a distance equal to the coherence length of the radiation. Thus, the approximation of rectilinear motion of the heavy particles is correct if

$$\frac{2c}{\omega}\left[\gamma^{-2}+2(1-n_j)\right]^{-1} < 2c\left(\frac{\gamma^2}{\omega\omega_{B\mathrm{p}}^2\sin\theta}\right)^{1/3}, \tag{138}$$

or, more compactly,

$$\left(\frac{\omega_{B\mathrm{p}}\sin\theta}{\omega\gamma}\right)^{2/3} < \gamma^{-2}+2(1-n_j)\,. \tag{139}$$

For estimates we consider the least favorable case, in which the particle is moving strictly transversely to the magnetic field. For ordinary waves we then find the same applicability condition as before:

$$\gamma < \frac{\omega_{\mathrm{p}}}{\omega_{B\mathrm{p}}}\,. \tag{140}$$

For extraordinary waves we find [with the use of Eqn (123)]

$$\omega > \omega_* = \omega_{B\mathrm{p}}\gamma^2\,. \tag{141}$$

The curvature of the trajectory thus does not affect the radiation of extraordinary waves at any frequency if

$$\gamma < \left(\frac{\omega_{\mathrm{p}}}{\omega_{B\mathrm{p}}}\right)^{1/2}. \tag{142}$$

At

$$\gamma < \left(\frac{\omega_{B\mathrm{e}}}{\omega_{B\mathrm{p}}}\right)^{1/2} = \left(\frac{m_{\mathrm{p}}}{m_{\mathrm{e}}}\right)^{1/2} \approx 43 \tag{143}$$

the curvature of the trajectory is unimportant at frequencies $\omega_* < \omega < \omega_{B\mathrm{e}}$ but is essential at lower frequencies. However, the suppression of the extraordinary-wave radiation at $\omega < \omega_*$ has only a slight effect on the total energy of the transition radiation in magnetized plasma. Assuming the parameters typical for solar flares, we find that conditions (140)–(143) are usually satisfied, since the energies of the protons produced even by the most powerful flares are rarely in excess of 20 GeV [56] ($\gamma \sim 20$). In the laboratory, on the other hand, one could apparently arrange various regimes for transition radiation, in particular, when the curvature of the trajectory of the heavy particles is important.

Thus, the ordinary and extraordinary waves are generated in magnetized plasma quite differently, which, particularly, results in highly polarized radiation. When a particle moves along the magnetic field, the transition radiation decreases significantly at frequencies $\omega/\omega_{B\mathrm{e}} < 1$ due to suppression of the transverse motion of the plasma electrons by the magnetic field. In the case of transverse motion of a relativistic particle (a proton), ordinary waves are emitted considerably more efficiently than extraordinary waves (for $\omega_{B\mathrm{e}}/\omega_{\mathrm{p}} \gg 1$). The transition radiation by electrons moving transversely to the magnetic field is suppressed strongly by the curvature of the trajectories of the electrons. At frequencies $\omega/\omega_{B\mathrm{e}} > 1$, the polarization of the radiation can be rather high as well. The degree of polarization depends mainly on the magnetic field strength in this case. This could be used for finding an independent estimate of magnetic fields, e.g., by observing the radio emission from solar flares.

3. Transition radiation generated by particles with arbitrary energy

Section 2 studies in detail the transition radiation (TR) generated by ultra-relativistic particles under various conditions. In particular, TR has been found to be produced effectively by relatively low-energy particles with

$$\gamma < \frac{\omega_{\mathrm{p}}}{\omega_B}\,, \tag{144}$$

where $\gamma = E/Mc^2$ is the Lorentz factor of particle, ω_{p} is the plasma frequency, and $\omega_B = QB/Mc$ is the gyrofrequency of the particle. Natural plasmas frequently contain a broad spectrum of charged particles, falling with energy, e.g., $\mathrm{d}N_{\mathrm{e}} \propto N_{\mathrm{e}}E^{-\xi}\,\mathrm{d}E$. Emission by moderately- and non-relativistic particles can appear to be essential in this case. This section calculates the TR emitted by charged particles with arbitrary (i.e., not necessarily relativistic) energy in a plasma with a broad spectrum of random density inhomogeneities (35).

Along with the spectral and angular distributions of the radiation intensity by a charge of arbitrary energy, we also derive the emissivity of an ensemble of particles with a power-law spectrum as well as coefficients of transition absorption (or amplification), which is important for the purpose of application.

3.1 Transition radiation in isotropic plasma

As has been discussed [28, 19], the source of the TR is the plasma electron current excited by the quasi-stationary field of a fast charged particle:

$$\mathbf{j}^m_{\omega,\mathbf{k}} = \frac{\mathrm{i}e^2}{m\omega}\int \mathrm{d}\mathbf{k}'\,\mathbf{E}^Q_{\omega,\mathbf{k}-\mathbf{k}'}\,\delta N_{\mathbf{k}'}\,, \tag{145}$$

where e and m are the electron charge and mass, $\delta N_{\mathbf{k}'}$ is the variation in the electron density of the medium, and $\mathbf{E}^Q_{\omega,\mathbf{k}-\mathbf{k}'}$ is the quasi-stationary electric field of the radiating particle. The field of the particle is defined from its current

$$\mathbf{j}^Q_{\omega,\mathbf{k}-\mathbf{k}'} = \frac{Q\mathbf{v}}{(2\pi)^3}\,\delta\left[\omega-(\mathbf{k}-\mathbf{k}')\mathbf{v}\right] \tag{146}$$

(Q is the particle charge and v is its velocity) with the use of the Green function. Now, in contrast to the ultra-relativistic limit (Section 2), we must take into account not only the transverse but also the longitudinal Green function [57, 58]. As a result the quasi-stationary field $\mathbf{E}^Q$ takes the form

$$E^{Q,\,i}_{\omega,\mathbf{k}-\mathbf{k}'} = \frac{4\pi\mathrm{i}q\delta\left[\omega-(\mathbf{k}-\mathbf{k}')\mathbf{v}\right]}{(2\pi)^3}\,\frac{\omega\left[v_i-(\mathbf{k}-\mathbf{k}')_i\,\omega/k^2\right]}{c^2\left[(\mathbf{k}-\mathbf{k}')^2-k^2\right]}\,. \tag{147}$$

The energy emitted by the current (145) at frequency ω in the direction $\mathbf{n}$ is described by the expression [similar to Eqn (24)]

$$\mathcal{E}_{\mathbf{n},\omega} = (2\pi)^6\,\frac{\omega^2}{c^3}\,\varepsilon^{1/2}\left\langle\left|\mathbf{n}\times\mathbf{j}^m_{\omega,\mathbf{k}}\right|^2\right\rangle, \tag{148}$$

where $\varepsilon = 1-\omega_{\mathrm{p}}^2/\omega^2$ is the dielectric permeability of the plasma. The account of the value $\varepsilon^{1/2}$ in Eqn (148) is a must,

since we intend to describe TR correctly at all frequencies $\omega \geqslant \omega_p$, also including $\omega \approx \omega_p$, where ε differs substantially from unity. The ultra-relativistic treatment is valid for relativistic particles $\gamma \gg 1$ at high frequencies $\omega \gg \omega_p$, where $\varepsilon \approx 1$.

Spectral-angular distribution of TR. The use of expressions (145)–(148) enables us to derive the distribution of the radiation intensity per unit frequency per unit solid angle:

$$I_{\mathbf{n},\omega} = \frac{8\pi e^4 q^2}{m^2 c^3 \omega^2 \varepsilon^{3/2}} \int d\mathbf{k}' \, |\delta N|^2_{\mathbf{k}'} \, \frac{\left([\mathbf{n}\times\mathbf{v}] + [\mathbf{n}\times\mathbf{k}']\omega/k^2\right)^2}{\left[(\mathbf{k}-\mathbf{k}')^2/k^2 - 1\right]^2} \times \delta\left[\omega - (\mathbf{k}-\mathbf{k}')\mathbf{v}\right] . \quad (149)$$

The integrand in Eqn (149) depends on all three dummy variables (including the azimuth angle φ' of the vector $\mathbf{k}'$). To perform the integration of Eqn (149) it is convenient to assume that the particle moves in the direction parallel to the z axis, while the vector $\mathbf{k}$ is in the (x,z) plane. Then the azimuth angle φ' is equal to the angle between the projection of the vector $\mathbf{k}'$ on the (x,y) plane and the x axis (the projection of the vector $\mathbf{n}$ on the same plane) (Fig. 7a). The radiation intensity (149) passes into

$$I_{\mathbf{n},\omega} = \frac{8\pi e^4 Q^2}{v m^2 c^3 \omega^2 \varepsilon^{3/2}} \int_0^\infty k' \, dk' \, |\delta N|^2_{\mathbf{k}'} \Phi , \quad (150)$$

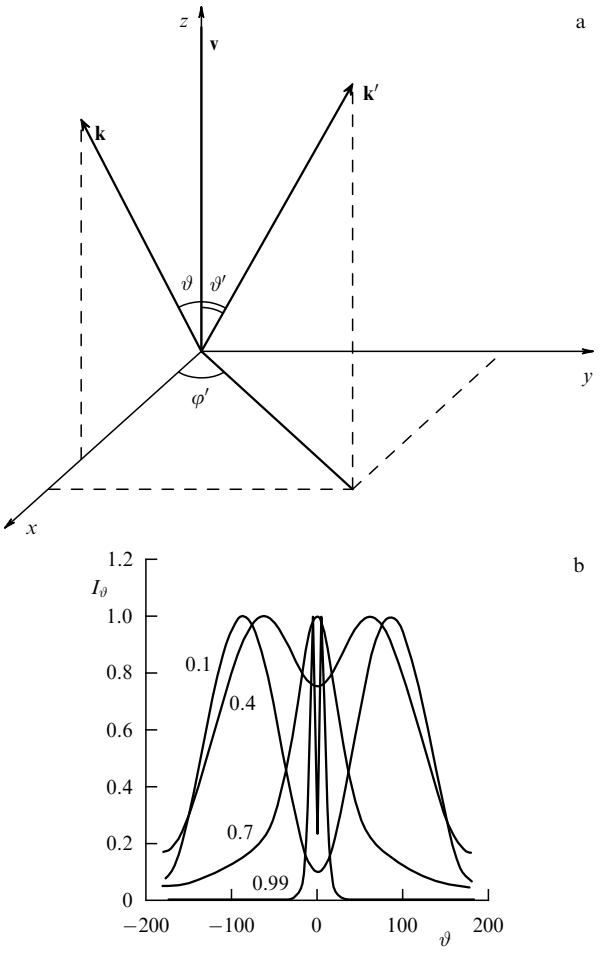

Figure 7. (a) Coordinate system. (b) Normalized angular distribution of transition radiation for various values of v/v_{ph} (labels on curves).

where

$$\Phi = \int_{-1}^{1} d\cos\vartheta' \, \delta(\cos\vartheta' - \cos\vartheta_r) \int_0^{2\pi} \frac{k^4 \, d\varphi'}{(a + b\cos\varphi')^2} \times \left[[\mathbf{n}\times\mathbf{v}]^2 + \frac{\omega^2 k'^2}{k^4}(1 - \cos^2\vartheta\cos^2\vartheta' - 2\cos\vartheta\cos\vartheta'\sin\vartheta\sin\vartheta'\cos\varphi' - \sin^2\vartheta\sin^2\vartheta'\cos^2\varphi') + \frac{2v\omega k'}{k^2}(\cos\vartheta'\sin^2\vartheta - \cos\vartheta\sin\vartheta\sin\vartheta'\cos\varphi') \right], \quad (151)$$

$\cos\vartheta_r = -(\omega - kv\cos\vartheta)/k'v$, $\quad a = k'^2 - 2kk'\cos\vartheta\cos\vartheta'$, $b = -2kk'\sin\vartheta\sin\vartheta'$. The integration over $d\cos\vartheta'$ is performed trivially using the δ function and gives rise to a Θ function, $\Theta(1-\cos^2\vartheta_r)$, associated with the obvious requirement $\cos^2\vartheta_r \leqslant 1$. Replacing $\cos\vartheta'$ by $\cos\vartheta_r$ in Eqn (151) and expanding the resulting expression into the simplest fractions, we find

$$\Phi = \Theta(1-\cos^2\vartheta_r) \int_0^{2\pi} k^4 \, d\varphi' \times \left\{ -\frac{\omega^2}{4k^6} + \left(\frac{\omega^2 k'^2}{2k^6} + \frac{\omega v}{k^3}\cos\vartheta \right)(a + b\cos\varphi')^{-1} + \left[v^2\sin^2\vartheta + \frac{\omega v}{k}\left(2 - \frac{k'^2}{k^2}\right)\cos\vartheta - \frac{\omega^2 k'^4}{4k^6} + \frac{\omega^2 k'^2}{k^4} - \frac{2\omega^2}{k^2} \right](a + b\cos\varphi')^{-2} \right\} . \quad (152)$$

Performing the integrals with respect to $d\varphi'$ in Eqn (152) (which are tabulated) and simplifying the results in terms of their power in $\cos\vartheta$ in the last term and combining common terms, we find the following:

$$\Phi = \frac{\pi\omega^2}{2k^2}\,\Theta(1-\cos^2\vartheta_r)\left\{ -1 + \frac{\beta^{-2}\cos^2\vartheta + \beta^{-1}\cos\vartheta + (1-\beta^{-2})(1 - y^2/2 + y^4/4) + y^2/2}{\left[\cos^2\vartheta + \beta(y^2-2)\cos\vartheta + \beta^2 - y^2 + y^4/4\right]^{1/2}} + (1-\beta^{-2})\left(1 - \frac{y^2}{2}\right)^2 \times \frac{\beta(1-y^2)\cos\vartheta - \beta^2 + y^2/2 - y^4/4}{\left[\cos^2\vartheta + \beta(y^2-2)\cos\vartheta + \beta^2 - y^2 + y^4/4\right]^{3/2}} \right\} , \quad (153)$$

where $\beta = \omega/kv$, $y = k'/k$. Thus, the spectral-angular distribution of the TR intensity reduces to a single integration over the spectrum of the plasma density inhomogeneities:

$$I_{\mathbf{n},\omega} = \frac{4\pi e^4 Q^2}{v m^2 c^3 \varepsilon^{3/2}} \int_{\beta - \cos\vartheta}^\infty y \, dy \, |\delta N|^2_{\mathbf{k}'} F(y, \beta, \cos\vartheta) , \quad (154)$$

where $F(y,\beta,\cos\vartheta) = 2k^2\Phi/\pi\omega^2\Theta(1-\cos^2\vartheta_r)$. However, it is impossible to integrate Eqn (154) analytically with the power-law spectrum (35). Figure 7b displays the normalized angular distribution of the TR intensity at different values of the parameter kv/ω, obtained by numerical integration of Eqn (154). In the non-relativistic range the radiation is similar to that from a dipole and its maximum occurs at angles of order 90° with respect to the particle velocity. As kv/ω increases the radiation maximum approaches the direction in which the particle is moving, and a strong directivity is observed for the radiation in the direction of the velocity vector in the ultra-relativistic limit. Note that in calculating

the TR in the ultra-relativistic limit (39) the radiation intensity in the forward direction ($\vartheta = 0$) vanishes. In Figure 7b we see $I(\vartheta = 0) > 0$, which is provided by the longitudinal proper field of the fast particle included here, but neglected there (39).

We proceed now to calculating the **TR intensity over the full solid angle**:

$$I_\omega = 2\pi \int_{-1}^{1} I_{\mathbf{n},\omega}\, \mathrm{d}\cos\vartheta\,. \tag{155}$$

Changing the order of integration with respect to $\mathrm{d}y$ and $\mathrm{d}\cos\vartheta$ we find

$$I_\omega = \frac{8\pi^3 e^4 Q^2}{v m^2 c^3 \varepsilon^{3/2}} \left(\int_{\beta-1}^{\beta+1} y\,\mathrm{d}y \int_{\beta-y}^{1} \mathrm{d}\cos\vartheta + \int_{\beta+1}^{\infty} y\,\mathrm{d}y \int_{-1}^{1} \mathrm{d}\cos\vartheta \right) |\delta N|^2_{\mathbf{k}'}\, F(y,\beta,\cos\vartheta)\,. \tag{156}$$

Since the spectrum $|\delta N|^2_{\mathbf{k}'}$ does not depend on the angle ϑ for isotropically distributed inhomogeneities, only the function F is integrated over the angle. We introduce two new functions F_1 and F_2:

$$F_1 = \int_{\beta-y}^{1} F\,\mathrm{d}\cos\vartheta\,, \qquad F_2 = \int_{-1}^{1} F\,\mathrm{d}\cos\vartheta\,. \tag{157}$$

Taking into account the variation interval of y in each of the integrals, we find

$$F_1 = \frac{(y+1-\beta)(y^2-2)^2\left[1+\beta(y+1)\right]}{2\beta^2 y(y+2)} + (y+1-\beta) \times \left(-\frac{3}{4\beta}\, y^3 + \frac{3\beta-1}{4\beta^2}\, y^2 + \frac{6\beta+1}{2\beta^2}\, y - \frac{1}{2\beta^2} - \frac{5}{2\beta} - 1 \right) + \left(\frac{5\beta^2-3}{8\beta^2}\, y^4 - \frac{2\beta^2-1}{\beta^2}\, y^2 + \frac{3\beta^2-1}{\beta^2} \right) \ln\frac{y(\beta+1)}{(y+2)(\beta-1)}\,, \tag{158}$$

$$F_2 = \frac{3-5\beta^2}{2\beta^2}\, y^2 + \frac{3\beta^2-1}{\beta^2} + \frac{\beta^2-1}{\beta^2(y^2-4)} - \left(\frac{5\beta^2-3}{8\beta^2}\, y^4 - \frac{2\beta^2-1}{\beta^2}\, y^2 + \frac{3\beta^2-1}{\beta^2} \right) \ln\left(1-\frac{4}{y^2}\right). \tag{159}$$

Substitution of the spectrum of the equilibrium thermal fluctuations $|\delta N|^2_{\mathbf{k}'}$ into Eqn (156) with the use of Eqns (158), (159) results in the intensity of the polarization bremsstrahlung. This problem is analyzed in Ref. [59], see Section 4 as well. Unfortunately, the integration cannot be completely carried out in terms of elementary functions.

Consider the emission that arises when super-thermal fluctuations are present in the plasma. After expressing the spectrum (35) by the dimensionless variable y

$$|\delta N|^2_{\mathbf{k}'} = \frac{v-1}{4\pi}\, \frac{k_0^{v-1}\langle \Delta N^2\rangle}{k^{v+2}}\, y^{-v-2}\,, \tag{160}$$

the intensity of radiation can be written as

$$I_\omega = \frac{2\pi^2 (v-1) e^4 Q^2 \langle \Delta N^2\rangle k_0^{v-1}}{v m^2 c^3 \varepsilon^{3/2} k^{v+2}} \times \left\{ \int_{\beta-1}^{\beta+1} F_1 y^{-v-1}\,\mathrm{d}y + \int_{\beta+1}^{\infty} F_2 y^{-v-1}\,\mathrm{d}y \right\}. \tag{161}$$

Then, expression (161) is calculated by expanding the functions F_1 and F_2 into the simplest fractions and integrating by parts the terms which contain logarithms. After simplifying and performing some identities we find

$$I_\omega = \frac{8\pi^2 (v-1)}{(4-v)(2-v)}\, \frac{v e^4 Q^2 \langle \Delta N^2\rangle k_0^{v-1}}{\omega^2 m^2 c^3 \varepsilon^{3/2} k^v} \times \sum_{\sigma=\pm 1} \left\{ (\beta+\sigma)^{-v} \left[\frac{2(\beta\sigma)^3}{v(v-1)} + \frac{2(\beta\sigma)^2}{v-1} + \frac{v^2+2v+16}{4(v+1)} \left(\frac{v+2}{v}\, \beta\sigma + 1 \right) \right] + (v^2-2v+8)\, \frac{(v+6)\beta^2 - (v+2)}{4v}\, \sigma \int_{\beta-\sigma}^{\infty} \frac{y^{-v-1}\,\mathrm{d}y}{y+2\sigma} \right\}. \tag{162}$$

The summation over $\sigma = \pm 1$ is introduced in Eqn (162) to make it more compact; the integral that remains in Eqn (162) can be expressed in terms of hypergeometric functions [60]. Equation (162) is valid for a charged particle of arbitrary energy moving rectilinearly at frequencies $\omega > \omega_\mathrm{p}$, except for a small region near ω_p, $\omega \lesssim \omega_\mathrm{p}(1 + v_\mathrm{T}^2/v^2)$, where v_T is the thermal velocity of the plasma electrons. In order to describe the intensity I_ω correctly in this region we must take into account the spatial dispersion of the plasma. We just note for a moment that in isotropic plasma the spatial dispersion gives rise to the substitution:

$$\varepsilon^{-3/2} \to F(\alpha)\,, \qquad \alpha = \frac{\varepsilon}{3}\left(\frac{v}{v_\mathrm{T}}\right)^2, \tag{163}$$

where the function $F(\alpha)$ represents a strong narrow peak in the spectrum close to the frequency ω_p. We refer to this part of the radiation as resonant TR. Under the condition $(\omega - \omega_\mathrm{p})/\omega_\mathrm{p} \gg (v_\mathrm{T}/v)^2$ we have $F(\alpha) \approx \varepsilon^{-3/2}$ and expression (162) is valid. In the opposite limit $\omega \to \omega_\mathrm{p}$, $\alpha \ll 1$ we have $F(\alpha) \approx (1/18)\varepsilon^{1/2}(v/v_\mathrm{T})^4$. If we note that $\beta \gg 1$ holds here we find

$$I_\omega(\omega \to \omega_\mathrm{p}) = \frac{16\pi^2 (v-1)}{27(v+2)}\, \varepsilon^{1/2}\, \frac{e^4 Q^2 \langle \Delta N^2\rangle k_0^{v-1}}{c^3 m^2} \left(\frac{v}{v_\mathrm{T}}\right)^4 \frac{v^{v+1}}{\omega_\mathrm{p}^{v+2}}\,. \tag{164}$$

Let us proceed now to finding asymptotic representations of the expression $S = \sum_{\sigma=\pm 1} \ldots$, which depends on β, for small and large values of $\beta - 1$.

Ultra-relativistic limit. For $(\beta - 1) \ll 1$ we should put $\beta = 1$ everywhere except in terms of the form $(\beta - 1)$, and neglect y in comparison with 2 in the denominator of the integrand. Then we find

$$S = \frac{(4-v)(2-v)}{2v^2(v+1)}\, (\beta-1)^{-v}\,. \tag{165}$$

Substituting Eqn (165) into Eqn (162) and setting $v = c$, $\varepsilon = 1$ in the coefficient, we find the ultra-relativistic limit of TR (46), which is correct for $\gamma \gg 1$, $\omega \gg \omega_\mathrm{p}$.

Non-relativistic limit. In the opposite limiting case, $(\beta - 1) \gg 1$, the quantities $(\beta \pm 1)^{-v}$ could be expanded in powers of $1/\beta$, where the first non-vanishing terms of this expansion arise only in the fourth order. Taking the integrals

to the same accuracy over $1/\beta$ we find

$$S = \frac{4(4-\nu)(2-\nu)}{3(\nu+2)}\,\beta^{-\nu}. \tag{166}$$

Finally, for $(\beta-1) \gg 1$, we have

$$I_\omega^{\mathrm{NR}} = \frac{32\pi^2(\nu-1)}{3(\nu+2)}\,\frac{e^4Q^2\langle\Delta N^2\rangle k_0^{\nu-1}}{c^3m^2\omega^{\nu+2}}\,F(\alpha)\,v^{\nu+1}. \tag{167}$$

Note that expression (167) is also valid for the TR of relativistic particles in the limit $\omega \to \omega_{\mathrm{p}}$, since in this case we have $(\beta-1) \gg 1$.

Using the asymptotic forms (165), (166) and applying the standard procedure for fitting the numerical results for the function S by an analytical formula we arrive at the result:

$$S = \frac{(4-\nu)(2-\nu)}{2\nu^2(\nu+1)}(A_1 + A_2), \tag{168}$$

where

$$A_1 = (\beta-1)^{-\nu} + \frac{8\nu^3+8\nu^2-3\nu-6}{3(\nu+2)}\,\beta^{-\nu}, \tag{169}$$

$$A_2 = -\frac{400(1.18\nu-2.17\nu+1.18)}{3(\nu+2)}\,\beta^{-3.03\nu-1.14}. \tag{170}$$

Retaining only the quantity A_1 [consisting of the asymptotic forms (165), (166)] in Eqn (168) yields the correct order of magnitude (the error is less than a factor of two), and the correction A_2 provides an average accuracy $\sim 10\%$ and maximum error $\sim 20\%$. Thus, the intensity of the transition radiation of a charged particle of arbitrary energy at all frequencies $\omega \geqslant \omega_{\mathrm{p}}$ is given by the expression

$$\begin{aligned} I_\omega = {} & \frac{4\pi^2(\nu-1)}{\nu^2(\nu+1)}\,\frac{e^4Q^2\langle\Delta N^2\rangle k_0^{\nu-1}}{m^2c^3}\,\frac{v}{k^\nu\omega^2}\,F(\alpha) \\ & \times\left[\left(\frac{\omega}{kv}-1\right)^{-\nu} + \frac{8\nu^3+8\nu^2-3\nu-6}{3(\nu+2)}\left(\frac{kv}{\omega}\right)^{\nu}\right. \\ & \left. - \frac{400(1.18\nu^2-2.17\nu+1.18)}{3(\nu+2)}\left(\frac{kv}{\omega}\right)^{3.03\nu+1.14}\right]. \end{aligned} \tag{171}$$

Figure 8a displays the spectra of TR calculated according to both Eqn (171) and the relativistic asymptotic forms for various values of the particle momentum. It demonstrates that the relativistic expressions provide a good description of the emission from high-energy particles at high frequencies, while near the plasma frequency a strong narrow peak appears which exceeds the level of the 'background' by several orders of magnitude.

These results can be used under laboratory conditions to analyze experiments with mono-energetic particle beams. For astrophysical applications it is often necessary to average the spectra over the energy distribution of the emitting particles as well.

TR from an ensemble of particles. Usually the spectrum of emitting particles in astrophysical sources can be represented in the form

$$\mathrm{d}N_{\mathrm{e}} = (\xi-1)N_{\mathrm{e}}(x > x_0)\,\frac{x_0^{\xi-1}\,\mathrm{d}x}{x^\xi}, \qquad x_0 < x < x_1, \tag{172}$$

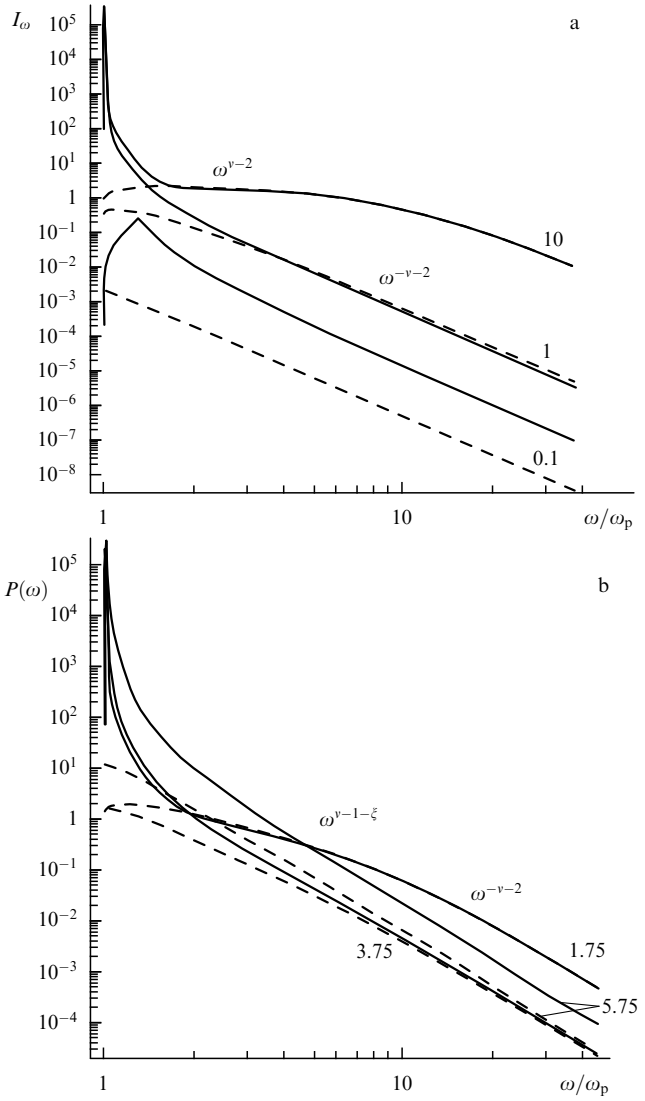

Figure 8. (a) Set of transition radiation spectra for various values of the dimensionless momentum of the charged particle $x = p/mc$ (the labels at curves). (b) Radiation by a charged particle ensemble with a power-law distribution over momentum for various spectral indices (labels on the curves). The dashed curves represent spectra plotted with the use of relativistic asymptotic forms.

where $x = p/mc$ is the dimensionless particle momentum. Then the emission from the ensemble of particles with the spectrum (172) can be written as follows:

$$P_\omega = \frac{4\pi^2(\nu-1)(\xi-1)}{\nu^2(\nu+1)}\,\frac{e^4Q^2\langle\Delta N^2\rangle k_0^{\nu-1}}{m^2c^2}\,N_{\mathrm{e}}(x > x_0)\,\frac{G(\omega)}{k^\nu\omega^2}, \tag{173}$$

where

$$\begin{aligned} G(\omega) = {} & \int_{x_0}^{x_1}\frac{F(\alpha)x_0^{\xi-1}\,\mathrm{d}x}{(1+x^2)^{0.5}x^{\xi-1}} \\ & \times\left[(\beta-1)^{-\nu} + \frac{8\nu^3+8\nu^2-3\nu-6}{3(\nu+2)}\,\beta^{-\nu}\right. \\ & \left. - \frac{400(1.18\nu-2.17\nu+1.18)}{3(\nu+2)}\,\beta^{-3.03\nu-1.14}\right], \end{aligned} \tag{174}$$

and the velocity v which enters the definition of α (see below) should be expressed in terms of the dimensionless momentum:

$$\frac{v}{c} = \frac{x}{(1+x^2)^{1/2}} \,. \tag{175}$$

Let us start with the analysis of the asymptotic behavior of the radiation spectrum in the region $\omega \gg \omega_p$, when the peak as $\omega \to \omega_p$ is unimportant. As will become clear, the shape of the corresponding asymptotic forms is different in three various cases: (1) $\xi > 2\nu + 1$, (2) $\nu + 2 < \xi < 2\nu + 1$, (3) $\xi < \nu + 2$. If the number of particles falls off sufficiently rapidly ($\xi > 2\nu + 1$) with increasing x, then the main contribution to the emission comes from the non-relativistic particles. Then we can set $x = v/c$ and integrate Eqn (174) over $\mathrm{d}v$ from v_0 to infinity. Here it is necessary to evaluate the integral $\int_{v_0}^{\infty} x^{\nu+1-\xi}\,\mathrm{d}x$ [see the asymptotic form (165)], and it obviously converges for

$$\xi > \nu + 2 \,, \tag{176}$$

which always holds in this region, since $\nu + 2 < 2\nu + 1$ for $\nu > 1$ and the radiation spectrum can be written in the form

$$P_\omega = \frac{32\pi^2(\nu-1)}{3(\nu+2)(\xi-\nu-2)} \frac{e^4 Q^2 \langle \Delta N^2 \rangle k_0^{\nu-1}}{m^2 c^3} N_e(\nu > \nu_0) \frac{v_0^{\nu+1}}{\omega^{\nu+2}} \,. \tag{177}$$

In the other limiting case $\xi < \nu + 2$, the main contribution to the radiation at these frequencies is associated with the ultra-relativistic particles. The integration of Eqn (174) for $\omega < \min\{\omega_p^2/\omega_{Be}, \omega_p\gamma_1\}$, where $\gamma_1 = (1 + x_1^2)^{1/2}$ is the maximum Lorentz factor in the spectrum (172), yields

$$P_\omega = \frac{8\pi^2(\nu-1)\Gamma\left[(\xi+1)/2\right]\Gamma\left[(2\nu-\xi+1)/2\right]}{\nu^2(\nu+1)\Gamma(\nu)} \times x_0^{\xi-1} N_e \frac{e^4 Q^2 \langle \Delta N^2 \rangle}{c m^2 \omega_p^3} \left(\frac{2k_0 c}{\omega_p}\right)^{\nu-1} \left(\frac{\omega_p}{\omega}\right)^{\xi+1-\nu} \,. \tag{178}$$

Finally, for

$$\nu + 2 < \xi < 2\nu + 1 \tag{179}$$

both expressions (177), (178) are correct, and the total spectrum is given by their sum. Since the emission spectrum in the relativistic case $\omega^{\nu-1-\xi}$ is flatter than in the non-relativistic case $\omega^{-\nu-2}$, the emission produced by non-relativistic particles dominates at lower frequencies, while the emission comes from the relativistic particles dominates at higher frequencies; the contribution of particles with $E_{kin} \sim mc^2$ is unessential.

Figure 8b displays the emissivity $P(\omega)$ of the particle ensemble as a function of frequency for three different values of ξ corresponding to the three intervals described (we set $\nu = 1.5$ in generating the plots). The solid curves are the results of calculations by the exact formula (174), while the dashed curves correspond to the relativistic asymptotic forms. The figure demonstrates a good agreement between the asymptotic forms and the exact calculations. The value of the TR intensity at the peak that remains after integration over the particle spectrum can be several orders of magnitude greater than the 'background' level of the emission.

3.2 Resonant transition radiation

General remarks. Resonant effects in transition radiation have already been discussed in Section 2 for TR produced by ultra-relativistic particles. They are the strong enhancement of TR intensity at the threshold of Cherenkov generation of extraordinary waves or that at cyclotron frequency if $\omega_{Be} > \omega_p$. A similar effect occurs near another plasma eigen frequency, namely, at the Langmuir frequency ω_p [57]. This effect can be regarded as more general, since it takes place independently on the ratio of gyrofrequency to plasma frequency. We refer to the transition radiation generated near the plasma frequency as *resonant transition radiation* (RTR).

Calculation of RTR. Since the phase velocity of transverse waves near ω_p is considerably greater than the speed of light, so $v/v_{ph} \ll 1$ holds for any $v < c$, we may keep only the longitudinal field of the fast particle (the non-relativistic approximation) to calculate the resonant transition radiation to an accuracy of $(v/v_{ph})^2$. However, the dielectric permeability that enters the expression for this field should be written taking into account the spatial dispersion $\varepsilon(\omega, \mathbf{k}) = \varepsilon(\omega) - 3k^2d^2 + i\varepsilon''$. Then the intensity of the resonant transition radiation can be represented in the form

$$I^R_{\mathbf{n},\omega} = \frac{8\pi e^4 Q^2 \varepsilon^{1/2}}{m^2 c^3} \int k'^2\,\mathrm{d}k' \times \frac{[\mathbf{n}\times\mathbf{k}']^2 \delta\left[\omega - (\mathbf{k}-\mathbf{k}')\mathbf{v}\right] |\delta N|^2_{\mathbf{k}'}\,\mathrm{d}\varphi\,\mathrm{d}\cos\vartheta}{(\mathbf{k}-\mathbf{k}')^4 \left\{\left[\varepsilon(\omega) - 3(\mathbf{k}-\mathbf{k}')^2 d^2\right]^2 + \varepsilon''^2\right\}} \,, \tag{180}$$

where $d = v_T/\omega_p$ is the Debye radius; the imaginary part ε'' of the dielectric permeability is introduced to eliminate the divergence when Eqn (180) is integrated. Note that $\varepsilon(\omega) \ll 1$ and $k \ll k'$ at the frequencies considered. This enables us to neglect $\mathbf{k}$ in comparison with $\mathbf{k}'$ everywhere except in the resonant denominator. Then it is convenient to integrate Eqn (180) over the angles of the vector $\mathbf{n}$, i.e., find the energy emitted over the full solid angle (the directivity pattern corresponds to that of a dipole in this case):

$$I^R_\omega = \frac{32\pi^3 e^4 Q^2 \varepsilon^{1/2}}{v m^2 c^3} \int_{\omega/v}^{\infty} \frac{\mathrm{d}k'}{k'} |\delta N|^2_{\mathbf{k}'} \times \int_{-1}^{1} \frac{\sin^2\vartheta\,\mathrm{d}\cos\vartheta}{\left[\varepsilon(\omega) + 6kk'd^2\cos\vartheta - 3k'^2d^2\right]^2 + \varepsilon''^2} \,. \tag{181}$$

In expression (181) we have also performed the trivial integration over the azimuth angle, $\int d\varphi \ldots = 2\pi$, ϑ is the angle between the vector $\mathbf{k}'$ and the particle velocity $\mathbf{v}$. Breaking up the integrand into the simplest fractions and integrating over the angle ϑ, we obtain:

$$I^R_\omega = \frac{32\pi^3 e^4 Q^2 \varepsilon^{1/2}}{v m^2 c^3} \int_{\omega/v}^{\infty} \frac{\mathrm{d}k'}{k'} |\delta N|^2_{\mathbf{k}'} \frac{J_\vartheta}{36k^2k'^2d^4} \,, \tag{182}$$

where

$$J_\vartheta = a \ln\frac{(a+1)^2 + b^2}{(a-1)^2 + b^2} - 2 + \frac{1 + b^2 - a^2}{b} \times \left[\pi\Theta(1 - a^2 - b^2) + \arctan\frac{2b}{a^2 + b^2 - 1}\right] \,, \tag{183}$$

and $a = [3k'^2d^2 - \varepsilon(\omega)]/(6kk'd^2)$, $b = \varepsilon''/(6kk'd^2)$. Let us analyze the expression for J_ϑ (183) in more detail. The case of

a transparent medium corresponds to the limit $b \to 0$. Then for $a^2 \leqslant 1$ we have $J_\vartheta \to \infty$ as π/b. This divergence has a clear physical origin. The matter is that for $a^2 \leqslant 1$ the condition for Vavilov–Cherenkov radiation is fulfilled for longitudinal (plasma) waves. Hence, the particle field for the respective values of $\omega, \mathbf{k}, \mathbf{k}'$ is not quasi-stationary but propagating, and its interaction with the plasma inhomogeneities corresponds to scattering of already emitted quanta, rather than the production of new ones. The mean free path of the Cherenkov plasmons in an infinite transparent medium is infinite, which is the very reason for this divergence. In order to calculate the intensity of the transition radiation, regarded as the result of conversion of the quasi-stationary field of the particle into propagating waves [19], we must exclude values $a^2 \leqslant 1$ from the range of integration over $\mathrm{d}k'$.

In this case the function J_ϑ can be simplified. Discarding the term $\pi\Theta(1-a^2-b^2)$ and expanding $\arctan x$ in a series based on the smallness of its argument for $a^2 > 1$, we find:

$$J_\vartheta = \left[a \ln \frac{(a+1)^2+b^2}{(a-1)^2+b^2} - 4\right]\Theta(a^2-1)\,. \tag{184}$$

The quantity J_ϑ has a singularity in the limit $b \to 0$, $a^2 \to 1$, but this singularity is integrable. This can easily be shown if we expand J_ϑ in powers of $1/a$, the expansion converges within $1/|a| < 1$. Retaining the first non-vanishing term of this expansion

$$J_\vartheta \simeq \frac{4}{3a^2}\,\Theta(a^2-1) \tag{185}$$

ensures an accuracy of better than 30%. After substitution of Eqn (185) into Eqn (182) and transition to the dimensionless variable $\mu = k'v/\omega$, we can write the resonant transition radiation spectrum in the form

$$I_\omega^{\mathrm{R}} = \frac{32\pi^2(v-1)}{27}\,\frac{e^4Q^2\varepsilon^{1/2}}{vm^2c^3}\,k_0^{v-1}\langle\Delta N^2\rangle\left(\frac{v}{\omega}\right)^{v+2}\left(\frac{v}{\omega d}\right)^4 \times \int_1^\infty \frac{\mathrm{d}\mu\,\Theta(a^2-1)}{\mu^{v+3}(\mu^2-\alpha)^2}\,, \tag{186}$$

where $\alpha = \varepsilon/3(v/\omega d)^2 \approx \varepsilon/3(v/v_{\mathrm{T}})^2$. For arbitrary values of the spectral index v, the integral in Eqn (186) can be expressed in terms of hypergeometric functions. In fact, the shape of the peak has only a weak dependence on the spectral index, so it is convenient to use the result of integrating Eqn (186) for $v = 2$, which can be expressed in terms of elementary functions:

$$\begin{aligned}\Phi(\alpha) &\equiv \int_1^\infty \frac{\mathrm{d}\mu\,\Theta(a^2-1)}{\mu^5(\mu^2-\alpha)^2}\\ &= \frac{1}{\alpha^3}\left[\frac{1}{1-\alpha}+2+\frac{\alpha}{2}+\frac{3}{\alpha}\ln(1-\alpha)\right]\Theta(\omega_1-\omega)\\ &+\frac{1}{\alpha^4}\,\frac{c}{2\times 3^{0.5}v_{\mathrm{T}}}\left(1-\frac{6\times 3^{0.5}v_{\mathrm{T}}}{c}\ln\frac{c}{2\times 3^{0.5}v_{\mathrm{T}}}\right)\\ &\times\Theta(\omega-\omega_1)\Theta(\omega_2-\omega)+\left\{\frac{1}{\alpha^4}\,\frac{c}{3^{0.5}v_{\mathrm{T}}}\right.\\ &\left.+\frac{1}{\alpha^3}\left[\frac{1}{1-\alpha}+2+\frac{\alpha}{2}+\frac{3}{\alpha}\ln(\alpha-1)\right]\right\}\Theta(\omega-\omega_2)\,,\end{aligned} \tag{187}$$

where

$$\omega_{1,2} = \omega_{\mathrm{p}}\left[1+\frac{3}{2}\left(\frac{v_{\mathrm{T}}}{v}\right)^2\left(1\mp\frac{2\times 3^{0.5}v_{\mathrm{T}}}{c}\right)\right]. \tag{188}$$

Further, it is convenient to transit from the function $\Phi(\alpha)$ to another function

$$\begin{aligned}F(\alpha) &= \frac{2\varepsilon^{1/2}}{9}\left(\frac{v}{v_{\mathrm{T}}}\right)^4\Phi(\alpha)\\ &= 2\varepsilon^{-3/2}\left(\frac{1}{\alpha}\left[\frac{1}{1-\alpha}+2+\frac{\alpha}{2}+\frac{3}{\alpha}\ln(1-\alpha)\right]\Theta(\omega_1-\omega)\right.\\ &+\frac{1}{\alpha^2}\,\frac{c}{2\times 3^{0.5}v_{\mathrm{T}}}\left(1-\frac{6\times 3^{0.5}v_{\mathrm{T}}}{c}\ln\frac{c}{2\times 3^{0.5}v_{\mathrm{T}}}\right)\\ &\times\Theta(\omega-\omega_1)\Theta(\omega_2-\omega)+\left\{\frac{1}{\alpha^2}\,\frac{c}{3^{0.5}v_{\mathrm{T}}}+\right.\\ &\left.\left.+\frac{1}{\alpha}\left[\frac{1}{1-\alpha}+2+\frac{\alpha}{2}+\frac{3}{\alpha}\ln(\alpha-1)\right]\right\}\Theta(\omega-\omega_2)\right),\end{aligned} \tag{189}$$

since for large frequencies $\omega \gg \omega_{\mathrm{p}}$, $\alpha \gg 1$ we have $F(\alpha) \approx \varepsilon^{-3/2}(\omega)$, and the respective expression merges with the overall transition radiation spectrum (162). Thus, the TR spectrum which is correct at all frequencies $\omega \geqslant \omega_{\mathrm{p}}$ is found after substituting $\varepsilon^{-3/2} \to F(\alpha)$ in Eqn (162) [see Eqn (171)]. It is easy to see that at high frequencies $\omega \gg \omega_{\mathrm{p}}$ the role of the spatial dispersion is minor, i.e., $F(\alpha) \approx \varepsilon^{-3/2} \approx 1$; at low frequencies, $\alpha \ll 1$, we have $F(\alpha) \approx (\varepsilon^{1/2}/18)(v/v_{\mathrm{T}})^4 \propto (\omega-\omega_{\mathrm{p}})^{1/2}$, while near the maximum of the spectrum $\alpha \approx 1$ we have $F(\alpha) \sim v^3c/v_{\mathrm{T}}^4$.

Total energy of RTR. Now let us find the total energy emitted by the resonant transition mechanism. Integrating the spectrum (167) that is valid near ω_{p} over frequency for particles of arbitrary energy, we find

$$I_{\mathrm{tot}}^{\mathrm{R}} = \frac{64\pi^2(v-1)}{45(v+2)}\,\frac{e^4Q^2\langle\Delta N^2\rangle k_0^{v-1}}{c^3m^2}\left(\frac{v}{\omega_{\mathrm{p}}}\right)^{v+1}\frac{vc}{v_{\mathrm{T}}^2}\,. \tag{190}$$

The comparison of Eqn (190) with the energy emitted in the ultra-relativistic region (50) proves the resonant TR by particles with $\gamma < c^2/v_{\mathrm{T}}^2$ to be more intensive than standard TR. For $\gamma > c^2/v_{\mathrm{T}}^2$ most of the energy is emitted at frequencies $\omega_{\mathrm{m}} \sim \omega_{\mathrm{p}}\gamma > \omega_{\mathrm{p}}c^2/v_{\mathrm{T}}^2$.

If the charged particle is moving in a plasma with gradually varying density [with some distribution $\Phi(\omega_{\mathrm{p}})$ over the plasma frequencies], then the bulk of the observed emission at frequency ω comes from the regions of the plasma with $\omega_{\mathrm{p}} \approx \omega$. To estimate the TR from these (large-scale) non-uniform sources it is convenient to use the approximation

$$I_\omega^{\mathrm{R}} = \frac{64\pi^2(v-1)}{45(v+2)}\,\frac{e^4Q^2\langle\Delta N^2\rangle k_0^{v-1}}{c^3m^2}\left(\frac{v}{\omega_{\mathrm{p}}}\right)^{v+1}\frac{vc}{v_{\mathrm{T}}^2}\,\delta(\omega-\omega_{\mathrm{p}})\,, \tag{191}$$

which should be convolved with the function $\Phi(\omega_{\mathrm{p}})$.

RTR from an ensemble of particles. In order to obtain the TR generated by an ensemble of particles with a broad spectrum we should convolve expression (191) with the spectrum (172):

$$P_\omega^{\mathrm{R}} = \frac{2(v-1)}{45(v+2)}\,\frac{(\xi-1)\Gamma[(\xi-1)/2]\Gamma[(v-\xi+3)/2]}{\Gamma[(v+2)/2]} \times \frac{e^2}{c}\,x_0^{\xi-1}N_{\mathrm{e}}\omega_{\mathrm{p}}^2\,\frac{\langle\Delta N^2\rangle}{N^2}\left(\frac{k_0c}{\omega_{\mathrm{p}}}\right)^{v-1}\frac{c^2}{v_{\mathrm{T}}^2}\,\delta(\omega-\omega_{\mathrm{p}})\,. \tag{192}$$

The main contribution to this expression comes from particles of moderate relativistic energy with $E_{\rm kin} \sim mc^2$.

Let us evaluate the contribution provided by the scattering of Cherenkov plasmons [i.e. the pole contribution discarded in Eqn (183)] to the entire spectrum of the radiation produced in a randomly inhomogeneous plasma. The total intensity of Cherenkov radiation of plasmons is given by the well-known expression [61]:

$$I_{\rm tot}^{\rm p} = \frac{e^2\omega_{\rm p}^2}{v} \ln\frac{v}{v_{\rm T}}\,, \tag{193}$$

accordingly, the fraction of plasmons scattered per unit time into transverse waves does not exceed the ratio of the probability for a plasmon to be scattered into a transverse wave to the probability for the plasmon to be scattered into another plasmon, $w_{lt}/w_{ll} \approx v_{\rm T}^3/c^3$ [62].

So the radiation intensity provided by the pole contribution (i.e., by the scattering of Cherenkov plasmons into transverse waves) appears to be small in comparison to RTR.

3.3 Resonant transition radiation in magnetic field

The total RTR energy found in Section 3.2 is rather large for the mechanism to be important in nature. However, the objects, which can produce RTR, contain magnetic fields substantially affecting the particle motion, the matter dispersion, and emission of electromagnetic waves.

The analysis of the particle path curvature effect on TR (Section 2) proves that for

$$\frac{\omega_{\rm p}}{\omega_B} \gg 1\,, \tag{194}$$

where $\omega_B = eB/mc$ is the electron gyrofrequency, the curvature is unessential for the frequencies $\omega < \omega_{\rm p}(\omega_{\rm p}\gamma/\omega_B)^{1/2}$, where γ is the Lorentz factor of the particle. This is particularly valid around the plasma frequency. We consider the magnetic field effect on the plasma dispersion [63], while neglecting any curvature of the particle path keeping up the case of relatively small fields (194).

Calculation of RTR in a magnetic field. The phase velocity of electromagnetic waves is mach larger than the speed of light (and, respectively, than the particle speed) at frequencies $\omega \sim \omega_{\rm p}$. Hence, the non-relativistic approximation is correct for particle with arbitrary energy. General equations for the RTR intensity should take into account the presence of ordinary ($\sigma = {\rm o}$) and extraordinary ($\sigma = {\rm x}$) waves in magnetized plasma as well as the magnetic field effect on the longitudinal dielectric permeability of the plasma:

$$\varepsilon(\omega, \mathbf{k}-\mathbf{k}') = \varepsilon(\omega) - 3(\mathbf{k}-\mathbf{k}')^2 d^2 - \frac{\omega_{\rm p}^2\omega_B^2}{\omega^4}\sin^2\theta + {\rm i}\varepsilon''\,, \tag{195}$$

where θ is the angle between the magnetic field $\mathbf{B}$ and the vector $(\mathbf{k}-\mathbf{k}')$. Then, the RTR intensity of each magneto-ionic mode reads

$$I_{\mathbf{n},\omega}^{{\rm R},\sigma} = \frac{4\pi e^4 Q^2 n_\sigma}{m^2c^3}\int {\rm d}^3k' \times \frac{[\mathbf{n}\times\mathbf{k}']^2\delta[\omega - (\mathbf{k}-\mathbf{k}')\mathbf{v}]\,|\delta N|_{\mathbf{k}'}^2}{(\mathbf{k}-\mathbf{k}')^4\left\{\left[\varepsilon(\omega) - 3(\mathbf{k}-\mathbf{k}')^2 d^2 - (\omega_{\rm p}^2\omega_B^2/\omega^4)\sin^2\theta\right]^2 + \varepsilon''^2\right\}}\,, \tag{196}$$

where Q, $\mathbf{v}$ are the charge and velocity of the emitting particle, $\mathbf{n}$ is the unit vector in the direction of wave propagation, m, e are the electron mass and charge, $|\delta N|_{\mathbf{k}'}^2$ is the spectrum of plasma density inhomogeneities, and ε'' is the imaginary part of dielectric permeability. Since the mutual orientation of the vectors $\mathbf{B}$, $\mathbf{v}$, $\mathbf{n}$ is arbitrary, the integrand in Eqn (196) depends on the azimuth angle $\varphi_{\mathbf{k}'}$. Unfortunately, this dependence prevents complete calculation of the respective integrals. Therefore, we consider RTR by a particle ensemble with an anisotropic distribution function

$$f(\mathbf{p}) = f(p, \theta_v) \tag{197}$$

that depends on the polar angle θ_v between the magnetic field $\mathbf{B}$ and velocity $\mathbf{v}$, and does not depend on the azimuth angle φ_v. This kind of anisotropic function covers the majority of astrophysical applications. The intensity of RTR from the particle ensemble can obviously be written as

$$P_{\mathbf{n},\omega}^{{\rm R},\sigma} = \frac{4\pi e^4 Q^2 n_\sigma}{m^2c^3}\int {\rm d}^3p\, f(p,\theta_v)\int {\rm d}^3k' \times \frac{[\mathbf{n}\times\mathbf{k}']^2\delta\left[\omega - (\mathbf{k}-\mathbf{k}')\mathbf{v}\right]|\delta N|_{\mathbf{k}'}^2}{(\mathbf{k}-\mathbf{k}')^4\left\{\left[\varepsilon(\omega) - 3(\mathbf{k}-\mathbf{k}')^2 d^2 - (\omega_{\rm p}^2\omega_B^2/\omega^4)\sin^2\theta\right]^2 + \varepsilon''^2\right\}}\,. \tag{198}$$

Let us expand the distribution function in a series over Legendre polynomials:

$$f(p,\theta_v) = \frac{1}{4\pi}\sum_{l=0}^{\infty} F_l(p) P_l(\cos\theta_v)\,. \tag{199}$$

First of all, we calculate the integral over the angle of velocity (momentum) vector. We set the $\mathbf{k}'$ direction as z axes and express $P_l(\cos\theta_v)$ through the angles θ and $\theta_{\mathbf{k}'\mathbf{v}}$ (this is the angle between the velocity $\mathbf{v}$ and vector $\mathbf{k}'$) according to the well-known combination formula [30, p. 132]:

$$P_l(\cos\theta_v) = \sum_{m=-l}^{l} P_l^{|m|}(\cos\theta_{\mathbf{k}'\mathbf{v}})\, P_l^{|m|}(\cos\theta)\exp({\rm i}m\varphi_v)\,. \tag{200}$$

Integrals over azimuth angle φ_v do not vanish for the terms with $m = 0$ only, and integration over ${\rm d}\cos\theta_{\mathbf{k}'\mathbf{v}}$ is easy to perform due to the δ function. This results in

$$P_{\mathbf{n},\omega}^{{\rm R},\sigma} = \frac{2\pi e^4 Q^2 n_\sigma}{m^2c^3}\sum_{l=0}^{\infty}\int\frac{p^2 F_l(p)\,{\rm d}p}{v} \times \int_{\omega/v}^{\infty}\frac{{\rm d}k'}{k'^3}\,|\delta N|_{\mathbf{k}'}^2\, P_l\!\left(\frac{\omega}{k'v}\right)\int {\rm d}\varphi_{k'}\,{\rm d}\cos\theta \times \frac{[\mathbf{n}\times\mathbf{k}']^2 P_l(\cos\theta)}{\left[\varepsilon(\omega) - 3k'^2 d^2 - \omega_{\rm p}^2\omega_B^2/\omega^4 + (\omega_{\rm p}^2\omega_B^2/\omega^4)\cos^2\theta\right]^2 + \varepsilon''^2}\,. \tag{201}$$

We should note that the terms of the series with even l only contribute to the radiation intensity. Integrating over ${\rm d}\varphi_{k'}$ and substituting $x = \cos\theta$, we find

$$P_{\mathbf{n},\omega}^{{\rm R},\sigma} = \frac{2\pi^2 e^4 Q^2 n_\sigma}{m^2c^3}\sum_{l=0}^{\infty}\int\frac{p^2 F_{2l}(p)\,{\rm d}p}{v} \times \int_{\omega/v}^{\infty}\frac{{\rm d}k'}{k'^3}|\delta N|_{\mathbf{k}'}^2\, P_{2l}\!\left(\frac{\omega}{k'v}\right)\frac{\omega^8}{\omega_{\rm p}^4\omega_B^4} \times \int_{-1}^{1}\frac{\left[1+\cos^2\theta_n + (1-3\cos^2\theta_n)x^2\right]P_{2l}(x)\,{\rm d}x}{(x^2-a)^2 + b^2}\,, \tag{202}$$

where

$$a = -\frac{\varepsilon(\omega)\omega^4}{\omega_{\rm p}^2\omega_B^2} + \frac{3k'^2 d^2\omega^4}{\omega_{\rm p}^2\omega_B^2} + 1\,, \qquad b = \frac{\varepsilon''\omega^4}{\omega_{\rm p}^2\omega_B^2}\,.$$

The case of a transparent (non-absorbing) medium corresponds to the limit $b \to 0$. If this happens in the parameter region $0 < a < 1$, then the integrals over $\mathrm{d}x$ in Eqn (202) diverge. The physical origin of this divergence and the way to regularize it are discussed in Section 3.2 in detail: the region $0 < a < 1$ should be omitted when integrating Eqn (202). Actually, this can be done by multiplication of the integrand by $\Theta[3k'^2d^2 - \varepsilon(\omega) - 6kk'd^2]$ for $a > 1$ and by $\Theta[\varepsilon(\omega) - 3k'^2d^2 - \omega_p^2\omega_B^2/\omega^4 - 6kk'd^2]$ for $a < 0$, where $\Theta(z)$ is the unit step function:

$$P_{\mathbf{n},\omega}^{\mathrm{R},\sigma} = \frac{4\pi^2 e^4 Q^2 n_\sigma}{m^2 c^3} \sum_{l=0}^{\infty} \int_{p_0}^{\infty} \frac{p^2 F_{2l}(p)\,\mathrm{d}p}{v} \times \int_{\omega/v}^{\infty} \frac{\mathrm{d}k'}{k'^3} |\delta N|_{\mathbf{k}'}^2 P_{2l}\left(\frac{\omega}{k'v}\right) \frac{\omega^8}{\omega_p^4 \omega_B^4} J_{2l}(a)\,, \qquad (203)$$

where

$$J_{2l}(a) = \int_0^1 \frac{\left[1 + \cos^2\theta_n + (1 - 3\cos^2\theta_n)x^2\right] P_{2l}(x)\,\mathrm{d}x}{(x^2 - a)^2} \times \Theta\left[3k'^2d^2 - \varepsilon(\omega) - 6kk'd^2\right] + \int_0^1 \frac{\left[1 + \cos^2\theta_n + (1 - 3\cos^2\theta_n)x^2\right] P_{2l}(x)\,\mathrm{d}x}{(x^2 - a)^2} \times \Theta\left[\varepsilon(\omega) - 3k'^2d^2 - \frac{\omega_p^2\omega_B^2}{\omega^4} - 6kk'd^2\right]. \qquad (204)$$

Thus, expression (204) is reduced to the calculation of integrals like

$$\int_0^1 \frac{x^{2n}\,\mathrm{d}x}{(x^2 \pm x_0^2)^2} \qquad (205)$$

for $n = 0, 1, 2\ldots$, which can be done within elementary functions, i.e., the RTR can be completely calculated if the particle anisotropy is known.

Let us consider **the isotropic mono-energetic fast particle distribution** (normalized by one particle) in more detail:

$$F_0 = \frac{1}{p_0^2}\,\delta(p - p_0)\,, \qquad F_l = 0 \quad \text{at} \quad l \neq 0\,. \qquad (206)$$

We denote the RTR by this particle distribution as $I_{\mathbf{n},\omega}^{\mathrm{R},\sigma}$. The integration of Eqn (205) for $n = 1, 2$ yields

$$I_{\mathbf{n},\omega}^{\mathrm{R},\sigma} = \frac{2\pi^2 e^4 Q^2 n_\sigma}{v m^2 c^3} \frac{\omega^8}{\omega_p^4 \omega_B^4} \times \int_{\omega/v}^{\infty} \frac{\mathrm{d}k'}{k'} |\delta N|_{\mathbf{k}'}^2 \left(\Theta\left[3k'^2d^2 - \varepsilon(\omega) - 6kk'd^2\right] \times \left\{ (1 + \cos^2\theta_n)\left[\frac{1}{a(a-1)} + \frac{1}{2a^{3/2}} \ln\frac{a^{1/2}+1}{a^{1/2}-1}\right] + (1 - 3\cos^2\theta_n)\left(\frac{1}{a-1} + \frac{1}{2a^{1/2}} \ln\frac{a^{1/2}-1}{a^{1/2}+1}\right)\right\} + \Theta\left[\varepsilon(\omega) - 3k'^2d^2 - \frac{\omega_p^2\omega_B^2}{\omega^4} - 6kk'd^2\right] \times \left\{ (1 + \cos^2\theta_n)\left[\frac{1}{|a|(|a|+1)} + \frac{1}{|a|^{3/2}} \arctan\left(|a|^{-1/2}\right)\right] + (1 - 3\cos^2\theta_n)\left[\frac{\arctan\left(|a|^{-1/2}\right)}{|a|^{1/2}} - \frac{1}{|a|+1}\right]\right\}\right). \qquad (207)$$

If the spectral index ν in Eqn (35) is arbitrary, then the integrals in Eqn (207) can be expressed through special functions. However, RTR is generated in the narrow frequency range $\omega \sim \omega_p$, and the results depend weakly on the shape of the inhomogeneity spectrum. Hence, we calculate the spectrum for a particular case $\nu = 2$, which allows integration in standard (elementary) functions. We accept $\omega \sim \omega_p$ everywhere except for $\varepsilon(\omega)$ and approximate logarithms and arc tangents by the first terms of Taylor expansions. This ensures an accuracy of order of 20%.

The RTR intensity takes the form

$$I_{\mathbf{n},\omega}^{\mathrm{R},\sigma} = \frac{\pi e^4 Q^2 n_\sigma}{3vm^2c^3} \langle \Delta N^2 \rangle k_0 \left(\frac{v}{\omega}\right)^4 \Phi\,, \qquad (208)$$

where the function Φ is defined by:

$$\Phi = \frac{3}{4}\left(\frac{\omega}{v}\right)^4 \frac{\omega_p^4}{\omega_B^4} \int_{(\omega/v)^2}^{\infty} \frac{\mathrm{d}x}{x^3} \left(\Theta\left[3xd^2 - \varepsilon(\omega) - 6kx^{1/2}d^2\right] \times \left[2\sin^2\theta_n\left(\frac{1}{a-1} - \frac{1}{a} + \frac{1}{a^2}\right) + \frac{4(3\cos^2\theta_n - 1)}{3a^2}\right] + \Theta\left[\varepsilon(\omega) - 3xd^2 - \frac{\omega_B^2}{\omega_p^2} - 6kx^{1/2}d^2\right] \times \left\{ \Theta(1 - |a|)\frac{\pi(1 + \cos^2\theta_n)}{2|a|^{3/2}} + \Theta(|a| - 1)\left[2\sin^2\theta_n\left(\frac{1}{|a|} - \frac{1}{|a|+1} + \frac{1}{a^2}\right) + \frac{4(3\cos^2\theta_n - 1)}{3a^2}\right]\right\}\right). \qquad (209)$$

The presence of Θ functions in the integrand of Eqn (209) restricts the integration region (differently for various frequencies). The respective integration of Eqn (209) yields

$$\Phi \equiv \Phi(\alpha, \beta) = \frac{3}{4}\frac{\omega_p^4}{\omega_B^4}(\Phi_1 + \Phi_2 + \Phi_3 + \Phi_4)\,, \qquad (210)$$

where (the subscript n of the emission angle θ_n is further omitted for the simplicity)

$$\Phi_1 = \Theta(\omega_1 - \omega)\left\{ 2\beta\sin^2\theta\left[\frac{\beta}{2\alpha(\alpha-\beta)} + \frac{(2\alpha-\beta)\beta^2}{\alpha^2(\alpha-\beta)} + \frac{\ln(1-\alpha+\beta)}{(\alpha-\beta)^3} - \frac{\ln(1-\alpha)}{\alpha^3}\right] + \frac{2(3\cos^2\theta + 1)}{3}\beta^2\left[\frac{1}{(\alpha-\beta)^3(1-\alpha+\beta)} + \frac{2}{(\alpha-\beta)^3} + \frac{1}{2(\alpha-\beta)^2} + \frac{3\ln(1-\alpha+\beta)}{(\alpha-\beta)^4}\right]\right\}, \qquad (211)$$

$$\Phi_2 = \Theta(\omega - \omega_1)\left\{ 2\beta\sin^2\theta\left[\frac{1}{\alpha^3}\left(\ln\frac{c}{2\times 3^{1/2}v_T} - \frac{3}{2}\right) - \frac{1}{(\alpha-\beta)^3}\ln\frac{1 + 2\times 3^{1/2}v_T/c}{\beta/\alpha + 2\times 3^{1/2}v_T/c} + \frac{3\alpha-\beta}{2\alpha^2(\alpha-\beta)^2}\right] + \frac{2(3\cos^2\theta + 1)}{3}\beta^2\left[\frac{1}{\alpha(\alpha-\beta)^3(\beta/\alpha + 2\times 3^{1/2}v_T/c)} + \frac{2}{\alpha(\alpha-\beta)^3} + \frac{1}{2\alpha^2(\alpha-\beta)^2} + \frac{3}{(\alpha-\beta)^4}\ln\frac{\beta/\alpha + 2\times 3^{1/2}v_T/c}{1 + 2\times 3^{1/2}v_T/c}\right]\right\}, \qquad (212)$$

$$\Phi_3 = \Theta(\omega-\omega_2)\Theta(\omega_3-\omega)\frac{\pi(1+\cos^2\theta)}{2}\,\beta^{3/2} \times\left(\frac{2}{(\alpha-\beta)^3}\left\{\frac{c}{2\times 3^{1/2}v_{\rm T}\left[\alpha(\alpha-\beta)\right]^{1/2}}\right\}^{1/2} +\left[\frac{1}{2(\alpha-\beta)}+\frac{5}{4(\alpha-\beta)^2}-\frac{15}{4(\alpha-\beta)^3}\right]\frac{1}{(\alpha-\beta-1)^{1/2}}\right), \tag{213}$$

$$\Phi_4 = \Theta(\omega-\omega_3)\left[\frac{\pi(1+\cos^2\theta)}{2}\,\beta^{3/2} \times\left(\frac{2}{(\alpha-\beta)^3}\left\{\frac{c}{2\times 3^{1/2}v_{\rm T}\left[\alpha(\alpha-\beta)\right]^{1/2}}\right\}^{1/2} -\frac{8\alpha^2-41\alpha\beta+48\beta^2}{4(\alpha-\beta)^3(\alpha-2\beta)^2} \times\frac{1}{\left\{\beta+2\times 3^{1/2}(v_{\rm T}/c)\left[\alpha(\alpha-2\beta)\right]^{1/2}\right\}^{1/2}}\right) +2\beta\sin^2\theta\left\{\frac{1}{(\alpha-\beta)^3}\ln\frac{(\alpha-\beta-1)(\alpha-2\beta)}{\beta+2\times 3^{1/2}(v_{\rm T}/c)\left[\alpha(\alpha-2\beta)\right]^{1/2}} -\frac{1}{\alpha^3}\ln\frac{(\alpha-1)(\alpha-2\beta)}{2\beta+2\times 3^{1/2}(v_{\rm T}/c)\left[\alpha(\alpha-2\beta)\right]^{1/2}} +\frac{(2\alpha-\beta)\beta(\alpha-2\beta-1)}{\alpha^2(\alpha-\beta)^2(\alpha-2\beta)}+\frac{\beta(\alpha-2\beta-1)(\alpha-2\beta+1)}{2\alpha(\alpha-\beta)(\alpha-2\beta)^2}\right\} +\frac{2(3\cos^2\theta+1)}{3}\,\beta^2 \times\left(\frac{1}{(\alpha-\beta)^3\left\{\beta+2\times 3^{1/2}(v_{\rm T}/c)\left[\alpha(\alpha-2\beta)\right]^{1/2}\right\}} +\frac{3}{(\alpha-\beta)^4}\ln\frac{(\alpha-\beta-1)(\alpha-2\beta)}{\beta+2\times 3^{1/2}(v_{\rm T}/c)\left[\alpha(\alpha-2\beta)\right]^{1/2}} -\frac{1}{(\alpha-\beta)^3(\alpha-\beta-1)}+\frac{2(\alpha-2\beta-1)}{(\alpha-\beta)^3(\alpha-2\beta)} +\frac{(\alpha-2\beta-1)(\alpha-2\beta+1)}{2(\alpha-\beta)^2(\alpha-2\beta)^2}\right)\right]. \tag{214}$$

Here

$$\alpha=\frac{\varepsilon}{3}\left(\frac{v}{v_{\rm T}}\right)^2,\qquad \beta=\frac{\omega_B^2}{3\omega_{\rm p}^2}\left(\frac{v}{v_{\rm T}}\right)^2, \tag{215}$$

$$\omega_1=\omega_{\rm p}\left[1+\frac{3}{2}\left(\frac{v_{\rm T}}{v}\right)^2\left(1-\frac{2\times 3^{0.5}v_{\rm T}}{c}\right)\right], \tag{216}$$

$$\omega_2=\omega_{\rm p}\left\{1+\frac{\omega_B^2}{2\omega_{\rm p}^2}+\frac{3}{2}\left(\frac{v_{\rm T}}{v}\right)^2\left[1+\frac{2\times 3^{0.5}v_{\rm T}}{c}(1+\beta)^{1/2}\right]\right\}, \tag{217}$$

$$\omega_3=\omega_{\rm p}\left\{1+\frac{\omega_B^2}{\omega_{\rm p}^2}+\frac{3}{2}\left(\frac{v_{\rm T}}{v}\right)^2\left[1+\frac{2\times 3^{0.5}v_{\rm T}}{c}(1+2\beta)^{1/2}\right]\right\}. \tag{218}$$

The function $\Phi(\alpha,\beta)$ has its limit at high frequency ($\omega\gg\omega_{\rm p}$)

$$\Phi(\alpha,\beta)\approx\varepsilon^{-2}(\omega), \tag{219}$$

that allows this expression to be merged with the transition radiation spectra at high frequencies (when the spatial dispersion is unessential) for any spectral index ν (162):

$$I^{\sigma}_{\mathbf{n},\omega}=\frac{\pi(\nu-1)}{2\nu^2(\nu+1)}\,\frac{e^4Q^2n_\sigma}{m^2c^3}\,\langle\Delta N^2\rangle k_0^{\nu-1}\frac{v}{k^\nu\omega^2}\,\Phi(\alpha,\beta) \times\left[\left(\frac{\omega}{kv}-1\right)^{-\nu}+\frac{8\nu^3+8\nu^2-3\nu-6}{3(\nu+2)}\left(\frac{kv}{\omega}\right)^\nu -\frac{400(1.18\nu^2-2.17\nu+1.18)}{3(\nu+2)}\left(\frac{kv}{\omega}\right)^{3.03\nu+1.14}\right]. \tag{220}$$

The spectrum (220) is correct for the frequency range $\omega_{\rm p}\leqslant\omega\ll\omega_{\rm p}(\omega_{\rm p}\gamma/\omega_B)^{1/2}$. The curvature of the fast particle trajectory affects the TR spectrum [Eqn (47)] at even higher frequencies [where $\Phi(\alpha,\beta)\approx\varepsilon^{-2}\approx 1$].

Limiting cases. The intensity (220) can be simplified close to the plasma frequency:

$$I^{{\rm R},\sigma}_{\mathbf{n},\omega}=\frac{4\pi(\nu-1)}{3(\nu+2)}\,\frac{e^4Q^2n_\sigma}{\nu m^2c^3}\,\langle\Delta N^2\rangle k_0^{\nu-1}\left(\frac{v}{\omega}\right)^{\nu+2}\Phi(\alpha,\beta)\,. \tag{221}$$

Let us analyze in more detail the function $\Phi(\alpha,\beta)$ describing RTR. Without magnetic field we have:

$$\lim_{\beta\to 0}n_\sigma\Phi(\alpha,\beta)=F(\alpha)\,, \tag{222}$$

where the function $F(\alpha)$ is defined by Eqn (189). According to Eqns (211) – (218), the magnetic field starts to affect the shape of the function $\Phi(\alpha,\beta)$ when $\beta>2\times 3^{1/2}v_{\rm T}/c$, that is

$$\frac{\omega_B^2}{\omega_{\rm p}^2}>\frac{6\times 3^{1/2}v_{\rm T}^3}{v^2c}\,, \tag{223}$$

and the magnetic field effect becomes most pronounced for $\beta\gg 1$. The physical origin of the effect is the change of the plasma dispersion in the presence of magnetic field under condition (223).

Consider the function $\Phi(\alpha,\beta)$ for $\omega\to\omega_{\rm p}$. The expansion of the function Φ_1 (211) for small α yields

$$\Phi_1=\beta\sin^2\theta\left[\frac{1}{3}-\frac{1}{2\beta}+\frac{1}{\beta^2}-\frac{\ln(1+\beta)}{\beta^3}\right] +\frac{2(3\cos^2\theta+1)}{3}\,\beta^2\left[\frac{1}{2\beta^2}+\frac{3\ln(1+\beta)}{\beta^4}-\frac{1}{\beta^3(1+\beta)}-\frac{2}{\beta^3}\right]. \tag{224}$$

For $\beta\ll 1$ this reads:

$$\Phi(\alpha,\beta)\to\frac{1}{18}\,\frac{v^4}{v_{\rm T}^4}\,. \tag{225}$$

For $\beta\gg 1$ the respective asymptotic form depends on the angle. If $\sin^2\theta$ is not too small, then

$$\Phi(\alpha,\beta)\to\frac{1}{18\beta}\,\frac{v^4}{v_{\rm T}^4}\sin^2\theta \tag{226}$$

is β times less than function (225), and if $\sin^2\theta\approx 0$, then

$$\Phi(\alpha,\beta)\to\frac{1}{9\beta^2}\,\frac{v^4}{v_{\rm T}^4} \tag{227}$$

is β^2 times less than function (225).

Without the magnetic field the peak of RTR spectrum (compare with Section 3.2) is

$$(n_\sigma \Phi)_{\max} \sim \frac{v^3 c}{v_T^4} . \tag{228}$$

The presence of a magnetic field gives rise to a difference in the ordinary and extraordinary wave generation due to the difference in their refractive indices, which are equal to (for $\omega_B/\omega_p \ll 1$):

$$n_\sigma^2 = 1 - \frac{\omega_{c\sigma}^2}{\omega^2} , \quad \omega > \omega_{c\sigma} , \quad \omega_{co} = \omega_p ,$$
$$\omega_{cx} = \sqrt{\omega_p^2 + \frac{\omega_B^2}{4}} + \frac{\omega_B}{2} . \tag{229}$$

Respectively, the resonant transition radiation of extraordinary waves is suppressed strongly in comparison to the radiation of ordinary waves if the cut-off frequency for extraordinary waves ω_{cx} exceeds the frequency ω_3.

For ordinary waves at $2\sqrt{3}\, v_T/c < \beta \ll 1$, we have

$$(n_o \Phi)_{\max} \sim \frac{v^2}{v_T^2} \frac{\omega_p}{\omega_B} \left(\frac{c}{v_T}\right)^{1/2} , \tag{230}$$

and at $\beta \gg 1$,

$$(n_o \Phi)_{\max} \sim \left(\frac{v}{v_T}\right)^{5/2} \left(\frac{\omega_p}{\omega_B}\right)^{1/2} \left(\frac{c}{v_T}\right)^{1/2} . \tag{231}$$

Thus, the magnetic field suppresses the RTR intensity. The intensity I^R displays inverse proportionality to the magnetic field $I^R_{\max} \propto B^{-1}$ (for $\beta \ll 1$), and then, for higher field $\beta \gg 1$ (when most of the RTR is polarized as ordinary mode) the decrease occurs more slowly, $I^R_{\max} \propto B^{-1/2}$. This change is provided by the shift of the RTR peak towards higher frequencies for $\beta \gg 1$, where the refractive index n_o reaches larger values. The functions $n_\sigma \Phi(\alpha, \beta)$ are plotted in Fig. 9 for $\sigma = o, x$ and a few values of the particle velocity and the magnetic field.

Total energy of RTR. Let us calculate the total (integrated over frequency) energy emitted by the resonant transition mechanism. If the magnetic field is weak enough [namely, $\beta \ll 2 \times 3^{1/2} v_T/c$ is fulfilled for ordinary waves, besides, the condition $\omega_B/\omega_p \ll 3(v_T/v)^2$ is required for extraordinary waves], then

$$I_{\mathbf{n}}^\sigma = \frac{8\pi(\nu-1)}{45(\nu+2)} \frac{e^4 Q^2 \langle \Delta N^2 \rangle k_0^{\nu-1}}{c^3 m^2} \left(\frac{v}{\omega_p}\right)^{\nu+1} \frac{vc}{v_T^2} \tag{232}$$

for each normal mode ($\sigma = o, x$), which equals one half of intensity (190) divided by 4π (the difference of 4π is connected with the difference in normalization: Eqn (190) is normalized to the full solid angle, while Eqn (232) is normalized to unity). Naturally, the intensity $I_{\mathbf{n}}^\sigma$ does not depend on the direction of radiation for this case.

If $\beta \gg 2 \times 3^{1/2} v_T/c$, the integration of the terms in Φ_3 and Φ_4 proportional to $(c/v_T)^{1/2}$ contributes the bulk to the total RTR intensity

$$I_{\mathbf{n}}^o = I_{B,\mathrm{tot}} J_o(\beta) , \tag{233}$$

where

$$I_{B,\mathrm{tot}} = \frac{\pi^2(\nu-1)}{(\nu+2)} \frac{1+\cos^2\theta}{2^{3/2} \times 3^{1/4}} \frac{e^4 Q^2 \langle \Delta N^2 \rangle k_0^{\nu-1}}{c^3 m^2} \times \left(\frac{v}{\omega_p}\right)^{\nu+1} \left(\frac{c}{v_T}\right)^{1/2} \frac{\omega_p}{\omega_B} , \tag{234}$$

$$J_o(\beta) = \frac{4}{\beta^2} \left[\frac{(1+\beta)^{9/4}}{9} - \frac{(1+\beta)^{5/4}}{5} + \frac{4}{45} \right] . \tag{235}$$

The magnetic field affects the RTR of extraordinary waves even more strongly, because besides modification of the function Φ, it modifies the respective refractive index (229). The function Φ is changed if $\beta \gg 2 \times 3^{1/2} v_T/c$, while the effect of magnetic field on the refractive index is essential for $\gamma > 1$, where

$$\gamma = \frac{\omega_B}{3\omega_p} \left(\frac{v}{v_T}\right)^2 . \tag{236}$$

For particles with low energy,

$$v < v_* = \left(\frac{\sqrt{3}\, c}{2 v_T}\right)^{1/2} v_T , \tag{237}$$

the main effect is the modification of the function Φ, the value γ reaches unity for an even stronger field. For this case we have

$$I_{\mathbf{n}}^x = I_{B,\mathrm{tot}} J_{x1}(\gamma) , \tag{238}$$

where

$$J_{x1}(\gamma) = \frac{2}{\gamma^2} \begin{cases} \dfrac{(1-\gamma)^{5/2}}{5} - \dfrac{(1-\gamma)^{3/2}}{3} + \dfrac{2}{15} , & \gamma < 1 , \\ \dfrac{2}{15} , & \gamma > 1 . \end{cases} \tag{239}$$

For the condition $v > v_*$, opposite to Eqn (237), the effect of magnetic field on Φ can be entirely neglected (the respective expressions are obtained in Section 3.2), while the modification of the refractive index n_x (229) in comparison to that in isotropic plasma should be taken into account properly. The result is

$$I_{\mathbf{n}}^x = \frac{4\pi(\nu-1)}{9(\nu+2)} \frac{e^4 Q^2 \langle \Delta N^2 \rangle k_0^{\nu-1}}{c^3 m^2} \left(\frac{v}{\omega_p}\right)^{\nu+1} \frac{vc}{v_T^2} J_{x2}(\gamma) , \tag{240}$$

where

$$J_{x2}(\gamma) = \frac{1}{3} \begin{cases} \dfrac{3\pi}{16\gamma^{5/2}} - \dfrac{3}{8\gamma^{5/2}} \arctan \sqrt{\dfrac{1-\gamma}{\gamma}} - \dfrac{3\sqrt{1-\gamma}}{8\gamma^2} \\ \quad - \dfrac{\sqrt{1-\gamma}}{4\gamma} + \sqrt{1-\gamma} , & \gamma < 1 , \\ \dfrac{3\pi}{16\gamma^{5/2}} , & \gamma > 1 . \end{cases} \tag{241}$$

Functions $J_{o,x}$ can be simplified for limiting cases. For small field, we have

$$J_o(\beta) = \frac{1}{2} \left(1 + \frac{\beta}{6}\right) , \quad \beta \ll 1 , \tag{242}$$

$$J_{x1}(\gamma) = \frac{1}{2} \left(1 - \frac{\gamma}{3}\right) , \quad \gamma \ll 1 \tag{243}$$

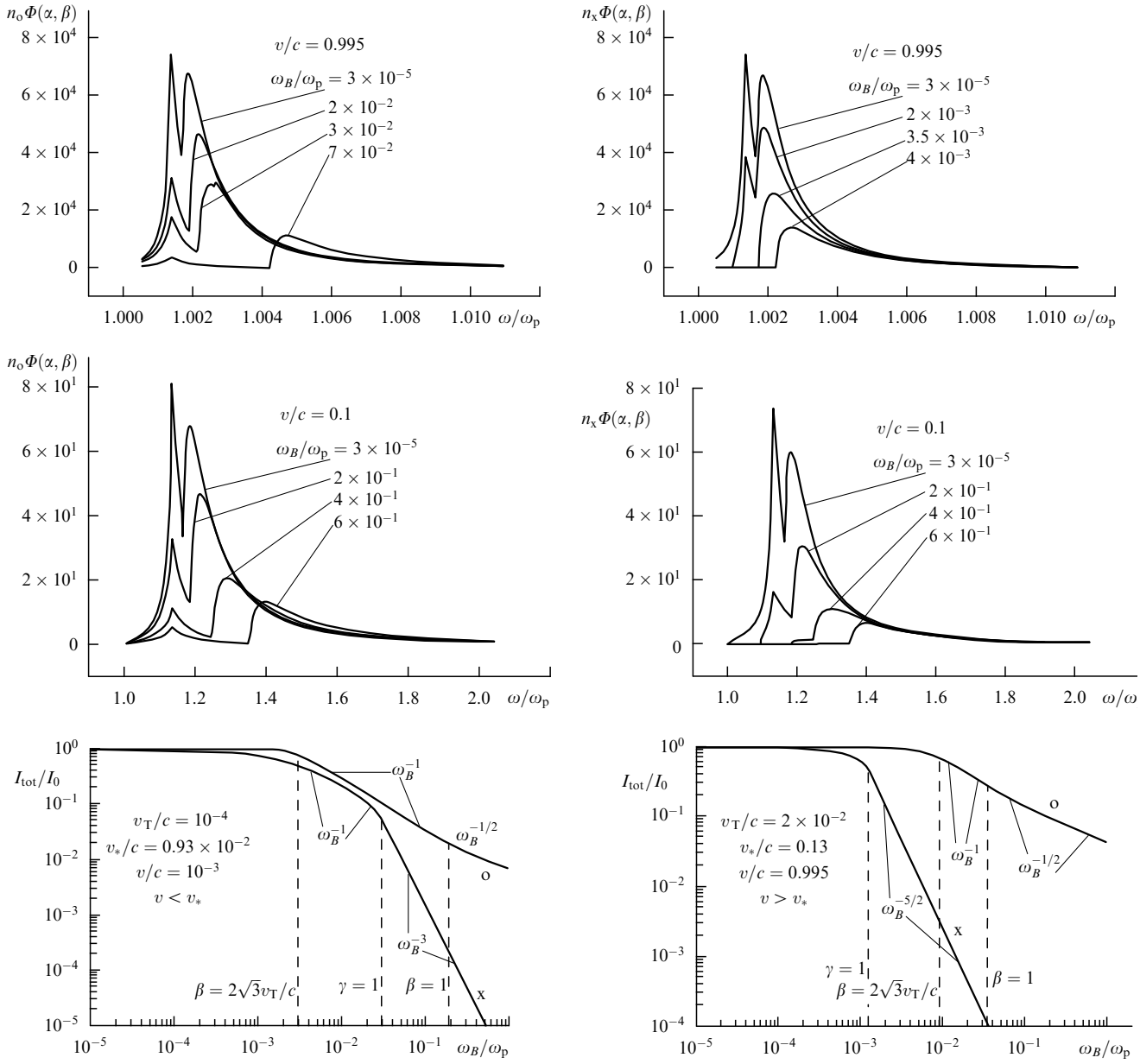

Figure 9. Spectra of resonant transition radiation of ordinary and extraordinary waves in plasma with $v_T/c = 0.0315$. For fast particles (top panel) the increase of the magnetic field suppresses the RTR of extraordinary waves first and then it provides a decrease (and shift) of the peak in the ordinary wave spectrum. For slow particles (middle panel) the peaks are originally broader than for fast particles; the difference in the spectra of radiation of the two normal modes is less prominent than before, while the suppression effect is somewhat stronger for extraordinary waves. The bottom panel displays the dependence of the total (integrated over frequency) RTR intensity on the magnetic field strength for a 'slow' (left) and 'fast' (right) particle. I_0 is the total intensity without the magnetic field. For $\gamma < 1$ the curves for o and x waves follow each other in general (the degree of polarization is less than 50%), while for $\gamma > 1$ the emission intensity of extraordinary waves decreases rapidly and the radiation becomes fully (100%) polarized.

(note, both asymptotic forms are only correct if $\beta \gg 2\times3^{1/2}v_T/c$), and

$$J_{x2}(\gamma) = \frac{2}{5}\left(1-\frac{5\gamma}{14}\right), \qquad \gamma \ll 1\,. \tag{244}$$

The degree of RTR polarization

$$P = \frac{I_{\mathbf{n}}^{o} - I_{\mathbf{n}}^{x}}{I_{\mathbf{n}}^{o} + I_{\mathbf{n}}^{x}} \tag{245}$$

is obviously not large for this case (it is determined by the major of two quantities β and γ); the sense of polarization corresponds to the ordinary mode.

For stronger magnetic field, we have

$$J_o(\beta) = \frac{4\beta^{1/4}}{9}\,, \qquad \beta \gg 1\,, \tag{246}$$

$$J_{x1}(\gamma) = \frac{4}{15\gamma^2}\,, \qquad \gamma > 1\,, \qquad v < v_*\,, \tag{247}$$

$$J_{x2}(\gamma) = \frac{\pi}{16\gamma^{5/2}}\,, \qquad \gamma > 1\,, \qquad v > v_*\,. \tag{248}$$

Respectively, RTR is strongly polarized as o mode for $\gamma > 1$ (independently of the β value).

Thus, the total energy of RTR for ordinary waves equals $I_{\mathbf{n}}^{\mathrm{o}} = I_{B,\mathrm{tot}}/2$ if $2\sqrt{3}\,v_{\mathrm{T}}/c < \beta < 1$ and

$$I_{\mathbf{n}}^{\mathrm{o}} = \frac{2^{1/2}\pi^2(\nu-1)}{(\nu+2)}\,\frac{1+\cos^2\theta}{9\times 3^{1/2}}\,\frac{e^4Q^2\langle\Delta N^2\rangle k_0^{\nu-1}}{c^3m^2} \times\left(\frac{v}{\omega_{\mathrm{p}}}\right)^{\nu+1}\left(\frac{\omega_{\mathrm{p}}}{\omega_B}\right)^{1/2}\left(\frac{cv}{v_{\mathrm{T}}^2}\right)^{1/2} \tag{249}$$

if $\beta > 1$ ($\omega_B/\omega_{\mathrm{p}} > \sqrt{3}\,v_{\mathrm{T}}/v$); and for extraordinary waves it equals $I_{\mathbf{n}}^{\mathrm{x}} = I_{B,\mathrm{tot}}/2$ if $\beta > 2\sqrt{3}\,v_{\mathrm{T}}/c$ and $\gamma < 1$, or

$$I_{\mathbf{n}}^{\mathrm{x}} = \frac{6\pi^2(\nu-1)}{5(\nu+2)}\,\frac{1+\cos^2\theta}{2^{1/2}\times 3^{1/4}}\,\frac{e^4Q^2\langle\Delta N^2\rangle k_0^{\nu-1}}{c^3m^2} \times\left(\frac{v}{\omega_{\mathrm{p}}}\right)^{\nu+1}\left(\frac{\omega_{\mathrm{p}}}{\omega_B}\right)^{3}\frac{c^{1/2}v_{\mathrm{T}}^{3.5}}{v^4}\,, \qquad v < v_*\,, \tag{250}$$

$$I_{\mathbf{n}}^{\mathrm{x}} = \frac{\sqrt{3}\,\pi^2(\nu-1)}{4(\nu+2)}\,\frac{e^4Q^2\langle\Delta N^2\rangle k_0^{\nu-1}}{c^3m^2} \times\left(\frac{v}{\omega_{\mathrm{p}}}\right)^{\nu+1}\left(\frac{\omega_{\mathrm{p}}}{\omega_B}\right)^{5/2}\frac{cv_{\mathrm{T}}^3}{v^4}\,, \qquad v > v_* \tag{251}$$

if $\gamma > 1$ ($\omega_B/\omega_{\mathrm{p}} > 3v_{\mathrm{T}}^2/v^2$). The total radiation energy of both modes equals the sum of the respective expressions for ordinary and extraordinary waves. The result is twice Eqn (232) for a weak field, Eqn (234) for an intermediate field, while the contribution of extraordinary waves is negligible for a strong field (the contribution decreases with increasing velocity if $\nu < 3$). So the radiation is strongly polarized as o mode.

Figure 9 displays the dependence of the total energy of RTR on the magnetic field (more precisely, $\omega_B/\omega_{\mathrm{p}}$) for both fast and slow particles.

Natural plasma is non-uniform usually. Hence, if the respective distribution function over the plasma frequency is broader than the peak in the spectrum of RTR, then the peak can be approximated by

$$I_{\mathbf{n},\omega}^{\mathrm{R},\sigma} = I_{\mathbf{n}}^{\sigma}\delta(\omega-\omega_*)\,, \tag{252}$$

where the frequency ω_* corresponds to the peak in the RTR spectrum and is close to the local plasma frequency.

The role of anisotropy of the fast particle ensemble. Consider how RTR changes if the fast particles are distributed anisotropically. We approximate the actual anisotropy by the second Legendre polynomial, namely

$$F(p,\mu) = \frac{1}{p_0^2}\,\delta(p-p_0)\bigl[1+AP_2(\mu)\bigr]\,, \tag{253}$$

where $\mu = \cos\theta_v$.

All the calculations are similar to the previous ones, while the expressions for the RTR spectrum turn out to be rather bulky. For simplicity, we restrict the consideration to RTR integrated over frequency only.

For a weak magnetic field we have

$$I_{\mathbf{n}}^{\mathrm{o,x}} = I_{\mathbf{n}}^{\mathrm{o,x}(0)}\left(1-\frac{A}{4}\right), \tag{254}$$

where $I_{\mathbf{n}}^{\mathrm{o,x}(0)}$ is the total energy of RTR for the isotropic particle distribution. Since, the distribution function (253) is defined positively for $-1 < A < 2$ only, then

$$\frac{I_{\mathbf{n}}^{\sigma(0)}}{2} \leqslant I_{\mathbf{n}}^{\sigma} \leqslant \frac{5I_{\mathbf{n}}^{\sigma(0)}}{4}\,. \tag{255}$$

Thus, the RTR intensity increases for flattened distributions ($A < 0$), and decreases for elongated ones ($A > 0$) in comparison to an isotropic distribution.

This conclusion is also valid for a strong magnetic field, while the exact expressions are different from the above. Similar calculations can be performed to the end for more complicated distribution functions (which are expressed with Legendre polynomials of higher orders) as well.

RTR by an isotropic particle distribution with a power-law spectrum over momentum. Let us consider RTR generated by an isotropic distribution of charged particles with a power-law dependence of the momentum (172). Many different asymptotic forms arise depending on the parameters involved, since the parameter β depends on the velocity of the particle and the main integration interval over $\mathrm{d}x$ is specified by the interrelation between spectral indices ν and ξ. The integration of Eqns (232), (249)–(251) with the spectrum (172) is easy to perform, so we give here the respective results:

$$P_1 = \frac{4\pi(\nu-1)(\xi-1)}{45(\nu+2)}\,\frac{\Gamma\bigl[(\xi-1)/2\bigr]\Gamma\bigl[(\nu-\xi+3)/2\bigr]}{\Gamma\bigl[(\nu+2)/2\bigr]} \times\frac{e^4Q^2\langle\Delta N^2\rangle k_0^{\nu-1}}{m^2c^3}\,x_0^{\xi-1}N_{\mathrm{e}}\left(\frac{c}{\omega_{\mathrm{p}}}\right)^{\nu+1}\frac{c^2}{v_{\mathrm{T}}^2}\,, \tag{256}$$

$$P_2 = \frac{8\pi(\nu-1)(\xi-1)}{45(\nu+2)(\xi-\nu-3)}\,\frac{e^4Q^2\langle\Delta N^2\rangle k_0^{\nu-1}}{m^2c^3} \times N_{\mathrm{e}}\left(\frac{v_0}{\omega_{\mathrm{p}}}\right)^{\nu+1}\frac{cv_0}{v_{\mathrm{T}}^2}\,, \qquad v_0 = x_0c\,, \tag{257}$$

$$P_3 = \frac{\pi(\nu-1)(\xi-1)}{3(\nu+2)}\left[\frac{8}{15(\nu+3-\xi)}+\frac{\pi(1+\cos^2\theta)}{8(\xi-\nu-2)}\right] \times\frac{e^4Q^2\langle\Delta N^2\rangle k_0^{\nu-1}}{m^2c^3}\,x_0^{\xi-1} \times N_{\mathrm{e}}\left(\frac{c}{\omega_{\mathrm{p}}}\right)^{\nu+1}\frac{c^2}{v_{\mathrm{T}}^2}\left[\frac{\omega_{\mathrm{p}}}{\omega_B}\left(\frac{6\times 3^{1/2}v_{\mathrm{T}}^3}{c^3}\right)^{1/2}\right]^{\nu+3-\xi}, \tag{258}$$

$$P_4 = \frac{\pi^2(\nu-1)(\xi-1)\Gamma\bigl[(\xi-1)/2\bigr]\Gamma\bigl[(\nu-\xi+2)/2\bigr]}{8\times 2^{1/2}3^{1/4}(\nu+2)\Gamma\bigl[(\nu+1)/2\bigr]} \times(1+\cos^2\theta)\,\frac{e^4Q^2\langle\Delta N^2\rangle k_0^{\nu-1}}{m^2c^3} \times x_0^{\xi-1}N_{\mathrm{e}}\left(\frac{c}{\omega_{\mathrm{p}}}\right)^{\nu+1}\left(\frac{c}{v_{\mathrm{T}}}\right)^{1/2}\frac{\omega_{\mathrm{p}}}{\omega_B}\,, \tag{259}$$

$$P_5 = \frac{\pi^2(\nu-1)(\xi-1)\Gamma\bigl[(\xi-1)/2\bigr]\Gamma\bigl[(\nu-\xi+2.5)/2\bigr]}{9\times 6^{1/2}(\nu+2)\Gamma(\nu/2+3/4)} \times(1+\cos^2\theta)\,\frac{e^4Q^2\langle\Delta N^2\rangle k_0^{\nu-1}}{m^2c^3} \times x_0^{\xi-1}N_{\mathrm{e}}\left(\frac{c}{\omega_{\mathrm{p}}}\right)^{\nu+1}\left(\frac{\omega_{\mathrm{p}}}{\omega_B}\right)^{1/2}\frac{c}{v_{\mathrm{T}}}\,, \tag{260}$$

$$P_6 = \frac{\pi(\nu-1)(\xi-1)}{3^{(\xi+1-\nu)/2}(\nu+2)}\left[\frac{8}{5(\nu+3-\xi)}+\frac{\pi}{4(\xi+2-\nu)}\right] \times \frac{e^4Q^2\langle\Delta N^2\rangle k_0^{\nu-1}}{m^2c^3}\, x_0^{\xi-1} N_e\left(\frac{c}{\omega_p}\right)^{\nu+1} \times \left(\frac{\omega_p}{\omega_B}\right)^{(\nu+3-\xi)/2}\left(\frac{c}{v_T}\right)^{\xi-\nu-1}, \quad (261)$$

$$P_7 = \frac{\pi^2(\nu-1)(\xi-1)\left[7(\xi-\nu)+46\right](1+\cos^2\theta)}{20\times 2^{1/2}3^{1/4}3^{(\xi-\nu)/2}(\nu+2)\left[4-(\xi-\nu)^2\right]} \times \frac{e^4Q^2\langle\Delta N^2\rangle k_0^{\nu-1}}{m^2c^3}\, x_0^{\xi-1} N_e\left(\frac{c}{\omega_p}\right)^{\nu+1} \times \left(\frac{\omega_p}{\omega_B}\right)^{(\nu+4-\xi)/2}\left(\frac{v_T}{c}\right)^{\nu-\xi+1.5}, \quad (262)$$

$$P_8 = \frac{\pi^2(\nu-1)(\xi-1)(1+\cos^2\theta)}{4\times 2^{1/2}3^{1/4}(\nu+2)(\xi-\nu-2)}\,\frac{e^4Q^2\langle\Delta N^2\rangle k_0^{\nu-1}}{m^2c^3} \times N_e\left(\frac{v_0}{\omega_p}\right)^{\nu+1}\left(\frac{c}{v_T}\right)^{1/2}\frac{\omega_p}{\omega_B}. \quad (263)$$

Table 1 is a guide to the asymptotic forms. A weak magnetic field, $\omega_B/\omega_p < 3v_T^2/c^2$, does not affect the radiation, so the first line of the table describes the radiation of each transverse eigen mode.

It is important to note that highly polarized radiation arises if the particles with $v > (3\omega_p/\omega_B)^{1/2}v_T$ $(\gamma > 1)$ contribute the bulk to the integrals over momentum. For a power-law distribution of particles (with $v_0 \sim v_T$) it requires relatively hard spectra (small ξ), while the radiation is highly polarized for any hardness of the particle spectrum if $v_0 > (3\omega_p/\omega_B)^{1/2}v_T$.

The factor of RTR excess over standard (non-resonant) transition radiation varies from c^2/v_T^2 in a weak magnetic field to $(c/v_T)(\omega_p/\omega_B)^{1/2}$ in the strong field.

The magnetic field's influence on the plasma dispersion considerably affects the properties of resonant transition radiation. Indeed, a decrease of the peak and total RTR intensity, and a shift and broadening of the peak occur. The emission by an isotropic particle ensemble depends on the emission direction, the degree of polarization can be rather strong (up to 100%), and the sense of polarization corresponds to o mode.

The equations found in Sections 2, 3 can be applied to both laboratory experiments and astrophysical objects, because all important physical effects are taken into account (the averaging of the expressions in gradually non-uniform plasma is trivial). It is important that the high intensity of the radiation makes it competitive with respect to other generally used mechanisms of non-thermal emission.

3.4 Absorption of transition radiation

Besides the emissivity, the absorption coefficient should be calculated to apply any particular emission mechanism to observations. Monograph [28] discusses stimulated TR and derives some of its important general properties. In particular, stimulated TR does not arise if the medium's inhomogeneities have an isotropic distribution, and the TR intensity is described by ultra-relativistic expressions. Reference [64] considers stimulated TR generated when a dense flow of particles is incident upon the sharp boundary of two media.

The study of stimulated emission is of primary interest at those frequency ranges where the intensity of TR generated by a single particle is large enough, because a rather large optical depth may be achieved at these frequencies [65].

Let us apply the method of Einstein coefficients to deduce the RTR growth (damping) rate. We use the standard approach [28] with the proper account of strong frequency dispersion, because the dispersion effects are very important at the plasma frequency. We accept that $N_{\mathbf{k},\sigma}$ is the number density of σ-mode photons with wave-vector $\mathbf{k}$ and $w_{\mathbf{p}}^{\sigma}(\mathbf{k},\mathbf{k}')$ is the probability of emitting a photon with momentum $\hbar\mathbf{k}$ by a particle with momentum $\mathbf{p}$ when the particle is exchanging the momentum $\hbar\mathbf{k}'$ with the medium.

The particle momentum after emission of a single photon is obviously $\mathbf{p}-\hbar(\mathbf{k}-\mathbf{k}')$. The probability $w_{\mathbf{p}}^{\sigma}(\mathbf{k},\mathbf{k}')$ is connected with the intensity of spontaneous emission per unit volume by the simple expression:

$$I_p^{\sigma} = \int \hbar\omega_{\sigma}(\mathbf{k}) w_{\mathbf{p}}^{\sigma}(\mathbf{k},\mathbf{k}')\,\mathrm{d}\mathbf{k}'\,\frac{\mathrm{d}\mathbf{k}}{(2\pi)^3} = \int \hbar\omega_{\sigma}(\mathbf{k}) w_{\mathbf{p}}^{\sigma}(\mathbf{k},\mathbf{k}')\,\mathrm{d}\mathbf{k}'\,\frac{\omega^2 n_{\sigma}^2\,\mathrm{d}(\omega n_{\sigma})/\mathrm{d}\omega}{(2\pi)^3 c^3}\,\mathrm{d}\omega\,\mathrm{d}\Omega_{\mathbf{k}}, \quad (264)$$

where n_{σ} is the refractive index of the respective mode.

The probability of stimulated emission and absorption are proportional to $N_{\mathbf{k},\sigma}w_{\mathbf{p}}^{\sigma}(\mathbf{k},\mathbf{k}')$. However, the emission is produced by the particles with the momentum $\mathbf{p}$ (at the top level), while the absorption is provided by the particles with the momentum $\mathbf{p}-\hbar(\mathbf{k}-\mathbf{k}')$ (at bottom level). Thus, the

Table 1.

Parameters	Type of wave	$\xi < \nu+3/2$	$\nu+3/2 < \xi < \nu+2$	$\nu+2 < \xi < \nu+5/2$	$\nu+5/2 < \xi < \nu+3$	$\nu+3 < \xi$
$\frac{3v_T^2}{c^2} < \frac{\omega_B}{\omega_p} < \frac{\sqrt{6\sqrt{3}}\,v_T^{3/2}}{c^{3/2}}$	o	P_1	P_1	P_1	P_1	P_2
	x	P_6	P_6	P_6	P_6	P_2
$\frac{\sqrt{6\sqrt{3}}\,v_T^{3/2}}{c^{3/2}} < \frac{\omega_B}{\omega_p} < \frac{\sqrt{3}\,v_T}{c}$	o	P_4	P_4	P_3	P_3	P_2
	x	P_6	P_6	P_6	P_6	P_2
$\frac{\sqrt{3}\,v_T}{c} < \frac{\omega_B}{\omega_p} < \left(\frac{6\sqrt{3}\,v_T}{c}\right)^{1/2}$	o	P_5	P_5	P_3+P_5	P_3	P_2
	x	P_7	P_7	P_3	P_3	P_2
$\left(\frac{6\sqrt{3}\,v_T}{c}\right)^{1/2} < \frac{\omega_B}{\omega_p} < 1$	o	P_5	P_5	P_5+P_8	P_8	P_8
	x	P_7	P_7	P_8	P_8	P_8

equation for the balance of the number of photons reads:

$$\frac{\mathrm{d}N_{\mathbf{k},\sigma}}{\mathrm{d}t} = 2\gamma_{\mathbf{k},\sigma}N_{\mathbf{k},\sigma} = N_{\mathbf{k},\sigma}\int w_{\mathbf{p}}^{\sigma}(\mathbf{k},\mathbf{k}')(f_{\mathbf{p}} - f_{\mathbf{p}-\hbar(\mathbf{k}-\mathbf{k}')})\,\mathrm{d}\mathbf{k}'\,\mathrm{d}\mathbf{p}\,, \tag{265}$$

where $\gamma_{\mathbf{k},\sigma}$ is the growth rate of the radiation field amplitude, and f_{p} is the distribution function of fast particles. Thus, the growth rate can be written as

$$\gamma_{\mathbf{k},\sigma} = \frac{1}{2}\,\frac{(2\pi)^3c^3}{\omega^3 n_\sigma^2\,\mathrm{d}(\omega n_\sigma)/\mathrm{d}\omega}\int\frac{\mathrm{d}I_p^{\sigma}}{\mathrm{d}\omega\,\mathrm{d}\Omega_{\mathbf{k}}\,\mathrm{d}\mathbf{k}'}(\mathbf{k}-\mathbf{k}')\,\frac{\mathrm{d}f}{\mathrm{d}\mathbf{p}}\,\mathrm{d}\mathbf{k}'\,\mathrm{d}\mathbf{p}\,. \tag{266}$$

The combination $\mathrm{d}I_p^{\sigma}/\mathrm{d}\omega\,\mathrm{d}\Omega_{\mathbf{k}}\,\mathrm{d}\mathbf{k}'$ represents the spectral-angular distribution of the intensity of spontaneous emission per unit plasma volume, when the plasma loses the momentum $\hbar\mathbf{k}'$.

The use of a spherical coordinate system in the space of momentum with the axis z along the external magnetic field $\mathbf{B}$ is convenient for calculating $\mathrm{d}f/\mathrm{d}\mathbf{p}$. Substituting the expression for the gradient in spherical coordinates and assuming the distribution function to be independent of the azimuth angle, we find finally:

$$\gamma_{\mathbf{k},\sigma} = \frac{1}{2}\,\frac{(2\pi)^3c^3}{\omega^2 n_\sigma^2\,\mathrm{d}(\omega n_\sigma)/\mathrm{d}\omega}\int\frac{\mathrm{d}I_p^{\sigma}}{\mathrm{d}\omega\,\mathrm{d}\Omega_{\mathbf{k}}\,\mathrm{d}\mathbf{k}'}\,\frac{1}{pv} \times\left\{p\,\frac{\partial f}{\partial p} + \left[\frac{v(\mathbf{k}-\mathbf{k}')\mathbf{B}}{\omega B} - \mu\right]\frac{\partial f}{\partial\mu}\right\}\mathrm{d}\mathbf{k}'\,\mathrm{d}\mathbf{p}\,, \tag{267}$$

where $\mu = \cos\theta_{\mathbf{vB}}$ is the cosine of the angle between the velocity of particle and the external magnetic field.

The TR absorption coefficient $\kappa_\omega = \gamma/v_{\mathrm{gr}} \approx \gamma/c$ is calculated in Ref. [66] at high frequencies (in the ultra-relativistic limiting case). Both electrons and protons contribute to it, so that

$$\kappa_\omega = \frac{\pi(\nu-1)(\xi-1)(\xi+2)}{2\nu^2(\nu+2)}\left(\frac{N_{\mathrm{cr}}}{M}+\frac{N_{\mathrm{e}}}{m}\right) \times\frac{q^2\omega_{\mathrm{p}}^4}{c\omega^5}\,\frac{\langle\Delta N^2\rangle}{N^2}\left(\frac{2k_0c}{\omega}\right)^{\nu-1}\left(\frac{\omega}{\omega_{\mathrm{p}}}\right)^{2\nu}F\left(\nu,\frac{\xi}{2},\frac{\xi+2}{2};-\frac{\omega^2}{\omega_{\mathrm{p}}^2}\right), \tag{268}$$

where N_{cr}, M are the number density and mass of relativistic nuclei, and $F(\alpha,\beta,\gamma;x)$ is the hypergeometric function. It can be expanded at high frequencies into a series valid for $x \gg 1$:

$$F\left(\nu,\frac{\xi}{2},\frac{\xi+2}{2};-\frac{\omega^2}{\omega_{\mathrm{p}}^2}\right) = \frac{\xi}{\xi-2\nu}\left(\frac{\omega_{\mathrm{p}}}{\omega}\right)^{2\nu}\left[1+\frac{\nu(\xi-2\nu)}{2\nu-\xi+2}\,\frac{\omega_{\mathrm{p}}^2}{\omega^2}\right] + \frac{\Gamma(\nu-\xi/2)\Gamma(\xi/2+1)}{\Gamma(\nu)}\left(\frac{\omega_{\mathrm{p}}}{\omega}\right)^{\xi}. \tag{269}$$

According to Eqns (268), (269), the radiation intensity [for the optically thick regime ($L\kappa_\omega \gg 1$)] is

$$J_\omega = \frac{P_\omega}{\kappa_\omega} \propto \omega^3 \quad\text{at}\quad 2\nu > \xi \quad\text{and}\quad \propto \omega^{2\nu+3-\xi} \quad\text{at}\quad 2\nu < \xi\,. \tag{270}$$

Equation (268) shows that the contribution from the electron component is important even if their number density is less than the number density of relativistic nuclei. The spectral behavior (270) differs in the general case from the respective laws for synchrotron ($J_\omega^{\mathrm{s}} \propto \omega^{2.5}$) and blackbody ($J_\omega^{\mathrm{T}} \propto \omega^2$) emissions. Estimates show that the optical thickness of astrophysical objects, which is related to (standard) transition radiation, is typically much less than unity.

Let us go back to the absorption of resonant transition radiation. In the presence of magnetic field the value $\mathrm{d}I_p^{\sigma}/\mathrm{d}\omega\,\mathrm{d}\Omega_{\mathbf{k}}\,\mathrm{d}\mathbf{k}'$ is

$$\frac{\mathrm{d}I_p^{\sigma}}{\mathrm{d}\omega\,\mathrm{d}\Omega_{\mathbf{k}}\,\mathrm{d}\mathbf{k}'} = \frac{4\pi e^4q^2n_\sigma}{m^2c^3} \times\frac{[\mathbf{n}\times\mathbf{k}']^2\delta\big[\omega-(\mathbf{k}-\mathbf{k}')\mathbf{v}\big]|\delta N|_{\mathbf{k}'}^2}{(\mathbf{k}-\mathbf{k}')^4\big\{\big[\varepsilon(\omega)-3(\mathbf{k}-\mathbf{k}')^2d^2-(\omega_{\mathrm{p}}^2\omega_B^2/\omega^4)\sin^2\theta\big]^2+\varepsilon''^2\big\}}\,, \tag{271}$$

where θ is the angle between the vector $\mathbf{k}'$ and the magnetic field. We should emphasize that the magnetic field produces two effects at least: it modifies the spectrum of spontaneous RTR through the variation of the plasma dispersion, and provides the selected direction that is necessary to produce an anisotropic distribution of fast electrons.

If the distribution of the particles is isotropic [note, the distribution is normalized by d^3p contrary to Eqn (172)],

$$f(\mathbf{p}) = \frac{\zeta-3}{4\pi p_0^3}\,N_{\mathrm{e}}\left(\frac{p_0}{p}\right)^{\zeta}, \tag{272}$$

the angular derivative in Eqn (267) vanishes, and the RTR growth rate reads:

$$\gamma_{\mathbf{k},\sigma} = \frac{\zeta}{2}\,\frac{(2\pi)^3c^3}{\omega^2n_\sigma^2\,\mathrm{d}(\omega n_\sigma)/\mathrm{d}\omega}\int\frac{4\pi f(\mathbf{p})p\,\mathrm{d}p}{v}\int I_{\mathbf{n},\omega}^{\sigma}\,\frac{\mathrm{d}\Omega_{\mathbf{p}}}{4\pi}\,, \tag{273}$$

where

$$I_{\mathbf{n},\omega}^{\sigma} = \int\frac{\mathrm{d}I_p^{\sigma}}{\mathrm{d}\omega\,\mathrm{d}\Omega_{\mathbf{k}}\,\mathrm{d}\mathbf{k}'}\,\mathrm{d}\mathbf{k}'$$

is the spectral-angular distribution of RTR. The last integration in Eqn (273) has already been performed in the previous sections for the power-law distribution (35) of density inhomogeneities; it has the form (221). Substitution of Eqns (221), (272) into Eqn (273) yields

$$\gamma_{\mathbf{k},\sigma} = -\frac{\zeta(2\pi)^4(\nu-1)(\zeta-3)}{3(\nu+2)}\,\frac{e^6p_0^{\zeta-3}N_{\mathrm{e}}k_0^{\nu-1}\langle\Delta N^2\rangle}{m^2\omega^{\nu+4}n_\sigma\,\mathrm{d}(\omega n_\sigma)/\mathrm{d}\omega} \times\int\Phi(\alpha,\beta)\,\frac{v^\nu\,\mathrm{d}p}{p^{\zeta-1}}\,. \tag{274}$$

The RTR damping rate is expressed here as a single integral from the function $\Phi(\alpha,\beta)$ over momentum. The integration cannot be performed within standard (elementary) functions for a general case. Nevertheless, the integral is obviously specified by the integration region $p \sim mc$, because the integrand decreases more or less fast (with power laws) for both $p < mc$ and $p > mc$. Taking into account the asymptotic forms of $\Phi(\alpha,\beta)$ when v decreases, the integral is estimated as

$$\int\Phi(\alpha,\beta)\,\frac{v^\nu\,\mathrm{d}p}{p^{\zeta-1}} = \Phi_c(\alpha,\beta)\,\frac{c^\nu}{(mc)^{\zeta-2}} \times\frac{\Gamma\big[(\nu-\zeta+5)/2\big]\Gamma\big[(\zeta-2)/2\big]}{2\Gamma\big[(\nu+3)/2\big]}\,, \tag{275}$$

where $\Phi_c(\alpha,\beta)$ is defined as $\Phi(\alpha,\beta)$ at $v=c$ (the index 'c' of the function $\Phi_c(\alpha,\beta)$ is hereafter omitted). Substitution of Eqn (275) into Eqn (274) finally gives rise to

$$\gamma_{\mathbf{k},\sigma}=\frac{\zeta(v-1)(\zeta-3)\Gamma\big[(v-\zeta+5)/2\big]\Gamma\big[(\zeta-2)/2\big]}{6(v+2)\Gamma\big[(v+3)/2\big]n_\sigma\,\mathrm{d}(\omega n_\sigma)/\mathrm{d}\omega}\,\frac{e^2N_\mathrm{e}}{m\omega_\mathrm{p}}$$
$$\times\left(\frac{\omega_\mathrm{p}}{\omega}\right)^{v+4}\left(\frac{k_0c}{\omega_\mathrm{p}}\right)^{v-1}\left(\frac{p_0}{mc}\right)^{\zeta-3}\frac{\langle\Delta N^2\rangle}{N^2}\,\Phi(\alpha,\beta)\,, \qquad (276)$$

where the factor $(\omega_\mathrm{p}/\omega)^{v+4}$ can be omitted when RTR is analyzed because the peak frequency is close to the plasma frequency. The RTR damping rate can exceed the collisional damping rate of the waves. For example, if $N\sim10^{10}$ cm^{-3}, $T\sim10^6$ K (the parameters are typical for coronal loops at the Sun), the collisional damping rate is

$$\nu_\mathrm{ei}\approx60\,\frac{N}{T^{3/2}}\approx600\ \mathrm{s}^{-1}\,. \qquad (277)$$

The RTR damping rate for the same plasma parameters and

$$\left(\frac{k_0c}{\omega_\mathrm{p}}\right)^{v-1}\frac{\langle\Delta N^2\rangle}{N^2}\approx10^{-4}\,,\qquad N_\mathrm{e}\left(\frac{p_0}{mc}\right)^{\zeta-3}\approx10^3\ \mathrm{cm}^{-3} \qquad (278)$$

is

$$\gamma^\sigma=10^3\ \mathrm{s}^{-1}\,. \qquad (279)$$

3.5 Transition maser emission

Let us concentrate on stimulated (maser) resonant transition radiation. Astrophysical plasma frequently contains magnetic structures. These structures (e.g. magnetic traps) may give rise to anisotropic distributions of super-thermal particles. The anisotropic distributions may be unstable with respect to the generation of particular electromagnetic mode(s) under appropriate conditions. Excitation of Langmuir waves by beams of non-thermal particles and cyclotron (maser) instability of transverse waves in magnetized plasma [67] are good examples of these instabilities. The conditions providing the instability of resonant transition radiation and the respective growth rates are of special interest here.

The absorption coefficient for an anisotropic particle distribution can be calculated like the intensity of radiation (Section 3.3) by means of expansion of the angular distribution over Legendre polynomials. However, if the real anisotropy is approximated by the lowest Legendre polynomials:

$$f(p,\mu)=f_0(p)\big[1+A_1(p)P_1(\mu)+A_2(p)P_2(\mu)\big]\,, \qquad (280)$$

then the RTR amplification does not happen.

Indeed, the contribution of the flow-like term $A_1(p)P_1(\mu)$ is proportional to the factor kv/ω, which is small at the peak (at $\omega\sim\omega_3$)

$$\frac{kv}{\omega}\sim\frac{\omega_B}{\omega_\mathrm{p}}\,. \qquad (281)$$

Hence, the weak flow anisotropy modeled by the first Legendre polynomial ($-1\leqslant A_1\leqslant1$ because the distribution function must be positive) does not provide the instability. The even part of the distribution function, $A_2(p)P_2(\mu)$, does not contain any small factor. Nevertheless, the positive contribution connected with the derivative over the angle is less (by the absolute value) than the negative contribution from the derivative over momentum. Thus, an anisotropy of this kind is too weak to provide the instability of RTR.

Two model distribution functions are further analyzed to find the anisotropy required for providing the instability. The first one

$$f(p,\mu)\propto\exp a\mu\,,\qquad\frac{\partial f}{\partial\mu}=af \qquad (282)$$

is not even, and it contains a flow component. The main positive contribution is produced here by the term $(kv\cos\theta)/\omega$, while the main negative one is by the term $p\,\partial f/\partial p$. Thus,

$$p\,\frac{\partial f}{\partial p}+\left[\frac{v(\mathbf{k}-\mathbf{k}')\mathbf{B}}{\omega B}-\mu\right]\frac{\partial f}{\partial\mu}\cong\left(-\zeta+a\,\frac{v}{c}\,n_\sigma\cos\theta\right)f(p,\mu)\,. \qquad (283)$$

At the RTR peak we have $n_\sigma\approx\omega_B/\omega_\mathrm{p}$. Since the region of $v\sim c$ contributes the bulk to the integral over momentum, the RTR instability is possible for

$$a>\frac{\zeta}{n_\sigma}\approx\frac{\zeta\omega_\mathrm{p}}{\omega_B}\,. \qquad (284)$$

If $\zeta>3$, $\omega_\mathrm{p}/\omega_B\sim3$ we have $a>10$, hence most of the fast electrons should be concentrated within a cone of angle less or of the order of 25°. Expansion of the distribution function (282) in Eqn (283) (i.e., after taking the derivative over μ!) and keeping the first term of the expansion provides an accuracy of about 30%. Thus, the growth rate differs from Eqn (276) by the replacement of the factor $-\zeta$ by $-\zeta+(v/c)an_\sigma\cos\theta$. The largest amplification occurs along the magnetic field, while the waves damp in the transverse direction.

Let us consider a distribution function even over μ that does not contain any contribution from the term $v\mathbf{kB}/\omega B$. The integration over angles yields

$$p\,\frac{\partial f}{\partial p}-\left(v\,\frac{\mathbf{k}'\mathbf{B}}{\omega B}+\mu\right)\frac{\partial f}{\partial\mu}\to(-\zeta+1)f<0\,, \qquad (285)$$

for any even distribution function if most of the particles move transversely to the magnetic field, $\mu\ll1$.

However, if the derivative $\partial f/\partial\mu$ is large for $\mu\sim1$, the instability of RTR is possible. We assume the distribution function to be independent of μ for $|\mu|<\mu_1$ and to decrease linearly down to zero when $|\mu|$ increases up to unity [$f(p,\mu)=N_\mathrm{e}f(p)f(\mu)$]:

$$f(\mu)=\frac{1}{1+\mu_1}\begin{cases}1, & |\mu|<\mu_1\,,\\ \dfrac{1-\mu}{1-\mu_1}\,, & \mu_1<|\mu|<1\,,\end{cases} \qquad (286)$$

$$\frac{\partial f}{\partial\mu}=\begin{cases}0\,, & |\mu|<\mu_1\,,\\ -\dfrac{1}{1-\mu_1^2}\,, & \mu_1<|\mu|<1\,.\end{cases} \qquad (287)$$

The calculations cannot be performed analytically to the very end for this case. Nevertheless, some simplifications can be used in the peak region because $k'_\mathrm{eff}\gg\omega/v$. Since the contribution to the integration over the angle $\theta_{\mathbf{k}'\mathbf{B}}$ in Eqns (267), (271) is small for terms proportional to

$\cos^{2n}\theta_{\mathbf{k}'\mathbf{B}}$ in comparison to the terms free from the factor $\cos\theta_{\mathbf{k}'\mathbf{B}}$ in the numerator, the expansion of μ over the angles $\theta_{\mathbf{k}'\mathbf{B}}$ and $\theta_{\mathbf{k}'\mathbf{v}}$ reduces to

$$\mu = \cos\theta_{\mathbf{k}'\mathbf{B}}\cos\theta_{\mathbf{k}'\mathbf{v}} + \sin\theta_{\mathbf{k}'\mathbf{B}}\sin\theta_{\mathbf{k}'\mathbf{v}}\cos\phi_{\mathbf{B}\mathbf{v}} \approx \left[1-\left(\frac{\omega}{k'v}\right)^2\right]^{1/2}\cos\phi_{\mathbf{B}\mathbf{v}}\,. \quad (288)$$

The use of (288) yields

$$\int \mathrm{d}\mathbf{p}\,\delta(\omega+\mathbf{k}'\mathbf{v})\left[-\zeta f(p,\mu)-\mu\frac{\partial f}{\partial\mu}\right] = \pi\int\frac{f(p)p^2\,\mathrm{d}p}{k'v}\left\{-\zeta+\frac{2\left[1-(\omega/k'v)^2-\mu_\mathrm{I}^2\right]^{1/2}}{\pi(1-\mu_\mathrm{I}^2)}\right\}. \quad (289)$$

Hence, the growth rate of the RTR instability takes the form

$$\gamma^\sigma = \frac{(2\pi)^5 e^6 N_\mathrm{e}}{4m^2\omega^2 n_\sigma\,\mathrm{d}(\omega n_\sigma)/\mathrm{d}\omega}\int\frac{f(p)\,p\,\mathrm{d}p}{v^2} \times\int\mathrm{d}k'\,\mathrm{d}x\,(1+\cos^2\theta_n)|\delta N|^2_{\mathbf{k}'} \times\frac{-\zeta+2\left[1-(\omega/k'v)^2-\mu_\mathrm{I}^2\right]^{1/2}/\left[\pi(1-\mu_\mathrm{I}^2)\right]}{\mathbf{k}'\left\{\left[\varepsilon(\omega)-3(\mathbf{k}-\mathbf{k}')^2d^2-(\omega_\mathrm{p}^2\omega_B^2/\omega^4)(1-x^2)\right]^2+\varepsilon''^2\right\}}\,. \quad (290)$$

Further calculations are very similar to those done in Section 3.3. The only difference is that now we may keep just the largest terms (in the peak region), because the next terms [without the factor $(c/v_\mathrm{T})^{1/2}$)] would provide over-accuracy of Eqn (290). Finally, we have

$$\gamma^\sigma = \frac{(\nu-1)(\zeta-3)(\nu+3)\pi^5 e^6 N_\mathrm{e}N^2}{3^{3/2}(\nu-\zeta+5)(\zeta-2)m^3\omega_\mathrm{p}^5 n_\sigma\,\mathrm{d}(\omega n_\sigma)/\mathrm{d}\omega} \times\left(\frac{p_0}{mc}\right)^{\zeta-3}\left(\frac{c}{v_\mathrm{T}}\right)^3\left(\frac{k_0c}{\omega_\mathrm{p}}\right)^{\nu-1}\frac{\langle\Delta N^2\rangle}{N^2}\left(\frac{\omega_\mathrm{p}}{\omega_B}\right)(1+\cos^2\theta_n) \times\frac{\left(c/(2\times3^{1/2}v_\mathrm{T})\right)^{1/2}}{(\alpha-\beta)^3\left[\alpha(\alpha-\beta)\right]^{1/4}}\left[-\zeta+\frac{2(1-\varkappa^2-\mu_\mathrm{I}^2)^{1/2}}{\pi(1-\mu_\mathrm{I}^2)}\right], \quad (291)$$

where $\varkappa=\omega_\mathrm{p}v_\mathrm{Te}/\omega_B c$; α and β are defined by Eqn (215) with $v=c$. The amplification along the fields is two times stronger than that transverse to the field for this model. Note that for $\mu_\mathrm{l}\ll 1$ the last factor in brackets in Eqn (291) tends to $-\zeta+2/\pi<0$. The small difference between it and Eqn (285) arises because the linear decrease is too slow to reach the asymptotic form (285), while the two expressions are in good qualitative agreement. The value in brackets reaches its maximum $-\zeta+1/\pi\varkappa$ at $\mu_\mathrm{l}^2=1-2\varkappa^2$; the growth rate decreases for both larger and smaller μ_l. Thus, the distribution function even over angle provides the instability if the particles are lacking close to $|\mu|=1$ in the region of the width $\Delta\theta\cong\varkappa$. For other angles, $f(\mu)$ can be an arbitrary slow-varying function. Such a distribution can arise in magnetic traps, which are typical for planetary and stellar magnetospheres.

Let us estimate **the growth rate** (291) and the required parameters of the magnetic trap for ionospheric plasma. For $(k_0c/\omega_\mathrm{p})^{\nu-1}\langle\Delta N^2\rangle/N^2\cong10^{-4}$, $(p_0/mc)^{\zeta-3}N_\mathrm{e}\cong10^{-5}$ cm^{-3}, $\omega_\mathrm{p}/\omega_B\cong3$, $\mu_\mathrm{l}^2=1-2\varkappa^2$, $\omega_\mathrm{p}\cong3\times10^7$ s^{-1}, $v_\mathrm{T}/c\cong10^{-3}$ the growth rate is $\gamma^\sigma\cong80$ s^{-1}. The ratio B/B_max providing the required shape of the distribution function $f(\mu)$ is $B/B_\mathrm{max}=2\varkappa^2\cong2\times10^{-5}$.

Let us discuss the most important outcome of **the study of the absorption of resonant transition radiation in magnetic field.** The RTR absorption coefficient can exceed the absorption coefficient provided by thermal electrons close to the plasma frequency.

Anisotropic distributions of fast electrons can provide instability of RTR. The respective exponential growth of this (maser) RTR can give rise to a large brightness temperature of the generated radio emission, like other coherent mechanisms, i.e., cyclotron maser and plasma mechanisms. The mechanisms have widely been applied for the interpretation of various kinds of radio emission from the Sun, planets and stars; mainly, for the emission revealing fast temporal variability like millisecond solar radio spikes [67].

The basic properties of maser RTR, which can be tested observationally, are

— maser RTR does not produce any harmonic emission: only emission close to the local plasma frequency can be amplified;

— the waves are amplified along the external magnetic field preferentially;

— the RTR instability is insensitive to details of the energy spectrum of electrons in the 1 MeV region. Hence, the maser RTR can or cannot be accompanied by soft gamma-ray emission, contrary to cyclotron maser emission.

The comparison of maser RTR with other coherent mechanisms. The plasma mechanism produces waves around ω_p and $2\omega_\mathrm{p}$ (and at the third harmonic, but very seldom). Cyclotron maser emission arises around the lowest harmonics of cyclotron frequency; non-integer 'harmonic' ratios are possible [68–71]. Then, according to Ref. [67] cyclotron maser emission cannot be accompanied by soft gamma-ray emission and must be accompanied by hard X-ray emission [i.e., the number of fast electrons with $E_\mathrm{kin}>(0.5-1)$ MeV should be small enough].

Presently, the important role of cyclotron maser and plasma mechanism for solar corona and planetary magnetospheres has reliably been proved. The possible role of the transition maser emission is still absolutely unstudied.

4. Polarization bremsstrahlung

This section considers a limiting case of transition radiation, where density inhomogeneities are related to the thermal fluctuations in the medium. This radiation mechanism is referred to as polarization bremsstrahlung (the terms 'transition bremsstrahlung' and 'dynamic bremsstrahlung' are also used in the literature for the very same emission process), since the dynamic polarizability of the medium is the primary physical reason for the electromagnetic wave generation in this case. The theory of this problem (see Refs [59, 72–76], monographs [28, 5], and references there) uses two different approaches to describe the emission. The first of them, the macroscopic treatment, is based on the methods of macroscopic electrodynamics. First, currents and charges induced by the fast particles moving in the medium are calculated and then radiation fields are found from the Maxwell equations. The second approach, microscopic, describes movement and emission of an individual background electron by methods of quantum or classical mechanics. The result obtained is summed over all electrons and averaged over the electron distribution in the medium. Obviously, the second approach has wider range of applicability because it starts with an elementary particle interac-

tion. However, such calculations are too expensive mathematically, so they are worth using only when the first method fails. Accordingly, monograph [5] uses the microscopic method to describe the emission of only the simplest interacting systems (collisions of a particle with one atom, atom with atom etc.), while the classical approach is used for most of the cases.

Section 4.1 applies the microscopic approach to find the spectrum of polarization bremsstrahlung in equilibrium isotropic plasma. The general expression for the intensity of polarization bremsstrahlung (PB) in the plasma is obtained taking into account the interaction between particles and collective plasma excitations. The emission spectrum is specified by the correlation function of the plasma density. Inelastic processes associated with excitation of single plasma electrons are shown to contribute the bulk to the emission in the frequency range $\omega > c/d$ (where d is the Debye radius in the plasma). At lower frequencies three main processes make a comparable contribution to PB: scattering of the fast particle field by Debye spheres (the proper transition bremsstrahlung), emission by individual excited electrons, and emission by electrons with simultaneous plasmon excitation. The two latter processes are analogous to ionization and polarization losses of a fast particle in plasma.

Section 4.2 studies the PB spectrum in the vicinity of a resonant singularity, i.e., when the radiation frequency is approaching the plasma frequency.

Section 4.3 considers PB in a medium in the frequency range $c/v_0\sqrt{\varepsilon(\omega)} < 1$, where the Vavilov – Cherenkov effect takes place. In this frequency range, the PB intensity is found to rise by one – two orders of magnitude in comparison with the frequency range $c/v_0\sqrt{\varepsilon(\omega)} > 1$. This increase can be interpreted as a result of the scattering of Cherenkov quanta by the electron shells of atoms. In this case, PB can be observed in spite of the Vavilov – Cherenkov radiation being more powerful, since the PB is emitted largely outside the Cherenkov cone.

The next three sections study the influence of the external magnetic field on PB. Section 4.4 considers a weak magnetic field that does not affect the spectrum of thermal plasma fluctuations, while provides differences in the dispersion of emitted normal waves related to weak plasma gyrotropy [82], which results in the generation of polarized radiation. The degree of polarization is determined here by the magnetic field strength.

Section 4.5 deals with a stronger magnetic field [77]: $\omega_{Be} \gg \omega_{pe}$ (where ω_{pe} is the electron plasma frequency, $\omega_{Be} = eB/mc$ is the electron gyrofrequency). The considered magnetic field has a substantial effect on the correlation function of plasma density fluctuations, while it is not strong enough to suppress the motion of particles transverse to the magnetic field completely.

Finally, Section 4.6 discusses ultra-strong magnetic field, where the motion of all charged particles in the plasma is one-dimensional.

4.1 Microscopic theory of the polarization bremsstrahlung by fast particles in equilibrium plasma

This section offers the theory of PB in non-degenerate plasma based on the tight similarity with the theory of electromagnetic wave scattering in a plasma [79]. The general treatment accounts for both the interaction of plasma particles and various types of plasma excitations.

Let us first deduce a general expression for the PB intensity in a plasma. The radiation field of non-relativistic charged particles at a distance R is described by the expression

$$\mathbf{E}_{\mathbf{n}}(\mathbf{R},t) = \frac{e}{cR}\left[\mathbf{n}\times\left[\mathbf{n}\times\dot{\boldsymbol{\beta}}\right]\right]\Big|_{t'}, \qquad t' = t - \frac{|\mathbf{R}|}{c}, \quad \mathbf{n} = \frac{\mathbf{R}}{R}, \quad \dot{\boldsymbol{\beta}} = \frac{\dot{\mathbf{v}}}{c}. \tag{292}$$

Here we use the perturbation theory assuming that the plasma electron followed an unperturbed trajectory $\mathbf{r}(t)$ before collision to find the acceleration of the electron by the fast particle field $\mathbf{E}^{Q}$:

$$\dot{\boldsymbol{\beta}}(t) = \frac{e}{mc}\,\mathbf{E}^{Q}\big(\mathbf{r}(t);t\big). \tag{293}$$

The field of radiation by all electrons is

$$\mathbf{E}_{\mathbf{n}}(\mathbf{R},t) = \frac{e}{cR}\int \mathrm{d}\mathbf{r}\int \mathrm{d}\mathbf{v}\,F_{\mathrm{e}}(\mathbf{r},\mathbf{v},t)\left[\mathbf{n}\times\left[\mathbf{n}\times\dot{\boldsymbol{\beta}}\right]\right]\Big|_{t'}, \tag{294}$$

where $F_{\mathrm{e}} = \sum_a \delta\big[\mathbf{r}-\mathbf{r}_a(t)\big]\delta\big[\mathbf{v}-\mathbf{v}_a(t)\big]$ is the microscopic phase density, and

$$n_{\mathrm{e}}(\mathbf{r},t) = \sum_a \delta\big[\mathbf{r}-\mathbf{r}_a(t)\big] = \int \mathrm{d}\mathbf{v}\,F_{\mathrm{e}}(\mathbf{r},\mathbf{v},t) \tag{295}$$

is the microscopic number density of plasma electrons. The radiation intensity can be expressed with the use of the Poynting vector for the field (294). To obtain the spectral density of radiation, we expand the radiation field into the Fourier integral over time, which provides the intensity of a monochromatic radiation component at frequency ω:

$$I_{\mathbf{n},\omega} = \frac{cr_0^2 N}{4\pi^2 T}\int \mathrm{d}\mathbf{k}'\,\mathrm{d}\mathbf{k}''\,\mathrm{d}\omega'\,\mathrm{d}\omega'' \times\left[\mathbf{E}^{Q}_{\mathbf{k}',\omega'}\cdot\mathbf{E}^{Q}_{\mathbf{k}'',\omega''} - (\mathbf{n}\cdot\mathbf{E}^{Q}_{\mathbf{k}',\omega'})(\mathbf{n}\cdot\mathbf{E}^{Q}_{\mathbf{k}'',\omega''})\right] \times S(\mathbf{k}-\mathbf{k}',\omega-\omega',\mathbf{k}-\mathbf{k}'',\omega-\omega''), \qquad T\to\infty. \tag{296}$$

Here, $\mathbf{k} = (\omega/c)\mathbf{n}(1-\omega_{\mathrm{p}}^2/\omega^2)^{1/2}$, $\mathbf{n}$ is the unit vector, N is the mean electron number density, $r_0 = e^2/mc^2$, T is the total time of fast particle motion,

$$S(\mathbf{k}_1,\omega_1,\mathbf{k}_2,\omega_2) = \left\langle\frac{n_{\mathrm{e}}(\mathbf{k}_1,\omega_1)n_{\mathrm{e}}^{*}(\mathbf{k}_2,\omega_2)}{N}\right\rangle \tag{297}$$

is the correlation function of the electron density, n_{e} is defined by Eqn (295), and the averaging is performed over the plasma electron distribution function.

Let us consider a classical equilibrium plasma composed of electrons with the number density n_{e} and ions with the number density $n_{\mathrm{i}} = n_{\mathrm{e}}/Z$. The number density $n_{\mathrm{e}}(\mathbf{r},t)$ in Eqn (295) can be written as a sum

$$n_{\mathrm{e}} = N + n_{1\mathrm{e}}, \qquad \langle n_{1\mathrm{e}}\rangle = 0. \tag{298}$$

The calculation of $n_{1\mathrm{e}}(\mathbf{r},t)$ has repeatedly been performed in the literature [78, 79], so we use the well-known result [79]. Then calculating the function $S(\mathbf{k}_1,\omega_1,\mathbf{k}_2,\omega_2)$ according to Eqn (297), we find

$$S(\mathbf{k}_1,\omega_1,\mathbf{k}_2,\omega_2) = \frac{(2\pi)^3}{V}\,\delta(\mathbf{k}_1-\mathbf{k}_2)\delta(\omega_1-\omega_2)S(\mathbf{k}_1,\omega_1), \tag{299}$$

where V is the volume of plasma. The dependence on the differences in arguments appeared since the plasma is assumed to be statistically uniform and stationary. The function $S(\mathbf{k}_1, \omega_1)$ is given by the expression [79]:

$$S(\mathbf{k}_1, \omega_1) = \frac{2\pi}{k_1} \left| 1 - \frac{G_e(\mathbf{k}_1, \omega_1)}{\varepsilon(\mathbf{k}_1, \omega_1)} \right|^2 f_e\left(\frac{\omega_1}{k_1}\right) + \frac{2\pi Z}{k_1} \left| \frac{G_e(\mathbf{k}_1, \omega_1)}{\varepsilon(\mathbf{k}_1, \omega_1)} \right|^2 f_i\left(\frac{\omega_1}{k_1}\right), \quad (300)$$

Here, $f_{e,i} = \left(\sqrt{\pi}\langle v_{e,i}\rangle\right)^{-1} \exp\left(-v^2/\langle v_{e,i}\rangle^2\right)$ is the one-dimensional Maxwell distribution function, $\varepsilon = 1 + G_e$ is the plasma dielectric permeability. Expression (300), being the integrand in Eqn (296), provides a pole singularity when $\varepsilon(\mathbf{k}_1, \omega_1) \to 0$. The integral (296) can be expressed as a sum of two terms. The first of them is defined as integration over all the range of variables $\mathbf{k}'$, ω', $\mathbf{k}''$, ω'' except for the poles. The second term is defined as a contribution of pole points. Let us denote them as $I^{(1)}$ and $I^{(2)}$. The first term allows for $f_{e,i}$ to perform the transition $\langle v_{e,i}\rangle \to 0$, i.e., $f_{e,i} \approx \delta(v)$ and $(k_1\sqrt{\pi}\langle v_e\rangle)^{-1} \exp(-\omega_1^2/k_1^2\langle v_e\rangle^2) \approx \delta(\omega_1)$. This corresponds to neglecting the Doppler shift in the frequency of radiation generated by an electron with velocity $\langle v_e\rangle$, $\langle v_e\rangle/c \ll 1$. The electric field of the fast particle with a velocity $v^Q \sim c$ is given by

$$\mathbf{E}^Q_{\mathbf{k},\omega} = \frac{4\pi i Q}{(2\pi)^3} \frac{\mathbf{k} - \mathbf{v}^Q(\mathbf{k}\mathbf{v}^Q)/c^2}{k^2 - (\omega^2/c^2)(1 - \omega_p^2/\omega^2)} \delta(\omega - \mathbf{k}\mathbf{v}^Q). \quad (301)$$

Substituting Eqns (300) and (299) into Eqn (296) and carrying out the passage $\langle v_{e,i}\rangle \to 0$, we obtain the final expression for the radiation intensity

$$I^{(1)}_{\mathbf{n},\omega} = \frac{4cr_0^2 N Q^2}{v^Q (2\pi)^2} \int_{-\infty}^{\infty} d^2\chi \left[\chi^2 + \frac{\omega^2}{(v^Q)^2\gamma^4} - \left(\mathbf{n}\mathbf{k}' - \frac{\mathbf{n}\mathbf{v}^Q\omega}{c^2}\right)^2\right] \times \left[\chi^2 + \frac{\omega^2}{(v^Q)^2}\left(\frac{1}{\gamma^2} + \frac{\omega_p^2}{\omega^2}\right)\right]^{-2} \times \left\{\frac{(\mathbf{k} - \mathbf{k}')^4 d^4}{\left[1 + (\mathbf{k} - \mathbf{k}')^2 d^2\right]^2} + \frac{Z}{\left[1 + (\mathbf{k} - \mathbf{k}')^2 d^2\right]^2}\right\}, \quad (302)$$

$(\mathbf{k}')_z = \omega/v^Q$, $\mathbf{n} = \mathbf{k}/k$, $\mathbf{k}'_\perp = \boldsymbol{\chi}$, $\gamma = \left[1 - (v^Q)^2/c^2\right]^{-1/2}$ is the Lorentz factor of the fast particle, and d is the Debye radius. Let us now consider the contribution of the pole term to Eqn (300). In the pole we have $\operatorname{Re}\varepsilon(\mathbf{k}_1, \omega_1) \to 0$, $\operatorname{Re} G_e(\mathbf{k}_1, \omega_1) \to -1$. Let us use the formula

$$\frac{1}{|\varepsilon|^2} = \pi(\operatorname{Im}\varepsilon)^{-1} \frac{1}{\pi} \frac{\operatorname{Im}\varepsilon}{|\operatorname{Im}\varepsilon|^2 + |\operatorname{Re}\varepsilon|^2} \overset{\substack{\operatorname{Re}\varepsilon \to 0 \\ \operatorname{Im}\varepsilon \ll 1}}{\to} \pi(\operatorname{Im}\varepsilon)^{-1}\delta(\operatorname{Re}\varepsilon). \quad (303)$$

Then

$$S(\mathbf{k}_1, \omega_1) = \frac{2\pi}{k_1} f_e\left(\frac{\omega_1}{k_1}\right) \frac{\pi\delta\left[\operatorname{Re}\varepsilon(\mathbf{k}_1, \omega_1)\right]}{\operatorname{Im}\varepsilon(\mathbf{k}_1, \omega_1)}, \quad (304)$$

$$\operatorname{Im}\varepsilon = \sqrt{\pi}\,\frac{1}{k_1^2 d^2}\,\frac{\omega_1}{k_1\langle v_e\rangle} \exp\left(-\frac{\omega_1^2}{k_1^2\langle v_e\rangle^2}\right), \qquad \operatorname{Re}\varepsilon = 1 - \frac{\omega_p^2}{\omega^2}.$$

Thus, we obtain finally:

$$S(\mathbf{k}_1, \omega_1) = \pi k_1^2 d^2 \left[\delta(\omega - \omega_p) + \delta(\omega + \omega_p)\right], \qquad |\mathbf{k}_1| < \frac{1}{d}. \quad (305)$$

The second term in Eqn (300) has a factor $f_i(\omega_1/k_1)/\operatorname{Im}\varepsilon(\mathbf{k}_1, \omega_1)$, so it is exponentially small in comparison with the first term because $\langle v_i\rangle \ll \langle v_e\rangle$. The physical nature of the pole is the presence of plasmons. Indeed, expression (296) [with Eqn (305) substituted in it] describes the radiation of transverse quanta generated by background electrons when their collective excitation, plasmon, arises (or disappears). The condition $k_1 < 1/d$ is associated with the fact that the momentum of a plasmon can not exceed $\hbar/d$.

The total radiation intensity can be expressed as a sum of three terms. Two of them are determined by Eqn (302) and describe the emission of plasma electrons interacting with each other [the first term in braces in Eqn (302)] and with plasma ions [the second term in Eqn (302)]. The third term is obtained by substituting Eqn (305) into Eqn (296) and accounts for the contribution of the pole of the dielectric permeability. The radiation intensity can be divided into three terms because there are a few ways to transfer the momentum of fast particle to the plasma during radiation: (1) single plasma electrons receive the momentum; (2) momentum is transferred to a group of electrons surrounding an ion (to the Debye sphere), (3) plasma excitation (plasmon) receives the momentum. Other channels of momentum transfer, for example, to ion-acoustic waves, can be neglected because they contain the respective small parameter $(m_e/m_i)^2$.

Integrating expressions (302) and (296) with the use of Eqn (305) is possible in a general form. Nevertheless, we consider various restricted frequency regions, which simplifies the calculations and provides convenient asymptotic forms. For each component of the total radiation $I_\omega = I_\omega^{(1)\mathrm{el}} + I_\omega^{(1)\mathrm{ion}} + I_\omega^{(2)}$ we obtain the following expressions.

(a) Single electron contribution (inelastic component):

$$\omega_p < \omega < \frac{c}{d}, \qquad I_\omega^{(1)\mathrm{el}} = \frac{16}{3} r_0^2 Q^2 N \ln\frac{mcd}{\hbar}, \quad (306)$$

$$\frac{c}{d} < \omega < \frac{mc^2}{\hbar}, \qquad I_\omega^{(1)\mathrm{el}} = \frac{16}{3} r_0^2 Q^2 N \ln\frac{mc^2}{\hbar\omega\sqrt{1/\gamma^2 + \omega_p^2/\omega^2}}.$$

A decrease of the radiation intensity of single electrons at low frequencies is related to the screening effects. The range of small values of transferred momentum is responsible for the emission at low frequencies, while the momentum less than $\hbar/d$ is gained by a group of electrons rather than a single electron in a plasma, which leads to an increase of the effective mass of the electron and to a decrease of the radiation intensity.

(b) Electrons surrounding an ion (proper polarization bremsstrahlung, elastic contribution). The spectrum is studied in detail in Ref. [28], where analytical expressions for different frequency ranges are given. The entire spectrum is shown in Fig. 10; for $\omega_p < \omega < c/d$ we have

$$I_\omega^{(1)\mathrm{ion}} = \frac{16}{3\left[\varepsilon(\omega)\right]^{3/2}} Z r_0^2 Q^2 N \ln\frac{c}{\omega_p d}. \quad (307)$$

(c) The component associated with plasmons:

$$\omega_p < \omega < \frac{c}{d}, \qquad I_\omega^{(2)} = \frac{8}{3} r_0^2 Q^2 N,$$
$$\frac{c}{d} < \omega < \frac{c}{d}\gamma^2, \qquad I_\omega^{(2)} = \frac{8}{3} r_0^2 Q^2 N \left(\frac{c}{\omega d}\right)^2, \quad (308)$$
$$\omega > \frac{c}{d}\gamma^2, \qquad I_\omega^{(2)} = 0.$$

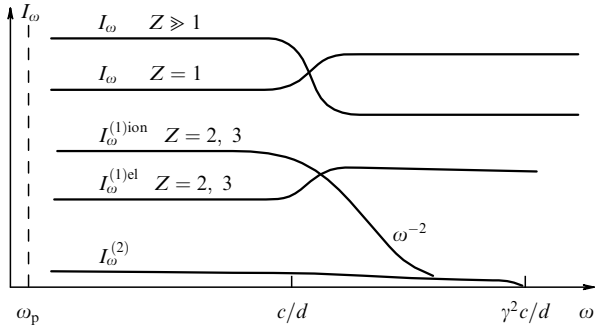

Figure 10. Spectrum of polarization bremsstrahlung I_ω and the respective components for various charges Z of the background nucleus.

The intensity of the component $I_\omega^{(2)}$ associated with plasmons becomes zero because the wavelength of the plasmon cannot be less than d. The three components of the radiation intensity are plotted in Fig. 10.

At low frequencies ($\omega_\text{p} < \omega < c/d$) either the ion component ($Z > 3$) or the electron and ion components ($Z = 1-3$) can contribute the bulk to the emission. The contribution of the plasmon component is a few (8 – 10) times less. For higher frequencies ($\omega \gg c/d$) the radiation intensity is determined by (inelastic) single electron excitations, the contributions of ion (elastic) and plasmon components are unessential. Figure 10 displays the entire (sum over all contribution) intensity of PB for $Z = 1$ and $Z \gg 1$. For electrons, PB dominates the Bethe – Heitler radiation in the frequency range, where the density effect occurs, $\omega_\text{p} < \omega < \omega_\text{p}\gamma$, and up to $\omega \sim mc^2/\hbar$ for heavy fast particles (ions and nuclei).

4.2 Resonant polarization bremsstrahlung

Let us consider the effect similar to the resonant transition radiation but provided by thermal fluctuations of background plasma, i.e., resonant polarization bremsstrahlung [80].

Akopyan and Tsytovich [81] studied polarization bremsstrahlung (PB) for two limiting cases of high and low frequencies. For high frequencies $\omega_\text{p} \ll \omega \ll \omega_\text{p} v/v_\text{T}$ the PB intensity is

$$I_\omega^\text{p} = \frac{16}{3}\, I_0 \varepsilon^{-3/2}\left(\ln\frac{v\omega_\text{p}}{v_\text{T}\omega} - \frac{1}{2}\right), \qquad I_0 = \frac{e^2 Q^2 e_\text{i}^2 n_\text{i}}{vm^2c^3}, \quad (309)$$

where Q is the fast particle charge, e and m are the electron charge and mass, and e_i and n_i are the ion charge and number density in a plasma. This expression is obtained by standard methods of the theory of emission in media (see, for example, Ref. [28]) neglecting the spatial dispersion in the photon Green functions. Evidently, Eqn (309) approaches infinity if the frequency formally approaches the plasma frequency $\omega \to \omega_\text{p}$. Therefore, paper [81] considered as a special case the range of low frequencies $(\omega - \omega_\text{p})/\omega_\text{p} \ll v_\text{T}^2/v^2$, where the spatial dispersion must be taken into account in the Green functions but one can assume that $\omega = \omega_\text{p}$. The following expression was obtained for the PB intensity:

$$I_\omega^\text{p} = \frac{2}{27}\, I_0 \varepsilon^{1/2}\left(\frac{v}{v_\text{T}}\right)^4. \quad (310)$$

Monographs [28, 5] present the same result but with a numerical coefficient of 2 instead of 2/27. However, the more recent monograph (see Ref. [5, pp. 57 – 60]) indicates that Eqn (309) is valid in wider range $(\omega - \omega_\text{p})/\omega_\text{p} \gg v_\text{T}^2/v^2$, and particularly at frequencies $(\omega - \omega_\text{p})/\omega_\text{p} \approx v_\text{T}^2/v^2$, where both Eqns (309) and (310) are comparable in value. This value was declared to give the correct estimate of the radiation intensity in order of magnitude

$$I_\text{max} \sim I_0\left(\frac{v}{v_\text{T}}\right)^3. \quad (311)$$

The increase of PB intensity near the plasma frequency was referred to as resonant polarization bremsstrahlung (RPB) [5]. Note that the effect was estimated using extrapolation of the correct asymptotic forms outside the region of their applicability, while proper joint account of temporal and spatial dispersion in the photon Green functions was not performed.

The calculations of PB spectra valid for any frequencies $\omega_\text{p} \leqslant \omega \ll \omega_\text{p} v/v_\text{T}$, carried out below, show that a true value of RPB in the maximum is about c/v_T times higher than the estimate (311) [5], and that the asymptotic form (309) is valid only for $\omega > 2\omega_\text{p}$.

Let us consider the emission generated near the plasma frequency, where the phase velocities of transverse waves are much larger than the speed of light $v_\text{ph} \gg c$, so, $v/v_\text{ph} \ll 1$ for any particle. Hence, the use of a longitudinal Green function alone (non-relativistic approximation) is sufficient to calculate RPB. The dielectric permeability in the Green function has to involve the spatial dispersion $\varepsilon(\omega, \mathbf{k}) = \varepsilon(\omega) - 3k^2d^2 + \mathrm{i}\varepsilon''$. Then the RPB intensity can be expressed in a form similar to Eqn (180):

$$I_{\mathbf{n},\omega}^\text{p} = \frac{8\pi Z^2 e^4 Q^2 \varepsilon^{1/2}}{m^2c^3} \times \int k'^2\, \mathrm{d}k'\, \frac{[\mathbf{n}\times\mathbf{k}']^2 \delta\left[\omega - (\mathbf{k}-\mathbf{k}')\mathbf{v}\right] |\delta N|_{\mathbf{k}'}^2\, \mathrm{d}\varphi\, \mathrm{d}\cos\vartheta}{(\mathbf{k}-\mathbf{k}')^4\left\{\left[\varepsilon(\omega) - 3(\mathbf{k}-\mathbf{k}')^2 d^2\right]^2 + \varepsilon''^2\right\}}, \quad (312)$$

where

$$|\delta N|_\mathbf{k}^2 = \frac{n_\text{i}}{(2\pi)^3(1+k^2d^2)^2}. \quad (313)$$

To simplify the integration of Eqn (312), we apply an approximation for the equilibrium fluctuation spectrum (313), namely, we assume $|\delta N|_{\mathbf{k}'}^2 = n_\text{i}/(2\pi)^3$ if $k' < d^{-1}$ and $|\delta N|_{\mathbf{k}'}^2 = 0$ if $k' > d^{-1}$. Here, $d = v_\text{T}/\omega_\text{p}$ is the Debye radius, $Z = e_\text{i}/e$; the imaginary part of the dielectric permeability ε'' is kept to regularize the divergence when integrating Eqn (312). Note that for the frequencies considered we have $\varepsilon(\omega) \ll 1$ and $k \ll k'_\text{min} = \omega_\text{p}/v < k'$. This allows us to neglect $\mathbf{k}$ in comparison with $\mathbf{k}'$ everywhere excluding the resonant denominator. It is convenient further to integrate Eqn (312) over angles of vector $\mathbf{n}$, which provides the energy emitted into the full solid angle

$$I_\omega^\text{p} = \frac{32\pi^3 Z^2 e^4 Q^2 \varepsilon^{1/2}}{vm^2c^3} \int_{\omega/v}^{1/d} \frac{\mathrm{d}k'}{k'}\, |\delta N|_{\mathbf{k}'}^2 \times \int_{-1}^{1} \frac{\sin^2\vartheta\, \mathrm{d}\cos\vartheta}{\left[\varepsilon(\omega) + 6kk'd^2\cos\vartheta - 3k'^2d^2\right]^2 + \varepsilon''^2}. \quad (314)$$

Here, we also integrated over the azimuth angle: $\int \mathrm{d}\varphi \ldots = 2\pi$, while ϑ is the angle between vector $\mathbf{k}'$ and

particle velocity $\mathbf{v}$. Expanding into the simplest fractions and integrating over the angle results in:

$$I_\omega^{\mathrm{p}} = \frac{32\pi^3 Z^2 e^4 Q^2 \varepsilon^{1/2}}{v m^2 c^3} \int_{\omega/v}^{1/d} \frac{\mathrm{d}k'}{k'} \, |\delta N|^2_{\mathbf{k}'} \, \frac{J_\vartheta}{36 k^2 k'^2 d^4} \,, \quad (315)$$

where J_ϑ is defined by Eqn (183), which reduces to Eqn (185) like in Section 3.2. Substituting Eqn (185) into Eqn (315) and introducing the dimensionless variable $\mu = k'v/\omega$, we can express the RPB spectrum as

$$I_\omega^{\mathrm{p}} = \frac{16}{3} I_0 F(\alpha) \,, \qquad F(\alpha) = \frac{\varepsilon^{1/2}}{9} \left(\frac{v}{\omega d}\right)^4 \int_1^{\mu_{\max}} \frac{\mathrm{d}\mu}{\mu} \, \frac{\Theta(a^2-1)}{(\mu^2-\alpha)^2} \,, \quad (316)$$

where $\mu_{\max} \approx v\omega_{\mathrm{p}}/v_{\mathrm{T}}\omega$. Integrating in Eqn (316) is carried out using standard functions:

$$\begin{aligned} F(\alpha) = {} & \frac{\varepsilon^{1/2}}{18} \left(\frac{v}{\omega d}\right)^4 \left(\left[\frac{1}{\alpha(1-\alpha)} + \frac{1}{\alpha^2} \ln(1-\alpha) \right] \Theta(\omega_1 - \omega) \right. \\ & + \frac{1}{\alpha^2} \frac{c}{2 \times 3^{0.5} v_{\mathrm{T}}} \left(1 - \frac{2 \times 3^{0.5} v_{\mathrm{T}}}{c} \ln \frac{c}{2 \times 3^{0.5} v_{\mathrm{T}}} \right) \\ & \times \Theta(\omega - \omega_1) \Theta(\omega_2 - \omega) \\ & + \left\{ \frac{1}{\alpha^2} \frac{c}{3^{0.5} v_{\mathrm{T}}} + \frac{1}{\alpha} \left[\frac{1}{1-\alpha} - \frac{1}{\mu_{\max}^2 - \alpha} + \frac{1}{\alpha} \ln \frac{(\alpha-1)\mu_{\max}^2}{\mu_{\max}^2 - \alpha} \right] \right\} \\ & \times \Theta(\omega - \omega_2) \Theta(\omega_3 - \omega) \\ & + \left[\frac{1}{\alpha^2} \frac{c}{2 \times 3^{0.5} v_{\mathrm{T}}} - \frac{1}{\alpha(\alpha-1)} + \frac{1}{\alpha^2} \ln \frac{(\alpha-1)c}{2 \times 3^{0.5} v_{\mathrm{T}}} \right] \\ & \times \Theta(\omega - \omega_3) \Theta(\omega_4 - \omega) \\ & \left. + \left\{ \frac{1}{\alpha} \left[\frac{1}{\alpha - \mu_{\max}^2} - \frac{1}{\alpha - 1} + \frac{1}{\alpha} \ln \frac{(\alpha-1)\mu_{\max}^2}{\alpha - \mu_{\max}^2} \right] \right\} \Theta(\omega - \omega_4) \right) . \end{aligned} \quad (317)$$

Here, $\omega_{1,2}$ are defined by Eqn (188), and

$$\omega_{3,4} = 2\omega_{\mathrm{p}} \left(1 \mp \frac{3 \times 3^{0.5} v_{\mathrm{T}}}{4c} \right) . \quad (318)$$

Note the sharp changes of the slope at frequencies $\omega_{1,2}$ in the spectrum are associated with the physical nature of the process considered (radiation properties change abruptly when the system parameters overcome Cherenkov's threshold), whereas changes at frequencies $\omega_{3,4}$ correspond to the approximation used for $|\delta N|^2_{\mathbf{k}'}$. However, the latter is unimportant for the RPB effect considered here.

Let us discuss the results obtained. The properties of function (317) near frequency ω_{p} are close to those of function (189), i.e., the results display only a weak dependence on the spectral index of inhomogeneities, which supports the assumption made in Section 3.2. At high frequencies $\omega_{\mathrm{p}} \ll \omega \ll \omega_{\mathrm{p}} v/v_{\mathrm{T}}$, the calculated RPB spectrum (316), (317) turns into the asymptotic form (309). However, formula (309) is correct for $\omega > 2\omega_{\mathrm{p}}$ only, rather than for $(\omega - \omega_{\mathrm{p}})/\omega_{\mathrm{p}} > v_{\mathrm{T}}^2/v^2$ as was declared earlier [5]. The reason is the specific shape of the spectrum of thermal fluctuation in the plasma, which remains flat up to small scales of about d, hence the contribution of the upper limit in integral (316) is important. At low frequencies, $\omega \to \omega_{\mathrm{p}}$, we obtain Eqn (310).

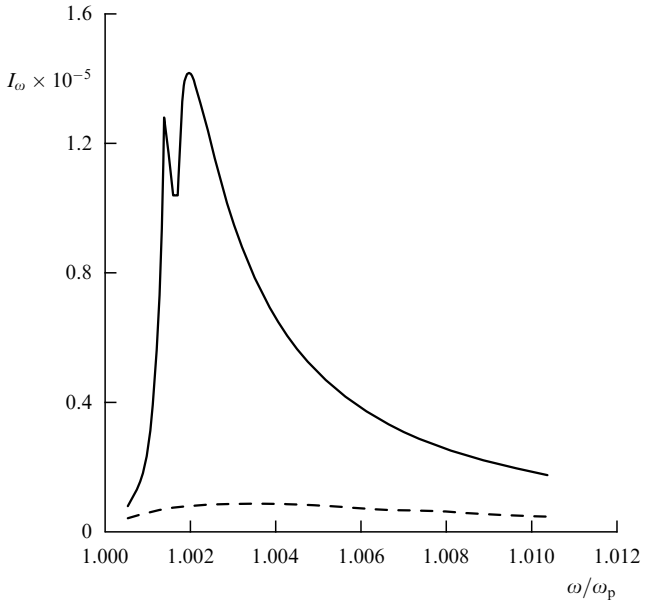

Figure 11. Spectrum of resonant polarization bremsstrahlung (solid line). The dashed line is the spectrum composed of asymptotic forms (309), (310) given in Ref. [5, p. 57].\

But in the spectral peak, $\alpha \approx 1$, we have

$$I_{\max}^{\mathrm{p}} \sim I_0 \frac{v^3 c}{v_{\mathrm{T}}^4} \quad (319)$$

unlike estimate (311). Figure 11 displays the shape of RPB peak calculated by Eqn (317).

The total RPB energy emitted at all the frequencies is

$$I_{\mathrm{tot}}^{\mathrm{p}} = \frac{8}{27} I_0 \omega_{\mathrm{p}} \frac{vc}{v_{\mathrm{T}}^2} \,. \quad (320)$$

This result is larger than the power of standard PB (without the peak) by a factor of vc/v_{T}^2, and c/v_{T} times larger than the estimate of the RPB effect in Ref. [5].

4.3 Polarization bremsstrahlung by fast particles in the presence of the Vavilov–Cherenkov effect

Let us consider one more resonant effect arising in the frequency range where the condition of the Vavilov–Cherenkov radiation for transverse waves is fulfilled. This section proves the two channels of emission (Vavilov–Cherenkov and polarization bremsstrahlung) to interact with each other, which results in a substantial (1–2 orders of magnitude) increase of PB intensity. Though the PB is emitted simultaneously with the more powerful Vavilov–Cherenkov radiation, both mechanisms can easily be separated in experiment because the PB has broader angular distribution. Since the Vavilov–Cherenkov emission of transverse waves does not occur in isotropic plasma, this section considers an atomic medium. The results obtained can be generalized to the Vavilov–Cherenkov effect in a magnetized plasma (see Section 2.4.) taking into account the optical anisotropy of the medium.

One of the Feynman diagrams corresponding to polarization bremsstrahlung is shown in Fig. 1b. Passing from the state $|p_{\mathrm{i}}\rangle$ to the state $|p_{\mathrm{f}}\rangle$, a fast particle emits a virtual quantum with momentum $(\mathbf{q}, q_0)$, which affects an atomic

electron providing emission of a photon. The final state of the atomic electron $|n_f\rangle$ may either coincide with the initial one $|n_i\rangle$ (proper elastic emission) or belong to an excited atom state (inelastic process). The intensity of the elastic polarization bremsstrahlung I_ω, corresponding to the process shown in Fig. 1b, is described by the expression:

$$I_\omega = \frac{16}{3}\, nZ^2 r_0^2 Q^2 \left[\frac{m\omega^2}{e^2}\,\alpha(\omega)\right]^2 \ln\frac{c\gamma}{\omega R}\,, \qquad \omega \leqslant \frac{c}{R}\,. \tag{321}$$

Here, ω is the frequency of the emitted quantum, n is the number density of atoms, Z is the nucleus charge, $R = \hbar/Zme^2$ is the atom radius, r_0 is the classical radius of electron, Q, γ are the charge and Lorentz factor of the fast particle, and $\alpha(\omega)$ is atomic polarizability [not confuse with a value α defined by Eqn (215)]. The intensity of inelastic polarization bremsstrahlung is less than that of elastic by a factor of $Z\ln(c\gamma/\omega R)/\ln(mcR/\hbar)$ and may be omitted for atoms with high Z.

When deriving Eqn (321), the emission of an isolated atom disturbed by a fast particle was calculated and the result was multiplied by the number of atoms with the use of the vacuum Green function of a photon. However, dielectric permeability $\varepsilon(\mathbf{q},\omega)$ effect on both the virtual photon and propagation of the produced quantum should be properly taken into account in a medium. It is necessary if a large number of atoms is located within a coherence length l_c (it is defined as the value inverse to the projection of wave vector $\mathbf{q}$ of the virtual photon on the direction of particle velocity), i.e.,

$$n^{-1/3} \ll l_c\,, \tag{322}$$

where n is the number density of atoms in the medium. Note that monograph [28] applies the dielectric permeability to the range of high frequencies $\omega \gg I_a$ (I_a is the ionization potential of the atoms), where

$$\alpha(\omega) = \frac{e^2}{m\omega^2}\,, \qquad \varepsilon = 1 - \frac{\omega_p^2}{\omega^2}\,. \tag{323}$$

This leads to the replacement of $\ln(c\gamma/\omega R)$ by $\ln(c/\omega_p R)$ in Eqn (321). Meanwhile, of primary interest is the frequency range $\omega \leqslant I_a$ because the radiation intensity increases at these frequencies [$\alpha(\omega)$ is high when ω approaches the intrinsic frequencies of atoms] and $\varepsilon(\omega)$ differs strongly from unity in this frequency range. Moreover, for $\varepsilon(\omega) > 1$ Vavilov–Cherenkov radiation is generated besides polarization bremsstrahlung in the medium.

Let us analyze the expression for the radiation intensity I_ω involving the Green function of a virtual photon explicitly and taking into account the dielectric permeability [28]

$$I_\omega = \frac{8Z^2}{3\varepsilon^{3/2}}\, nr_0^2 Q^2 \left[\frac{m\omega^2}{e^2}\,\alpha(\omega)\right]^2 \times \int_0^{1/R^2} \frac{q_\perp^2\,\mathrm{d}q_\perp^2\,\delta(\varepsilon_i - \varepsilon_f - \omega)\,\mathrm{d}\varepsilon_f}{\left|\mathbf{q}^2 - \varepsilon(\omega)\omega^2/c^2\right|^2}\,. \tag{324}$$

Here, $q_\perp$ is the component of the vector $\mathbf{q}$ perpendicular to the particle velocity $\mathbf{v}_0$; $q_\parallel = \omega/v_0$, $\mathbf{q}^2 = q_\perp^2 + q_\parallel^2$; $\varepsilon(\omega)$ is the dielectric permeability of the system composed of non-interacting atoms being in the ground state, and ε_i and ε_f are the initial and final energy of the fast particle, respectively. In the range of frequencies $(v_0^2/c^2)\,\mathrm{Re}\,\varepsilon(\omega) < 1$ the integrand in Eqn (324) has no singularity, so the integration is trivial:

$$I_\omega = \frac{16Z^2}{3\varepsilon^{3/2}}\, nr_0^2 Q^2 \left[\frac{m\omega^2}{e^2}\,\alpha(\omega)\right]^2 \ln\frac{c}{\omega R\left[1 - \varepsilon(\omega)v_0^2/c^2\right]^{1/2}}\,. \tag{325}$$

(This coincides with Eqn (321) taking into account the medium dielectric permeability.) For $(v_0^2/c^2)\,\mathrm{Re}\,\varepsilon(\omega) > 1$, a singularity appears in the integrand of Eqn (324). This integral, denoted as I, has the form:

$$I = \int_0^{1/R^2} \frac{q_\perp^2\,\mathrm{d}q_\perp^2}{\left|\mathbf{q}_\perp^2 - (\omega^2/v_0^2)\left[\varepsilon(\omega)v_0^2/c^2 - 1\right]\right|^2}\,, \qquad \omega = \varepsilon_i - \varepsilon_f\,. \tag{326}$$

This singularity is associated with the possible arrival of a virtual photon onto the mass surface. As a result, if $(v_0^2/c^2)\,\mathrm{Re}\,\varepsilon(\omega) > 1$, the polarization bremsstrahlung can be described as the output of two successive processes: generation of a Cherenkov quantum by a relativistic particle and scattering of the quantum by an atomic shell (here, the Cherenkov quantum exists over a length of about $\sim q_\parallel^{-1} = v_0/\omega$).

Actually, the pole singularity in Eqn (326) can be regularized by introducing the imaginary part of the energy ω of the virtual photon. The imaginary part is caused by both the imaginary part of a dielectric permeability ε'' ($\varepsilon = \varepsilon' + \mathrm{i}\varepsilon''$) and the imaginary parts (or finite lifetime in a certain energy state) of the energy of the fast particle and atomic electron in the ground state, due to the law of energy conservation [δ function in Eqn (324)]. The lifetime of a fast particle τ is determined by the collisions between the particle and background atoms as well as by the emission of Cherenkov quanta:

$$\tau^{-1} = \sigma v_0 n + \int \frac{Q^2}{\hbar c}\left[1 - \frac{c^2}{v_0^2\varepsilon'(\omega)}\right]\mathrm{d}\omega\,, \tag{327}$$

where σ is the cross-section of collision between the particle and atom. The atomic electron lifetime in the ground state can be regarded as infinitely large. The imaginary part of the dielectric permeability is

$$\varepsilon''(\omega) = \frac{4\pi ne^2}{m_e}\sum_{k=0}^{\infty} \frac{f_{0k}^2\omega\Gamma_{0k}}{(\omega^2 - \omega_{0k}^2)^2 + \omega^2\Gamma_{0k}^2}\,, \tag{328}$$

where f_{0k} is the oscillator force of atom transition with frequency ω_{0k} and bandwidth Γ_{0k}. Thus, the total energy bandwidth Γ in the pole denominator in Eqn (326) is determined by the expression

$$\Gamma(\omega) = \tau^{-1} + \omega\varepsilon''(\omega)\,. \tag{329}$$

Let us calculate integral (326) excluding the pole singularity by introducing Γ:

$$\begin{aligned} I &= \int_0^{1/R^2} \frac{q_\perp^2\,\mathrm{d}q_\perp^2}{\left|q_\perp^2 - (\omega^2/v_0^2)\left[\varepsilon(\omega)v_0^2/c^2 - 1\right] - (\mathrm{i}\omega/c^2)\Gamma(\omega)\right|^2} \\ &= \pi\Theta\left[\frac{\varepsilon'(\omega)v_0^2}{c^2} - 1\right]\left[\frac{\varepsilon'(\omega)v_0^2}{c^2} - 1\right]\frac{\omega}{\Gamma} \\ &\quad + 2\ln\left\{\frac{v_0}{\omega R}\left[\left(\frac{v_0^2}{c^2}\,\varepsilon' - 1\right)^2 + \frac{\Gamma^2 v_0^2}{\omega^2 c^2}\right]^{-1/4}\right\}. \end{aligned} \tag{330}$$

The first term in Eqn (330) is caused by the pole singularity, the second, by the rest of the range of integration. Obviously, the first term in Eqn (330) describes the intensity of polarization bremsstrahlung related to the Cherenkov part of the fast particle field, while the second does it for the quasi-stationary electromagnetic field of the particle. For $(v_0^2/c^2)\varepsilon'(\omega) > 1$ and $\Gamma \ll \omega$ the first term dominates [recall that it disappears altogether for $(v_0^2/c^2)\varepsilon'(\omega) < 1$] and the respective radiation intensity can be expressed as

$$I_\omega^{(1)} = \frac{8\pi Z^2}{3} nr_0^2 \left[\frac{m\omega^2}{e^2}\,\alpha(\omega)\right]^2 \lambda\hbar\omega \times \frac{(\omega Q^2/\hbar c)(1 - c^2/v_0^2\varepsilon')}{\Gamma}\,\frac{v_0^2}{c^2}\,. \tag{331}$$

The second term gives a result similar to Eqn (325):

$$I_\omega^{(2)} = \frac{16Z^2}{3\varepsilon'^{3/2}} nr_0^2 Q^2 \left[\frac{m\omega^2}{e^2}\,\alpha(\omega)\right]^2 \times \ln\left\{\frac{v_0}{\omega R}\left[\left(\frac{v_0^2}{c^2}\,\varepsilon' - 1\right)^2 + \frac{\Gamma^2 v_0^2}{\omega^2 c^2}\right]^{-1/4}\right\}. \tag{332}$$

Equation (331) can be interpreted as follows. The term $8\pi/3nr_0^2\lambda$ is the number of atoms in the cylinder with the base $\sigma_{\rm Th}$ and the height $\lambda = c/\omega\varepsilon'^{1/2}$ ($\sigma_{\rm Th}$ is the Thompson cross-section), the factor $[m\omega^2\alpha(\omega)/e^2]^2$ allows for the difference between polarizability of an atomic shell and free electrons. Their product determines the total effective number of electrons, scattering Cherenkov quanta, taking into account the electron bonds in atoms and the coherent nature of quantum scattering by the entire atomic shells. The term $\hbar\omega$ is the energy of the scattered (and emitted) quantum, the value $\omega Q^2(1 - c^2/v_0^2\varepsilon')/\hbar c\Gamma$ is the ratio of the probability of emitting a Cherenkov quantum to the total probability of decay of the state of the emitting fast particle. Apparently, the last term cannot be higher than unity.

Let us compare the two components (331) and (332) of polarization bremsstrahlung:

$$\frac{I_\omega^{(1)}}{I_\omega^{(2)}} = \frac{\pi\varepsilon' v_0^2\omega\left[1 - c^2/v_0^2\varepsilon'(\omega)\right]}{2\Gamma c^2 \ln\left\{(v_0/\omega R)\left[(\varepsilon' v_0^2/c^2 - 1)^2 + \Gamma^2 v_0^2/\omega^2 c^2\right]^{-1/4}\right\}}\,. \tag{333}$$

The pole contribution $I_\omega^{(1)}$ existing only in the range of parameters $(v_0^2/c^2)\varepsilon'(\omega) > 1$) predominates if the resonance nature of the process is pronounced clearly

$$\frac{\omega}{\Gamma} > \frac{2c^2 \ln\left\{(v_0/\omega R)\left[(\varepsilon' v_0^2/c^2 - 1)^2 + \Gamma^2 v_0^2/\omega^2 c^2\right]^{-1/4}\right\}}{\pi\varepsilon' v_0^2\left[1 - c^2/v_0^2\varepsilon'(\omega)\right]}\,. \tag{334}$$

Figure 12 displays the dependences describing both considered contributions to polarization bremsstrahlung for the particular case:

$$\varepsilon(\omega) = 1 - \frac{5\Gamma}{\omega - \omega_0 + i\Gamma/2}\,. \tag{335}$$

The pole contribution reaches the peak when the real part of the dielectric permeability has its maximum. Standard PB reaches its maximum at the threshold of the Vavilov–Cherenkov radiation. For the medium described by

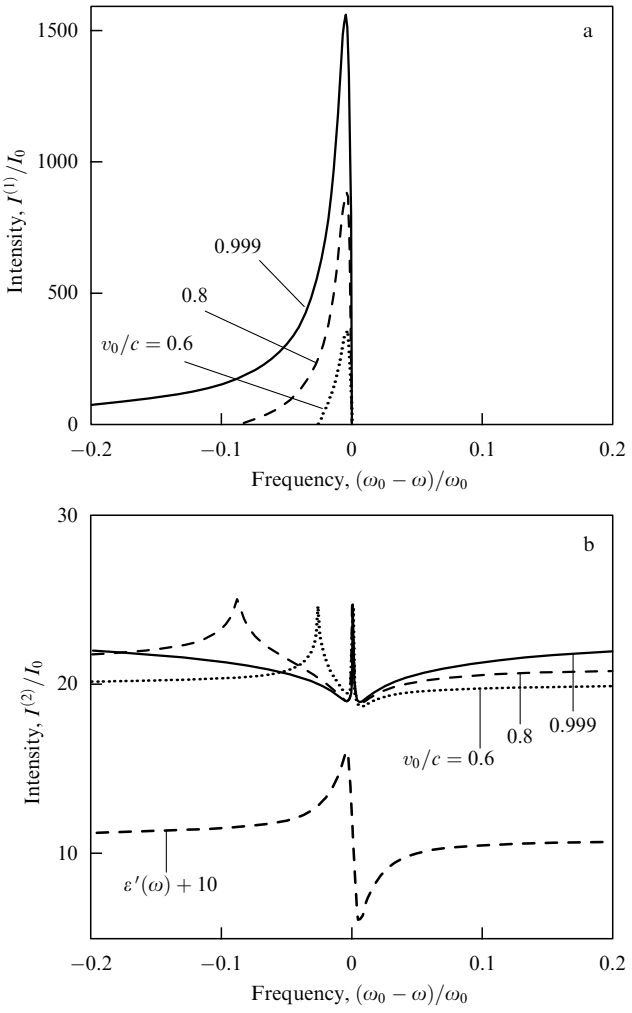

Figure 12. Pole (a) and standard (b) components of polarization bremsstrahlung for various velocities of fast particle ($v_0/c = 0.6, 0.8, 0.999$). The plot (b) also displays the real part of the dielectric permeability (335) for $\omega_0/\Gamma = 100$. The larger the value $\varepsilon'(\omega)$ the stronger the pole contribution $I^{(1)}$ exceeds the standard contribution $I^{(2)}$. The standard contribution has its maximum at the Cherenkov threshold.\

Eqn (335), the spectral intensity of the pole contribution dominates in the limited frequency range, whereas the total PB energy (integrated over all frequencies) is determined by the standard contribution $I^{(2)}$.

Now let us compare the increase of the standard PB (contribution $I^{(2)}$) with the qualitatively similar resonant PB considered in Section 4.2. In both cases, the physical reason for the increase of PB intensity is the Vavilov–Cherenkov generation of intrinsic modes in the medium: plasma waves in Section 4.2 or transverse ones in this section. It is important to emphasize that the magnitude of the increase of PB intensity is considerably different in these two cases: the increase of the intensity shown in Fig. 12 is about 20%, while for RPB it is a few orders of magnitude. This difference can be accounted for by a different structure of the dependence of the integrands on the transferred momentum (this is a result of the difference in the dispersion laws for potential and transverse eigen modes). In this section, the spatial dispersion is unessential, so the account of the frequency dependence of the dielectric permeability, $\varepsilon(\omega)$, is sufficient, which results in the logarithmic dependence on frequency at the resonance. For RPB the

resonance nature of the process is more pronounced because the dielectric permeability, $\varepsilon(\omega, \mathbf{q})$, depends on the transferred momentum and the result of integration is described by the power-law functions.

Note the radiation intensity (331) coincides with the intensity of scattering of pre-emitted Cherenkov quanta. Indeed, the number of Cherenkov quanta N^{VC} generated per unit time, per unit frequency, and per unit solid angle, is expressed as

$$N^{\mathrm{VC}}_{\omega,\theta} = \frac{Q^2}{2\pi\hbar c}\left[1 - \frac{c^2}{v_0^2\varepsilon'(\omega)}\right]\delta\left(\cos\theta - \frac{c}{v_0\varepsilon'^{1/2}}\right), \qquad (336)$$

where θ is the angle between the wave vector of the Cherenkov quantum and the particle velocity $\mathbf{v}_0$. For the lifetime $1/\Gamma$ of the system in a certain state, $N^{\mathrm{VC}}_{\omega}/\Gamma$ photons are emitted (recall the polarization of the Vavilov – Cherenkov radiation is such that the electric field vector belongs to the plane of $\mathbf{v}_0$ and the direction of radiation). The differential cross-section of scattering of the quantum by the atomic shell depends on the frequency and propagation direction; it is equal to

$$\frac{\mathrm{d}^2\sigma}{\mathrm{d}\omega'\,\mathrm{d}\Omega} = \frac{3}{8\pi}\,\sigma_{\mathrm{Th}}\left[\frac{m\omega^2}{e^2}\alpha(\omega)\right]^2\delta(\omega-\omega')\sin^2\chi, \qquad (337)$$

where χ is the angle between the electric field vector of the incident quantum and the direction of scattering:

$$\sin^2\chi = 1 - \sin^2\theta\cos^2\vartheta - \cos^2\theta\sin^2\vartheta\cos^2(\varphi-\phi) + \frac{1}{2}\sin 2\theta\sin 2\vartheta\cos(\varphi-\phi). \qquad (338)$$

Here, ϑ is the angle between the direction of the scattered quantum and fast particle velocity, and φ and ϕ are azimuth angles.

The probability of scattering w of the Cherenkov quantum equals

$$\frac{\mathrm{d}w}{\mathrm{d}\omega\,\mathrm{d}\Omega} = \frac{c}{\varepsilon'^{1/2}}\,n\,\frac{\mathrm{d}^2\sigma}{\mathrm{d}\omega\,\mathrm{d}\Omega}. \qquad (339)$$

The number of secondary scattered quanta N_ω is

$$N_\omega = \int \frac{\mathrm{d}w}{\mathrm{d}\omega\,\mathrm{d}\Omega}\,\frac{N^{\mathrm{VC}}_{\omega',\theta}}{\Gamma}\,\mathrm{d}\omega'\,\sin\vartheta\sin\theta\,\mathrm{d}\theta\,\mathrm{d}\vartheta\,\mathrm{d}\varphi\,\mathrm{d}\phi. \qquad (340)$$

The respective intensity (340) of scattered radiation $I_\omega = \hbar\omega N_\omega$ coincides with formula (331). Note the angular distribution of the scattered quanta is almost isotropic and specified mainly by the angular dependence of the cross-section. The structure of expression (340) is identical to the case of bremsstrahlung by a relativistic particle on an excited atom [83]. This is not an accidental coincidence: the Feynman diagrams of bremsstrahlung with de-excitation and polarization bremsstrahlung are equivalent in topology; in both cases, a virtual photon can arrive at the mass surface. When the lifetime of the fast particle energy state is governed by the emission only, we have

$$\frac{\omega}{\Gamma} = \frac{\omega}{(Q^2/\hbar c)\int(1 - c^2/v_0^2\varepsilon')\,\mathrm{d}\omega} \approx \frac{\hbar c}{Q^2} \approx 137 \qquad (341)$$

and $I^{(1)}_\omega$ is two orders of magnitude higher than the standard polarization radiation.

Let us discuss now the physical interpretation of the emission under study. It represents the influence of the Vavilov – Cherenkov effect on polarization bremsstrahlung, while this is not a linear superposition of these two effects. The extra contribution $I^{(1)}_\omega$ to polarization bremsstrahlung is caused by the scattering of Cherenkov quanta by atomic shells, while the effect described by Eqn (332) for $I^{(2)}_\omega$ arises due to atomic shell excitation by the quasi-stationary field of the fast particle. According to estimate (333), the contribution stimulated by the Vavilov – Cherenkov effect can dominate in many cases.

Furthermore, we should compare $I^{(1)}_\omega$ with the spectral densities of other emission mechanisms, namely, the Vavilov – Cherenkov effect and bremsstrahlung, to evaluate the possibility to observe the effect experimentally.

The intensity of the Vavilov – Cherenkov radiation exceeds $I^{(1)}_\omega$ since the latter is the effect of higher order of smallness in respect to the electron charge

$$\frac{I^{(1)}_\omega}{I^{\mathrm{VC}}_\omega} \approx \frac{\omega}{\Gamma}\,\sigma_{\mathrm{Th}} n\lambda \ll 1. \qquad (342)$$

However, Cherenkov quanta with frequency ω propagate only at the angle $\cos\theta = c/v_0\varepsilon'^{1/2}$ to the fast particle velocity, while polarization bremsstrahlung has a broad angular distribution $(1+\cos^2\vartheta)$ close to isotropic and, in particular, it exists well outside the Cherenkov cone. Indeed, polarization bremsstrahlung results from the scattering of Cherenkov quanta by non-relativistic electrons of atomic shells. The cross-section of scattering is known to be weakly anisotropic for this case.

The ratio of pole contribution $I^{(1)}$ to standard bremsstrahlung obeying the Bethe – Heitler equation can be much larger than unity:

$$\frac{I^{(1)}_\omega}{I^{\mathrm{BH}}_\omega} = \frac{\pi\left[(m\omega^2/e^2)\alpha(\omega)\right]^2\omega(1 - c^2/v_0^2\varepsilon')}{2\Gamma\varepsilon'\ln(mv_0^2/\hbar\omega)}. \qquad (343)$$

However, the standard bremsstrahlung contains a pole contribution if the condition for the Vavilov – Cherenkov effect is fulfilled as well as PB. The contribution (that can be interpreted as Compton scattering of Cherenkov quanta by the fast particle) is yet to be calculated.

Thus, the pole contribution to emission (PB considered above and, possibly, a similar contribution to standard bremsstrahlung) is concluded to dominate all other emission mechanisms outside the Cherenkov cone in some frequency ranges, and it can easily be observed in this range of angles.

The considered contribution to PB is nonzero for the same frequencies, where the condition of the Vavilov – Cherenkov effect is fulfilled because this contribution is associated with elastic scattering of Cherenkov photons by background atoms without changing frequency. Obviously, inelastic processes (Raman-like scattering) related either to atom excitation or de-excitation or to emission or absorption of intrinsic (collective) excitation of the medium (plasmon, magnon, phonon, etc.) are possible as well. For example, Section 4.1 along with the elastic contribution $I^{(1)\mathrm{ion}}_\omega$ considers the emission accompanied by excitation (driving out) of a single electron $I^{(1)\mathrm{el}}_\omega$ and emission with simultaneous plasmon emission or absorption $I^{(2)}_\omega$.

Obviously, inelastic contributions are modified as well as elastic ones when the condition for the Vavilov – Cherenkov effect is fulfilled. It is important that these contributions can

be essential at those frequencies where the Vavilov–Cherenkov condition is not fulfilled, since the respective elementary processes go with changing frequency.

4.4 Polarization of transition bremsstrahlung in a weak magnetic field

The calculation of PB in the presence of a magnetic field can be carried out according to the same algorithm as the calculation of transition radiation in a gyrotropic plasma (see Section 2.4). However, we should take into account some important differences between PB and transition radiation. Firstly, there is no high directivity of PB along the fast particle velocity [5], so the small-angle approximation is incorrect even for ultra-relativistic particles. For the same reason, the longitudinal field of the fast particle should be taken into account together with its transverse field. Secondly, most of the plasma fluctuation energy corresponds to scales of about the electron Debye radius d. Hence, in the most interesting frequency range

$$\omega_{\mathrm{p}} \ll \omega < \omega \frac{c}{v_{\mathrm{T}}} \tag{344}$$

the transferred momentum $\tilde{k} \simeq d^{-1}$ (when emitting a photon) is much larger than the wave number of the emitted quantum $\tilde{k} \gg k = 2\pi/\lambda$. The inverse inequality is valid for transition radiation.

The energy emitted per normal mode by a particle for the entire time of its motion in a plasma can still be expressed in the form (88). The spectrum of equilibrium thermal fluctuations has the form (313), while the electric field $\mathbf{E}^{Q}$ can be expressed by the particle current $\mathbf{j}$ using the longitudinal and transverse Green functions:

$$\begin{aligned} \mathbf{E}^{Q}_{\omega,\mathbf{k}} &= \frac{4\pi \mathrm{i}}{\omega}\left[\sum_{\sigma}\frac{(\mathbf{j}\cdot\mathbf{a}^{*}_{\sigma})\mathbf{a}_{\sigma}}{n^2-n^2_{\sigma}} - \frac{(\mathbf{j}\cdot\mathbf{k})\mathbf{k}}{k^i\varepsilon_{ij}k^j}\right], \\ \mathbf{j} &= \mathbf{j}_{\omega,\mathbf{k}} = \frac{Q\mathbf{v}}{(2\pi)^3}\,\delta(\omega-\mathbf{k}\mathbf{v}), \end{aligned} \tag{345}$$

where $\mathbf{a}_{\sigma}$ ($\sigma = \pm 1$) are the vectors of polarization for ordinary and extraordinary waves, and n_{σ} are the respective refractive indices, $n_{\sigma} = kc/\omega_{\sigma}$.

Taking into account these relations, the PB intensity of the mode j can be expressed as

$$I_{j,\mathbf{n},\omega} = \frac{8\pi e^4 Q^2}{m^2c^3\omega^2}\int |\delta N|^2_{\mathbf{k}-\mathbf{k}'}|\mathbf{A}^{*}_{j,\mathbf{k}'}\cdot\mathbf{F}_{\mathbf{k}'}|^2\delta(\omega-\mathbf{k}'\cdot\mathbf{v})\,\mathrm{d}\mathbf{k}', \tag{346}$$

where $A^{\alpha}_{j,\mathbf{k}} = \chi_{\alpha\beta}a^{\beta}_{j,\mathbf{k}} = (1/v)[(1-n_j^2)a^{\alpha}_{j,\mathbf{k}} + n_j^2(\boldsymbol{\varkappa}\cdot\mathbf{a}_{j,\mathbf{k}})\varkappa^{\alpha}]$, $v = \omega_{\mathrm{p}}^2/\omega^2$, $\boldsymbol{\varkappa} = \mathbf{k}/k$,

$$\mathbf{F}_{\mathbf{k}} = \sum_{\sigma}\frac{(\mathbf{j}\cdot\mathbf{a}^{*}_{\sigma})\mathbf{a}_{\sigma}}{n^2_{\sigma}-n^2} - \frac{(\mathbf{j}\cdot\mathbf{k})\mathbf{k}}{k^i\varepsilon_{ij}k^j}. \tag{347}$$

We consider a weakly gyrotropic plasma, where all the values depending on the magnetic field can be expanded into series. The exact form of the expansion of the vector of polarization and the refractive indices of normal modes depends on the relation between $u^{1/2} = \omega_{B\mathrm{e}}/\omega$ and $\cos\alpha$, where α is the angle between the wave vector and magnetic field. We focus on case (96), where the magnetic field influence on emission is especially strong. When expanding the functions depending on $\mathbf{k}'$ into series, we also use approximation (96) since the integral over the angles in the range $\cos\alpha \leqslant u^{1/2}$ contributes little to the polarization of radiation.

With the accuracy of the first order with respect to the small parameter $u^{1/2}/\cos\alpha$, the refractive indices and polarization vectors of normal modes can be expressed as

$$n_j^2 = 1 - v\bigl(1 - ju^{1/2}|\cos\alpha|\bigr), \tag{348}$$

$$\mathbf{a}_j = \mathbf{a}^0_{j\perp} - j\frac{u^{1/2}\sin^2\alpha}{4|\cos\alpha|}\,\mathbf{a}^0_{-j\perp} - \mathrm{i}vu^{1/2}\boldsymbol{\varkappa}\sin\alpha, \tag{349}$$

where

$$\mathbf{a}^0_{j\perp} = 2^{-1/2}\bigl[\hat{\mathbf{x}} - \mathrm{i}j\hat{\mathbf{y}}\,\mathrm{sgn}\,(\cos\alpha)\bigr], \tag{350}$$

and $\hat{\mathbf{x}}$, $\hat{\mathbf{y}}$ are the unit main vectors of the polarization ellipse

$$\hat{\mathbf{x}} = \frac{\mathbf{B}\times\boldsymbol{\varkappa}}{|\mathbf{B}\times\boldsymbol{\varkappa}|}, \qquad \hat{\mathbf{y}} = \boldsymbol{\varkappa}\times\hat{\mathbf{x}}. \tag{351}$$

Substituting Eqns (348), (349) into Eqn (346), we can integrate the obtained expression within the range (344). As a result, we obtain

$$I_{j,\mathbf{n},\omega} = I^{(0)}_{\mathbf{n},\omega} + \Delta I_{j,\mathbf{n},\omega}, \tag{352}$$

where

$$I^{(0)}_{\mathbf{n},\omega} = J_0\frac{1+\cos^2\theta}{2}\Bigl(\ln D - 2\Bigr) \tag{353}$$

is the half of the radiation intensity in isotropic plasma, while the additional term $\Delta I_{j,\mathbf{n},\omega}$ depends on the wave type

$$\begin{aligned} \Delta I_{j,\mathbf{n},\omega} = J_0 ju^{1/2}\Bigg(\Bigg\{&(1+\cos^2\theta)|\cos\alpha| \\ &+ \frac{\sin^2\alpha}{4v^2|\cos\alpha|}\bigl[(\hat{\mathbf{y}}\cdot\mathbf{v})^2 - (\hat{\mathbf{x}}\cdot\mathbf{v})^2\bigr] \\ &+ \mathrm{sgn}\,(\cos\alpha)\,\frac{2^{1/2}\sin\alpha}{v}(\hat{\mathbf{y}}\cdot\mathbf{v})\cos\theta\Bigg\}(\ln D - 2) \\ &+ \frac{\cos\theta|\cos\alpha|}{1+\omega^2/\omega_{\mathrm{p}}^2\gamma^2}\Bigg). \end{aligned} \tag{354}$$

Equations (353), (354) use the following designations

$$J_0 = \frac{zNe^4Q^2}{2\pi m^2c^4}, \qquad D = \frac{c^2}{d^2\omega^2(\omega_{\mathrm{p}}^2/\omega^2 + \gamma^{-2})}, \tag{355}$$

where θ is the angle between the wave vector and particle velocity.

The last term in Eqn (354) without the large factor $(\ln D - 2)$ is related to the correction arising from the expansion of the transverse Green function in the series. Later on, this term is discarded, which actually corresponds to the use of the Green function for isotropic plasma in Eqn (345).

For a bound source of radiation with the characteristic size L, the Fourier phases of the density fluctuations $\delta N_{\mathbf{k}_1}$, $\delta N_{\mathbf{k}_2}$ are statistically independent if $|\mathbf{k}_1 - \mathbf{k}_2| \gg L^{-1}$. When radiating in the direction $\mathbf{n}$ the normal waves with wave vectors $\mathbf{k}_{\mathrm{o}}$, $\mathbf{k}_{\mathrm{e}}$, spatial harmonics of the spectrum of density inhomogeneities with the wave vectors

$$\tilde{\mathbf{k}}\cdot\mathbf{v} = \mathbf{k}_{\mathrm{o}}\cdot\mathbf{v} - \omega, \qquad \tilde{\mathbf{k}}\cdot\mathbf{v} = \mathbf{k}_{\mathrm{e}}\cdot\mathbf{v} - \omega \tag{356}$$

are involved in the scattering process. If the direction of radiation satisfies the condition of strong Faraday rotation,

$$|\cos\theta||k_{\rm o}-k_{\rm e}| \gg L^{-1}\,, \tag{357}$$

then the phase difference between the normal waves is a random value, so the radiation is polarized circularly (within the first approximation over $u^{1/2}/|\cos\alpha|$). The degree of polarization in a given direction is

$$P_{\mathbf{n},\omega}=\frac{I_1-I_{-1}}{I_1+I_{-1}}=-u^{1/2}\left(|\cos\alpha|+\frac{1}{1+\cos^2\theta}\times\left\{\frac{\sin^2\alpha}{4v^2|\cos\alpha|}\left[(\hat{\mathbf{y}}\cdot\mathbf{v})^2-(\hat{\mathbf{x}}\cdot\mathbf{v})^2\right]+\operatorname{sgn}(\cos\alpha)\frac{2^{1/2}\sin\alpha}{v}(\hat{\mathbf{y}}\cdot\mathbf{v})\cos\theta\right\}\right). \tag{358}$$

Note, $P_{\mathbf{n},\omega}$ has no azimuth symmetry with respect to **B**. This is due entirely to the approximation used for the steady rectilinear motion of the particle. Therefore, azimuth asymmetry of the polarization can be observed experimentally if the typical size of the plasma is much less than the particle gyro-radius.

When the inequality opposite to Eqn (357) is fulfilled, the phase difference between complex amplitudes of normal waves is a well-defined value

$$\Delta\phi\approx\operatorname{sgn}(\cos\alpha)(2\psi-\pi)\,, \tag{359}$$

where ψ is the angle between the projections of vectors **v** and **B** on the plane transverse to the wave-vector, and the angle is counted from the projection of **B** in the anti-clockwise direction. In other words, the radiation is almost completely linearly [up to the terms of order of $u^{1/2}/|\cos\alpha|$, $(\ln D)^{-1}$, $L|\cos\theta||k_1-k_{-1}|$)] polarized.

If the length of the Faraday rotation is much larger than the source sizes, the polarization of radiation is linear up to terms of order of $u^{1/2}/|\cos\alpha|$ like in isotropic plasma, the degree of polarization is

$$P_{\mathbf{n},\omega}=\cos^2\theta\,. \tag{360}$$

The emission produced by an ensemble of particles may be of interest too. As an example, let us consider the emission by mono-energetic electrons with an isotropic velocity distribution. In this case, the polarization is circular for any quasi-longitudinal ($|\cos\alpha|\gg u^{1/2}$) direction of the emission. When averaging Eqn (358) over velocity directions, the contribution of sign-alternating terms vanishes and the polarization of radiation receives the form

$$P=-2u^{1/2}|\cos\alpha|\,. \tag{361}$$

Like for transition radiation, the polarization corresponds to predominant emission of extraordinary waves but with somewhat higher degree of polarization [cf. Eqn (99)].

4.5 Effect of an external magnetic field on the spectra of polarization bremsstrahlung

Let us consider the case when the fast particle velocity is parallel to the external constant uniform magnetic field since effect of the field B_0 on the radiation spectrum is largest within such geometry (disturbed background electrons move transversely to the field). The field is assumed to be strong enough to affect the spectrum of plasma density fluctuations. The radiation is calculated in the range of frequencies $\omega\gg\omega_B$ when the field influence on the dispersion of transverse waves is small.

In a magnetized plasma, the function $S(\mathbf{k}_1,\omega_1)$ considered in Section 4.1 has the form [79]

$$S(\mathbf{k}_1,\omega_1)=2\sqrt{\pi}\left|1-\frac{H_{\rm e}}{\varepsilon_L}\right|^2\sum_{l=-\infty}^{\infty}\exp(-k_{1\perp}^2\rho_{\rm e}^2)I_l(k_{1\perp}^2\rho_{\rm e}^2)\times\frac{\exp\left\{-\left[(\omega-l\omega_B)/k_{1\parallel}\langle v_{\rm e}\rangle\right]^2\right\}}{k_{1\parallel}\langle v_{\rm e}\rangle}+2\sqrt{\pi}\,Z\left|\frac{H_{\rm e}}{\varepsilon_L}\right|^2\exp\left(-\frac{\omega_1^2}{k_1^2\langle v_{\rm i}\rangle^2}\right), \tag{362}$$

where $\varepsilon_L=1+H_{\rm e}$ is the longitudinal dielectric permeability of the magnetized plasma, ω_B is the electron cyclotron frequency, $\rho_{\rm e}=\langle v_{\rm e}\rangle/\omega_B$; $k_{1\perp}$, $k_{1\parallel}$ are the components of vector $\mathbf{k}_1$ across and along the magnetic field, and $I_l(x)$ is the modified Bessel function. In expression (362) we neglected the influence of the field B_0 on ion motion (partially magnetized plasma) and the transverse types of oscillations in the magnetized plasma. The longitudinal dielectric receptivity $H_{\rm e}$ of the magnetized plasma is [79]

$$H_{\rm e}(\mathbf{k},\omega)=\frac{1}{k^2d^2}\left\{1-\sum_{l=-\infty}^{\infty}\exp(-k_\perp^2\rho_{\rm e}^2)\,I_l(k_\perp^2\rho_{\rm e}^2)\times\frac{\omega}{\omega-l\omega_B}\left[2x_l\exp(-x_l^2)\int_0^{x_l}\exp(p^2)\,{\rm d}p+{\rm i}\pi^{1/2}x_l\exp(-x_l^2)\right]\right\},\qquad x_l=\frac{\omega-l\omega_B}{k_\parallel\langle v_{\rm e}\rangle}\,. \tag{363}$$

When substituting Eqns (362), (299) into integral (296), the integral cannot be calculated within standard functions, however the integral can be estimated for the strong magnetic field limit ($\rho_{\rm e}\ll d$).

When this condition is fulfilled, the space-charge cloud screening every ion takes a form stretched along the field with a size of $\sim\rho_{\rm e}$ in the transverse direction. The intensity of ion contribution to the spectrum decreases by $(\rho_{\rm e}/d)^4$ times at low frequencies [this is associated with the $(\rho_{\rm e}/d)^2$ times decrease of the transverse (with respect to the magnetic field) plasma polarizability, the square of the polarizability determining the radiation intensity],

$$I_\omega^{(1){\rm ion}}\approx\left(\frac{\rho_{\rm e}}{d}\right)^4\frac{16}{3}\,Zr_0^2Q^2N\ln\frac{c}{\rho_{\rm e}\omega_{\rm p}}\,,\qquad \omega_B\ll\omega<\frac{c}{\rho_{\rm e}}\,, \tag{364}$$

while at $\omega>c/\rho_{\rm e}$, the intensity falls exponentially with increasing frequency.

The intensity of (inelastic) radiation produced by single electrons decreases by a factor of $\ln(mc\rho_{\rm e}/\hbar)/\ln(mcd/\hbar)$ in the range $\omega_{\rm p}<\omega<c/\rho_{\rm e}$ because a momentum higher than $\hbar/\rho_{\rm e}$ is required to detach an electron [i.e., the decrease is much weaker than for the 'ion' contribution, so for $Z(\rho_{\rm e}/d)^4\ll1$ the electron contribution dominates at all frequencies $\omega\gg\omega_B$]. The effective range of the transferred momenta responsible for the emission by single electrons becomes narrower under these conditions, which results in a logarithmic decrease of the intensity. The intensity remains

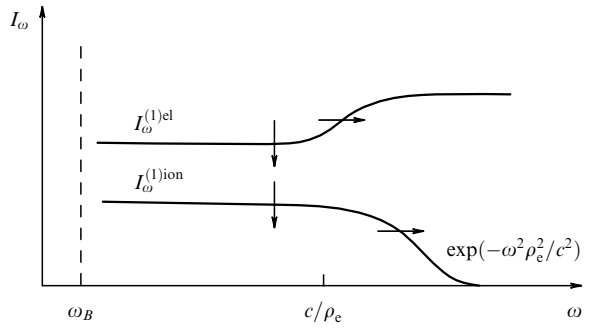

Figure 13. Influence of magnetic field on components of polarization bremsstrahlung.

unchanged at higher frequencies. Figure 13 displays the overview of the spectrum. The arrows indicate the directions as the spectrum changes with increases of the field B_0. The contribution of the longitudinal oscillations (plasmons) to the emission is a few percent. It should be noted that for $\rho_\mathrm{e} \ll d$ we have $\omega_\mathrm{p} < \omega_B$, so in the vicinity of ω_B (and, possibly near its lowest harmonics) the cyclotron emission and absorption may be rather essential.

4.6 Polarization bremsstrahlung in a strong magnetic field

As was stressed in Section 4.1, polarization bremsstrahlung is caused by the scattering of the quasi-stationary field of a fast particle by background particles into electromagnetic waves. This section considers this process in an ultra-strong magnetic field $\omega_B \gg \gamma c/d$, when both thermal plasma electrons and relativistic electrons ($\gamma \gg 1$) move strictly along the magnetic field lines [84]. So, the emission is one dimensional in nature. Here, the emission is strongly suppressed because it is caused by the longitudinal field of the ultra-relativistic particle, which is γ^2 times weaker than traverse one. This approximation can be used if the frequency of radiation satisfies the condition $\omega \ll \omega_B/\gamma$. We accept $\omega \gg \omega_\mathrm{p}$ as well.

In this range of frequencies the plasma is a highly gyrotropic medium; the plasma intrinsic modes are the ordinary wave and slow extraordinary wave [62]. The expression for refractive indices and polarization vectors are given in Section 2.4, where transition radiation in gyrotropic plasma is considered. It is important that the polarization of each eigen mode is almost linear if their directions of propagation are not too close to the magnetic field direction. In the ordinary wave the electric fields vector lies in the plane $(\mathbf{k}, \mathbf{B})$, while in the slow extraordinary wave this vector is perpendicular to the plane. Since the electric current has only one component here, the ordinary waves are generated much more effectively than extraordinary waves (in agreement with the results of Section 2.4, see Fig. 6). Hence, in this section we give the formulae for PB of ordinary waves only.

The radiation spectrum is calculated in a similar way as in Section 4.1 with only one exception. The acceleration in Eqn (292) and the field of relativistic particle (301) have only one component parallel to the particle velocity and magnetic field. The calculation details are published in Ref. [84], we give the final result only. At high frequencies $\omega > 2\gamma^2 c/d$ we have:

$$I_\omega(\vartheta) = \frac{2r_0^2 Q^2 n_\mathrm{i} Z^2}{\gamma^2}\left(\frac{c}{\omega d}\right)^4 \frac{\sin^2\vartheta(1+\gamma^2\sin^2\vartheta)}{\left[1-(v/c)\cos\vartheta\right]^2}\,. \qquad (365)$$

Strictly speaking, Eqn (365) was obtained within the 'quasi-transverse' approximation, when condition (128) is fulfilled, i.e. Eqn (365) is valid for the angles

$$\theta > \left(\frac{2\omega}{\omega_B}\right)^{1/2}. \qquad (366)$$

However, since there is no sharp directivity along the magnetic field for the emission (365) (see Fig. 14a), the approximation used is adequate for this case. For high energies $\gamma \gg 1$, the radiation intensity (365) integrated over all angles does not depend on energy explicitly:

$$I_\omega = \frac{8}{3} r_0^2 Q^2 n_\mathrm{i} Z^2 \left(\frac{c}{\omega d}\right)^4. \qquad (367)$$

If we compare Eqn (367) with the intensity of standard bremsstrahlung in the high magnetic field

$$I_\omega^{\mathrm{BH}} = \frac{8r_0^2 Q^2 n_\mathrm{i} Z^2}{3\gamma^2}\,, \qquad \omega > \frac{2\gamma^2 c}{d}\,, \qquad (368)$$

we find that the polarization mechanism is negligible in comparison with standard bremsstrahlung in the range of high frequencies $\omega > 2\gamma^2 c/d$.

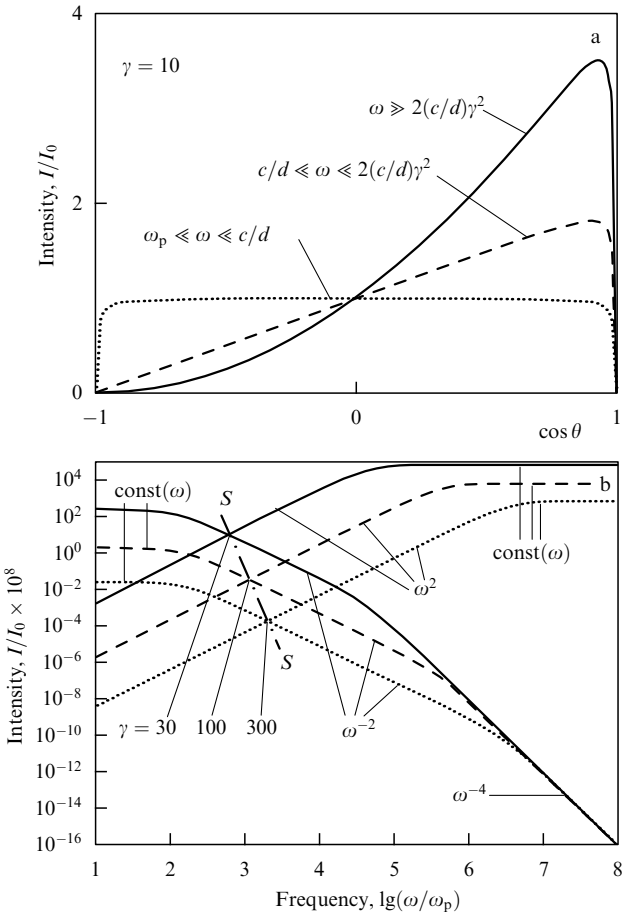

Figure 14. Angular (a) and spectral (b) distributions of polarization bremsstrahlung in the presence of a very strong magnetic field. The PB has no strong directivity at any frequencies; the dependence of angle is very slight at low frequencies. $c/v_\mathrm{T} = 10^2$ is accepted for plotting the spectra. PB dominates to the left on the line $S-S$ corresponding to Eqn (375), the usual bremsstrahlung dominates to the right.

At frequencies $c/d \ll \omega \ll 2\gamma^2 c/d$ and $\omega_p \ll \omega \ll c/d$ we have, respectively:

$$I_\omega(\vartheta) = \frac{2r_0^2 Q^2 n_i Z^2}{\gamma^4} \frac{c^2}{\omega^2 d^2} \frac{\sin^2\vartheta}{1-(v/c)\cos\vartheta}\,, \tag{369}$$

$$I_\omega(\vartheta) = \frac{4r_0^2 Q^2 n_i Z^2}{\gamma^2} \frac{\sin^2\vartheta}{1+\gamma^2\sin^2\vartheta}\,. \tag{370}$$

Equation (370) shows transition bremsstrahlung to depend weakly on the angle at relatively low frequencies $\omega_p \ll \omega \ll c/d$ in the range $\gamma^{-1} < \vartheta < \pi/2$, while for small angles it approaches zero as $\sin^2\vartheta$ (see Fig. 14a).

Integrating Eqns (369) and (370) over the full solid angle, yields the respective spectral intensities:

$$I_\omega = \frac{4r_0^2 Q^2 n_i Z^2}{\gamma^4}\left(\frac{c}{\omega d}\right)^2 (\ln 2\gamma - 1)\,, \tag{371}$$

$$I_\omega = \frac{8r_0^2 Q^2 n_i Z^2}{\gamma^4}\,. \tag{372}$$

In the same frequency ranges the intensity of standard bremsstrahlung is expressed as

$$I_\omega^{BH} = \frac{4r_0^2 Q^2 n_i Z^2}{3\gamma^6}\left(\frac{\omega d}{c}\right)^2\left(\ln\frac{2\gamma^2\omega d}{c} - 1\right), \quad \frac{c}{d} \ll \omega \ll \frac{2\gamma^2 c}{d}\,, \tag{373}$$

$$I_\omega^{BH} = \frac{8r_0^2 Q^2 n_i Z^2}{\gamma^6}\left(\frac{\omega d}{c}\right)^2 (\ln 2\gamma - 1)\,, \quad \omega_p \ll \omega \ll \frac{c}{d}\,. \tag{374}$$

Comparing formulae (371), (372) and (373), (374), we can conclude that polarization bremsstrahlung dominates in the plasma in the presence of a strong magnetic field if

$$\omega < \omega_* = \frac{\sqrt{\gamma}\,c}{d}\,, \tag{375}$$

and the frequency ω_* belongs to the range $c/d \ll \omega \ll 2\gamma^2 c/d$. Figure 14b displays the polarization bremsstrahlung and standard bremsstrahlung for various energies of the relativistic particle, the line $S-S$ corresponding to Eqn (375) divides the regions, where one or other contribution predominates. In the range $\omega_p \ll \omega \ll c/d$, where the length of the emitted wave $\lambda \gg d$, the polarization bremsstrahlung always dominates in the strong magnetic field because thermal plasma electrons producing dynamic polarizability emit coherently when scattering virtual photons, which results in the maximal intensity of radiation. As to interference between standard and polarization bremsstrahlung, it is unimportant because of the different frequency and energy dependences in the respective equations.

To finalize, we note that the total bremsstrahlung of a fast particle in plasma depends substantially on the radiating frequency and particle energy in the presence of a strong magnetic field. In the range $\omega \gg 2\gamma^2 c/d$ the emission is provided by the standard bremsstrahlung mechanism, which has the largest intensity in this range. The polarization bremsstrahlung dominates at low frequencies (375); its intensity reaches the maximal value in the range $\omega_p \ll \omega \ll c/d$. The maximal PB level (372) in this range of frequencies is γ^2 times less than that of standard bremsstrahlung (368) at high frequencies $\omega \gg 2\gamma^2 c/d$.

In conclusion we recall that PB consists of three different contributions $I_\omega^{(1)ion}$, $I_\omega^{(1)el}$, $I_\omega^{(2)}$ according to the results of Section 4.1. In an isotropic medium without a magnetic field, the first contribution is Z times larger than the others and, so, it dominates for $Z \gg 1$. For this reason (as well as for simplicity) this section considers the contribution $I_\omega^{(1)ion}$ only. However, Section 4.5 proves that the magnetic field affects these contributions differently. For example, the electron contribution $I_\omega^{(1)el}$ dominates under the conditions considered in Section 4.5. The contributions $I_\omega^{(1)el}$ and $I_\omega^{(2)}$ have not been considered yet in the literature in the presence of the ultra-strong magnetic field discussed in this section.

5. Astrophysical applications of the theory of transition radiation

The theory of transition radiation is a rather broad field of physics today [28]. The respective experimental data, which have been obtained for the past decades, agree excellently with the TR theory for both a single boundary and periodic media [4, 10, 85–89]. Furthermore, coherent TR generated by bunches of ultra-relativistic electrons passing through a metallic foil has been observed in the far infrared range [90] as well as in the X-ray range [91].

While TR is a rather general effect and the theory is pretty simple and nice, the effect has not been widely applied in astrophysics (and, generally, for natural conditions) yet.

Probably, the first attempt to apply the TR theory in astrophysics was done in Ref. [92]. That paper employed the formulae valid for a single boundary to calculate TR generated by high-energy charged particles interacting with cosmic dust in the interstellar medium. The calculated TR intensity (with the use of independent data on the amount of cosmic dust and the flux of cosmic rays) was shown to agree with the observed intensity of the diffuse *galactic soft X-ray emission*. However, later papers [93, 94] noted the size of a single dust grain to be about three orders of magnitude less than the TR formation zone. Thus, the intensity of X-ray TR is about 0.1% of the observed value.

Transition radiation by relativistic nuclei on random plasma inhomogeneities was applied to account for low-frequency excess in radio spectra of some *radio galaxies* at decametric wavelengths [66]. Large values of the background number density $N \sim 10^2$ cm^{-3} of the emitting plasma were found to be required for the theory to fit observations. The lobes of radio galaxies are known to be much more tenuous, $N \sim 10^{-2}-10^{-3}$ cm^{-3}, so a sufficient TR level could only have been provided by denser nuclei of the radio galaxies. However, the spatial resolution is too low in the decametric range to specify where the decametric radiation originates (i.e., from the nucleus or lobes). TR could contribute to the infrared excess observed in some *active galactic nuclei* [95], as well as to continuum *millimeter radiation from stars* when the synchrotron mechanism fails [96].

Some quantitative estimates of transition radiation in natural conditions have already been done in the review. For example, the effect of TR suppression by a magnetic field is evaluated at the end of Section 2.2, and by scattering at the end of Section 2.3.

Resonant transition radiation has been discovered and calculated properly just recently [57, 63]; consequently this effect has not been widely used for applications (in spite of its high intensity). Below we discuss the generation of TR and RTR in cosmic plasmas in more detail.

5.1 Generation of transition radiation in the interstellar medium

The diffuse galactic radio emission is known to have a power-law distribution from a few MHz to a few GHz and to be produced by electrons of cosmic rays propagating in galactic magnetic field due to the synchrotron mechanism [97]. Hence, the synchrotron radiation carries information about the relativistic electrons and the magnetic field. However, the radiation originates and propagates in the interstellar medium (ISM) that affects the radiation properties. When the frequency of observation decreases, the Faraday effect starts to depolarize the radiation. Then, free–free absorption and the density effect (Razin–Tsytovich effect) become essential at lower frequencies. Thus, the (low-frequency) synchrotron radiation carries information on the ISM itself (its number density, temperature, spatial distribution etc.).

From this point of view, the analysis of the galactic radio emission at very low frequencies, $f \leqslant 3$ MHz, where the spectrum is qualitatively different from that at high frequencies [98], is of primary interest. We should emphasize that the radiation intensity drops by more than two orders of magnitude when the frequency decreases ten times only, and no shape of energetic spectrum of relativistic electrons can account for this low-frequency cutoff.

It is very important that less intensive emission mechanisms can contribute to the total spectrum at low frequencies where the synchrotron emission is exponentially small. The mechanisms are Compton emission by relativistic electrons on small-scale fields [32, 99, 100] that is suppressed by the density effect but less effectively than synchrotron emission, and transition radiation on density fluctuations that is not suppressed by the thermal plasma at all.

To obtain the transition radiation level we use the modern data on the electron density inhomogeneities in the disc derived from the analysis of radio source scintillations in the ISM. The spectrum of inhomogeneities $|\delta N|^2_{\mathbf{k}}$ is found to fit a power-law for most of the lines of sight [101]:

$$|\delta N|^2_{\mathbf{k}} = C_N^2 k^{-\alpha}, \qquad \frac{2\pi}{l_0} < k < \frac{2\pi}{l_1}, \tag{376}$$

where $l_1 \approx c/f_\mathrm{p} \approx 10^7$ cm, $l_0 \geqslant 10^{14}$ cm,

$$\alpha = \nu + 2 = \frac{11}{3} \pm 0.3, \tag{377}$$

and f_p is the plasma frequency. On average over the disc with thickness $L \approx 1$ kpc and radius $R \approx 20$ kpc the value C_N^2 is [101]

$$C_N^2 \approx 10^{-3.5}\ \mathrm{m}^{-20/3}. \tag{378}$$

A region of enhanced scattering with $C_N^2 \sim 1\ \mathrm{m}^{-20/3}$ is situated (4 ± 2) kpc from the galactic center, while some clumps reveal much higher scattering with the largest value $C_N^2 \approx 10^5\ \mathrm{m}^{-20/3}$ in NG6334 at 1.7 kpc from the Sun.

For the Kolmogorov spectrum (376) and the minimal value of C_N^2 (378) we find

$$\langle \Delta N^2 \rangle = (1-3) \times 10^{-10}\ \mathrm{cm}^{-6} \tag{379}$$

on scales $l < 2\pi c/\omega_B \approx (2-3) \times 10^9$ cm responsible for transition radiation generation. With $\bar{N} \approx 0.025\ \mathrm{cm}^{-3}$ [101] we have

$$\frac{\langle \Delta N^2 \rangle}{N^2} \approx (2-5) \times 10^{-7}. \tag{380}$$

The output spectrum of transition radiation depends strongly on the actual distribution of the mean electron density over the emitting volume (see Section 3). We calculate the spectrum for two limiting models of the distribution. The first one assumes that the plasma frequencies f_p are distributed uniformly in the range $f_\mathrm{p} = (2.0 \pm 0.5)$ kHz. Further, we accept $\langle \Delta N^2 \rangle / N^2 \approx 3 \times 10^{-7}$ and $\nu = \alpha - 2 = 1.7$ [101]. Here, resonant transition radiation (Section 3) is generated at the lowest frequencies $f \sim f_\mathrm{p}$, while usual transition radiation (Section 2) is generated at higher frequencies by relativistic particles. The respective contribution is the curve tr1 in Fig. 15a. The spectrum has the frequency dependence $P_\mathrm{tr1} \propto f^{-1.1}$ at $f \gg f_\mathrm{p}$.

The second model (the curve tr2 in Fig. 15b) uses the distribution of the mean electron density derived from the relation between the emission measure and dispersion measure in the ISM [102]:

$$F(f_\mathrm{p}) = \frac{0.5 f_\mathrm{p0}^{0.5}}{f_\mathrm{p}^{1.5}}, \qquad f_\mathrm{p0} < f_\mathrm{p} < f_\mathrm{pm} \simeq 20\ \mathrm{kHz}, \tag{381}$$

where $F(f_\mathrm{p})$ is the filling factor of the regions with plasma frequency f_p in the warm ISM, and f_p0 is the typical value of the ISM plasma frequency $f_\mathrm{p0} \approx 2$ kHz. Averaging the transition radiation spectrum with distribution function (381) gives:

$$P^\mathrm{tr2} = 0.5 \tilde{K}_\mathrm{tr} \frac{e^2}{c} N_\mathrm{e} \omega_\mathrm{p0} \frac{\langle \Delta N^2 \rangle}{N^2} \frac{c^2}{v_\mathrm{T}^2} \left(\frac{k_0 c}{\omega_\mathrm{p0}} \right)^{\nu-1} \left(\frac{\omega_*}{\omega} \right)^{\nu-1.5}, \tag{382}$$

where $\omega_* = 2\pi f_* = \omega_\mathrm{p}^2/\omega_B$ (actually, a smaller factor can enter Eqn (382) instead of c^2/v_T^2 due to the magnetic field effect, see Section 3); the ratio of TR (382) to synchrotron emission at the frequency ω_* is

$$\frac{P^\mathrm{tr2}}{P^\mathrm{s}} \simeq 3 \times 10^{-3} \frac{c^2}{v_\mathrm{T}^2} \frac{\langle \Delta N^2 \rangle}{N^2} \left(\frac{k_0 c}{\omega_\mathrm{p0}} \right)^{\nu-1.5} \left(\frac{\omega_*}{\omega_\mathrm{p0}} \right)^{\xi-\nu+1.5}. \tag{383}$$

Transition radiation (382) provides a nearly flat spectrum (with spectral index 0.2) similar to the free–free emission. Note that the transition radiation (382) exceeds the free–free radiation of warm ISM if $\langle \Delta N^2 \rangle / N^2 > 10^{-9}$. It is important that if the level of density inhomogeneities were larger than 3×10^{-7} (and the distribution function (381) is correct for local ISM), or $\nu < 1.6-1.7$, or $f_\mathrm{pm} \gg 20$ kHz, the intensity of transition radiation would exceed the measured intensity at 0.1–0.2 MHz. Thus, the value

$$\frac{\langle \Delta N^2 \rangle}{N^2} = 3 \times 10^{-7} \tag{384}$$

is the upper limit for the small scale density fluctuation level in the local ISM if distribution (381) is correct.

Finally, Fig. 15c shows the expected intensity of ultra-low-frequency background galactic radiation reduced by free-free absorption in the galactic disc. The two theoretical curves reflect the two considered models for the distribution of the thermal electron density. Transition radiation clearly dominates any other emission mechanism at $f < 50$ kHz. Thus,

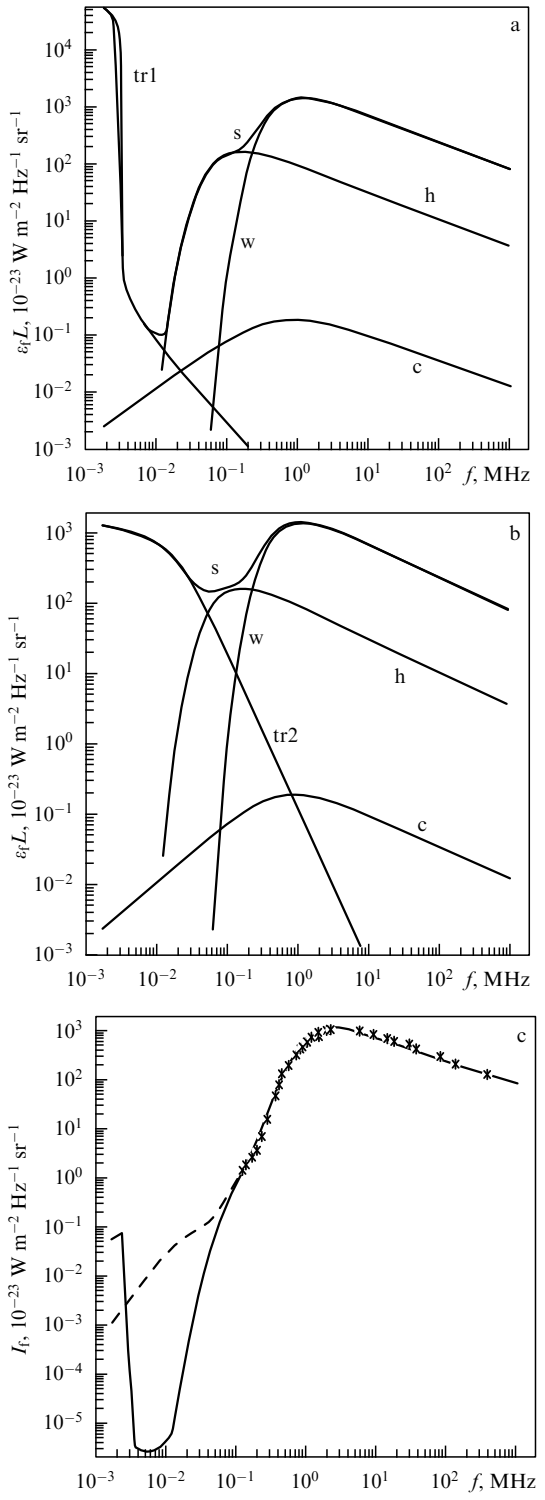

Figure 15. Various components of the volume emissivity of the galactic disc according to paper [98]: w is the synchrotron emission in warm gas, h is the synchrotron emission in hot gas, c is the inverse Compton emission on small-scale magnetic fields, tr is transition radiation calculated for two different models (a and b), s is the sum of all components. (c) The intensity of the background galactic radio emission accounting for free – free absorption in diffuse warm ISM. The asterisks display available observational data in the range 0.13 – 408 MHz. The solid curve corresponds to the model tr1 (a), the dashed one to the model tr2 (b). Within the model tr2, transition radiation dominates at $f < 100$ kHz.

observations of the galactic transition radiation at these extremely low frequencies would provide us with averaged characteristics of the small-scale structure of the local interstellar medium.

So far, the lowest frequency observations, $f = 0.13-2.6$ MHz, of the background radio emission of the Galaxy were performed by the satellite IMP-6 [103] 30 years ago. Recent observations performed by the WIND spacecraft at $f > 0.2$ MHz [104, 105] agree well (within a factor of 2) with older ones [103, 106, 107].

All the observations cited have been made from Earth orbit, where the interference level (of solar and terrestrial origin) is rather large. Hence, it is exceedingly difficult to observe at low frequencies. The study of the low-frequency background radiation of the Galaxy can be promoted substantially by a spacecraft like CASSINI [108] traveling far from the Sun and Earth. Particularly, such missions can contribute significantly to observations of transition radiation generated in the local interstellar (and/or interplanetary) medium.

5.2 Estimate of transition radiation intensity in the solar corona

Relativistic particles and magnetized turbulent plasma are typical for most astrophysical objects. However, many sources like radio galaxies and supernova remnants are rather tenuous, so they produce transition radiation in a low frequency range that is inaccessible to observations from the Earth due to absorption in the interstellar medium and the opacity of the Earth's atmosphere. Contrarily, the plasma frequencies of the solar atmosphere belong to the frequency range covered by the usual ground based radio telescopes.

Solar radio bursts are well known to reveal a prominent variety. Both the difference in physical conditions at the source and the different microscopic emission mechanisms dominating in various events [109] provide the variety of solar radio emission types. There is no doubt that bremsstrahlung, gyro-synchrotron (both incoherent and coherent), and plasma mechanisms are important for the production of solar radio emission [67, 109]. The role of transition radiation generated by fast particles in a plasma with random inhomogeneities is still unclear, while there is ample observational and theoretical evidence for the presence of non-thermal particles (particularly, relativistic) and turbulence in flares (for details see Ref. [110]).

Modeling of flaring electromagnetic emission requires taking into account that the primary energy release occurs in arch-like magnetic structures, rather than in uniform plasma. The legs of arch end in the dense photosphere, while the top of arch is located in more rarefied corona (Fig. 16). Hence, the

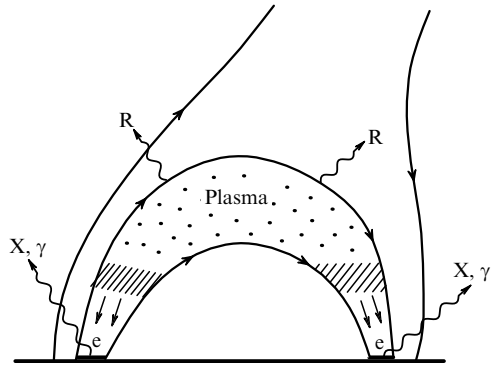

Figure 16. Magnetic loop in the solar corona.

charged particles accelerated by the energy release propagate in a medium with varying parameters (number density, temperature, and magnetic field). Consequently, radio emission (R) originates at high (rarefied) levels of the magnetic loop, while hard X-ray and gamma-ray radiation (X, γ) are generated (by bremsstrahlung) at the dense legs of the arch.

The intensity of transition radiation has been discussed to be rather large close to the local plasma frequency. It is important that the plasma mechanism based on the instability of plasma waves and their consequent conversion into radio waves can contribute to the very same frequency range. The instability requires the fast particle distribution to be anisotropic (say, beam-like or loss-cone). Transition radiation can dominate (at the plasma frequency) if the fast electrons are distributed more or less isotropically and the conditions for plasma wave instability are not fulfilled. This is probably the case for continuum decimetric and microwave bursts of solar radio emission. The high frequency emission is, no doubt, generated by gyro-synchrotron emission of energetic electrons [109], while low-frequency emission can be produced by the transition mechanism.

Section 5.1 uses independent data on the spectrum of the ISM density inhomogeneities to calculate the transition radiation generated in ISM. Unfortunately, data of this kind are not available for the solar atmosphere (and for solar flares, in particular). However, the interpretation of flare radio emission can be improved being analyzed together with hard X-ray and gamma-ray emission generated by the same accelerated electrons. The analysis of these hard emissions provides us with spectra and number densities of fast particles, hence, the account of hard X-ray and gamma-ray emissions is a must for the interpretation of radio data to be consistent.

Relativistic electrons generate both transition and gyro-synchrotron radio emission when they move in a magnetic trap filled by turbulent background plasma. However, the two mechanisms dominate in different frequency ranges, namely, the high-frequency part (to the right of the spectral peak) of observed spectrum is produced by the synchrotron mechanism [109], while the low-frequency part (to the left of the spectral minimum) is produced by transition radiation. This separation happens because synchrotron radiation decreases exponentially due to the plasma dispersion effect [53] at the frequencies $f < f_R = 2f_p^2/3f_B$, where f_p and f_B are the plasma and gyro-frequencies of the electron, while it is generated effectively at the frequencies (range I):

$$f > f_R \,. \tag{385}$$

If $f_p \gg f_B$, then transition radiation is produced at $f_p < f < f_R$ (range II), while it is suppressed by magnetic field at higher frequencies (see Section 2.2).

Let us start with an oversimplified model assuming the radio source to be uniform on average, so that resonant transition radiation is unessential at frequencies $f > f_p$. The flux of (standard) transition radiation in range II can be expressed as [110]

$$F_f^{tr} = \beta \times 10^6 \, \frac{f_p}{1\ \text{GHz}} \, \frac{VN_e(>1\ \text{MeV})}{10^{33}} \, \frac{\langle \Delta N^2 \rangle}{N^2} \left(\frac{f_p}{f}\right)^{\xi+1-\nu} \text{sfu} \tag{386}$$

(1 sfu $= 10^{-19}$ erg cm^{-2} s^{-1} Hz^{-1} is a solar flux unit), where $\langle \Delta N^2 \rangle$ and ν are the mean square and spectral index of inhomogeneities on scales $l_0 \sim 2c/f_p$, N is the number density of background electrons, and $\beta(\nu; \xi) \sim 1$ [for example $\beta(1.5; 3.5) \approx 3.3$, $\beta(1.7; 4) \approx 4.4$].

The flux of transition radiation can exceed the synchrotron flux: the ratio of transition radiation at $f \sim f_p$ (but outside the RTR peak!) to the peak of synchrotron radiation (at $f \approx f_R$) is

$$\frac{F^{tr}}{F^s} \sim \frac{\langle \Delta N^2 \rangle}{N} \left[\frac{f_p}{f_B}\right]^{\xi} \tag{387}$$

for an optically thin source. Estimate (387) can be larger than unity for dense plasma $f_p \gg f_B$.

Microwave solar bursts frequently display spectra with maxima and minima. We consider three solar flares observed at gamma range $E_\gamma > 300$ keV: 1980 June, 21; 1982 April, 02; and 1982 July, 09. The flares lasted about one minute in both radio and gamma ranges, so they are classified as impulsive flares [111]. Differential energy spectra of accelerated electrons are obtained with the use of the respective gamma-ray spectra [112], the number density of the electrons is found from cooperative analysis of microwave (gyro-synchrotron) and gamma (bremsstrahlung) radiation.

1982 July, 09 flare. This flare produced both decimetric and microwave radiation (Fig. 17) [113]. The real (gradually non-uniform) loop is assumed for simplicity to consist of two regions, dense legs and rarefied loop-top, which are assumed to be uniform on average. Hence, gamma-ray emission is generated in the lower source (loop legs), while radio emission is produced in the upper source (loop top).

Let us obtain the parameters of radio source from the microwave spectrum. We assume $f_p \sim 1$ GHz that is less than the frequency of the spectral minimum $f_{min} \approx 3$ GHz. The peak of microwave emission at $f_{max} \approx 9$ GHz is due to the Razin–Tsytovich effect if $B \approx 90$ G. Hence, the instantaneous number of fast electrons should be

$$VN_e(>1\ \text{MeV}) \approx 10^{32} \,, \tag{388}$$

to provide the observed flux of 700 sfu at the frequency f_{max}. As could be expected the estimate (388) is one order of magnitude less than the total (during the whole flare) number

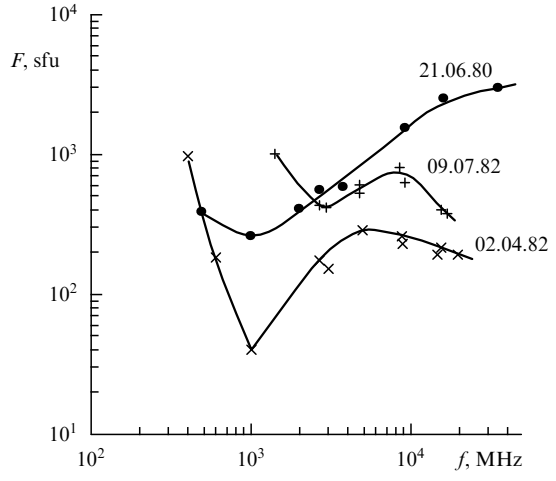

Figure 17. Radio spectra of three solar flares at the moments of the respective temporal peaks.

of accelerated electrons $N_{\rm tot}(>1\ {\rm MeV})\sim 10^{33}$ found from the gamma-ray fluence. The spectral index of the energy spectrum of electrons found from the slope of the high-frequency microwave spectrum, $\xi\approx 3.5$, is in good quantitative agreement with that found from gamma-ray data. Thus, the high frequency radiation can be consistently interpreted in terms of gyro-synchrotron emission from a uniform (on average) source.

Let us apply the TR theory to the low-frequency radiation. Substitution of Eqn (388), $f_{\rm p}$ and the observed flux 500 sfu at $f\approx 1.5$ GHz into Eqn (386) yields

$$\frac{\langle\Delta N^2\rangle}{N^2}\approx 6\times 10^{-4} \tag{389}$$

in scales $l_0\sim 2c/f_{\rm p}$.

The interpretation would be consistent if the radio emission generated at the lower source did not exceed the observed level. Assuming typical parameters $B\sim 200$ G, $N\sim 2\times 10^{11}$ cm^{-3} we have $f_{\rm R}\approx 20$ GHz, so synchrotron radiation from the lower source is unessential at these frequencies. Transition radiation from the lower source is less than the observed radio flux if

$$\frac{\langle\Delta N^2\rangle}{N^2}<4\times 10^{-4}\,. \tag{390}$$

The same analysis of the two other flares (see Ref. [114] for more details) shows that the low-frequency rise in the radio spectra is due to transition radiation if

$$\frac{\langle\Delta N^2\rangle}{N^2}\approx (1-2)\times 10^{-3}\,. \tag{391}$$

Thus, the cooperative use of the synchrotron and transition mechanisms provides a consistent model of radio emission generated during solar gamma flares (which are the most powerful ones).

The majority of solar flares do not produce gamma emission, while they produce hard X-ray emission. The low frequency rise can also be treated as transition radiation in this case providing a consistent interpretation [110].

Thus, the use of the theory of transition radiation is concluded to give *logically* consistent results. However, the obtained level of plasma inhomogeneities seems to be rather large, $\langle\Delta N^2\rangle/N^2\approx 10^{-4}-10^{-2}$, while less than unity. We should finally note that the estimates do not take into account the real large-scale inhomogeneity of the radio source and resonant transition radiation, which is more important for a non-uniform source.

5.3 Resonant transition radiation in solar flares

Resonant transition radiation from a uniform source is a narrow peak close to the plasma frequency. The actual shape of the RTR spectrum depends primarily on the real large-scale inhomogeneity of the medium producing this radiation.

Further calculations assume the distribution of the TR source 'over the plasma frequency' to obey a power-law at some range of plasma frequencies

$$F(\omega_{\rm p})=(\lambda-1)\frac{\omega_{\rm p0}^{\lambda-1}}{\omega_{\rm p}^{\lambda}}\,,\qquad \omega_{\rm p}>\omega_{\rm p0}\,, \tag{392}$$

where $\omega_{\rm p0}$ is the lowest plasma frequency at the source.

Eight different formulae describe the RTR intensity of ordinary and extraordinary waves depending on the ratio of the dimensionless parameters $\omega_B/\omega_{\rm p}$ and $v_{\rm T}/c$ (where $v_{\rm T}$ is the thermal velocity of the background electron, c is the speed of light) and on the interrelation between the spectral indices ξ and ν, see Section 3.3. The narrowness of the RTR peak allows us to approximate the RTR spectral density for each of the cases (256) – (263) by

$$P_{\omega}^{(i)}=P_i\,\delta(\omega-\omega_{\rm p})\,,\qquad 1\leqslant i\leqslant 8\,. \tag{393}$$

Integration of the intensity (393) with the distribution function (392) over the volume of the source located at a certain distance from the observer yields the flux of radio emission:

$$F_f=\frac{2\pi V}{R_{\rm s}^2}\int F(\omega_{\rm p})P^{(i)}\delta(\omega-\omega_{\rm p})\,{\rm d}\omega_{\rm p}\,, \tag{394}$$

where V is the volume of the emission source, and $R_{\rm s}$ is the distance between the Sun and the Earth.

The following relation between parameters is typically correct for solar decimetric and microwave bursts:

$$\frac{v_{\rm T}}{c}<\frac{\omega_B}{\omega_{\rm p}}<\left(\frac{v_{\rm T}}{c}\right)^{1/2}. \tag{395}$$

Here, if $\xi<\nu+2$, then the RTR of ordinary waves is P_5 (260); if $\xi>\nu+2.5$, then it is P_3 (258), and if $\nu+2<\xi<\nu+2.5$, then it is the sum of these two formulae. Let us consider the case of P_5 (260) in more detail. Substitution of Eqn (260) into Eqn (394) yields

$$F_f=\frac{V}{R_{\rm s}^2}\,C_5\,\frac{e^2}{c}(1+\cos^2\theta)\int f_{\rm p}x_0^{\xi-1}N_{\rm e}\,\frac{\langle\Delta N^2\rangle}{N^2}\left(\frac{k_0c}{\omega_{\rm p}}\right)^{\nu-1}\times\left(\frac{\omega_{\rm p}}{\omega_B}\right)^{1/2}\frac{c}{v_{\rm T}}\left(\frac{\omega_{\rm p0}}{\omega_{\rm p}}\right)^{\lambda}\delta(\omega-\omega_p)\,{\rm d}\omega_{\rm p}\,, \tag{396}$$

where

$$C_5=\frac{\pi^2(\lambda-1)(\nu-1)(\xi-1)\Gamma\left[(\xi-1)/2\right]\Gamma\left[(\nu-\xi+2.5)/2\right]}{36\times 6^{1/2}(\nu+2)\Gamma(\nu/2+3/4)}\,. \tag{397}$$

We should emphasize that the output of the integration (396) is specified by whether and how the parameters involved $\langle\Delta N^2\rangle$, k_0, ω_B depend on the plasma frequency $\omega_{\rm p}$. If each of the parameters depends on the plasma frequency (if any) by a power-law, the integration in Eqn (396) yields

$$F_f=C_5\,\frac{e^2f_{\rm p0}}{R_{\rm s}^2c}(1+\cos^2\theta)x_0^{\xi-1}VN_{\rm e}\,\frac{\langle\Delta N^2\rangle}{N^2}\left(\frac{k_0c}{\omega_{\rm p0}}\right)^{\nu-1}\times\left(\frac{\omega_{\rm p0}}{\omega_B}\right)^{1/2}\frac{c}{v_{\rm T}}\left(\frac{\omega_{\rm p0}}{\omega}\right)^{\alpha}. \tag{398}$$

The spectral index α is specified by partial power-laws. For example, if

$$\frac{\langle\Delta N^2\rangle}{N^2}={\rm const}\,,\qquad \frac{k_0c}{\omega_{\rm p}}={\rm const}\,,\qquad \frac{\omega_{\rm p}}{\omega_B}={\rm const}\,, \tag{399}$$

then

$$\alpha=\lambda-1\,; \tag{400}$$

if

$$\frac{\langle \Delta N^2 \rangle}{N^2} = \text{const}\,, \qquad k_0 = \text{const}\,(\omega_\text{p})\,, \qquad \omega_B = \text{const}\,(\omega_\text{p})\,, \tag{401}$$

then

$$\alpha = \lambda + \nu - 2.5 \tag{402}$$

etc. Further, we omit for simplicity the index '0' in $\omega_{\text{p}0}$ and use the notation ω_p. Substituting the well-known fundamental constants and the distance between the Sun and the Earth, $R_\text{s} = 1.49 \times 10^{13}$ cm, into Eqn (398), we obtain the RTR flux from a non-uniform source (in solar flux units):

$$F_f = 3.45 \times 10^5 C_5 (1 + \cos^2\theta)\, \frac{f_\text{p}}{1\ \text{GHz}}\, x_0^{\xi-1}\, \frac{VN_\text{e}}{10^{33}} \times \times \left(\frac{k_0 c}{\omega_\text{p}}\right)^{\nu-1} \frac{\langle \Delta N^2 \rangle}{N^2} \left(\frac{\omega_\text{p}}{\omega_B}\right)^{1/2} \frac{c}{v_\text{T}} \left(\frac{\omega_\text{p}}{\omega}\right)^{\alpha} \text{sfu}\,. \tag{403}$$

Expression (403) is correct [with the condition (395)] for rather hard spectra of fast electrons, $\xi < \nu + 2$. For softer spectra, $\nu + 2.5 < \xi < \nu + 3$, the use of RTR intensity P_3 (258) yields (for ordinary waves)

$$F_f = 3.45 \times 10^5 C_3\, \frac{f_\text{p}}{1\ \text{GHz}}\, x_0^{\xi-1}\, \frac{VN_\text{e}}{10^{33}} \left(\frac{k_0 c}{\omega_\text{p}}\right)^{\nu-1} \frac{\langle \Delta N^2 \rangle}{N^2} \times \frac{c^2}{v_\text{T}^2} \left[\frac{\omega_\text{p}}{\omega_B} \left(\frac{6 \times 3^{1/2} v_\text{T}^3}{c^3}\right)^{1/2}\right]^{\nu+3-\xi} \left(\frac{\omega_\text{p}}{\omega}\right)^{\alpha} \text{sfu}\,, \tag{404}$$

where

$$C_3 = \frac{\pi(\lambda-1)(\nu-1)(\xi-1)}{12(\nu+2)} \times \left[\frac{8}{15(\nu+3-\xi)} + \frac{\pi(1+\cos^2\theta)}{8(\xi-\nu-2)}\right]. \tag{405}$$

For the intermediate case, $\nu + 2 < \xi < \nu + 2.5$, the flux is described by the sum of expressions (403) and (404). The RTR is polarized as the ordinary mode (see Section 3.3) and the degree of polarization can be as high as 100%.

Moreover, solar flares frequently produce even softer electron distributions:

$$\xi > \nu + 3\,. \tag{406}$$

Indeed, the hard X-ray spectra (closely related to the spectrum of fast electrons injected into the loop) of solar flares are typically

$$F_E \propto E^{-\gamma_\text{X}}\,, \qquad 3 < \gamma_\text{X} < 7 \tag{407}$$

The respective energy spectra of the fast non-relativistic electrons accumulated inside the magnetic loop obey power-laws as well [115, 116]:

$$N(E) \propto E^{-\xi_E}\,, \qquad 2.5 < \xi_E < 8\,. \tag{408}$$

The spectral index ξ in the distribution over momentum (172) is defined in the non-relativistic region by ξ_E by the relation

$$\xi = 2\xi_E - 1 > 4\,. \tag{409}$$

So, (406) is fulfilled for the Kolmogorov spectrum of turbulence for $\xi > 4.7$.

For this case (and $\omega_B/\omega_\text{p} < (v_\text{T}/c)^{1/2}$), the transition radiation of each of the normal modes is described by the formula P_2 (257). For the total flux (the sum of the two modes), we find similarly to Eqns (403), (404) (the total radiation is weakly polarized for this case):

$$F_f = 3.45 \times 10^5 C_2\, \frac{f_\text{p}}{1\ \text{GHz}} \left(\frac{k_0 c}{\omega_\text{p}}\right)^{\nu-1} \frac{\langle \Delta N^2 \rangle}{N^2}\, x_0^{\nu+2} \times \frac{VN_\text{e}(> x_0)}{10^{33}}\, \frac{c^2}{v_\text{T}^2} \left(\frac{f_\text{p}}{f}\right)^{\alpha} \text{sfu}\,, \tag{410}$$

where

$$C_2 = \frac{4\pi(\lambda-1)(\nu-1)(\xi-1)}{45(\nu+2)(\xi-\nu-3)}\,. \tag{411}$$

Since the gradual source non-uniformity (392) does not affect the high-frequency (gyro-synchrotron) part of the radio spectrum substantially (see Section 5.2), let us concentrate on the estimate of resonant transition radiation.

We assume:

$$\lambda = \nu = 1.5\,, \qquad \xi = 3.5\,, \tag{412}$$

$$f_\text{p} = 1\ \text{GHz}, \quad VN_\text{e}(> 1\ \text{MeV}) = 10^{32}\,, \quad \left(\frac{\omega_\text{p}}{\omega_B}\right)^{1/2} \frac{c}{v_\text{T}} = 10^2\,, \tag{413}$$

$$k_0 = \frac{\omega_\text{p}}{c}\,, \qquad \cos^2\theta \approx 0.5\,. \tag{414}$$

Then, Eqn (403) yields the RTR flux:

$$F_f = 3 \times 10^6\, \frac{\langle \Delta N^2 \rangle}{N^2} \left(\frac{f_\text{p}}{f}\right)^{\alpha} \text{sfu}\,. \tag{415}$$

Hence, the RTR intensity is equal to 100 sfu at 1 GHz [with the parameters (412) – (414)], if there are plasma density inhomogeneities with the level

$$\frac{\langle \Delta N^2 \rangle}{N^2} = 3 \times 10^{-5} \tag{416}$$

on scales $l < l_0 = 2\pi c/\omega_\text{p}$ (if $f_\text{p} = 1$ GHz then $l = 30$ cm).

Steeper (softer) spectra of fast electrons require the use of Eqn (404) for the RTR intensity. For

$$\lambda = 2\,, \qquad \nu = 1.7\,, \qquad \xi = 4.5 \tag{417}$$

and the same values of parameters (413), (414), (416), Eqn (404) yields

$$F_f \approx 5000\ \text{sfu}\,. \tag{418}$$

This flux exceeds the flux (415) by more than an order of magnitude; hence, the inhomogeneity level (416) can provide radio emission with a flux in excess of 1000 sfu. This increase is due mainly to the enhanced number of non-relativistic fast electrons for the softer distribution with the same number of particles with $E_\text{kin} > 1$ MeV (413).

The RTR flux depends on many parameters, which could have seemed to give rise to significant uncertainty of the respective interpretation. However, detailed diagnostics

based on gyro-synchrotron, hard X-ray and gamma emissions usually provides a lot of parameters (the number of fast electrons, their spectrum, the magnetic field etc.). On top of this, soft X-ray and/or millimeter-wave emissions allow one to evaluate the temperature and the number density of the medium.

Thus, most of the parameters (ω_p, ω_B, v_T, VN_e, ξ) are determined from independent observations, and only the level of inhomogeneities $\langle \Delta N^2 \rangle / N^2$ and the spectral indices λ, ν, α remain undetermined. The value of α can properly be found from the slope of the low-frequency part of the radio spectrum (produced by transition radiation). Unfortunately, there is no universal relationship between α, on the one hand, and ν and λ, on the other; so their values remain uncertain. Nevertheless, ν and λ are numbers of the order of unity, so the lack of knowledge of their exact values does not result in any considerable uncertainty in the level of small-scale density inhomogeneities $\langle \Delta N^2 \rangle / N^2$ inferred from the low-frequency radio flux.

Let us consider, as an example, **a radio burst recorded on 1991 December, 24** [117], which clearly produced the decimetric transition radiation [118]. Figure 18 displays the radio spectra of this burst at successive times. Together with the spectra, the available observational data are temporal profiles and spectra of hard X-ray emission, soft X-ray emission, temporal profiles of radio emission at frequencies 410, 606, 1415, 2695, 4880, 8800, 15400 MHz, as well as images of the radio source at 333 and 1446 MHz.

The instantaneous number of emitting electrons $VN_e(> 10\ \text{keV})$ obtained from hard X-ray emission at the peak time is

$$VN_e(> 10\ \text{keV}) \approx 10^{38}\,, \tag{419}$$

when the hard X-ray spectral index is $\gamma_X = 4$. The respective spectral indices (over energy and momentum) of non-relativistic electrons trapped in the radio source are [119, 120]

$$\xi_E = 3.5\,, \qquad \xi = 6\,. \tag{420}$$

The temperature of the plasma producing the observed soft X-ray emission is

$$T \sim 7 \times 10^6\ \text{K} \qquad (v_T \approx 10^9\ \text{cm s}^{-1})\,. \tag{421}$$

Assuming the gyro-synchrotron mechanism to produce the microwave emission of this burst, we find

$$\begin{aligned} &f_p \approx 6 \times 10^8\ \text{GHz} \quad (N \approx 4 \times 10^9\ \text{cm}^{-3})\,, \\ &f_B \approx 8 \times 10^7\ \text{GHz} \quad (B \approx 30\ \text{G})\,. \end{aligned} \tag{422}$$

The high-frequency ($f = 8.8 - 15.4$ GHz) spectral index at the peak time is

$$\alpha_2 \approx 0.9 \tag{423}$$

and it increases to 1.75 later on. The microwave flux, spectra, and time profiles support the idea that both the hard X-ray and microwave emissions are produced by the fast electrons injected into the trap by a common source. However, the hard X-ray emission at 25 – 50 keV is bremsstrahlung produced by low-energy electrons of $E_{kin} \sim 50 - 100$ keV, while the microwave radiation is produced by gyro-synchrotron emission of high-energy electrons with a typical energy in excess of a few hundreds keV. The characteristic lifetime of the accelerated electrons in a magnetic trap increases with energy, which results in more smoothed time profiles of microwave emission (say, at $f = 4.88$ GHz, see Fig. 19) compared to the profiles of hard X-ray emission [119, 120].

The respective time profiles of decimetric radio emission reveal a tight similarity with the time profiles of hard X-ray emission, which indicates the dominant role of low-energy electrons in the generation of the decimetric emission. The correlation of these time profiles with the time profiles of microwave radiation is rather significant as well (while, it is weaker than between hard X-ray and decimetric emissions). Hence, the decimetric emission is produced by the very same fraction of fast electrons and in the very same magnetic loop as the hard X-ray emission. However, according to Ref. [117], the gyro-synchrotron mechanism cannot account for the observed spectral shape in the decimetric range. In particular, the low-frequency spectral index ($f = 1415 - 2695$ MHz)

$$\alpha_1 \approx 3 \tag{424}$$

is noticeably larger than the high-frequency one α_2 (423). Moreover, the gyro-synchrotron emission by electrons with $E_{kin} \sim 50 - 100$ keV (producing the decimetric emission) is rather ineffective. Willson [117] suggests the decimetric emission to be generated by the plasma mechanism. However, this would imply a much richer temporal fine structure than is really observed, because the plasma mechanism is an effect of kinetic instability, so the emission produced is not proportional to the number of fast electrons.

The most straightforward interpretation of the decimetric emission is provided by resonant transition radiation that is generated effectively by low-energy electrons. Suppose the dimensionless parameters (399) to be independent of the plasma frequency, then the spectral index in distribution

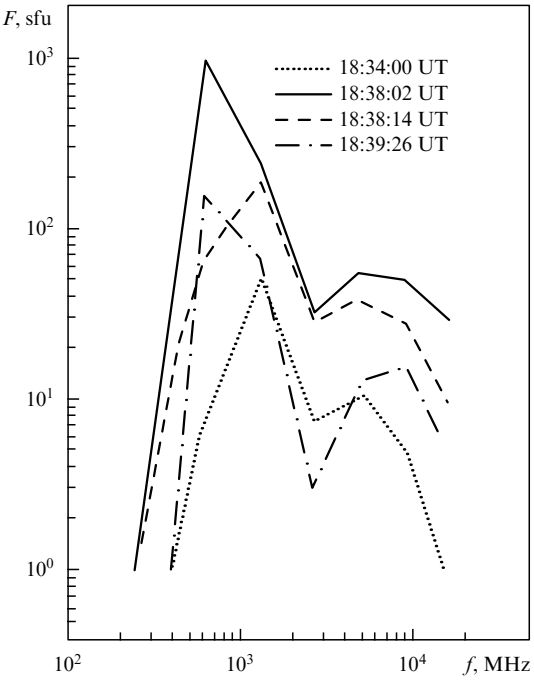

Figure 18. Radio spectra of the 1991 December, 24 solar flare at successive times (UT — Universal time).

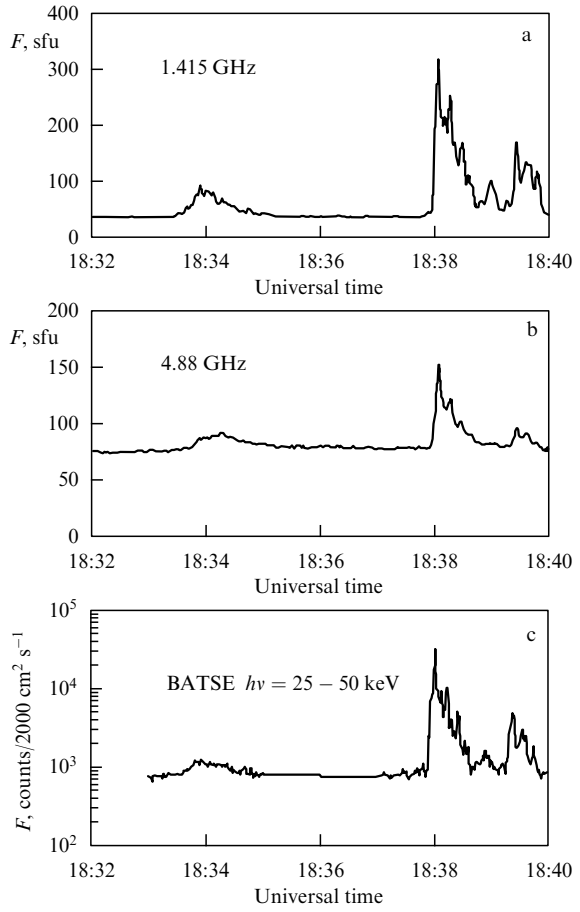

Figure 19. Temporal profiles of decimetric $f = 1.415$ GHz (a), microwave $f = 4.88$ GHz (b) and hard X-ray $E = 25-50$ keV (c) emissions for the 1991 December, 24 burst.

(392) is

$$\lambda = \alpha_1 + 1 \approx 4\,. \tag{425}$$

Assume further the spectrum of plasma inhomogeneities to be of Kolmogorov type:

$$\nu = 1.7\,. \tag{426}$$

The use of Eqns (419)–(422), (425), (426), $C_2 = 0.15$, and $x_0(10\text{ keV}) = 0.2$ yields the flux of the resonant transition radiation (410) at $f_p \approx 600$ MHz:

$$F_f = 0.7 \times 10^{10}\,\frac{\langle \Delta N^2 \rangle}{N^2}\ \text{sfu}\,, \tag{427}$$

where $\langle \Delta N^2 \rangle$ corresponds to the scales $l < c/f_p = 50$ cm, so that $k_0 c/\omega_p = 1$.

From the observed flux at $f = 606$ MHz,

$$F_{606} = 1300\ \text{sfu}\,, \tag{428}$$

we find

$$\frac{\langle \Delta N^2 \rangle}{N^2} \approx 2 \times 10^{-7}\,. \tag{429}$$

Thus, the rather low level of the plasma density inhomogeneities (429) provides the observed decimetric radio emission of the 1991 December, 24 flare. The sharp cutoff of the spectrum at $f < 600$ MHz can obviously be ascribed to a deviation of the actual distribution of the source plasma from the model one (392) at $f_p < 600$ MHz.

The importance of studying **small-scale turbulence** in the solar corona can hardly be overestimated, since it plays a key role in **fast particle kinetics** in the loops [121], **radio wave scattering** in the corona [122], the origin of **anomalous plasma kinetic coefficients** [123a] (particularly, in current sheets and shock waves [123b]) etc.

Finally it should be stressed that there are currently no means to study these extremely small-scale medium inhomogeneities except for the proposed analysis of resonant transition radiation. Note that the obtained level of the (dimensionless) plasma density inhomogeneities (429) for this particular flare is the same as in the interstellar medium (where it has been found by analyzing the scintillations of radio sources [101]).

5.4 Generation of resonant transition radiation in the Earth's ionosphere

Let us consider resonant transition radiation generated in the Earth's ionosphere. This problem is of particular interest because the ionosphere is the closest cosmic plasma to the Earth and therefore its properties are thoroughly studied.

The ionospheric plasma is known to be non-uniform with altitude. The number density of background electrons has its maximum in the F2 layer; the profile of the number density can be approximated there by a parabolic function

$$N = N_m\left[1 - \left(1 - \frac{z}{L}\right)^2\right], \tag{430}$$

where N_m is the peak (over the altitude) value of the electron number density, L is the effective scale of the F2 layer, and the coordinate z is counted from the level of $N = 0$. The plasma frequency calculated for N_m is referred to as the ionospheric *critical* frequency, f_{cr}.

The RTR intensity from a non-uniform source distributed over the sky is given by the integration of RTR emissivity over z and its averaging over the angles:

$$I_f = \left\langle \int P(f)\,\mathrm{d}z \right\rangle = \left\langle \int P(f)\,\frac{\mathrm{d}z}{\mathrm{d}f_p}\,\mathrm{d}f_p \right\rangle = \int P(f)\Phi(f_p)\,\mathrm{d}f_p\,, \tag{431}$$

where

$$\Phi = \left\langle \frac{\mathrm{d}z}{\mathrm{d}f_p} \right\rangle \tag{432}$$

represents the distribution function of the ionospheric plasma over plasma frequency.

The use of Eqn (430) yields for an ideal parabolic layer:

$$\Phi_z = \frac{\mathrm{d}z}{\mathrm{d}f_p} = \frac{L f_p}{f_{cr}^2\sqrt{1 - (f_p/f_{cr})^2}}\,, \quad \text{if} \quad f_p < f_{cr}\,,$$

$$\text{and} \quad \Phi_z = 0\,, \quad \text{if} \quad f_p > f_{cr}\,. \tag{433}$$

To average this function over the angles we take into account large-scale random ionospheric inhomogeneities, which are assumed to be distributed in accordance with the gaussian law:

$$\phi(f_p) = \frac{1}{\sqrt{\pi}\Delta f_p}\exp\left[-\frac{(f_p - f_0)^2}{\Delta f_p^2}\right], \tag{434}$$

where $\Delta f_p = (1/2) f_p \langle \Delta N_t^2 \rangle^{1/2}/N$, $\langle \Delta N_t^2 \rangle^{1/2}$ is the rms magnitude of large-scale random inhomogeneities of the electron number density, and f_0 is the mean plasma frequency at the level z.

The distribution function $\Phi(f_p)$ is obviously the convolution of these two functions (433), (434):

$$\Phi = \frac{L}{\sqrt{\pi}\,\Delta f_p f_{cr}^2} \int_0^{f_{cr}} \exp\left[-\frac{(f_p - f_0)^2}{\Delta f_p^2}\right] \frac{f_0\,\mathrm{d}f_0}{\sqrt{1-(f_0/f_{cr})^2}}\,. \quad (435)$$

For ionospheric conditions $\omega_B/\omega_p > (v_T/c)^{1/2}$, hence, the RTR is strongly polarized as o mode. We assume $\xi < \nu + 2.5$ for definiteness, so the RTR is described by formula P_5 (260). Substitution of Eqns (260), (435) into Eqn (431) finally yields the intensity of RTR generated in the Earth's ionosphere:

$$I_f = \frac{C(\theta) e^2 L}{\sqrt{\pi}\, c \Delta f_p} x_0^{\xi-1} N_e \frac{\langle \Delta N^2 \rangle}{N^2} \left(\frac{c}{l_0 f}\right)^{\nu-1} \left(\frac{f}{f_{cr}}\right)^2 \left(\frac{f}{f_B}\right)^{1/2} \times \frac{c}{v_T} \int_0^{f_{cr}} \exp\left[-\frac{(f-\delta f - f_0)^2}{\Delta f_p^2}\right] \frac{f_0\,\mathrm{d}f_0}{\sqrt{1-(f_0/f_{cr})^2}}\,, \quad (436)$$

where

$$C(\theta) = (1+\cos^2\theta) \times \frac{\pi^2(\nu-1)(\xi-1)\Gamma[(\xi-1)/2]\Gamma[(\nu-\xi+2.5)/2]}{36\times 6^{1/2}(\nu+2)\Gamma(\nu/2+3/4)}\,, \quad (437)$$

$\langle \Delta N^2 \rangle$ is the mean square of the *small-scale* density inhomogeneities at $l < l_0$ ($l_0 \sim 100$ m for this case), and $\delta f \approx f_B^2/f_p$ is the difference between the frequency of RTR peak and the local plasma frequency. We should note that $\langle \Delta N^2 \rangle$ differs from the value $\langle \Delta N_t^2 \rangle$ describing *large-scale* plasma inhomogeneities.

The RTR spectrum (436) could be measured by standard multi-frequency observations using, for example, the VDR-300 radio telescope operating in the frequency range 4.5–9.3 MHz [124]. However, it is easier to study the dependence of RTR on the ionospheric critical frequency that reveals considerable diurnal variation. Indeed, recording the radio intensity at a single frequency during the night-to-day passage [125] ensures observation of this dependence.

Figure 20 represents the theoretical dependence of the RTR intensity generated at $f = 5.6$ MHz (the frequency is relatively free from interference [126]) on the ionospheric critical frequency f_{cr} for the parameters typical for middle latitudes [127]. The estimated values of the RTR intensity are of the same order of magnitude as the background cosmic radio emission at these frequencies, thus the RTR must dominate at day time when the cosmic background is screened by the ionosphere.

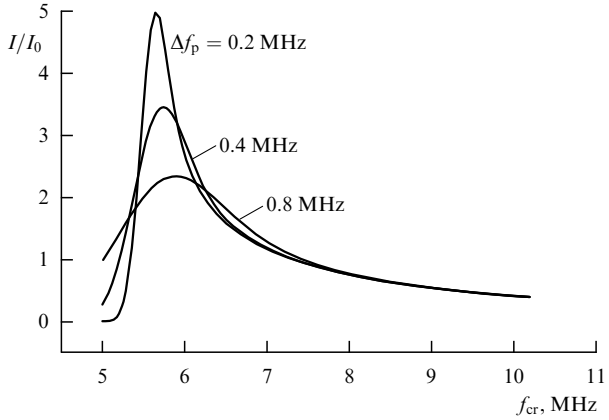

Figure 20. RTR generated in the Earth's magnetosphere versus the ionospheric critical frequency for various values of large-scale plasma density inhomogeneities. The parameters accepted are: $L = 1.3 \times 10^7$ cm, $f/f_B = 4$, $c/v_T = 2 \times 10^3$, $x_0^{\xi-1} N_e \langle \Delta N^2 \rangle / N^2 = 4 \times 10^{-7}$.

5.5 Further application of RTR to cosmic plasmas

The RTR intensity is so large that it should be produced at an observable level any time when fast electrons move in a plasma with small-scale inhomogeneities of the electron number density.

Let us discuss some important cases when RTR can be observed (or has been observed but has been interpreted differently or is not interpreted at all).

Type II bursts. Solar and interplanetary type II bursts are associated with shock waves traveling from the sun. Typically, an enhanced level of both plasma turbulence and accelerated particles accompanies the shock front. Hence, the RTR intensity from the shock region should be enhanced as well. If the shock wave is strong enough (the compression ratio is close to 4) the plasma densities in upstream and downstream regions are four times different. Thus, the characteristic frequencies of RTR peaks generated in these two regions are two times different providing the 'harmonic' structure of radiation with the ratio of frequencies 1:2.

Coronal mass ejections (CME) represent a prominent kind of solar activity strongly affecting interplanetary medium, geomagnetic phenomena etc. Paper [128] publishes radio spectra of some restricted regions of a CME recorded on 1998 April, 20 at frequencies 164, 236.6, 327 MHz and proves the radio emission to be generated by mildly relativistic electrons (0.5–5 MeV) by synchrotron radiation affected by the density effect (Razin–Tsytovich effect).

Transition radiation (from the same spatial regions of the CME) should dominate at lower frequencies where the synchrotron emission is suppressed strongly. Transition radiation might be discovered with the same frequency set when analyzing denser regions of the CME. The contribution of transition radiation can be discriminated as an excess of the radio flux at the frequency 164 MHz.

Low-frequency terrestrial radio emission. Many kinds of radio emission are known to originate in the auroral region of the Earth's magnetosphere [129]. Long ago the intensity of the emissions was found to correlate strongly with the flux of fast auroral electrons [130, 131]. Some of these emissions are fairly **narrow-band** and are concentrated within the range between local plasma- and upper-hybrid frequencies [129]. RTR is the most intensive in the very same frequency range and there can contribute the bulk of radiation. The mechanisms of **broad-band** auroral radiation, such as emission associated with ionization of atmospheric particles or emission associated with charge exchange between protons and atmospheric neutrals [72, 130, 132] are just particular cases of the (inelastic) polarization bremsstrahlung analyzed in Section 4.

Furthermore, RTR can be observed in experiments on ionospheric modification by power radio signals [21, 133] because both accelerated particles [134] and small-scale plasma density inhomogeneities [135, 136] originate there.

Planetary radio emissions. All giant planets are radio sources. They have a broad variety of kinds of radiation

[137] providing an ample field for the application of the TR theory. For example, the broad-band spectrum of Jovian radio emission displays a low-frequency rise [137, p. 43], and the respective radiation is polarized strongly (up to 100%) in the ordinary mode. Such radiation can easily be interpreted as resonant transition radiation.

The outer heliospheric boundary produces drifting bursts of radio emission ($f = 2-3$ kHz) [138]. Since a shock wave is assumed to be located there (hence, the level of plasma inhomogeneities should be enhanced) and the respective plasma frequencies are of the order of $f = 2-3$ kHz, the contribution of RTR to the bursts can be rather essential.

Transition maser emission is the generation of electromagnetic waves due to transition instability (i.e., when the coefficient of the transition absorption is negative, see Section 3.5). Section 3.5 evaluates the growth rate of the transition instability for **ionospheric plasma**, while it is unclear yet if the transition instability plays any role for the Earth's ionosphere.

The transition instability obviously requires an anisotropic distribution of fast electrons to operate. For example, solar and interplanetary **type III bursts** are produced by beams of fast electrons [109]. The plasma mechanism of radio emission is widely accepted for these bursts. Indeed, fast electron beams generate plasma waves easily. The plasma waves can further be converted into transverse waves due either to coalescence processes (providing second harmonic radio emission at twice the plasma frequency) or to scattering of the plasma waves on either background particles or low-frequency waves (providing fundamental plasma emission at the plasma frequency).

Type III bursts frequently reveal such a harmonic structure (with the ratio of frequencies 1:2). However, the plasma mechanism implies a weaker fundamental-to-harmonic intensity ratio (I_1/I_2) than is actually observed. RTR (normal or maser) could contribute to the generation of the fundamental emission of type III bursts.

6. Conclusions

Transition radiation is an exceedingly general phenomenon representing a broad branch of modern physics. A particular case of the phenomenon, namely, transition radiation arising under natural conditions, is discussed in detail in this paper. Natural sources of electromagnetic radiation are rather different from laboratory ones. For the latter case, the parameters of both medium and fast particles can be under control (for example, we can study the emission by monoenergetic particles, or localize a single boundary, or arrange a periodical medium etc.).

Astrophysical media (including interplanetary and ionospheric plasmas) are usually highly inhomogeneous. Gradual large-scale non-uniformity and small-scale random inhomogeneities of the density and/or field typically coexist. The role of a regular (large-scale) magnetic field is rather important; fast particles have broad energy spectra and (frequently) anisotropic angular distributions.

The theory of transition radiation generated by fast particles in magnetized plasma with random density inhomogeneities presented in this article includes all the counted physical effects. Hence, its application for the interpretation of astrophysical radiation is correct and provides reliable consistent results. Nevertheless, further development of the theory is strongly required, e.g., in respect to processes of wave absorption and scattering, the effect of large optical depth, maser effects, as well as detailed models for cosmic sources of transition radiation and their use in analyzing observations.

In essence, the use of the theory of transition radiation has just started and, no doubt, the field of its application will grow greatly in the near future.

The authors thank V L Ginzburg and the unknown referee for discussion of the basic problems of transition radiation, as well as T Bastian, D Gary, W Kurth, and Yu V Tokarev for the discussion of TR applications. This work was supported in part by RFBR (Grant No. 00-02-16356).

References

1. Ginzburg V L *Usp. Fiz. Nauk* **166** 1033 (1996) [*Phys. Usp.* **39** 973 (1996)]; **172** 373 (2002) [*Phys. Usp.* **45** 341 (2002)]
2. Ginzburg V L, Frank I M *Zh. Eksp. Teor. Fiz.* **16** 15 (1946); *J. Phys. USSR* **9** 353 (1945)
3. Bolotovskiĭ B M, Galst'yan E A *Usp. Fiz. Nauk* **170** 809 (2000) [*Phys. Usp.* **43** 755 (2000)]
4. Ter-Mikhaelyan M L *Vliyanie Sredy na Elektromagnitnye Protsessy pri Vysokikh Energiyakh* (High Energy Electromagnetic Processes in Condensed Media) (Erevan: Izd. AN Arm. SSR, 1969) [Translated into English (New York: Wiley-Intersci., 1972)]
5. Amus'ya M Ya et al. *Polyarizatsionnoe Tormoznoe Izluchenie Chastits i Atomov* (Polarization Bremsstrahlung by Particles and Atoms) (Exec. eds V N Tsytovich, I M Oĭringel') (Moscow: Nauka, 1987) [Translated into English: *Polarization Bremsstrahlung* (New York: Plenum Press, 1992)]
6. Frank I M *Izluchenie Vavilova–Cherenkova* (*Voprosy Teorii*) (Vavilov–Cherenkov Radiation. Theoretical Aspects) (Moscow: Nauka, 1988)
7. Tamm I E *Usp. Fiz. Nauk* **68** 387 (1959)
8. Tsytovich V N *Usp. Fiz. Nauk* **165** 89 (1995) [*Phys. Usp.* **38** 87 (1995)]
9. Akhiezer A I, Shul'ga N F *Usp. Fiz. Nauk* **137** 560 (1982) [*Sov. Phys. Usp.* **25** 541 (1982)]
10. Bazylev V A, Zhevago N K *Izluchenie Bystrykh Chastits v Veshchestve i vo Vneshnikh Polyakh* (Emission by Fast Particle in Media and in External Fields) (Moscow: Nauka, 1987)
11. Platonov K Yu, Toptygin I N, Fleĭshman G D *Usp. Fiz. Nauk* **160** (4) 59 (1990) [*Sov. Phys. Usp.* **33** 289 (1990)]
12. Platonov K Yu, Toptygin I N, Fleĭshman G D *Fiz. Plazmy* **16** 1517 (1990) [*Sov. J. Plasma Phys.* **16** 878 (1990)]
13. Tamoĭkin V V *Izv. Vyssh. Uchebn. Zaved. Radiofiz.* **11** 1879 (1968)
14. Ryzhov Yu A, Tamoĭkin V V *Izv. Vyssh. Uchebn. Zaved. Radiofiz.* **13** 358 (1970)
15. Tamoikin V V *Astrophys. Space Sci.* **53** 3 (1978)
16. Bass F G *Izv. Vyssh. Uchebn. Zaved. Radiofiz.* **2** 1015 (1959)
17. Tamoĭkin V V *Izv. Vyssh. Uchebn. Zaved. Radiofiz.* **14** 285 (1971)
18. Ermakova E N, Trakhtengerts V Yu *Fiz. Plazmy* **18** 1358 (1992)
19. Fleĭshman G D *Usp. Fiz. Nauk* **161** (1) 165 (1991) [*Sov. Phys. Usp.* **34** 86 (1991)]
20. Ermakova E N, Trakhtengerts V Yu *Fiz. Plazmy* **18** 1403 (1992)
21. Ermakova E N, Trakhtengerts V Yu *Izv. Vyssh. Uchebn. Zaved. Radiofiz.* **39** 286 (1996)
22. Bel'kov S A, Nikolaev Yu A, Tsytovich V N *Izv. Vyssh. Uchebn. Zaved. Radiofiz.* **23** 261 (1980)
23. Davydov V A *Izv. Vyssh. Uchebn. Zaved. Radiofiz.* **25** 1429 (1982)
24. Davydov V A *Izv. Vyssh. Uchebn. Zaved. Radiofiz.* **26** 1134 (1983)
25. Davydov V A *Izv. Vyssh. Uchebn. Zaved. Radiofiz.* **26** 1251 (1983)
26. Tamoĭkin V V, Bigarov S B *Zh. Eksp. Teor. Fiz.* **44** 1544 (1963) [*Sov. Phys. JETP* **17** 682 (1963)]
27. Vesnitskiĭ A I, Metrikin A V *Usp. Fiz. Nauk* **166** 1043 (1996) [*Phys. Usp.* **39** 983 (1996)]
28. Ginzburg V L, Tsytovich V N *Perekhodnoe Izluchenie i Perekhodnoe Rasseyanie* (Transition Radiation and Transition Scattering) (Moscow: Nauka, 1984) [Translated into English (Bristol: A. Hilger, 1990)]
29. Fleĭshman G D *Zh. Eksp. Teor. Fiz.* **99** 488 (1991) [*Sov. Phys. JETP* **72** 272 (1991)]

30. Landau L D, Lifshitz E M *Teoriya Polya* (The Classical Theory of Fields) (Moscow: Nauka, 1973) [Translated into English (Oxford: Pergamon Press, 1975)]
31. Baĭer V N, Katko V M, Fadin V S *Izluchenie Relyativistskikh Elektronov* (Emission by Relativistic Electrons) (Moscow: Atomizdat, 1973)
32. Toptygin I N, Fleishman G D *Astrophys. Space Sci.* **132** 213 (1987)
33. Migdal A B *Dokl. Akad. Nauk SSSR* **96** 49 (1954)
34. Dolginov A Z, Toptygin I N *Zh. Eksp. Teor. Fiz.* **51** 1771 (1966) [*Sov. Phys. JETP* **24** 1195 (1967)]
35. Garibyan G M *Zh. Eksp. Teor. Fiz.* **39** 332 (1960) [*Sov. Phys. JETP* **12** 237 (1961)]
36. Toptygin I N *Kosmicheskie Luchi v Mezhplanetnykh Magnitnykh Polyakh* (Cosmic Rays in Interplanetary Magnetic Fields) (Moscow: Nauka, 1983) [Translated into English (Dordrecht: D. Reidel, 1985)]
37. Ginzburg V L *Zh. Eksp. Teor. Fiz.* **10** 601 (1940)
38. Ginzburg V L *Zh. Eksp. Teor. Fiz.* **10** 608 (1940); *J. Phys. USSR* **3** 101 (1940)
39. Kolomenskiĭ A A *Zh. Eksp. Teor. Fiz.* **24** 167 (1953)
40. Kolomenskiĭ A A *Dokl. Akad. Nauk SSSR* **106** 982 (1956) [*Sov. Phys. Dokl.* **1** 133 (1956)]
41. Barsukov K A *Zh. Eksp. Teor. Fiz.* **36** 1485 (1959) [*Sov. Phys. JETP* **9** 1052 (1959)]
42. Ginzburg V L *Usp. Fiz. Nauk* **69** 537 (1959) [*Sov. Phys. Usp.* **2** 874 (1960)]
43. Bazylev V A, Zhevago N K *Usp. Fiz. Nauk* **160** (12) 47 (1990) [*Sov. Phys. Usp.* **33** 1021(1990)]
44. Arutyunov V A et al. *Zh. Tekh. Fiz.* **61** 1 (1991)
45. Biryukov V M, Kotov V I, Chesnokov Yu A *Usp. Fiz. Nauk* **164** 1017 (1994) [*Phys. Usp.* **37** 937 (1994)]
46. Bolotovskiĭ B M, Mergelyan O S *Opt. Spektrosk.* **18** 3 (1965) [*Opt. Spectrosc.* **18** 1 (1965)]
47. Pafomov V E *Zh. Eksp. Teor. Fiz.* **39** 134 (1960) [*Sov. Phys. JETP* **12** 97 (1961)]
48. Fleĭshman G D *Zh. Eksp. Teor. Fiz.* **101** 432 (1992) [*Sov. Phys. JETP* **74** 261 (1992)]
49. Lifshitz E M, Pitaevskiĭ E M *Fizicheskaya Kinetika* (Physical Kinetics) (Moscow: Nauka, 1979) [Translated into English (Oxford: Pergamon Press, 1981)]
50. Ginzburg V L *Teoreticheskaya Fizika i Astrofizika* 2nd ed. (Theoretical Physics and Astrophysics) (Moscow: Nauka, 1981) [Translated into English: Applications of Electrodynamics in Theoretical Physics and Astrophysics 2nd rev. Engl. ed. (New York: Gordon and Breach Sci. Publ., 1989)]
51. Éĭdman V Ya *Zh. Eksp. Teor. Fiz.* **34** 31 (1958) [*Sov. Phys. JETP* **7** 91 (1958)]; **36** 1335 (1959) [*Sov. Phys. JETP* **9** 947 (1959)]
52. Ginzburg V L *Rasprostranenie Elektromagnitnykh Voln v Plazme* (The Propagation of Electromagnetic Waves in Plasmas) (Moscow: Nauka, 1967) [Translated into English (Oxford: Pergamon Press, 1970)]
53. Pacholczyk A G *Radio Astrophysics*; *Nonthermal Processes in Galactic and Extragalactic Sources* (San Francisco: W.H. Freeman, 1970) [Translated into Russian (Moscow: Mir, 1973)]
54. Kapitza S P *Zh. Eksp. Teor. Fiz.* **39** 1367 (1960) [*Sov. Phys. JETP* **12** 943 (1961)]
55. Abramowitz M, Stegun I A *Handbook of Mathematical Functions with Formulas, Graphs, and Mathematical Tables* (New York: Dover Publ., 1965) [Translated into Russian (Moscow: Nauka, 1979)]
56. Mathews T, Venkatesan D *Nature* **345** 600 (1990)
57. Platonov K Yu, Fleĭshman G D *Zh. Eksp. Teor. Fiz.* **106** 1053 (1994) [*JETP* **79** 572 (1994)]
58. Fleishman G D, Platonov K Yu *Space Sci. Rev.* **68** 243 (1994)
59. Akopyan A V, Tsytovich V N *Zh. Eksp. Teor. Fiz.* **71** 166 (1976) [*Sov. Phys. JETP* **44** 87 (1976)]
60. Prudnikov A P, Brychkov Yu A, Marichev O I *Integraly i Ryady: Elementarnye Funktsii* (Integrals and Series: Elementary Functions) (Moscow: Nauka, 1981) [Translated into English (New York: Gordon and Breach Sci. Publ., 1986)]
61. Bredov M M, Rumyantsev V V, Toptygin I N *Klassicheskaya Elektrodinamika* (Classical Electrodynamics) (Moscow: Nauka, 1985)
62. Akhiezer A I (Ed.) *Elektrodinamika Plazmy* (Plasma Electrodynamics) (Moscow: Nauka, 1974) [Translated into English (International Series of Monographs in Natural Philosophy, Vol. 68) (Oxford: Pergamon Press, 1975)]
63. Platonov K Yu, Fleĭshman G D *Zh. Eksp. Teor. Fiz.* **108** 1942 (1995) [*JETP* **81** 1059 (1995)]
64. Istomin Ya N, Luk'yanov A V *Zh. Eksp. Teor. Fiz.* **97** 1578 (1990) [*Sov. Phys. JETP* **70** 987 (1990)]
65. Platonov K Yu, Fleĭshman G D *Izv. Vyssh. Uchebn. Zaved. Radiofiz.* **40** 941 (1997)
66. Fleĭshman G D *Astron. Zh.* **66** 932 (1989) [*Sov. Astron.* **33** 482 (1989)]
67. Fleĭshman G D, Mel'nikov V F *Usp. Fiz. Nauk* **168** 1265 (1998) [*Phys. Usp.* **41** 1157 (1998)]
68. Fleishman G D, Yastrebov S G *Solar Phys.* **154** 361 (1994)
69. Fleishman G D, Platonov K Yu, in *Magnetic Fields and Solar Processes*: *Proc. 9th European Meeting on Solar Physics, Florence, Italy, 12–18 September 1999* (ESA SP, 448, Ed. A Wilson) Vol. 2 (Noordwijk: ESA Publ. Division, ESTEC, 1999) p. 809
70. Fleishman G D, Platonov K Yu *Astrophys. Rep.* (Publ. Beijing Astron. Observ.) **36** 111 (2000)
71. Platonov K Yu, Fleĭshman G D *Astron. Zh.* **78** 238 (2001) [*Astron. Rep.* **45** 203 (2001)]
72. Toptygin I N *Zh. Eksp. Teor. Fiz.* **43** 1031 (1962) [*Sov. Phys. JETP* **16** 516 (1963)]
73. Astapenko V A et al. *Zh. Eksp. Teor. Fiz.* **88** 1560 (1985) [*Sov. Phys. JETP* **61** 930 (1985)]
74. Amus'ya M Ya et al. *Zh. Eksp. Teor. Fiz.* **88** 353 (1985) [*Sov. Phys. JETP* **61** 224 (1985)]
75. Amus'ya M Ya, Solov'ev A V, Korol' A V *Pis'ma Zh. Tekh. Fiz.* **12** 705 (1986)
76. Platonov K Yu, Toptygin I N, in *Tez. Dokl. XVI Vsesoyuzn. Soveshch. po Fiz. Vzaimodeĭstviya Zaryazhennykh Chastits s Kristallami* (Abstract in All-Union Conf. on Phys. of Charged Part. Interaction with Crystals) (Moscow: Izd. MGU, 1986) p.70
77. Platonov K Yu, Toptygin I N *Izv. Vyssh. Uchebn. Zaved. Radiofiz.* **32** 735 (1989)
78. Sitenko A G *Fluktuatsii i Nelineĭnoe Vzaimodeĭstvie Voln v Plazme* (Fluctuations and Non-Linear Wave Interactions in Plasmas) (Kiev: Naukova Dumka, 1977) [Translated into English (Oxford: Pergamon Press, 1982)]
79. Sheffield J *Plasma Scattering of Electromagnetic Radiation* (New York: Academic Press, 1975) [Translated into Russian (Moscow: Atomizdat, 1978)]
80. Platonov K Yu, Fleĭshman G D *Pis'ma Zh. Eksp. Teor. Fiz.* **59** 586 (1994) [*JETP Lett.* **59** 613 (1994)]
81. Akopyan A V, Tsytovich V N, Preprint FIAN No. 184 (Moscow: FIAN, 1978)
82. Korsakov V B, Fleĭshman G D *Izv. Vyssh. Uchebn. Zaved. Radiofiz.* **38** 887 (1995)
83. Batkin Ya S, Almaliev A N *Zh. Eksp. Teor. Fiz.* **88** 1958 (1985) [*Sov. Phys. JETP* **61** 1246 (1985)]
84. Akopyan A V, Tsytovich V N *Zh. Eksp. Teor. Fiz.* **72** 1824 (1977) [*Sov. Phys. JETP* **45** 957 (1977)]
85. Yuan L C L et al. *Phys. Rev. Lett.* **25** 1513 (1970)
86. Cherry M L et al. *Phys. Rev. D* **10** 3594 (1974)
87. Lorikyan M P, Sardaryan R A, Shikhlyarov K K *Izv. Akad. Nauk Arm. SSR Ser. Fiz.* **24** 159, 252 (1989)
88. Piestrup M A et al. *Phys. Rev. A* **45** 1183 (1992)
89. Ter-Mikhaelyan M L *Usp. Fiz. Nauk* **171** 597 (2001) [*Phys. Usp.* **44** 571 (2001)]
90. Happek U, Sievers A J, Blum E B *Phys. Rev. Lett.* **67** 2962 (1991)
91. Moran M J et al. *Phys. Rev. Lett.* **57** 1223 (1986)
92. Johansson S A E *Astrophys. Lett.* **9** 143 (1971)
93. Ramaty R, Bleach R D *Astrophys. Lett.* **11** 35 (1972)
94. Yodh G B, Artru X, Ramaty R *Astrophys. J.* **181** 725 (1973)
95. Gnedin Yu N, Private communication (1998)
96. Doyle J G, Mathioudakis M *Astron. Astrophys.* **241** L41 (1991)
97. Ginzburg V L, Syrovatskiĭ S I *Proiskhozhdenie Kosmicheskikh Lucheĭ* (The Origin of Cosmic Rays) (Moscow: Izd. AN SSSR, 1963) [Translated into English (Oxford: Pergamon Press, 1964)]
98. Fleishman G D, Tokarev Yu V *Astron. Astrophys.* **293** 565 (1995)
99. Getmantsev G G, Tokarev Yu V *Astrophys. Lett.* **12** 57 (1972)

100. Nikolaev Iu A, Tsytovich V N *Phys. Scripta* **20** 665 (1979)
101. Cordes J M et al. *Nature* **354** 121 (1991)
102. Pynzar' A V *Astron. Zh.* **70** 480 (1993) [*Astron. Rep.* **37** 245 (1993)]
103. Brown L W *Astrophys. J.* **180** 359 (1973)
104. Tokarev Yu V et al. *Pis'ma Astron. Zh.* **26** 643 (2000) [*Astron. Lett.* **26** 553 (2000)]
105. Manning R, Dulk G A *Astron. Astrophys.* **372** 663 (2001)
106. Alexander J K et al. *Astrophys. J. Lett.* **157** L163 (1969)
107. Novaco J C, Brown L W *Astrophys. J.* **221** 114 (1978)
108. Tokarev Yu V et al., in *Tez. Dokl. Vseross. Astron. Konf. St. Petersburg 2001 Aug. 6–12* (Abstracts of All-Russian Astron Conf.) (St. Petersburg: NIIKh SPbGU, 2001) p. 175
109. Bastian T S, Benz A O, Gary D E *Annu. Rev. Astron. Astrophys.* **36** 131 (1998)
110. Fleishman G D, Kahler S W *Astrophys. J.* **394** 688 (1992)
111. Kocharov G E et al., in *Problemy Solnechnykh Vspyshek* (Problems of Solar Flares) (Ed. V V Fomichev) (Moscow: Nauka, 1986) p. 176
112. Vestrand W T et al. *Astrophys. J.* **322** 1010 (1987)
113. *Solar Geophys. Data Pt. II* (436) (1980); (458) (1982); (461) (1983)
114. Fleishman G D, Kovaltsov G A, in *Yadernaya Astrofizika* (Nuclear Astrophysics) (Ed. G E Kocharov) (St. Petersburg: FTI, 1991) p. 102
115. Mel'nikov V F *Izv. Vyssh. Uchebn. Zaved. Radiofiz.* **37** 856 (1994)
116. Mel'nikov V F, Magun A *Izv. Vyssh. Uchebn. Zaved. Radiofiz.* **39** 1456 (1996)
117. Willson R F *Astrophys. J.* **413** 798 (1993)
118. Fleĭshman G D *Pis'ma Astron. Zh.* **27** 296 (2001) [*Astron. Lett.* **27** 254 (2001)]
119. Melnikov V F, Magun A *Solar Phys.* **178** 591 (1998)
120. Melnikov V F, Silva A V R, in *Magnetic Fields and Solar Processes: Proc. 9th European Meeting on Solar Physics, Florence, Italy, 12–18 September 1999* (ESA SP, 448, Ed. A Wilson) Vol. 2 (Noordwijk: ESA Publ. Division, ESTEC, 1999) p. 1053
121. Bespalov P A, Zaitsev V V, Stepanov A V *Astrophys. J.* **374** 369 (1991)
122. Bastian T S *Astrophys. J.* **426** 774 (1994)
123. (a) Priest E R, Forbes T *Magnetic Reconnection: MHD Theory and Applications* (Cambridge: Cambridge Univ. Press, 2000);
(b) Vaĭnshteĭn S I, Bykov A M, Toptygin I N *Turbulentnost', Tokovye Sloi i Udarnye Volny v Kosmicheskoĭ Plazme* (Turbulence, Current Sheets, and Shocks in Cosmic Plasma) (Moscow: Nauka, 1989) [Translated into English (The Fluid Mechanics of Astrophysics and Geophysics, Vol. 6) (Langhorne, Pa.: Gordon and Breach Science Publ., 1993)]
124. Tokarev Yu V, in *Tez. Dokl. XXV Abstract in Radio Astron. Conf., Pushchino, 1993 September, 20–24* (Pushchino: Pushchinskiĭ Nauchnyĭ Tsentr RAN, 1993) p. 209
125. Tokarev Yu V, Private Communication (2001)
126. Vinyaĭkin E N et al. *Astron. Zh.* **64** 987 (1987) [*Sov. Astron.* **31** 517 (1987)]
127. Taran V I *Geomagn. Aeronomiya* **41** 659 (2001) [*Geomagn. Aeron.* **41** 632 (2001)]
128. Bastian T S et al. *Astrophys. J.* **558** L65 (2001)
129. LaBelle J *J. Atmosph. Terrestr. Phys.* **51** 197 (1989)
130. Bozhkov A I, Osipov N K *Geomagn. Aeronomiya* **11** 1021 (1971) [*Geomagn. Aeron.* **11** 859 (1971)]
131. Osipov N K, Shevelev Yu G *Geomagn. Aeronomiya* **13** 674 (1973) [*Geomagn. Aeron.* **13** 573 (1973)]
132. Rappoport V O, Éĭdman V Ya *Geomagn. Aeronomiya* **5** 930 (1965)
133. Thidé B, Kopka H, Stubbe P *Phys. Rev. Lett.* **49** 1561 (1982)
134. Carlson H C, Wickwar V B, Mantas G P *J. Atmosph. Terrestr. Phys.* **44** 1089 (1982)
135. Inhester B, Fejer J A, Das A C *J. Geophys. Res.* **86** 9101 (1981)
136. Kelley M C et al. *J. Geophys. Res.* **100** 17367 (1995)
137. Ryabov B P, Gerasimova N N *Dekametrovoe Sporadicheskoe Radioizluchenie Yupitera* (Jovian Decametric Sporadic Radio Emission) (Kiev: Naukova Dumka, 1990)
138. Kurth W S et al. *Nature* **312** 27 (1984)